72-11,564

HALL, Jr., Wilton Earl, 1941-
COMPUTATIONAL METHODS FOR THE SYNTHESIS OF
ROTARY-WING VTOL AIRCRAFT CONTROL SYSTEMS.

Stanford University, Ph.D., 1971
Engineering, aeronautical

University Microfilms, A XEROX Company, Ann Arbor, Michigan

THIS DISSERTATION HAS BEEN MICROFILMED EXACTLY AS RECEIVED

COMPUTATIONAL METHODS FOR THE SYNTHESIS OF ROTARY-WING VTOL AIRCRAFT CONTROL SYSTEMS

A DISSERTATION
SUBMITTED TO THE DEPARTMENT OF AERONAUTICS AND ASTRONAUTICS
AND THE COMMITTEE ON GRADUATE STUDIES
OF STANFORD UNIVERSITY
IN PARTIAL FULFILLMENT OF THE REQUIREMENTS
FOR THE DEGREE OF
DOCTOR OF PHILOSOPHY

By

Wilton Earl Hall, Jr.
August 1971

I certify that I have read this thesis and that in my opinion it is fully adequate, in scope and quality, as a dissertation for the degree of Doctor of Philosophy.

Arthur E. Bryson Jr.
(Principal Adviser)

I certify that I have read this thesis and that in my opinion it is fully adequate, in scope and quality, as a dissertation for the degree of Doctor of Philosophy.

Daniel G. Dodd

I certify that I have read this thesis and that in my opinion it ~~is~~ fully adequate, in scope and quality, as a dissertation for the degree of Doctor of Philosophy.

Gene L. Franklin
(Electrical Engineering)

Approved for the University Committee
on Graduate Studies:

Dean of Graduate Studies

PLEASE NOTE:

Some Pages have indistinct print. Filmed as received.

UNIVERSITY MICROFILMS

ABSTRACT

A design procedure is developed which models a rotary-wing VTOL aircraft as two coupled rigid bodies which represent the rotor and fuselage respectively. Previous design approaches for the synthesis of VTOL aircraft controllers have treated rotor and fuselage as dynamically uncoupled systems, and generally the rotor dynamics have been neglected in synthesizing the fuselage controls. Only the low-speed flight regime around hover is considered for this design. The equations for the rotor dynamics and rotor forces on the fuselage are obtained from an analysis of blade motions. The controls-fixed dynamic response of the two rigid body approximation is determined for a typical vehicle with an articulated rotor and also with a hingeless rotor.

A controller has been designed for the two rigid body approximation using eigenvector decomposition of the Euler-Lagrange equations of quadratic synthesis. Through a unique statement of these equations, eigenvector decomposition is applied to the model follower and smoothing problems. A new computer program, using an improved QR eigensystem solver routine, is developed. The program also determines the steady state RMS response of an optimally controlled system to random winds.

This computer program is used to design high and low order controllers for hovering vehicles. The effects of the order of the rotor representations on this controller are evaluated. It is found that the controller for the two rigid body model requires rotor state feedback gains comparable in magnitude to fuselage state gains for a quadratic cost which involves only fuselage state. Furthermore, it is found that controller design based on lower order rotor models can lead to reduced damping and even instability in the complete rotor fuselage approximation.

The application of a random rotor torque on the vehicle with the complete and reduced order controllers indicates an increase in RMS fuselage and rotor state response when the lower order controllers are used.

The possibility of blade instability due to rotor plane feedback is examined by multivariable Floquet theory. It is shown that such rotor

plane feedback may cause blade instability and it is concluded that such an analysis should be included in the control system design.

The dynamic models, analysis methods, and computer programs developed during this research should provide a major improvement in the performance prediction and control of rotary-wing VTOL aircraft.

CONTENTS

Chapter		Page
I	INTRODUCTION	1
	1.1 Statement and Discussion of Problem	1
	1.2 Previous Studies and Related Results	2
	1.3 Organization of This Thesis	4
	1.4 Summary of Contributions	6
II	BLADE EQUATIONS OF MOTION	8
	2.1 Introduction	8
	2.2 Representations of Blade Dynamics	8
	Kinematics	8
	Blade Equations of Motion	9
	2.3 Aerodynamic Forces and Moments	15
	Induced Velocity	16
	Reference Planes	18
	Aerodynamic Forces and Moments	20
	Reversed Flow	23
	2.4 Flap-Lag Blade Equations	23
	2.5 Summary	32
III	MODEL FUSELAGE DYNAMIC MODELS IN HOVER	33
	3.1 Introduction	33
	3.2 Averaging Over Blade State to Obtain Rotor Tilt Equations	35
	3.3 Averaging Over Blade State to Obtain Rotor Forces on Fuselage	36
	Moment Due to Flapping Spring Restraint	37
	Moments Due to Rotor Blade Inertia Shear Forces	39
	Moments Due to Airload Shear at Flapping Hinge	41
	Inplane Rotor Forces	43
	Total Rotor Forces on Fuselage	46
	3.4 A Tenth Order Roll-Pitch-Horizontal Translation Model	47
	Transformation to Canonical Form	51
	TRBM Eigensystem for a Vehicle with a Fully Articulated Rotor	53
	3.5 Rotor Rate (Eighth Order) and Rotor Position (Sixth Order) Roll-Pitch Horizontal Translation Models	60
	Characteristic Frequencies and Modes for the Sixth and Eighth Order Models	63

Page

3.6 Eigensystem Analysis of a Hypothetical Hingeless Rotored Vehicle 70
3.7 Summary 76

IV COMPUTATIONAL ASPECTS OF MODAL ANALYSIS AND CONTROL SYNTHESIS 78

4.1 Introduction 78
Solution Methods of the Matrix Riccati Equation . 78
4.2 Quadratic Synthesis Using Matrix Riccati Equations 79
4.2.1 Smoothing with Pre-Flight, In-Flight, and Post-Flight Data 80
Euler-Lagrange Equations 80
The Forward-Then-Backward Solution Using a Matrix Riccati Equation 82
The Backward-Then-Forward Solution Using a Matrix Riccati Equation 83
Combination of Forward and Backward Solutions at an Intermediate Time 85
4.2.2 Follower with Initial, In-Flight, and Final Goals 85
Equivalence to Smoother Problem 86
Euler-Lagrange Equations 86
4.3 Quadratic Synthesis Using Eigenvector Decomposition 87
Symmetry of Eigenvalues of the Euler-Lagrange Equations 87
Eigenvector Decomposition of the Euler-Lagrange Equations 89
Relationship to Steady-State Solutions of Matrix Riccati Equations 91
Eigenvalues and Eigenvectors of the Backward Smoother 93
Eigenvalues and Eigenvectors of the Forward Smoother 93
Eigenvalues and Eigenvectors of the Forward Filter 94
Eigenvalues and Eigenvectors of the Backward Filter 95
Eigenvalues and Eigenvectors of the Follower-Regulator 95
The Smoothed Covariance Matrix 96
An Example 96
4.4 Determining Mean Square Stochastic Response . . . 101

Page

4.5 Computational Considerations 103
4.6 The OPTSYS Computer Program 108
4.7 Time-Varying Solutions of the Constant Coefficient Homogeneous Euler-Lagrange Equations 115
4.8 Summary 118

V CONTROLLER SYNTHESIS FOR A ROTARY WING VTOL AIRCRAFT NEAR HOVER 120

5.1 Introduction 120
5.2 Design of Three Different Controllers Using the Two Rigid Body, Rotor Rate and Rotor Position Models 121
5.3 Closed Loop Vehicle Response Using the Three Controllers with Their Respective Models 125
5.4 Closed-Loop Vehicle Response Using the Three Controllers with the Complete Model 128
5.5 Mean Square Response of the Controlled Vehicle in the Presence of a Random Rotor Torque 135
5.6 Controller Design and Evaluation for a Hingeless Rotored VTOL Aircraft 136
5.7 Summary 142

VI EFFECT OF FORWARD SPEED AND ROTOR PLANE FEEDBACK ON BLADE STABILITY 144

6.1 Introduction 144
6.2 Computer Analysis of Periodic Excitation of Rotor Motions 144
6.3 Simple Flapping with Reverse Flow 145
6.4 Flap-Lag Instability at Low μ and γ 153
Equivalence of Blade Flapping State Feedback with Rotor State Feedback 153
Flap-Lag Instability for a Hypothetical Rotor . . 155
6.5 Summary 160

VII CONCLUSIONS AND RECOMMENDATIONS 161

7.1 Conclusions 161
7.2 Recommendations 162

Appendix A DERIVATION OF BLADE FLAP-PITCH-LAG EQUATIONS OF MOTION 164

Appendix B THE HAMILTONIAN AND SYMPLECTIC PROPERTIES OF THE CANONICAL SYSTEM 172

Appendix C FLOQUET THEORY 175

Page

Appendix D DESCRIPTION OF BLADE STABILITY PROGRAM 183

Appendix E LISTING OF OPTSYS 194

References 226

LIST OF FIGURES

Figure		Page
2.2.1	Blade Axis System	10
2.2.2	Inertial References Axes	11
2.2.3	Velocities and Rates in Fuselage Axes	11
2.3.1	Schematic of Blade Element Velocity Resolutions	19
2.3.2	Reverse Flow Regimes	29
3.3.1	Schematic of Rotor Blade Shear Forces	40
3.3.2	Schematic of Inplane Rotor Forces	44
3.4.1	Controls Fixed Eigenvalues for 10X10 F Matrix of Table 3.4.1 (TRBM)	55
3.4.2	Open Loop Low Frequency Eigenvectors for Tenth Order Model (TRBM)	57
3.4.3	Open Loop High Frequency Eigenvectors for Tenth Order Model (TRBM)	58
3.5.1	Open Loop Eigenvectors for Eighth Order Model (RRM)	67
3.5.2	Open Loop Eigenvectors for Sixth Order Model (RPM)	68
3.6.1	Controls-Fixed Eigenvalues of TRBM with Hingeless Rotor	71
3.6.2	Open Loop Low Frequency Eigenvectors for Tenth Order Hypothetical Hingeless-Rotored Model (TRBM)	72
3.6.3	Open Loop High Frequency Eigenvectors for Hingeless Rotor TRBM	73
3.6.4	Open Loop Low Frequency Eigenvectors for Eighth Order Hingeless Rotor Model (RRM)	74
3.6.5	Open Loop Low Frequency Eigenvectors for Sixth Order Hingeless Rotor Model (RPM)	75
4.6.1	Typical Output of OPTSYS	111
5.1.1	Schematic of TRBM, RRM, and RPM Controller Designs with Evaluation on the Respective Models	122
5.1.2	Schematic of TRBM, RRM, and RPM Controllers on TRBM	123
5.3.1	Mode Shapes Corresponding to the Three Low Frequency Closed Loop Eigenvalues	126
5.3.2	Mode Shapes Corresponding to Two High Frequency Closed Loop Eigenvalues (TRBM and RRM)	127
5.4.1	Comparison of Low Frequency Mode Shapes Using Full Order Feedback (TRBM Gains) with Mode Shapes Using Reduced Order Feedback (RRM and RPM Gains)	129

		Page
5.4.2	Comparison of High Frequency Mode Shapes Using Full Order Feedback (TRBM Gains) with Mode Shapes Using Reduced Order Feedback (RRM and RPM Gains)	130
5.6.1	Mode Shapes Corresponding to the Low Frequency Closed-Loop Eigenvalues (Hingeless Rotor)	138
5.6.2	Comparison of Low Frequency Mode Shapes Using Full Order Feedback (TRBM Gains) with Mode Shapes Using Reduced Order Feedback (RRM and RPM Gains)--(Hingeless Rotor Model)	140
5.6.3	Rotor Modes with Gains from TRBM, RRM, and RPM	141
6.3.1	Correlation of Stability Regimes with Lowis (LO1) . . .	148
6.3.2	Correlation with Reverse Flow Stability Regimes with Lowis (LO1)	149
6.3.3	Stability Regimes with Continuous Representation of Reverse Flow	151
6.3.4	Variation of $Re(s_\beta)$ with μ, $\gamma' = 11.2$	152
6.3.5	Variation of $Re(s_\beta)$ with μ, $\gamma = 11.2$	152
6.4.1	Effect of Velocity on $Re(s_\beta)$: $\bar{K}_\beta = \beta_o = 0$	156
6.4.2	Effect of Velocity on $Re(s_\beta)$ and $Re(s_\zeta)$: $\bar{K}_\beta = 0$.	157
6.4.3	Effect of Velocity on $Re(s_\beta)$ and $Re(s_\zeta)$: $\bar{K}_\beta = -.4$.	158
6.4.4	Effect of Velocity on $Re(s_\beta)$ and $Re(s_\zeta)$: $\bar{K}_\beta = +.4$.	159
C-1	Loci of Characteristic Multipliers	181
C-2	Characteristic Exponent Root Locus of 1/2 per Rev Transition	182
D-1	Blade Stability Program Sequencing	185

LIST OF TABLES

Table		Page
2.2.1	Blade Axes	9
2.3.1	Aerodynamic Coefficients	24
3.1.1	Flight Test Hover Derivatives for Sikorsky S-61	34
3.4.1	Elements of 10X10 F Matrix and 10X2 G Matrix for S-61 Sikorsky Helicopter (TRBM)	54
3.4.2	Comparison of Roots of 10th Order Hover Model--TRBM and Ref. C01	56
3.4.3	Relative Mode Shapes of 10th Order Open Loop Eigenvectors	59
3.5.1	Representation of Blade Dynamics	64
3.5.2	Elements of 8X8 F Matrix and 8X2 G Matrix for Rotor Rate Model (RRM)	65
3.5.3	Elements of 6X6 F Matrix and 6X2 G Matrix for Rotor Position Model (RPM)	66
3.5.4	Effect of Reduced Order Rotor Approximations on Hover Characteristic Frequencies	69
3.5.5	Open Loop Eigenvectors for RRM and RPM	69
3.6.1	Comparison of Hypothetical Hingeless Rotored TRBM Characteristic Frequencies with Reduced Rotor Model Frequencies	76
4.6.1	OPTSYS Input Requirements and Output Options	110
5.2.1	Control Gains for TRBM, RRM, RPM ($A_{\theta_F} = A_{\varphi_F} = A_{\bar{u}} = A_{\bar{v}} = B_{\theta_C} = B_{\theta_S} = 1.0$)	124
5.3.1	Closed Loop Eigenvalues of TRBM, RRM, and RPM	125
5.4.1	Closed Loop Eigenvalues of TRBM with RRM Controller and RPM Controller	128
5.4.2	Effects of Weighting Factors on Feedback Gains of the RPM Controller	132
5.4.3	Closed Loop Eigenvalues of the Sixth Order RRM as the Fuselage Attitude Weighting Factors of the Quadratic Cost are Increased	132
5.4.4	Effect of Weighting Factors in Quadratic Cost on Closed Loop Eigenvalues Using RPM Controller on Tenth Order Model	133
5.4.5	TRBM and RRM Feedback Gains for $A_{\theta_F} = A_{\varphi_F} = 100$	133

		Page
5.4.6	Closed Loop Eigenvalues with $A_{\theta_F} = A_{\varphi_F} = 100$	134
5.5.1	Root Mean Square Vehicle Response to a Random Lateral Rotor Torque Using Three Different Controller Designs	136
5.6.1	Control Gains for Hingeless Rotor TRBM, RRM, RPM . . .	137
5.6.2	Closed-Loop Eigenvalues of TRBM, RRM, and RPM (Hingeless Rotor Model)	139
5.6.3	Closed Loop Eigenvalues of TRBM with TRBM, RRM, and RPM Controllers (Hingeless Rotor)	139
5.6.4	Root Mean Square Vehicle Response to a Random Lateral Rotor Torque Using Three Different Hingeless Rotor Controller Designs	142
6.1.1	Floquet Stability Program Output	146
6.4.1	Hypothetical Rotor System Parameters	155
7.1	Topic Summaries by Chapter	161

SYMBOLS

Notation

Unlisted symbols are defined in the chapter where they appear.

English

a	lift curve slope (Ch. 2 and Ch. 3)
$\vec{a}_F^{O-I}$	acceleration of shaft plane relative to inertial frame with scalar value a_F^{O-I} (Ch. 2, 3)
A	matrix of state weighting coefficients in quadratic cost. In Chapter 5, $A = \text{diag}\{0,0,0,0, A_{\theta_F}, A_{\phi_F}, 0,0, A_{\bar{u}}, A_{\bar{v}}\}$.
$\mathcal{A}$	coefficient matrix of the $n(n+1)/2$ distinct elements of the covariance matrix (Ch. 4)
B	· blade tip loss factor (Ch. 2,6) · matrix of control weighting coefficients in quadratic cost (Ch. 4,5). In Chapter 5, $B = \text{diag}\{B_{\theta_c}, B_{\theta_s}\}$ · matrix of principal eigenvalues of C (Appendix C)
$\mathcal{B}$	real block diagonal matrix of eigenvalues [Eq. (4.4.5)]
c	blade chord [ft] (Ch. 2,3)
c_{do}	blade element profile drag coefficient (Ch. 4)
C	· optimal feedback gain, $C = -B^{-1}G^T(S_B)_{SS}$, (Ch. 4,5) · transition matrix at end of one rotor revolution, $\phi(T,t_o)$ (Appendix C)
$c_\beta^\beta \ldots c_{\beta\zeta}^\beta$ $c_\zeta^\zeta \ldots c_{\beta\zeta}^\zeta$	periodic coefficients of blade equations, (Ch. 2)
C_T	rotor thrust coefficient, $C_T = T/\rho\pi R^2(\Omega R)^2$, (Ch. 2,3)
CM	center of mass (Ch. 2,3,5)

$\mathcal{C}$	transformation from state to output for follower problem (Ch. 4)
$d\mathfrak{D}$	differential drag over a differential span of blade (Ch. 3)
$d\mathfrak{L}$	differential lift over a differential span of blade (Ch. 3)
dL	differential force normal to plane of rotation (Fig. 3.3.2)
dS	differential force in plane of rotation (Fig. 3.3.2)
D	solution matrix of time varying covariance equation (Ch. 4)
$\mathfrak{D}$	elemental profile drag force on blade (Ch. 3)
$e, \bar{e}$	$\bar{e} = e/R$, where e is the offset distance of the flapping hinge from the shaft (Ch. 2,3)
e_β, $\bar{e}_\beta$	equivalent offset distance for first flapping mode ($e_\beta = e$ for an articulated rotor); $\bar{e}_\beta = e_\beta/R$ (Ch. 2,3)
e_ζ, $\bar{e}_\zeta$	equivalent offset distance of a mode of first inplane lead-lag mode from the shaft; $\bar{e}_\zeta = e_\zeta/R$ (Ch. 2,3)
E	a solution matrix of the time-varying Riccati equation solution (Ch. 4)
$f^c_{11}, f^c_{12} \ldots f^c_{nn}$	elements of matrix F_c (Sec. 4.4)
F	open loop (controls-fixed) dynamics matrix of a system (Ch. 4,5)
F_c	closed loop dynamics matrix, F-GC (Sec. 4.4)
F_{x_F}, F_{y_F}	rotor inplane force resolved into fuselage coordinates (Ch. 3)
F_s	inertial shear force on fuselage from blade (Ch. 3)
$\mathcal{F}$	coefficient matrix of homogeneous continuous Euler-Lagrange equations (Ch. 4)
g	acceleration of gravity, 32.2 ft/sec^2
G	control distribution matrix of continuous system (Ch. 4)

$h, \bar{h}$	$\bar{h} = h/R$ where h is the height of rotor hub above vehicle CM (Ch. 3)
H	. measurement, or scaling, matrix of observations (Ch. 4)
	· angular momentum (Appendix A)
$\mathcal{H}$	scalar Hamiltonian (Ch. 4)
$\bar{\bar{I}}$	moment of inertia tensor (Appendix A)
I_{xx}	blade inertia about feathering axes (Appendix A, Ch. 2)
I_{yy}	blade flapping inertia (from e to R) (Appendix A, Ch. 2)
I_{zz}	blade inplane inertia (from e to R) (Appendix A, Ch. 2)
I_{xy}	blade product of inertia in blade x-y plane (Appendix A, Ch. 2)
I_β	equivalent blade flapping inertia (Ch. 2)
I_{θ_F}	fuselage pitch inertia (Ch. 3,4)
$I_{\theta'_F}$	equivalent fuselage pitch inertia for offset hinged rotor
I_{ϕ_F}	fuselage roll inertia
$I_{\phi'_F}$	equivalent fuselage roll inertia for offset hinged rotor
I_n	$n \times n$ identity matrix
I_{ψ_F}	yaw inertia of vehicle (Table 3.1.1)
$\hat{i}_{(\cdot)}, \hat{j}_{(\cdot)}, \hat{k}_{(\cdot)}$	unit vector triad in (B) (ζ), (S) or (F) plane
J	quadratic cost (Ch. 4,5)
$\bar{J}$	J with adjoined constraints (Ch. 4)
$\tilde{J}$	symplectic transformation matrix, $J = \begin{pmatrix} 0 & I_n \\ -I_n & 0 \end{pmatrix}$ (Appendix B)

K_v	induced velocity correction for forward flight [Eq. (2.3.6)]
K	Kalman filter gain, PH^TR^{-1} (Ch. 4)
$K_{\theta_R} \ldots K_{\bar{v}}$	optimal nondimensionalized feedback gains for lateral cyclic pitch [Eq. (5.1.1) and Ch. 5]
K_β	effective blade flapping torsional spring (Appendix A and Ch. 2)
$\bar{K}_\beta$	blade position feedback gain to blade pitch (rad/rad) [Eq. (6.4.1)]
$\bar{\bar{K}}_\beta$	blade rate feedback gain to blade pitch (rad/rad/sec) [Eq. (6.4.1)]
K_ζ	effective blade lead-lag torsional spring (Appendix A and Ch. 2)
K	real eigenvector matrix [Eq. (4.5.4)]
ℓ	lift of blade element normal to relative wind (Ch. 2,3)
L	total blade lift normal to reference plane (Ch. 2,3)
L_β	component of L normal to blade xy plane (Ch.2)
L_ζ	component of L normal to blade xz plane (Ch. 2)
$L_{(\cdot)}$	fuselage yaw moment derivative, $\partial L/\partial(\cdot)$ (Table 3.1.1)
$(L_{\theta_R} \ldots L_v)$	optimal nondimensionalized gains for longitudinal cyclic [Eq. (5.1.2) and Ch. 5]
m_v	mass of vehicle (Ch. 2,3)
M_B	mass of blade (Ch. 2)
M	relative magnitude of eigenvectors, $0 < M \leq 1$ (Ch. 3 and 5)
M_x, M_y, M_z	total airload moments about rotor blade x,y,z axes
$(M_{K_\beta})_{\theta_F}$, $(M_{K_\beta})_{\phi_F}$	rotor pitch and roll moments on fuselage from flapping elasticity [Eqs. (3.36) and (3.37)]

$(M_s)_{\theta_F}$, $(M_s)_{\phi_F}$ — rotor pitch and roll moments on fuselage from dynamic (d'Alembert) shear force at hinge offset [Eqs. (3.3.12) and (3.3.13)]

$(M_A)_{\theta_F}$, $(M_A)_{\phi_F}$ — rotor pitch and roll moments on fuselage from airload shear forces at hinge offset [Eqs. (3.3.17) and (3.3.18)]

$(M_e)_{\theta_F}$, $(M_e)_{\phi_F}$ — total rotor moment, sum of M_s and M_A [Eqs. (3.3.19) and (3.3.20)]

$(M_H)_{\theta_F}$, $(M_H)_{\phi_F}$ — fuselage moment from inplane rotor forces [Eqs. (3.3.29) and (3.3.30)]

M_{θ_F}, M_{ϕ_F} — total fuselage pitch and roll moment, in fuselage axes, sum of M_{K_β}, M_e, and M_H [Eqs. (3.3.31) and (3.3.32)]

M_β — flapping moment on blade (Ch. 2)

M_ζ — inplane lag moment on blade (Ch. 2)

$M_{(\cdot)}$ — fuselage pitch moment derivative, $\partial M/\partial(\cdot)$ (Table 3.3.1)

n — order of F, the system dynamics

N_B — number of rotor blades

$N_{(\cdot)}$ — fuselage roll moment derivative, $\partial N/\partial(\cdot)$ (Table 3.3.1)

p_i — real part of T_i (Ch. 4)

p_R — rotor roll rate, ϕ_R

p_F — fuselage roll rate, ϕ_F

P — covariance matrix (Ch. 4)

P' — normalized covariance (Ch. 4)

P_f — error covariance, $E\{[x(t_f) - x_f][x(t_f) - x_f]^T\}$

P_o — error covariance, $E\{[x(t_o) - x_o][x(t_o) - x_o]^T\}$

P_F — forward estimate error covariance matrix

P_B — backward estimate error covariance matrix

P_S — error covariance of smoothed estimate

q	scalar disturbance covariance (Ch. 4)
q_i	complex part of T_i (Ch. 4)
q_R	rotor roll rate, $\dot{\phi}_R$ (Ch. 3, 5)
q_F	fuselage pitch rate, $\dot{\phi}_F$ (Ch. 3,5)
Q	covariance of system random disturbances (Ch, 4,5)
Q'	normalized covariance of system random disturbances (Ch. 4)
r	. distance from blade element to shaft (Ch. 2,3)
	· scalar measurement noise covariance (Ch. 4)
R	· rotor radius (Ch. 2,3)
	· measurement noise covariance (Ch. 4)
RRM	rotor position model (Ch. 3,4,5)
RPM	rotor position model (Ch. 3,4,5)
s_i	an eigenvalue of $\mathcal{F}$ (Ch. 3,4,5)
$(s_i)_+$	s_i with real part greater than zero (Ch. 4)
$(s_i)_-$	s_i with real part less than zero (Ch. 4)
s_β	an eigenvalue of $\Phi(T,t_o)$ associated with flapping degree of freedom (Ch. 6, Appendix A)
s_ζ	an eigenvalue of $\Phi(T,t_o)$ associated with inplane lead-lag degree of freedom
S	· inplane force on a blade element
	· solution to Riccati equation of follower and information problems (Ch. 4,5)
S_o	initial weighting matrix on $x(t_o)$ [Eq. (4.2.3)]
S_f	final weighting matrix on $x(t_f)$ [Eq. (4.2.3)]
S_+	forward solution of control Riccati equation [Eq. (4.3.12)]
S_-	backward solution of control Riccati equation [Eq. (4.3.11)]

S_F	forward weighting matrix of control Riccati equation [Eq. (4.2.23a)]
S_B	backward weighting matrix of control Riccati equation [Eq. (4.2.15a)]
$\mathcal{S}$	$2n \times 2n$ matrix of $\mathcal{J}$ eigenvalues [Eq. (4.3.5)]
$\mathcal{S}_+$	$n \times n$ matrix of $\mathcal{S}$ whose real parts are greater than zero [Eq. (4.3.4)]
$\mathcal{S}_-$	$n \times n$ matrix of $\mathcal{S}$ whose real parts are less than zero [Eq. (4.3.4)]
t	time (t_o, initial time; t_f, final time; t_1, intermediate time) (Ch. 4)
Δt	time step of quadrature solution of Riccati equation (Ch. 4)
T	· rotor thrust (Ch. 2,3,6)
	· complex eigenvector matrix of $\mathcal{J}$ (Ch. 4)
T_i	i^{th} column of T (Ch. 4)
T_-	eigenvectors of T corresponding to $(s_i)_+$
T_+	eigenvectors of T corresponding to $(s_i)_-$
T_R	lowest common period of rotor frequency (Appendix C)
$T_{(\cdot)/(*)}$	matrix of transformation from frame $(\cdot)$ to frame $(*)$ (Appendix A)
TRBM	two rigid body model (Ch. 3,5)
u	control variable [Eq. (4.2.33)] or external disturbance [Eq. (4.2.2)]
u_I	fuselage longitudinal velocity components in inertial axes (Fig. 4.2.2)
u_F	fuselage longitudinal velocity in fuselage axes (Ch. 3)
$\bar{u}$	· nondimensionalized fuselage velocity, $u_F/\Omega R$
	· estimate of disturbance forces (Ch. 4)

U_R, U_T, U_P	relative wind velocities at blade in radial, tangential, and normal directions (Ch. 2)
U	total relative wind, $U = \sqrt{U_P^2 + U_P^2 + U_R^2}$ (Ch. 2,3)
u_R, u_T, u_P	nondimensionalized relative velocities, $U_R/\Omega R$, $U_T/\Omega R$, $U_P/\Omega R$
v	measurement noise (Ch. 4)
v_I	fuselage lateral velocity in inertial axes (Fig. 4.2.2)
v_F	fuselage lateral velocity in fuselage axes (Fig. 4.2.3)
$\bar{v}$	nondimensionalized fuselage velocity, $v_F/\Omega R$
V	· velocity of air far from rotor (Ch. 2)
	· velocity (Appendix A)
V'	total velocity through rotor [Eq. (2.3.2)]
x	· nondimensionalized span distance, r/R (Ch. 2)
	· state of system (Ch. 4)
$x_+^{(i)}$	i^{th} column of X_+
$x_-^{(i)}$	i^{th} column of X_-
x_o	pre-flight estimate of initial state, $x(t_o)$ [Eq. (4.2.1)]
x_f	independent estimate of final state, $x(t_f)$ [Eq. (4.2.1)]
$x(t_o)$	initial state (Ch. 4)
$x(t_f)$	final state (Ch. 4)
$\hat{x}_F$	forward Kalman filter estimate [Eq. (4.2.14)]
$\hat{x}_B$	backward Kalman filter estimate [Eq. (4.2.23)]

$x_\beta, y_\beta, z_\beta$ x_R, y_R, z_R x_S, y_S, z_S $x_\zeta, y_\zeta, z_\zeta$	coordinates in β, R, ζ, S frames
$X(t)$	$n \times n$ matrix formed from the first n rows and columns of the $2n \times 2n$ transition matrix of $\mathcal{F}$ (Ch. 4)
$X_{(\cdot)}$	longitudinal force derivative, $\partial X(\cdot)/\partial(\cdot)$ (Table 3.1.1)
X_+	first n rows of T_+
X_-	first n rows of T_-
X	covariance of state (Ch. 4)
$\hat{X}$	covariance of estimate (Ch. 4)
y	desired system output history [Eq. (4.2.33)]
y_B	backward information variable [Eq. (4.2.23a)]
y_F	forward information variable [Eq. (4.2.15a)]
$Y_{(\cdot)}$	lateral force derivative, $\partial Y/\partial(\cdot)$ (Table 3.1.1)
Y	$GB^{-1}G^T$ for smoother; GQG^T for follower (Ch. 4)
w	frequency (Ch. 4)
w_F	vertical fuselage velocity in fuselage axes (Ch. 2,3)
w_I	vertical fuselage velocity in inertial axes (Ch. 2,3)
w	random disturbance on system dynamics (Ch. 4)
W	$\mathcal{C}^T A \mathcal{C}$ for follower; $H^T R^{-1} H$ for smoother (Ch. 4)
z	· measurements of state x (Ch. 4) · $[x \ \lambda]^T$ [Eq. (4.5.1), Appendix B]

z'	normalized z [Eq. (4.5.2)]
$Z_{(\cdot)}$	vertical force derivative, $\partial Z/\partial(\cdot)$, (Table 3.1.1)

Greek

α	blade angle of attack (Ch. 2)
α_R	rotor angle of attack (Ch. 2)
α^*	generalized rotor angle of attack (Ch. 3)
β	blade flapping angle (Ch. 2,3,5,6)
β_o	blade coning angle (Ch. 2,6)
$\delta(t-\tau)$	impulse function (Kronecker's delta) (Ch. 4)
γ	blade Lock number, $\gamma = \rho a c R^4/I_\beta$
γ'	$\gamma/8$
Γ	distribution matrix of system random disturbances (Ch. 4)
ζ	· inplane blade angular deflection, positive in $+\psi$ direction (Ch. 2,3) · damping ratio (Ch. 4)
ζ'	real part of eigenvalues of example in Section 4.3
η	chordwise distance of blade element from feathering axes (Ch. 2)
η_o	bases vector of $\mathcal{F}$ [Eq. (4.7.2)]
θ	blade rotation angle about x_B axis
θ_c	lateral } cyclic pitch control
θ_s	longitudinal } cyclic pitch control
θ_F	fuselage pitch angle
θ_R	rotor pitch angle

θ_o	collective pitch angle
Θ_{con}	$[\theta_c \ \theta_s]^T$
λ	rotor inflow ratio (Ch. 2,3)
$\lambda(t)$	Lagrange multiplier (Ch. 4,5)
$\lambda_+^{(i)}$	i^{th} column of Λ_+
$\lambda_-^{(i)}$	i^{th} column of Λ_-
$\Lambda(t)$	$n \times n$ matrix formed from rows $n+1$ through $2n$ and first n columns of the $2n \times 2n$ transition matrix of $\mathcal{F}$ (Ch. 4)
Λ_+	second n rows of T_+
Λ_-	second n rows of T_-
μ	rotor advance ratio [Eq. (2.3.7)]
μ_x, μ_y	longitudinal and lateral velocities of rotor hub, divided by ΩR [Eqs. (3.3.33) and (3.3.34)]
$\bar{\nu}_o$	induced velocity in hovering [Eq. (2.3.1)]
ν_i	induced velocity in forward flight [Eq. (2.3.5)]
ξ	spanwise length variable of flapping section of blade (Ch. 2,3)
ξ_o	bases vector of $\mathcal{F}$ [Eq. (4.7.2)]
ρ	air density
ρ_B	blade mass/unit length (where $\rho_B R$ = blade mass, M_B)
σ	rotor solidity, $\sigma = N_B c/\pi R$
σ_i	real part of s_i
τ	sample time of a random variable for definition of age variable, $\delta(t-\tau)$ (Ch. 4)
ϕ	blade inflow angle, $\tan^{-1} u_p/u_T$ (Ch. 2,3)
ϕ_F	fuselage roll angle
ϕ_R	rotor roll angle

$\Phi(t,t_o)$	transition matrix (Appendix C)
ψ	rotor blade azimuth angle, positive along z_S, measured from downwind
ψ_F	fuselage yaw angle, positive along z_F
ω_β	blade flapping frequency in rotating coordinates for a spring restrained blade with no offset ($\bar{e} = 0$) [rad-sec]
ω_B	blade flapping frequency in rotating coordinates for spring restrained blade with offset [rad-sec]
ω_F	rotor blade frequency in nonrotating coordinates for a rotor with no offset hinges [rad-sec]
ω_R	rotor blade frequency in nonrotating coordinates for rotor with offset hinges [rad-sec]
ω_i	imaginary part of s_i (Ch. 4)
Ω	with no subscripts, Ω is the rotor angular velocity [rad-sec], otherwise Ω is a generalized angular velocity

Subscripts

B	coordinatized in blade frame
F	coordinatized in fuselage frame
I	inertial
$(\ )_{CM}$	blade center of mass
$(\ )_o$	trim value (Ch. 2,3,6)
$(\ )_{ss}$	steady state value of solution

Special Operations

$( )$	vector
$\bar{( )}$	nondimensionalized variable (except as noted)
$\bar{\bar{( )}}$	tensor
$\det\|\cdot\|$	determinant of $\cdot$
$\mathrm{Im}( )$	imaginary part of a complex variable
$\mathrm{Re}( )$	real part of a complex variable
$\otimes$	Kronecker product (Section 4.4)

• Let Θ be a vector. The symbol

$$\Theta_{\mathbf{c}}^{\mathbf{a-b}}\mathbf{q}$$

means:

let a, b, or c be F, S, B or R
(F = fuselage frame; S = shaft frame; B = blade frame; R = rotor frame)

(1) a-b requires Θ is the rate of axis frame a to axis frame b

(2) q is the component of Θ^{a-b} along the q axis of the reference frame

(3) c requires that Θ^{a-b} is a column vector coordinatized in frame c.

• Let Ω be the angular velocity

$$\Omega = \begin{pmatrix} \omega_x \\ \omega_y \\ \omega_z \end{pmatrix}$$

then

$$(\Omega\, x)$$

is equivalent to the matrix

$$\begin{bmatrix} 0 & -\omega_z & \omega_y \\ \omega_z & 0 & -\omega_x \\ -\omega_y & \omega_x & 0 \end{bmatrix}$$

- The derivative for a quantity x, x', means

$$(x)' = \frac{1}{\Omega} \frac{dx}{dt}$$

ACKNOWLEDGEMENT

I wish to thank my advisor, Professor Arthur E. Bryson, for his guidance, criticisms, and encouragement in this research effort. His insight into complex problems and ability to raise counterexamples helped the avoidance of several possible pitfalls.

The contributions of Professor Robert H. Cannon in the early phases of this work provided a firm foundation upon which many of the final results rest.

Professor Daniel B. DeBra and Professor Gene F. Franklin have made valuable suggestions which were helpful in the accomplishment and final documentation of the task. The many conversations with Professor Benjamin O. Lange and Professor John V. Breakwell certainly facilitated the development of some of the computational aspects of the problem.

Particular gratitude is expressed for the financial support from the U. S. Army Mobility Research and Development Command, Ames Directorate, under Contract NAS-2-5143. More specifically, the encouragement of Mr. Paul Yaggy and Mr. Dean Borgman of the contracting agency is deeply appreciated.

The author is indebted to Mrs. Diana Shull and Mrs. Connie Calica for their careful typing of a difficult manuscript.

Finally, the support and dedication of my wife, Donna, has proved invaluable.

This work is dedicated to Mandy.

Chapter I

INTRODUCTION

1.1 Statement and Discussion of Problem

The need for VTOL (Vertical Take-Off and Landing) aircraft is becoming more evident as new transportation requirements are established. As an element of an inter-urban and intra-urban network of STOL (Short Take-Off and Landing) aircraft and ground transit, the VTOL aircraft offers small terminal areas and random access. In addition, a particular class of VTOL aircraft, the rotary-wing type, offers efficient hover capability and reduced noise and downwash effects, as well as the inherent power safety factor of autorotation.

However, experience with rotary-wing vehicles, notably helicopters, has demonstrated many problems in achieving the promise of the concept. Vibration, rotor stability, handling qualities, high operating cost, and low speed are frequently cited as the principal disadvantages. Newer applications of the concept in the form of the winged compound vehicles, high speed stowed rotor designs, and the tilt rotor configurations, indicate possible elimination of some of these disadvantages.

Rotor dynamics and rotor interaction with the fuselage are common to all rotary-wing type vehicles. This research has been directed to the problem of controlling the rotor-fuselage combination. Two flight regimes are of particular importance for rotary-wing VTOL aircraft.

The first of these is the hover regime. The ability to hover over a particular point in the presence of winds is a requirement common to all rotary-wing aircraft. The primary objective of a hover control system is to reduce the work load on a pilot to avoid fatigue, but extremely precise hovering requirements will exceed even pilot control capability. Although such control systems have been designed in the past, they are gain limited by possible rotor instability. These systems rely only on fuselage based measurements and thus disregard any stabilizing information which might be provided by rotor measurements.

The second flight situation of interest is the high speed regime. The principal problem here is rotor instability due to the periodic airload excitation of the blade bending modes. Even if the blade oscillations are stable, they cause severe blade loading as aerodynamic damping decreases at higher speeds.

Satisfactory flying and vibration characteristics in these two regimes may be approached by passive design, wherein the rotor and fuselage design parameters are varied to achieve the desired end, or by active control, where automatic sensing and control devices augment the aircraft capabilities.

It is assumed in this work that the vehicle has been specified, and that an active control system is to be designed which minimizes rotor plane and fuselage motions in hover in the presence of random lateral and longitudinal gusts. The first requirement for such a design is an appropriate model of the rotor blade dynamics and the fuselage dynamics. This modeling requirement is one of the most important aspects of the entire problem. A "complete" analytical model of rotary-wing behavior is intractable. Hence, several classes of models are used, depending on the phenomenon of interest. A given control problem must be carefully formulated within the limits of the particular flight regime of interest.

Even with the simplified models used here, a difficult control synthesis problem still exists. Not only is the model of high order, it has a wide separation of characteristic frequencies. The high-order nature of the problem is tractable using the technique of multivariable quadratic synthesis. However, the wide separation of characteristic frequencies (rotor vs. fuselage) makes quadratic synthesis by integration of the matrix Riccati equation a time-consuming and expensive process. In addition, solution by this method gives little information about the response of the closed loop system without more calculation.

In summary, the basic problems to be treated in this thesis will be:

a) formulating mathematical models of coupled rotor-fuselage dynamics, and

b) designing control systems for these models.

1.2 Previous Studies and Related Results

The dynamics of rotary-wing VTOL aircraft have been a primary concern of many researchers, and only the efforts related to the particular emphasis of this thesis are described.

The analysis and design of helicopters in hover appears in the literature since before 1940. Of the early efforts, the results of Hohenemser (HO1) and Miller (MI1) are the most important in terms of modern analysis. The concept of the "quasi-steady" approximation was the basic contribution of Hohenemser. Although originally postulated in the late 1930's, this approximation achieved widespread use only after it was published in this country in 1948, and still serves as the basis of many analyses. The work of Miller, published in 1947, quantified the interaction of rotor and fuselage dynamics and introduced the concept of approximating the rotor by a first order rate model instead of Hohenemser's quasi-steady model.

In applying their results, the reduced order assumptions can lead to rotor instability in high gain control systems. Miller (MI2) and Ellis (EL1) showed such was the case for articulated rotored systems, and Shupe (SH2) demonstrated a similar result for hingeless rotored vehicles. All of these results were obtained using hover models in which the lateral and longitudinal modes were assumed decoupled.

In spite of this, fuselage-only models are still used for the design and analysis of modern hover control systems. Buffum and Robertson (BU1) discuss a hover control which neglects rotor dynamics. Narendra and Murphy (NA1) perform a quadratic control synthesis for a hover controller which is based on a coupled longitudinal-lateral fuselage model, but again neglected an explicit rotor model. Similarly, Crossley and Porter (CR2) designed a control system using pole assignment. Although GR1 used multivariable design with a simple rotor approximation for a high speed vehicle, the high speed allowed longitudinal-lateral decoupling and a "sub-optimal" design was done by simply deleting rotor feedback channels.

The design of controls for rotary-wing VTOL vehicles at high speeds is more difficult than for hover because the system dynamics have, so far, defied a conclusive analytical formulation. However, as speed of the vehicle increases, the aerodynamic forces on the fuselage increase and the rotor control problem depends increasingly on the effects of the feedback of fuselage states which respond to gusts. This necessitates the treatments of the periodic phenomena discussed in Section 1.1. Early studies by Horvay (HO4) and Shutler and Jones (SH1) treated simple high speed flapping instability by reducing the flapping equation to a Mathieu type equation and expanding the solution in terms of Mathieu functions. The same simple flapping equation, with an elementary consideration of reverse flow, was treated by Lowis (LO1). Lowis used Floquet theory to establish stability boundaries. The results of Horvay, Shutler, and Lowis were extended by Hohenemser and Peters to a four-bladed flapping rotor (HO3). This latter work solved the problem posed by Sissingh (SI1) by Floquet theory.

Concern for coupled flapping-inplane oscillation stability was expressed by Young (YO1) in a controversial 1965 paper. Work by Stammers (ST1, ST2), Duwalt and Daughaday (DU2) and Crimi (CR1) also used Floquet theory for solution of similar models.

The modern computational Floquet solution is based on finding the eigenvalues of a high order matrix. Efficient determination of such high order systems was made possible by the QR algorithm of Francis (FR3). This algorithm also plays an important role in the quadratic synthesis program of this thesis.

1.3 Organization of This Thesis

Chapter 2 is an introduction to rotor dynamics and quasi-steady rotor aerodynamics. Most of this chapter is also found in HA1, but typographical errors have been corrected and only the most important equations retained. The nonlinear equations of the coupled flap-lag-pitch motions of a non-flexible blade with offset, at arbitrary speed, are derived. By assumptions on the blade airloads, principally those of the quasi-steady state blade aerodynamics, these equations are re-

duced to the relations for flap-lag oscillations. The airload coefficient tables of Sissingh are extended to include flap-lag coupling and a new computational approach is suggested for handling reverse flow.

In Chapter 3, the rotor equations of Chapter 2 are specialized to the hover condition. A fuselage hover model is developed, and fuselage-rotor equations are derived in a fuselage-fixed frame as opposed to the inertial frame used in Miller (MI1). The rotor is treated as a rigid body, with pitch and roll degrees of freedom relative to the fuselage. This model is then used to determine the controls-fixed eigenvalues and eigenvectors for a typical vehicle with a fully articulated rotor, and for a hypothetical vehicle with a hingeless rotor, the effect of reduced-order rotor approximations on the controls-fixed response is determined by finding the eigensystem of an eighth order fuselage-rotor rate model and a sixth order fuselage-rotor position model.

Chapter 4 presents the theory for determining the regulator control gains for a constant coefficient continuous system, such as that of the hover controller. The theory of the modal analysis of the Euler-Lagrange equations is derived and application to the smoothing and filtering problems is given. Of particular note is the solution of the steady state Riccati equation for the Kalman filter, as well as the regulator problem. The transient solutions of the Euler-Lagrange equations and the Riccati equation are also given. The solution of the general linear matrix equation for determining the controlled state RMS response is discussed. A computer program for designing high order control systems is formulated.

In Chapter 5, the equations of Chapter 3 and the computer program discussed in Chapter 4 are used to design and evaluate three hover controllers. These three hover controllers, designed using tenth order, eighth order, and sixth order models respectively, are compared with respect to the resulting closed loop eigensystem and steady state response to a common random input.

Finally, in Chapter 4, the equations of Chapter 2 are examined by multivariable Floquet theory (Appendix C). The study of simple flapping

high speed instability with reverse flow extends the results of Lowis (L01). The flap-lag equations are also investigated to illustrate the effect of rotor position feedback on blade stability.

Chapter 7 presents the principal conclusions of this thesis.

1.4 Summary of Contributions

The principal contributions of this work may be grouped into three main categories:

A. Analytical Models and Assumptions

- Nonlinear dynamic equations for pitch-flap-lag oscillations (Chapter 2)
- Periodic linear and nonlinear aerodynamic coefficients for flap-lag coupling (Chapter 2);
- Hover equations of motion (with explicit treatment of first harmonic rotor dynamics), referenced to fuselage fixed coordinates (Chapter 3).

B. Computational Methods and Generalizations

- A computational algorithm for extending aero-coefficients to reverse flow (Chapter 2);
- A general method of reducing order of rotor dynamics which does not involve simply setting rotor derivatives to zero (Chapter 3);
- Transient and steady state solutions of the continuous constant coefficient Riccati equation using the eigensystem of the Euler-Lagrange equations of the regulator and smoothing problems (Chapter 4);
- Steady state gains for the forward and backward Kalman filters, deduced from the eigensystem of the smoothing problem (Chapter 4);
- Computational solutions of the general linear matrix equation and application to determine steady state RMS response of controlled system (Chapter 4).

C. Numerical Results

- Calculation of controls-fixed eigensystem for a typical fully articulated rotored helicopter and a hypothetical hingeless rotored helicopter;
- Comparison of effects of reduced order rotor models on the eigensystem of the complete model (Chapter 3);

- Design of tenth order hover controller for a typical fully articulated rotored helicopter and a hypothetical hingeless rotored helicopter. Comparison of performance of eighth order and sixth order hover controllers designed with lower order rotor models (Chapter 5);
- Evaluation of RMS state and control response of the tenth order, eighth order and sixth order controllers (Chapter 5);
- Determination of simple flapping stability regimes at high speed with continuous reverse flow representation (Chapter 6);
- Effect of rotor plane pitch and roll feedback on blade flap-lag stability (Chapter 6).

Chapter II

BLADE EQUATIONS OF MOTION

2.1 Introduction

A hinged, rigid blade is used as the model upon which to base stability and response calculations. This simplification is made for the following reasons:

a. Articulated rotors are common to many helicopters. For such rotors, the highest amplitude blade responses occur in the low frequency range around one oscillation per rotor revolution (one per rev.). The amplitude of the two per rev. mode is about ten per cent of the one per rev. amplitude. These low frequency flapping modes consist mostly of in-phase motion of all the blade elements which may be modeled by assuming a hinged, rigid blade.

b. For hingeless rotors, the first bending mode may be modeled as a rigid blade with a spring-loaded hinge offset from the center of rotation of the rotor. Several criteria for choosing the offset distance and the spring stiffness are discussed in YO1. At high speeds, hingeless rotors have a higher amplitude two per rev. response than articulated rotors, but the one per rev. response still predominates at low speeds. Hence, this approximation is useful around the hover regime.

c. The control systems of interest here are designed primarily on the basis of the rotor blade response in the low frequency range. Higher harmonic control is not a goal for this study, but is an important subject in itself. A complete design would include evaluation of the control on several of the rotor and fuselage higher harmonic responses. Even with these simplifications, the equations of motion are quite complex.

2.2 Representation of Blade Dynamics

Kinematics

Consider a rigid blade, attached with hinges at a distance e from

the center of rotation of the shaft, as shown in Fig. 2.2.1. The base reference axes X_s, Y_s and Z_s, are fixed with respect to a nonrotating shaft. The location and orientation of the rigid blade are specified by positive rotations as ordered in the following table.

Table 2.2.1. BLADE AXES

Rotation	Axis of Rotation	Angle	Axis System	Frame Symbol
			$\langle X_S, Y_S, Z_S \rangle$	S (shaft)
Azimuth	Z_S	ψ		
			$\langle X_R, Y_R, Z_R \rangle$	R (rotor)
Flapping	Y_R	$-\beta$		
			$\langle X_\beta, Y_\beta, Z_\beta \rangle$	
Inplane Lag	Z_β	ζ		
			$\langle X_\zeta, Y_\zeta, Z_\zeta \rangle$	L (inplane lag)
Pitch	X_ζ	θ		
			$\langle X_\theta, Y_\theta, Z_\theta \rangle$	B (blade)

The vehicle axes and coordinate convention is shown in Figs. 2.2.2 and 2.2.3. The shaft axis, Z_S, is parallel and oppositely directed to the fuselage fixed Z_F axis.

The direction cosine matrices corresponding to the rotations of Table 2.2.1 and the coordinates of Figs. 2.2.2 and 2.2.3 are used to resolve the velocities and angular rates into the rotating B frame. Appendix A lists the various transformations and vector equations for determining these quantities.

Blade Equations of Motion

The equations for flap-lag-pitch motions of a rigid hinged blade are derived in Appendix A. Several assumptions are used to simplify these equations for the purposes of this work:

(a) The rotor angular velocity is constant. (Most modern rotor systems are controlled automatically by engine controls to constant RPM.)

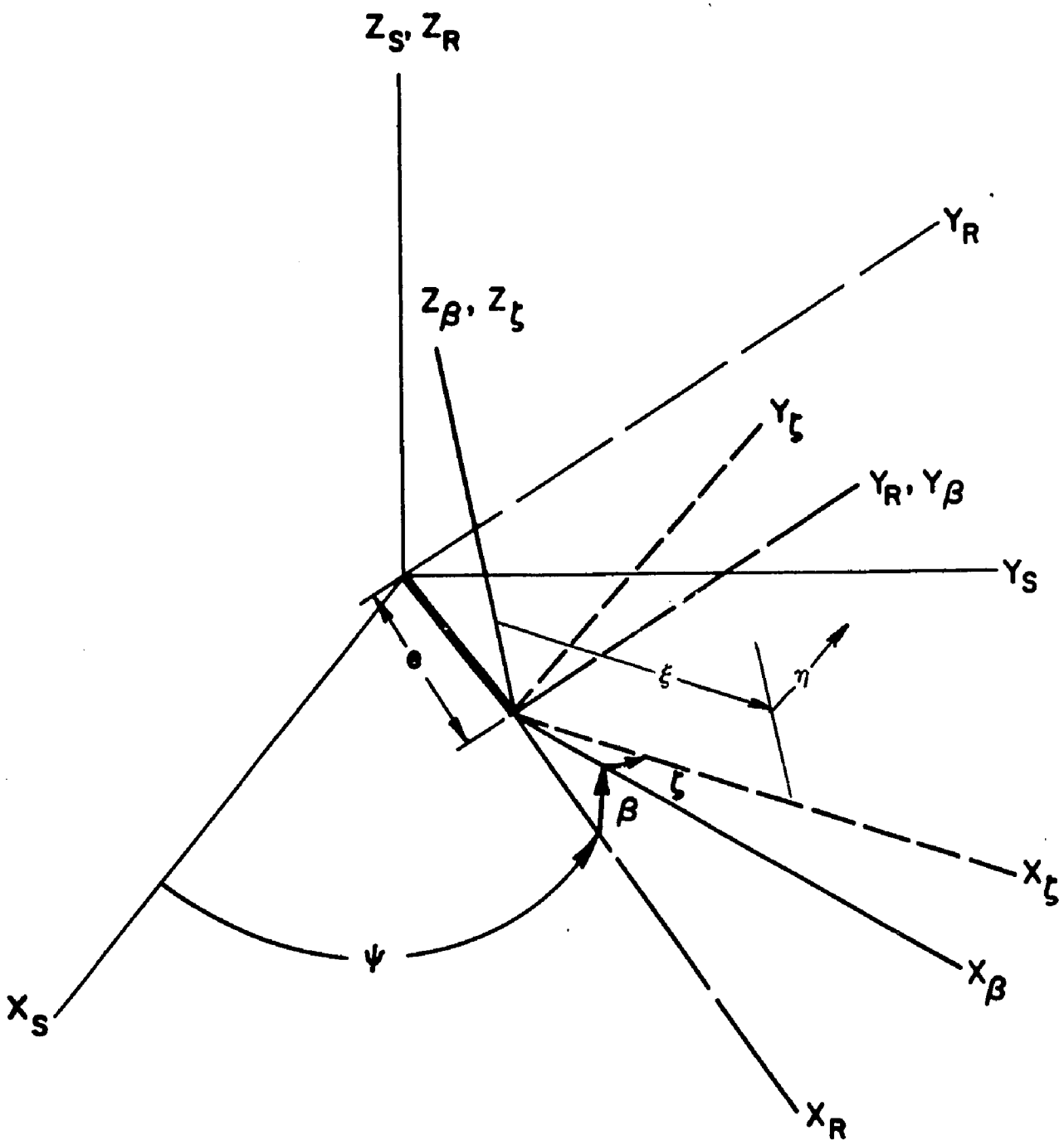

Fig. 2.2.1. BLADE AXIS SYSTEM

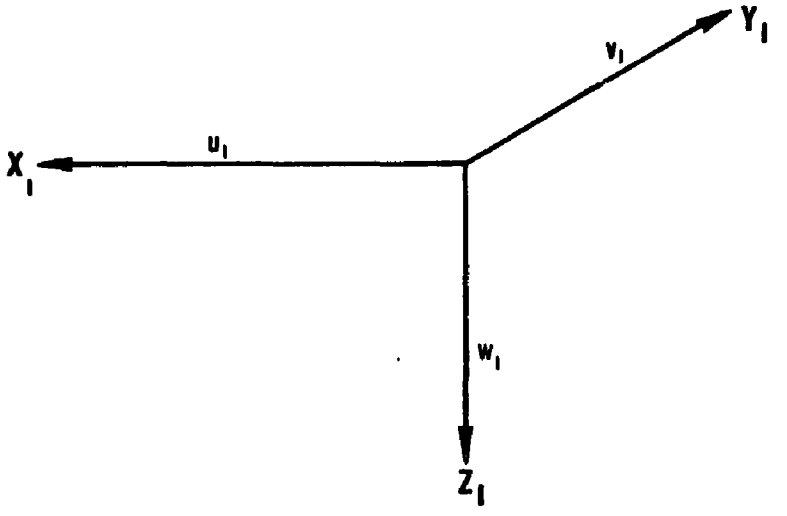

Fig. 2.2.2. INERTIAL REFERENCE AXES

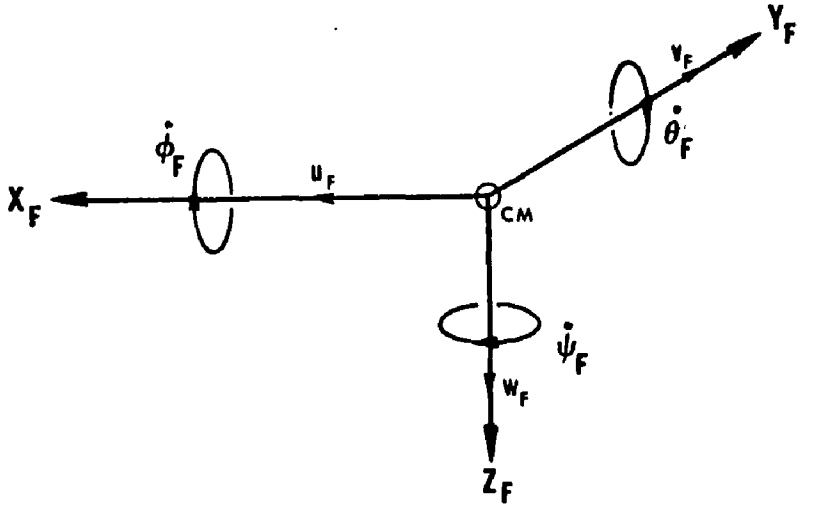

Fig. 2.2.3. VELOCITIES AND RATES IN FUSELAGE AXES

(b) Most rotor blades have symmetrical sections along the blade of small thickness ratio (approximately a thickness which is 10-15 per cent of the chord). Hence, it is assumed that the blade may be modeled as flat.

Assumptions (a) and (b) lead to an important approximation to the inertial properties of the blade,

$$I_{zz} - I_{yy} \cong I_{xx} \tag{2.2.1}$$

$$I_{xx} \ll I_{yy} \cong I_{zz} \tag{2.2.2}$$

where the inertias (in slug-ft^2) are

$I_{xx} \triangleq$ blade inertia about torsional blade axis, x_B

$I_{yy} \triangleq$ blade inertia about flapping axis, y_B

$I_{zz} \triangleq$ blade inertia about vertical z_B axis .

The complete blade equations, in the inplane lag frame, are then,

$$\frac{M_x}{I_{xx}} = [\ddot{\theta} + (\Omega^2+2\Omega\dot{\zeta})\theta - \zeta(\ddot{\beta}+\Omega^2\beta) + (-\ddot{\varphi}+2\Omega\dot{\theta}_F)\cos\psi + (\ddot{\theta}_F+2\Omega\dot{\varphi}_F)\sin\psi]$$

$$- \frac{I_{xy}}{I_{xx}}[\ddot{\beta} + (\Omega^2+2\Omega\dot{\zeta})\beta - \ddot{\zeta}\theta - (\ddot{\theta}_F+2\Omega\dot{\varphi}_F)\cos\psi + (\ddot{\varphi}_F-2\Omega\dot{\theta}_F)\sin\psi]$$

$$- \frac{M_B e\bar{\eta}_{CM}}{I_{xx}}[\Omega^2\beta - \Omega^2\zeta\theta + (\ddot{\theta}_F+2\dot{\varphi}_F\Omega)\cos\psi + (\ddot{\varphi}_F-2\Omega\dot{\theta}_F)\sin\psi] \tag{2.2.3}$$

$$\frac{M_y}{I_{yy}} = [\ddot{\beta} + (\Omega^2+2\Omega\dot{\zeta})\beta - (\ddot{\theta}_F+2\Omega\dot{\varphi}_F)\cos\psi + (-\ddot{\varphi}_F+2\Omega\dot{\theta}_F)\sin\psi]$$

(eq. cont.)

$$+\frac{3}{2}\frac{\eta_{CM}}{1-\bar{e}_\beta}\left[\ddot{\theta}+(\Omega^2+2\Omega\dot{\zeta})\theta-(\ddot{\beta}+\Omega^2\beta)\zeta+(\ddot{\varphi}_F-2\Omega\dot{\varphi}_F)\cos\psi\right.$$

$$\left.+(\ddot{\theta}_F+2\Omega\dot{\varphi}_F)\sin\psi\right]$$

$$+\frac{3}{2}\frac{\bar{e}_\beta}{1-\bar{e}_\beta}\left[\Omega^2\beta-(\ddot{\theta}_F+2\dot{\varphi}_F\Omega)\cos\psi-(\ddot{\varphi}_F-2\dot{\theta}_F)\sin\psi\right] \qquad (2.2.4)$$

$$\frac{M_z}{I_{zz}}=\ddot{\zeta}-2\Omega\dot{\beta}\beta+\frac{3}{2}\frac{\bar{e}_\zeta}{1-\bar{e}_\zeta}\Omega^2\zeta-\frac{3\bar{\eta}_{CM}\bar{e}_\zeta}{(1-\bar{e}_\zeta)^2}\Omega^2$$

$$+\ddot{\theta}_F\left[-\frac{3}{2(1-\bar{e}_\zeta)}\sin\psi-\frac{3\bar{\eta}_{CM}\bar{h}}{(1-\bar{e}_\zeta)^2}\cos\psi\right]+\ddot{\varphi}_F\left[\frac{3\bar{h}}{2(1-\bar{e}_\zeta)}\cos\psi\right.$$

$$\left.-\frac{3\bar{\eta}_{CM}\bar{h}}{(1-\bar{e}_\zeta)^2}\sin\psi\right]$$

$$+\dot{u}_F\left[\frac{3}{2(1-\bar{e}_\zeta)}\sin\psi-\frac{3\bar{\eta}_{CM}}{(1-\bar{e}_\zeta)^2}\cos\psi\right]+\dot{v}_F\left[\frac{3}{2(1-\bar{e}_\zeta)^2}\cos\psi\right.$$

$$\left.+\frac{3\bar{\eta}_{CM}}{(1-\bar{e}_\zeta)^2}\sin\psi\right]$$

(2.2.5)

where

$\langle M_x, M_y, M_z\rangle \triangleq$ components of external blade moments (airloads and stiffness of hinge)

M_B = total mass of rigid blade

$\bar{\eta}_{CM} = \frac{\eta_{CM}}{R}$, where η_{CM} is the chordwise distance of blade center of mass from torsional (feathering axis), positive along y_B axis

$\bar{e}_\beta = \frac{e_\beta}{R}$, where e_β is effective hinge point of first flapping mode

$\bar{e}_\zeta = \frac{e_\zeta}{R}$, where e_ζ is effective hinge point of first inplane mode

$\bar{h} = \frac{h}{R}$, where h is the height of the rotor hub above vehicle center of mass

$(\bar{u}_F, \bar{v}_F) = (u_F/R, v_F/R) \triangleq$ length dimensionless longitudinal and lateral velocities of vehicle, in vehicle axes.

Equations (2.2.3)-(2.2.5) are a new set of flap-lag-pitch dynamic relations for a first approximation of stability and response boundaries. Existing simplified analyses have derived either flap-lag or flap-pitch coupled equations, but not the flap-lag-pitch equations. If $\bar{\eta}_{CM}$ is large, coupling of all blade degrees of freedom should be considered. Alternately, if the feathering stiffness is reduced, torsional coupling should be considered even if $\bar{\eta}_{CM}$ is small.

For the purposes of this work, it is assumed that the blade has been designed such that $\bar{\eta}_{CM} = 0$ and that the torsional stiffness is such that the feathering uncoupled natural frequency is above twice per revolution. Then only flap-lag dynamics are significant, and the pertinent equations are:

$$\frac{M_y}{I_{yy}} = \ddot{\beta} + (\Omega^2+2\Omega\dot{\zeta})\beta - (\ddot{\theta}_F+2\Omega\dot{\varphi}_F)\cos\psi + (\ddot{\varphi}_F-2\Omega\dot{\theta}_F)\sin\psi$$

$$+ \frac{3}{2}\frac{\bar{e}_\beta}{1-\bar{e}_\beta}[\Omega^2\beta - (\ddot{\theta}_F+2\Omega\dot{\varphi}_F)\cos\psi + (-\ddot{\varphi}_F+2\Omega\dot{\theta}_F)\sin\psi] \qquad (2.2.8)$$

$$\frac{M_z}{I_{zz}} = \ddot{\zeta} - 2\Omega\beta\dot{\beta} + \frac{3}{2}\frac{\bar{e}_\zeta}{1-\bar{e}_\zeta}\Omega^2\zeta + \frac{3}{2}\frac{\bar{h}}{1-\bar{e}_\zeta}(-\ddot{\theta}_F\sin\psi + \ddot{\varphi}_F\cos\psi)$$

$$+ \frac{3}{2(1-\bar{e}_\zeta)}[\dot{\bar{u}}_F\sin\psi + \dot{\bar{v}}_F\cos\psi] . \qquad (2.2.9)$$

The dynamics of Eqs. (2.2.8) and (2.2.9) are the same as those of Hohenemser and Heaton (H02) with the exception of the effects of shaft angular and linear accelerations, which would be required if the shaft is flexible relative to the fuselage, and the effect of the offset in the inplane degree of freedom.

2.3 Aerodynamic Forces and Moments

The flow field over a rotating wing is so complex that a great many simplifying assumptions must be made to yield a tractable mathematical model. Most of these assumptions are now "classic" in the sense that they have been used for many years and substantiated by many researchers, both analytically and experimentally. The principal blade moments predicted by linear, quasi-steady aerodynamics are discussed in this section. The resulting expressions will be used in Chapter 3 and again in Chapter 6 to formulate mathematical models of rotor-fuselage dynamics and rotor dynamics.

The assumptions made in this section are listed below:

- The induced velocity is assumed constant across the rotor in hover (a correction for forward flight is derived).
- Radial flow along the blade is assumed to have no effect on blade aerodynamics.

- Unsteady aerodynamic effects are neglected, i.e., aerodynamic forces are assumed to be quasi-steady.
- The velocity differential introduced by finite hinge offset is neglected in predicting aerodynamic forces.
- The profile drag on the elements of the blade is neglected for blade motion studies, and only induced drag is considered.
- The inflow angle, φ, is sufficiently small that $\tan \varphi \sim \varphi$.
- The blade element lift curve is linear in angle of attack.
- Stall on the retreating blade tips is neglected, as well as compressibility on the advancing blade tips.

Induced Velocity

The thrust of the rotor is generated by imparting an increase in the velocity to the air passing through it. Although the distribution of this induced velocity over the rotor is a subject of much continuing research (WO2, for example), approximations are available which correlate well with flight tests.

The mean induced velocity, $\bar{v}_o$, in hover, as determined from momentum theory, is, for a rotor with N_B blades (SE1),

$$\bar{v}_o = \frac{T}{2\pi R^2 \rho B^2 V'} \tag{2.3.1}$$

where

B = tip loss factor = $1 - \frac{\sqrt{2C_T}}{N_B}$ (cf. Eq. (2.3.10))

T = rotor thrust normal to disc

R = rotor radius

ρ = air density

and

$$V' = [(\bar{v}_o - V \sin \alpha_R)^2 + (V \cos \alpha_R)^2]^{\frac{1}{2}} \quad * \qquad (2.3.2)$$

V = velocity of air far from rotor

α_R = angle between rotor plane and air velocity far from rotor

For high speed, $\bar{v}_o \ll V$ and

$$V' \sim V \qquad (2.3.3)$$

For hover, $V = 0$, and

$$\bar{v}_o = \sqrt{\frac{T}{2\pi\rho B^2 R^2}} \, . \qquad (2.3.4)$$

In addition, Glauert suggested an induced velocity distribution over the rotor disc in forward flight of

$$\bar{v}_i = \bar{v}_o (1 + \frac{Kr}{V} \cos \psi) \qquad (2.3.5)$$

where $\bar{v}_i$ is the induced velocity for the element, of the blade at azimuth ψ , r units from the center of rotation. An empirical value of K_v is (PA1)

$$K_v = \frac{4}{3} \frac{\mu}{\lambda} (1.2 + \frac{\mu}{\lambda}) \qquad (2.3.6)$$

where

$$\mu \triangleq \frac{V \cos \alpha_R}{\Omega R} \qquad \text{(rotor advance ratio)} \qquad (2.3.7)$$

*This relation was originally proposed by Glauert as a modification to his formula for the induced velocity of an elliptic wing flying with speed V' and generating a lift, T .

$$\lambda \triangleq \frac{\bar{v}_o - V \sin \alpha_R}{\Omega R} \qquad \text{(rotor inflow ratio)} . \qquad (2.3.8)$$

The angle α_R is found from Eqs. (2.3.1) and (2.3.2) and the definitions (2.3.7) and (2.3.8) as

$$\alpha_R = -\frac{\lambda}{\mu} + \frac{1}{2} \frac{C_T}{\mu (\mu^2+\lambda^2)^{\frac{1}{2}}} \qquad (2.3.9)$$

where

$$C_T = \frac{T}{\pi R^2 \rho (\Omega R)^2} \qquad (2.3.10)$$

is the thrust coefficient of the rotor.

Reference Planes

There exist various definitions of α_R, the rotor angle of attack, in the classical theory of rotor analysis. The relations Eqs. (2.3.1) through (2.3.10) do not define the angle of attack of the rotor.

For this study, the rotor angle of attack is taken as the angle between the velocity of the hub and the plane normal to the rotor shaft. Other reference planes are often used. The "no-feathering" plane is defined as the virtual plane in which an observer would see only blade flapping and no pitch change. The "tip path" plane is defined as the plane in which an observer would see no flapping, but only blade pitch changes.

In many studies the "no-feathering" axis is chosen as the basis for analyzing steady state rotor angles, since trim calculations may then be based on standard charts which give the rotor forces as functions of α, λ, and θ_o. For the reference plane as the rotor rotation plane, it is also necessary to specify the steady cyclic controls θ_c and θ_s and hence the trim calculation is slightly more involved. However, the plane

of rotation offers conceptual advantages and for this work, it is assumed that trim conditions are given. An excellent treatment of the various reference planes is given by Mil (MI3).

Since α_R is referenced to the shaft, $\bar{v}_i$ is the induced velocity along the shaft. It is assumed that the vertical velocity of the fuselage, w_F, is small.

From the discussion of Appendix A, assuming small angles, the flow at the blade elements in the plane of rotation is (see Fig. 2.3.1),

$$U_T = r\Omega + (r-e)\dot{\zeta} + (h\dot{\varphi}_F + v_F + \zeta u_F)\cos\psi + (-h\dot{\theta}_F + u_F - \zeta_V)\sin\psi \qquad (2.3.11)$$

and the component perpendicular to the plane of rotation is

$$U_p = (r-e)[\dot{\beta} + \Omega\zeta\beta] - (r\dot{\varphi}_F + v_F\beta)\sin\psi - (r\dot{\theta}_F - u_F\beta)\cos\psi$$
$$- u_I\theta_F + \bar{v}_i \qquad (2.3.12)$$

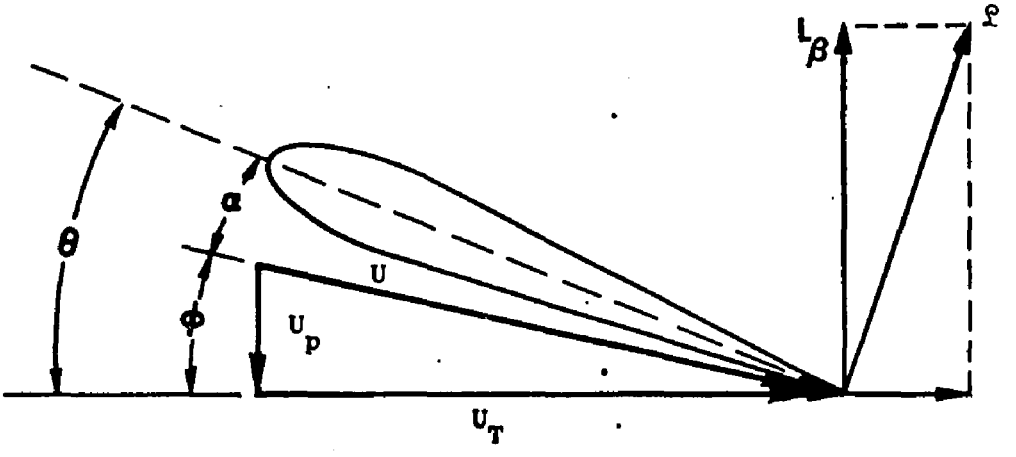

Fig. 2.3.1. SCHEMATIC OF BLADE ELEMENT VELOCITY RESOLUTIONS

Neglecting the offset hinge (aerodynamically only), and dividing by ΩR, Eqs. (2.3.11) and (2.3.12) become

$$\frac{U_T}{\Omega R} = x(1+\zeta') + (h\varphi_F' + \zeta\mu)\cos\psi + (-\bar{h}\theta_F' + \mu)\sin\psi \qquad (2.3.13)$$

$$\frac{U_P}{\Omega R} = x(\beta' + \zeta\beta) - (x\varphi_F' \sin\psi) - (x\theta_F' - \mu)\cos\psi + \lambda_i \qquad (2.3.14)$$

where time is measured in units of $1/\Omega$,

$$(\,)' = \frac{1}{\Omega}\frac{d}{dt}(\,),$$

and

$$x = r/R$$

$$\lambda_i = \frac{v_i}{\Omega R} - \mu\theta_F .$$

Classically, λ is defined as

$$\lambda = \frac{V \sin\alpha - v_i}{\Omega R} .$$

The former definition is used here because it is positive for powered flight and only powered flight is considered.

The neglect of the offset distance, e, in Eqs. (2.3.13) and (2.3.14) is justified by the small contribution of the inboard sections of the rotor blade to the integrated blade lift and flapping moment.

Aerodynamic Forces and Moments

The fundamental quasi-static relation for lift per unit span on an airfoil is

$$L = \frac{1}{2}\rho a c U^2 \alpha \qquad (2.3.15)$$

where

α = blade element angle of attack (rads)

a = lift curve slope (rad^{-1})

c = blade chord (ft)

ρ = density of air, .002378 ($slug/ft^3$)

$U = \sqrt{U_p^2+U_T^2}$ (ft/sec) .

Two integrals over a blade are of primary concern, namely, the total lift and the moments about the hinge. Since $U_p/U_T \ll 1$, the total lift and moment are given by:

$$L_\beta = \frac{1}{2}\rho ac\int_0^{BR}(U_T^2+U_p^2)(\theta-U_p/U_T)dr$$

$$= \frac{1}{2}\rho ac\int_0^{BR}U_T^2\left(1+\frac{U_p^2}{U_T^2}\right)(\theta-U_p/U_T)dr$$

$$\approx \frac{1}{2}\rho ac\int_0^{BR}(U_T^2\theta-U_pU_T)dr \qquad (2.3.16)$$

$$M_\beta \sim \frac{1}{2}\rho ac\int_0^{BR}(U_T^2\theta-U_pU_T)r\,dr\ . \qquad (2.3.17)$$

The quantity $\rho acR^4/I_{yy}$ is a fundamental parameter of rotor blade dynamics, being proportional to the ratio of airloads to dynamic loads of blade flapping. It is useful to convert the above expression for moment into a form factorable of this Lock number. The introduction of $u_T = U_T/\Omega R$ and $u_p = U_p/\Omega R$ with a change of variable of integration to $x = r/R$, gives

$$L_\beta = \frac{1}{2}\rho ac\,\Omega^2R^4\int_0^B(u_T^2\theta-u_Tu_p)dx \qquad (2.3.18)$$

$$M_\beta = \frac{1}{2}\rho a c\,\Omega^2 R^4 \int_0^B (u_T^2\theta - u_T u_p)x\,dx \qquad (2.3.19)$$

and the latter equation then becomes

$$\frac{M_\beta}{I_{yy}} = \frac{\gamma\Omega^2}{8}\int_0^B 4(u_T^2\theta - u_T u_p)x\,dx\ . \qquad (2.3.20)$$

The induced drag from the lift of the blade elements gives a moment related to inplane motion:

$$\frac{M_\zeta}{I_{zz}} = \frac{\gamma\Omega^2}{8}\int_0^B 4(u_p^2 - u_T u_p\theta)x\,dx\ . \qquad (2.3.21)$$

These expressions for M_β and M_ζ are first approximations to the quasi-static airloads produced by the β and ζ motions.

The geometric pitch angle θ is given by

$$\theta = \theta_o + x\theta_t + \theta_s \sin\Omega t + \theta_c \cos\Omega t + \bar{K}_\beta\beta \qquad (2.3.22)$$

where

θ_o = rotor collective pitch angle (rad)

θ_s, θ_c = rotor longitudinal and lateral cyclic angles (rad)

θ_t = blade twist (hub to tip) (rad)

$\bar{K}_\beta$ = gain on flapping position feedback to blade pitch control (rad/rad) .

Substitution of Eqs. (2.3.13), (2.3.14) and (2.3.22) into the moment equations (2.3.20) and (2.3.21) gives the coefficients of the state de-

pendent airloads, shown in Table 2.3.1. The twist effect, though small, is included for completeness.

Reversed Flow

The coefficients of Table 2.3.1 may be used to evaluate the effect of reversed flow on high speed blade motions.

One of the major deviations from simple periodicity of the airloads at high advance ratios is caused by this reversed flow over the retreating blade. This region is defined approximately by

$$x \leq -\mu \sin \psi \; ; \quad \pi < \psi < 2\pi \; ,$$

where x is the spanwise length variable. In this region, it may be assumed that the blade lift and drag are approximately reversed in direction relative to a coordinate system fixed in the blade. This characteristic may be used in simulating the reversed flow very simply on a digital computer. The shaded areas of Fig. 2.3.2 are the calculated reversed flow regions. For $\mu \leq 1$, the region is a circle of radius $\mu/2$ with center at $x = 0$, $y = -\mu/2$. For $\mu > 1$, the region is bounded by this circle and the edge of the rotor disc $x^2 + y^2 = 1$.

In the shaded regions for $\mu \leq 1$ new coefficients are defined from those of Table 2.3.1 by replacing B with $-\mu \sin \psi$ and multiplication by -1 . These coefficients are subtracted from the original coefficients and the results used as the state coefficients of the differential equations. For $\mu > 1$, the coefficients of Table 2.3.1 are simply multiplied by -1 .

This representation of the reversed flow regime is continuous as opposed to representations in which the entire blade is considered in reverse flow at a critical azimuth angle (LO1, SI1).

2.4 Flap-Lag Blade Equations

The torsional degree of freedom is assumed relatively rigid, such that high frequency oscillations of the blade spanwise pitch have little

Table 2.3.1. AERODYNAMIC COEFFICIENTS

Flapping Equation State Coefficients

- Rotor State Coefficients

$$C_o^\beta = -\frac{\gamma\Omega^2}{8}\left[\frac{4B^2}{3}\lambda + 2\mu B^2\lambda \sin\psi + \frac{4B^3}{3}\lambda K_v\cos\psi + \frac{2\mu B^3}{3}\lambda K_v\sin 2\psi\right]$$

$$C_\beta^\beta = \frac{\gamma\Omega^2}{8}\left[\frac{4\mu B^3}{3}\cos\psi + \mu^2B^2\sin 2\psi + K_\beta\left(B^4 + \frac{8}{3}\mu B^3\sin\psi + \mu^2B^2(1-c2\psi)\right)\right.$$

$$C_{\dot\beta}^\beta = \frac{\gamma\Omega}{8}\left[B^4 + \frac{4\mu B^3}{3}\sin\psi\right]$$

$$C_\zeta^\beta = \frac{\gamma\Omega^2}{8}\left[2\mu B^2\lambda\cos\psi + \lambda K_v\left(\frac{2B^3}{3}[1+\cos 2\psi]\right) - \theta_o\left(2\mu^2B^2\sin 2\psi + \frac{8}{3}\mu B^3\cos\psi\right)\right]$$

$$C_{\dot\zeta}^\beta = \frac{\gamma\Omega}{8}\left[\frac{4B^3}{3}\lambda + \lambda K_v B^4\cos\psi - \theta_o\left(2B^4 + \frac{8}{3}\mu B^3\sin\psi\right)\right]$$

$$C_{\beta\zeta}^{\beta\cdot} = \frac{\gamma\Omega}{8}\left[\frac{4}{3}\mu B^3\cos\psi\right]$$

$$C_{\beta\,\zeta}^{\beta\,\cdot} = C_{\dot\beta\zeta}^\beta + \frac{\gamma\Omega}{8}\left[K_\beta\left(2B^4 + \frac{8}{3}\mu B^3\sin\psi\right)\right]$$

$$C_{\beta\zeta}^\beta = \frac{\gamma\Omega^2}{8}\left[B^4 + \frac{4}{3}\mu B^3\sin\psi + \mu^2B^2(1+\cos 2\psi) + K_\beta\left(\frac{8}{3}\mu B^3\sin\psi + 2\mu^2B^2\sin 2\psi\right)\right]$$

(Table 2.3.1 continued)

- Inertial State Coefficients

$$C^{\beta}_{\dot{\theta}_F} = \frac{\gamma\Omega}{8}\left[-B^4\cos\psi - \frac{2\mu B^3}{3}\sin 2\psi - \lambda\,\bar{h}\left(2B^2 + \frac{4KB^3}{3}\right)\sin\psi\right]$$

$$C^{\beta}_{\dot{\phi}_F} = \frac{\gamma\Omega}{8}\left[-B^4\cos\psi - \frac{2\mu B^3}{3} + \frac{2\mu B^3}{3}\cos 2\psi + \lambda\,\bar{h}\left(2B^2 + \frac{4KB^3}{3}\right)\cos\psi\right]$$

- Control Coefficients

$$C^{\beta}_{\theta_o} = \frac{\gamma\Omega^2}{8}\left[B^4 + \frac{8}{3}\mu B^3\sin\psi + \mu^2B^2(1 - \cos 2\psi)\right]$$

$$C^{\beta}_{\theta_s} = C_{\theta_o}\sin\psi$$

$$C^{\beta}_{\theta_c} = C_{\theta_o}\cos\psi$$

- Correction for Twist (add to appropriate coefficient)

$$\delta C^{\beta}_{o} = \frac{\gamma\Omega^2}{8}\left[-\theta_t\left(\frac{4B^5}{5} + 2\mu B^4\sin\psi + \frac{2}{3}\mu^2B^2(1 - \cos 2\psi)\right)\right]$$

$$\delta C^{\beta}_{\zeta} = \frac{\gamma\Omega^2}{8}\left[-\theta_t\left(2B^4\cos\psi + \frac{4B^3}{3}\mu\sin 2\psi\right)\right]$$

$$\delta C^{\beta}_{\dot{\zeta}} = \frac{\gamma\Omega^2}{8}\left[-\theta_t\left(\frac{8}{5}B^5 + 2\mu B^4\sin\psi\right)\right]$$

(Table 2.3.1 continued)

- Inplane Coefficients

- Rotor State Coefficients

$$C_o^\zeta = \frac{\gamma\Omega^2}{8}\left[2\lambda^2 B^2 + \frac{8}{3}\lambda^2 B^3 K_V \cos\psi + \frac{\lambda^2 B^4 K_V^2}{2}(1 + \cos 2\psi)\right]$$

$$C_\zeta^\zeta = \frac{\gamma\Omega^2}{8}\left[2\mu B^2\lambda \cos\psi + \frac{2\mu B^3}{3}K_V\lambda (1 + \cos 2\psi)\right]\theta_o$$

$$C_{\dot\zeta}^\zeta = \frac{\gamma\Omega}{8}\left[\frac{4B^3\lambda}{3} + \lambda K_V B^4 \cos\psi\right]\theta_o$$

$$C_\beta^\zeta = \frac{\gamma\Omega^2}{8}\left[-4\lambda\mu B^2 \cos\psi - K_\beta\left(2\lambda\mu B^2 \sin\psi + \frac{4B^3}{3}\lambda + \lambda K_V B^4 \cos\psi + \frac{4\lambda\mu B^3 K_V}{3}\sin\psi\right) - \lambda K_V\left(\frac{4}{3}\mu B^3[1 + \cos 2\psi]\right) + \theta_o\left(\frac{4}{3}\mu B^3 \cos\psi + \mu^2 B^2 \sin 2\psi\right)\right]$$

$$C_{\dot\beta}^\zeta = \frac{\gamma\Omega}{8}\left[-\frac{8}{3}\lambda B^3 - \lambda K_V(2B^4 \cos\psi) + \theta_o\left(B^4 + \frac{4}{3}\mu B^3 \sin\psi\right)\right]$$

$$C_{\beta\dot\beta}^\zeta = \frac{\gamma\Omega}{8}\left[-\frac{8}{3}\mu B^3 \cos\psi - K_\beta\left(B^4 + \frac{4\mu B^3}{3}\sin\psi\right)\right]$$

$$C_{\beta\dot\zeta}^\zeta = \frac{\gamma\Omega}{8}\left[-K_\beta\left(\frac{4\lambda B^3}{3} + B^4\lambda K_V \cos\psi\right) + \theta_o\left(\frac{4}{3}\mu B^3 \cos\psi\right)\right]$$

(Table 2.3.1 continued)

· Inplane Rotor Coefficients (continued)

$$C^{\zeta}_{\dot{\beta}\zeta} = C^{\zeta}_{\beta\dot{\zeta}}$$

$$C^{\zeta}_{\dot{\beta}\zeta} = \frac{\gamma\Omega^2}{8}\left[-\frac{8}{3}\lambda B^3 - K_{\beta}\left(2\lambda\mu B^2\cos\psi + \frac{2}{3}\mu B^3\lambda K_V[1+\cos 2\psi]\right)\right.$$

$$\left. - \lambda K_V(2B^4\cos\psi) + \theta_o\left(B^4 + \frac{4}{3}\mu B^3\sin\psi + \mu^2B^2(1+\cos 2\psi)\right)\right]$$

· Inertial State Coefficients

$$C^{\zeta}_{\dot{\theta}_F} = \frac{\gamma\Omega}{8}\left[\frac{8}{3}\lambda B^3\cos\psi + \lambda B^4K_V(1+\cos 2\psi)\right]$$

$$C^{\zeta}_{\dot{\phi}_F} = \frac{\gamma\Omega}{8}\left[\frac{8}{3}\lambda B^3\sin\psi + \lambda B^3K_V\sin 2\psi\right]$$

· Control Coefficients

$$C^{\zeta}_{\theta_o} = -\frac{\gamma\Omega^2}{8}\left[2\mu B^2\lambda\sin\psi + \frac{4B^3}{3}\lambda + \lambda B^4K_V\cos\psi + \frac{2}{3}\mu B^3\psi\sin 2\psi\right]$$

$$C^{\zeta}_{\theta_s} = C_{\theta_o}\sin\psi$$

$$C^{\zeta}_{\theta_c} = C_{\theta_o}\cos\psi$$

(Table 2.3.1 continued)

- Inplane Equations: Twist Correction

$$\delta C^{\zeta}_{\zeta} = \frac{\gamma\Omega^2}{8}\theta_t\left[\lambda K_v\left(\frac{\mu B^4}{2}\right)(1 + \cos 2\psi) + \frac{4\mu B^3}{3}\lambda\cos\psi\right]$$

$$\delta C^{\zeta}_{\dot{\zeta}} = \frac{\gamma\Omega^2}{8}\theta_t\left[\lambda K_v B^4\cos\psi + \lambda B^4\right]$$

$$\delta C^{\zeta}_{\beta} = \frac{\gamma\Omega^2}{8}\theta_t\left[\mu B^4\cos\psi + \frac{2}{3}\mu^2 B^3\sin 2\psi\right]$$

$$\delta C^{\zeta}_{\dot{\beta}} = \frac{\gamma\Omega^2}{8}\theta_t\left[\frac{4B^5}{5} + \mu B^4\sin\psi\right]$$

$$\delta C^{\zeta}_{\beta\dot{\zeta}} = \frac{\gamma\Omega^2}{8}\theta_t\left[\mu B^4\cos\psi\right]$$

$$C^{\zeta}_{\dot{\beta}\,\zeta} = \delta C^{\zeta}_{\beta\dot{\zeta}}$$

$$\delta C^{\zeta}_{\beta\zeta} = \frac{\gamma\Omega^2}{8}\theta_t\left[\frac{4B^3\mu}{3} + \mu B^4\sin\psi + \frac{2\mu^2 B^3}{3}(1 + \cos 2\psi)\right]$$

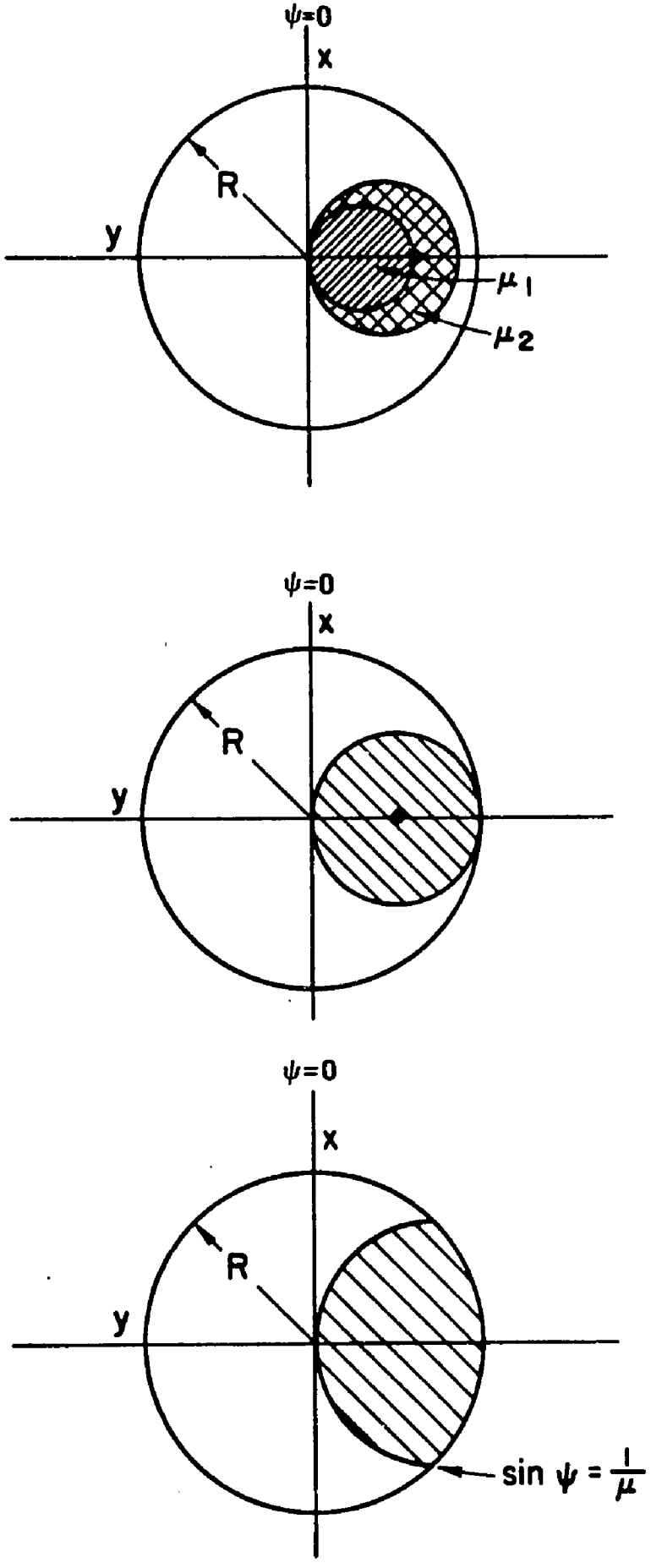

Fig. 2.3.2. REVERSE FLOW REGIMES

effect on the lower frequency flapping and inplane motions.

With the coefficients defined by Table 2.3.1, the flapping and inplane equations are:

$$\ddot{\beta} + \left[C^{\beta}_{\beta} + C^{\beta}_{\dot{\beta}\zeta}\zeta\right]\dot{\beta} + \left[\left\{1 + \left(\frac{3}{2}\frac{\bar{e}_{\beta}}{1-\bar{e}_{\beta}}\right) + \left(\frac{K_{\beta}}{I_{yy}\Omega^2}\right)\right\}\Omega^2 + C^{\beta}_{\zeta}\zeta + \left\{2\Omega + C^{\beta}_{\dot{\zeta}\beta}\right\}\dot{\zeta}\right]\beta$$

$$+ C^{\beta}_{\zeta}\zeta + C^{\beta}_{\dot{\zeta}}\dot{\zeta} + C^{\beta}_{\zeta\zeta}\zeta\dot{\zeta} - \left(1 + \frac{3}{2}\frac{\bar{e}}{1-\bar{e}}\right)\left[(\ddot{\theta}_F + 2\Omega\dot{\varphi}_F)\cos\psi + (-\ddot{\varphi}_F + 2\Omega\dot{\theta}_F)\sin\psi\right] + C^{\beta}_{\dot{\theta}_F}\dot{\theta}_F + C^{\beta}_{\dot{\varphi}_F}\dot{\varphi}_F$$

$$= C^{\beta}_{o} + C^{\beta}_{\theta_o}\theta_o + C^{\beta}_{\theta_s}\theta_s + C^{\beta}_{\theta_c}\theta_c \qquad (2.4.1)$$

$$\ddot{\zeta} + C^{\zeta}_{\dot{\zeta}}\dot{\zeta} + \left[\left\{\frac{K_{\zeta}}{I_{zz}\Omega^2} + \frac{3}{2}\frac{\bar{e}_{\zeta}}{1-\bar{e}_{\zeta}}\right\}\Omega^2 + C^{\zeta}_{\zeta}\right]\zeta - \Omega(2 + C^{\zeta}_{\beta\dot{\beta}})\beta\dot{\beta}$$

$$+ \frac{3}{2}\frac{\bar{h}}{(1-\bar{e})}\left[\ddot{\varphi}_F\cos\psi - \ddot{\theta}_F\sin\psi\right] + \frac{3}{2(1-\bar{e})}\left[\dot{\bar{u}}\sin\psi + \dot{\bar{v}}\cos\psi\right]$$

$$+ C^{\zeta}_{\beta}\beta + C^{\zeta}_{\dot{\beta}}\dot{\beta} + C^{\zeta}_{\zeta\beta}\zeta\beta + C^{\zeta}_{\beta\dot{\zeta}}\beta\dot{\zeta} + C^{\zeta}_{\dot{\theta}_F}\dot{\theta}_F + C^{\zeta}_{\dot{\varphi}_F}\dot{\varphi}_F$$

$$= C^{\zeta}_{o} + C^{\zeta}_{\theta_o}\zeta + C^{\zeta}_{\theta_s}\theta_s + C^{\zeta}_{\theta_s}\theta_c \qquad (2.4.2)$$

where

K_{β} = flapping torsional spring constant of the articulated rotor blade (or equivalent spring of hingeless rotor)

K_{ζ} = inplane torsional spring of rotor blade .

For the stability calculations of Chapter VI, the linearized* forms of Eqs. (2.3.1) and (2.4.2) are obtained by assuming

$$\beta = \beta_o + \delta\beta$$

$$\zeta = \zeta_o + \delta\zeta$$

and then writing β for $\delta\beta$ and ζ for $\delta\zeta$. Fuselage accelerations are neglected.

$$\ddot{\beta} + \left[C^{\beta}_{\dot{\beta}} + C^{\beta}_{\dot{\beta}\zeta}\zeta_o\right]\dot{\beta} + \left[\left\{1 + \left(\frac{3}{2}\frac{\bar{e}_\beta}{1-\bar{e}_\beta}\right) + \frac{K_\beta}{I_{yy}\Omega^2}\right\}\Omega^2 + C^{\beta}_{\beta} + C^{\beta}_{\beta\zeta}\zeta_o\right]\beta$$
$$+ \left[C^{\beta}_{\dot{\zeta}}\right]\dot{\zeta} + \left[C^{\beta}_{\zeta} + \left\{2\Omega + C^{\beta}_{\dot{\zeta}\beta}\right\}\beta_o + \left\{C^{\beta}_{\zeta\dot{\zeta}}\right\}\zeta_o\right]\zeta$$
$$= C^{\beta}_{o} + C^{\beta}_{\theta_o}\theta_o + C^{\beta}_{\theta_s}\theta_s + C^{\beta}_{\theta_c}\theta_c \qquad (2.4.3)$$

$$\ddot{\zeta} + \left[C^{\zeta}_{\dot{\zeta}} + C^{\zeta}_{\dot{\beta}\zeta}\beta_o\right]\dot{\zeta} + \left[\left\{\frac{K_\zeta}{I_{zz}\Omega^2} + \frac{3}{2}\left(\frac{\bar{e}_\zeta}{1-\bar{e}_\zeta}\right)\right\}\Omega^2 + C^{\zeta}_{\zeta} + C^{\zeta}_{\zeta\beta}\beta_o\right]\zeta$$
$$+ \left[C^{\zeta}_{\dot{\beta}}\right]\dot{\beta} + \left[C^{\zeta}_{\beta} - \Omega\left(2 + C^{\zeta}_{\dot{\beta}\beta}\right)\beta_o\right]\beta$$
$$= C_o\zeta_o + C^{\zeta}_{\theta}\theta_o + C^{\zeta}_{\theta_s}\theta_s + C^{\zeta}_{\theta_c}\theta_c \; . \qquad (2.4.4)$$

Such equations obviously depend on selection of appropriate constants β_o and ζ_o, which depend on the operating conditions of the vehicle.

The trim values of β_o may be approximated from the coefficients of Table 2.3.1. As mentioned previously, λ is found by solution of the equation (2.3.9) for a given α_R. Then, θ_o is found by integrating the lift along the blade. Knowing C_T and σ, the result is

*It is assumed that β_o and ζ_o represent stable operating points of a flight regime.

$$\theta_o = \frac{\frac{2C_T}{a\sigma} + \frac{\lambda}{2}}{\frac{1}{3}+\frac{1}{2}\mu^2} \,. \qquad (2.4.5)$$

Finally, β_o is found from equilibrium of flapping moments

$$\left(C_o^\beta = \left[\left(\omega_\beta^2 + \Omega^2\right) + C_\beta^\beta\right]\beta\right)$$

to be

$$\beta_o = \frac{\gamma}{2}\left[\frac{\theta_o}{4}\,(1+\mu^2) - \frac{\lambda}{3}\right] - \frac{\omega_\beta^2}{\Omega^2}\,. \qquad (2.4.6)$$

The value of ζ_o is set to zero in the studies of Chapter VI.

2.5 Summary

The equations for analysis of the motions of a hinged rigid blade have been derived. Based on the derivations of Appendix A, the pitch-lag-flap blade equations may be simplified by expressing the flapping and inplane inertias in terms of the geometry of a flat blade. Assumption of an infinite feathering axis stiffness then gives the flap-lag equations.

Quasi-steady aerodynamics are used to calculate the periodic airloads on the blades. Aerodynamic coefficients for the blade flap-lag motions are derived and given in Table 2.3.1. Coefficient corrections for non-uniform induced velocity over the rotor disc at high speeds is included, as well as corrections for twist and flapping angle feedback to the instantaneous blade pitch angle.

A method for studying the effects of reverse flow is described which uses the aerodynamic coefficients for normal flow, and hence no new coefficients are required.

Chapter III

ROTOR FUSELAGE DYNAMIC MODELS IN HOVER

3.1 Introduction

Since the hover regime is common to all types of rotary wing VTOL aircraft, the design of hover stability augmentation systems is an important problem.

In hover, and at low speeds around hover, the vertical and directional degrees of freedom are essentially uncoupled from the horizontal translation, pitch, and roll degrees of freedom (SE1, WO1). This decoupling actually depends on certain dimensions of the aircraft. For example, the longitudinal offset of the vehicle CM relative to the hub, either by shaft (pylon) attachment point displacement relative to the hub, or by shaft tilt, must be small for vertical motion decoupling. Similarly, an increase in tail rotor height will increase the directional-roll coupling, although this effect is moderated by the relatively small magnitude of the tail rotor thrust. Fuselage aerodynamic contributions are usually negligible in hover.

These aspects of the hover regime may be illustrated by the stability derivatives for a typical aircraft. Table 3.1.1 gives the stability derivatives for one configuration of the Sikorsky S-61 helicopter (Ref. CO1).* The lateral force Y derivatives have significant coupling with $\dot{\psi}_F$, the yaw rate. However, $\dot{\psi}_F$ may be controlled to zero independently of rotor forces by using the tail rotor. A similar situation occurs with respect to the vertical velocity, w_F, which may be controlled to zero almost independently by collective pitch, θ_o.

However, at higher speeds, the fuselage forces and moments increase, and the degrees of freedom couple strongly.

*Sikorsky engineers have normalized these derivatives. The force derivatives of the first three rows are normalized on the vehicle mass. The moment derivatives of the second three rows are normalized by the vehicle inertias.

	u(ft./sec.)	v(ft./sec.)	w(ft./sec.)	$\dot{\theta}_F$(rad./sec.)	$\dot{\varphi}_F$(rad./sec.)	$\dot{\psi}_F$(rad./sec.)
$\frac{X_{(\cdot)}}{m_v}$	-.0159 sec.$^{-1}$	-.00447 sec.$^{-1}$	0	1.76 $\frac{\text{ft.}}{\text{sec.-rad.}}$	0	0
$\frac{Y_{(\cdot)}}{m_v}$	.00447 sec.$^{-1}$	-.0334 sec.$^{-1}$	-.00509*sec.$^{-1}$	-1.61 $\frac{\text{ft.}}{\text{sec.-rad.}}$	-1.82 $\frac{\text{ft.}}{\text{sec.-rad.}}$	.645 $\frac{\text{ft.}}{\text{sec.-rad.}}$
$\frac{Z_{(\cdot)}}{m_v}$	0	0	-.324 sec.$^{-1}$	0	0	0
$\frac{M_{(\cdot)}}{I_{\theta_F}}$	.00261 $\frac{1}{\text{sec.ft.}}$	.00093 $\frac{1}{\text{sec.ft.}}$	-.00092 $\frac{1}{\text{sec.ft.}}$	- .371 $\frac{1}{\text{sec.-rad.}}$	2.28 $\frac{1}{\text{sec.-rad.}}$	0
$\frac{N_{(\cdot)}}{I_{\varphi_F}}$	0	.00845 $\frac{1}{\text{sec.ft.}}$	.00123 $\frac{1}{\text{sec.ft.}}$	0	0	-.306 $\frac{1}{\text{sec.-rad.}}$
$\frac{L_{(\cdot)}}{I_{\psi_F}}$	.0035 $\frac{1}{\text{sec.ft.}}$	-.0125 $\frac{1}{\text{sec.ft.}}$	-.00159 $\frac{1}{\text{sec.ft.}}$	- .854 $\frac{1}{\text{sec.-rad.}}$	-1.45 $\frac{1}{\text{sec.-rad.}}$	0

Table 3.1.1. FLIGHT TEST HOVER DERIVATIVES FOR SIKORSKY S-61 (Ref. C01) justify the assumption of decoupling the vertical and directional motions from the longitudinal-lateral motions.

3.2 Averaging Over Blade State to Obtain Rotor Tilt Equations

An observer fixed in inertial space sees a plane defined by the motion of the rotor blade tips (the "tip path plane"). This has led previous investigators to approximate the resultant rotor forces on the fuselage in terms of the roll angle, φ_R, and the pitch angle, θ_R, of the tip path plane. To determine φ_R and θ_R, we must average over one revolution of a blade. The flapping angle is approximated by its constant and first harmonic content:

$$\beta(t) \cong \beta_o(t) - \theta_R(t) \cos \Omega t - \varphi_R(t) \sin \Omega t \ . \qquad (3.2.1)$$

Only out-of-plane flapping motions are considered, i.e., $\zeta(t) \cong 0$ and Eq. (3.2.1) is substituted into Eq. (2.4.3). Since the resulting equation must be satisfied for all t, the coefficients of $\sin \Omega t$, $\cos \Omega t$, and the remainder are each set to zero.

This approximation is useful for determining stability of the coupled rotor fuselage motions since the most significant moments on the fuselage from the rotor arise from the once per revolution blade motion. Note there are possible instabilities associated with second or higher harmonics of the flapping angle (e.g., see Chapter 6).

In addition to Eq. (3.2.1), the pitch of the blade may be approximated by

$$\theta(t) = \theta_o + \theta_s \sin \Omega t + \theta_c \cos \Omega t \ . \qquad (3.2.2)$$

Performing the indicated substitutions, neglecting the effects of inplane oscillations, but including the first order fuselage pitch and roll acceleration moments, the following equations are obtained, for small motions about hover:

$$\ddot{\beta}_o + \frac{\gamma\Omega}{8} \dot{\beta}_o + \omega_B^2 \beta_o - \frac{1}{12} \gamma \mu_x \Omega (\dot{\varphi}_R + \dot{\varphi}_F) = \frac{\gamma\Omega^2}{8} \left[-\frac{4}{3}\lambda + \theta_o + \frac{4}{3} \mu_x \theta_c \right] \qquad (3.2.3)$$

$$\ddot{\theta}_R + \frac{\gamma\Omega}{8}\dot{\theta}_R + \omega_R^2\Omega^2\theta_R + 2\Omega\dot{\varphi}_R + \frac{\gamma\Omega^2}{8}\varphi_R + \ddot{\theta}_F\left(1+\frac{3}{2}\bar{h}\beta_o\right) + \frac{\gamma\Omega}{8}\dot{\theta}_F$$

$$+ 2\Omega\left(1+\frac{3}{2}\frac{\bar{e}}{1-\bar{e}}\right)\dot{\varphi}_F - \frac{4}{3}\frac{\gamma\Omega^2}{8}\beta_o\mu_x + \frac{\gamma\Omega^2}{8}\left(\frac{8}{3}\theta_o - 2\lambda\right)\mu_y$$

$$= -\frac{\gamma\Omega^2}{8}\theta_c \qquad (3.2.4)$$

$$\ddot{\varphi}_R + \frac{\gamma\Omega}{8}\dot{\varphi}_R + \omega_R^2\Omega^2\varphi_R - 2\Omega\dot{\theta}_R - \frac{\gamma\Omega^2}{8}\theta_R + \ddot{\varphi}_F\left(1+\frac{3}{2}\bar{h}\beta_o\right) + \frac{\gamma\Omega}{8}\dot{\varphi}_F$$

$$- 2\Omega\left(1+\frac{3}{2}\frac{\bar{e}}{1-\bar{e}}\right)\dot{\theta}_F + \frac{\gamma\Omega^2}{8}\left(\frac{8}{3}\theta_o - 2\lambda\right)\mu_x + \frac{4}{3}\frac{\gamma\Omega^2}{8}\beta_o\mu_y$$

$$= -\frac{\gamma\Omega^2}{8}\theta_s \qquad (3.2.5)$$

where

$$\bar{h} = h/R$$

$$\bar{e} = e/R$$

$$\omega_B^2 = 1 + \omega_R^2$$

$$\omega_R^2 = \frac{K_\beta}{I_\beta\Omega^2} + \frac{3}{2}\frac{\bar{e}}{1-\bar{e}}$$

For this work, the coning dynamics, Eq. (3.2.3) will be neglected since the effect of coning dynamics on fuselage pitch and roll responses is small in hover. However, the steady coning angle, β_o, is retained to account for its contribution to the speed damping of the vehicle.

3.3 Averaging Over Blade State to Obtain Rotor Forces on Fuselage

The rotor effects on the fuselage arise from three sources:

(a) Moments on the shaft from the flapping spring of the articulated rotor (or the effective flapping stiffness which repre-

sents the elasticity of the hingeless rotor);

(b) Moments on the shaft from the aerodynamic shear and inertial shear forces acting over the offset distance, e_β;

(c) Moments about the vehicle CM from the inplane rotor aerodynamic forces acting across the hub height from the CM.

Moment Due to Flapping Spring Restraint

Fully articulated rotor blades, where the flapping and inplane motions occur about hinges offset from the rotor hub, are still used on large helicopters. Although mechanically more complex, the fully articulated rotor has fewer problems of stability and blade stress. A physical spring is used on such rotors to control flapping amplitude.

A flexible hingeless rotor may be modeled approximately by a spring-loaded offset hinge (SH2). This equivalence of modeling between the fully articulated and the hingeless rotor is valid only so long as the first harmonic of rotor blade motion is predominant, and hence is restricted to low speed flight. The procedure for representing the hingeless rotor as an articulated rotor is to select the offset and the spring constant so that the first harmonic mode shape and unit force deflection are well approximated. Then the static blade moment and inertia are selected so that the corresponding first harmonic of the flapping motion is obtained.

As discussed in Appendix A, the restraint is modeled as a torsion spring at the flapping hinge point, with spring constant, K_β (moment per radian). The blade flapping natural frequency, viewed in the rotating blade frame, is given by

$$\left(\frac{\omega_B}{\Omega}\right)^2 = 1 + \frac{K_\beta}{I_\beta \Omega^2} + \frac{3}{2}\frac{\bar{e}_\beta}{1-\bar{e}_\beta}$$

$$\triangleq \left(\frac{\omega_\beta}{\Omega}\right)^2 + \frac{3}{2}\frac{\bar{e}_\beta}{1-\bar{e}_\beta} \quad . \tag{3.3.1}$$

In the fuselage-fixed, non-rotating frame, the rotor plane natural frequency is then

$$\left(\frac{\omega_R}{\Omega}\right)^2 = \left(\frac{\omega_B}{\Omega}\right)^2 - 1 \quad . \tag{3.3.2}$$

The effect of the spring on the shaft moment is found by averaging the periodic blade moment, $K_\beta\beta$, for each blade. This average moment is then resolved into its components in fuselage axes. The result is

$$\left(M_{K_\beta}\right)_{\theta_F} = \frac{N_B}{2} K_\beta \theta_R \tag{3.3.3}$$

$$\left(M_{K_\beta}\right)_{\varphi_F} = \frac{N_B}{2} K_\beta \varphi_R \tag{3.3.4}$$

but

$$\frac{K_\beta}{I_\beta \Omega^2} = \left(\frac{\omega_\beta}{\Omega}\right)^2 - 1 \triangleq \left(\frac{\omega_F}{\Omega}\right)^2 \tag{3.3.5}$$

so

$$\left(M_{K_\beta}\right)_{\theta_F} = \frac{N_B}{2} I_\beta \Omega^2 \omega_F^2 \theta_R \tag{3.3.6}$$

$$\left(M_{K_\beta}\right)_{\varphi_F} = \frac{N_B}{2} I_\beta \Omega^2 \omega_F^2 \varphi_R \qquad (3.3.7)$$

where

N_B = number of rotor blades

$\left(M_{K_\beta}\right)_{\theta_F}, \left(M_{K_\beta}\right)_{\varphi_F}$ = longitudinal and lateral components of rotor elastic moment in fuselage axes

Moments Due to Rotor Blade Inertia Shear Forces

The largest component of the blade inertia shear force at the flapping hinge arises from the centrifugal acceleration of the blade. If there is no flapping hinge offset, no net moment exists on the shaft.

Figure 3.3.1 illustrates the origin of the shear force. The d'Alembert forces are due to flapping acceleration and shaft plane acceleration, $\vec{a}_F^{O-I}$. The integrated inertial shear force in fuselage axes is

$$F_s \simeq \int_e^R \rho_B \left[(r-e_\beta)\ddot{\beta} + r\Omega^2\beta - \vec{a}_F^{O-I}\right] dr \qquad (3.3.8)$$

where

ρ_B = mass per unit length of blade

$$a_F^{O-I} = (\ddot{\theta}_F + 2\dot{\theta}_F\Omega) \cos \Omega t + (\ddot{\varphi}_F - 2\Omega\dot{\theta}_F) \sin \Omega t \; . \qquad (3.3.9)$$

Neglecting products of $\bar{e}_\beta$ with $\dot{\beta}$ and $\ddot{\beta}$,

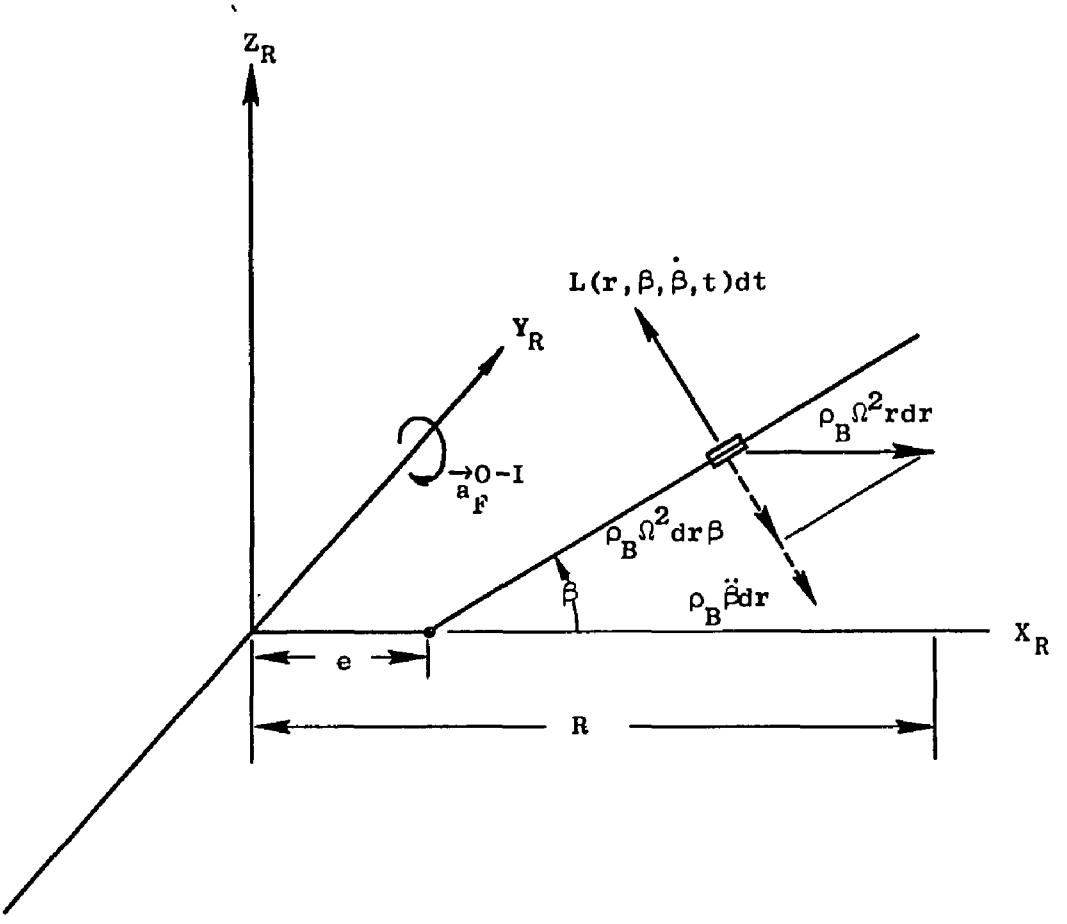

Fig. 3.3.1. SCHEMATIC OF ROTOR BLADE SHEAR FORCES

$$F_s = \frac{-\rho_B R^2}{2}\left\{\left[(\ddot{\theta}_R+\ddot{\theta}_F) + 2\Omega(\dot{\varphi}_R+\dot{\varphi}_F) - \theta_R\Omega^2\right]\cos\ \Omega t + \left[(\ddot{\varphi}_R+\ddot{\varphi}_F) - 2\Omega(\dot{\theta}_R+\dot{\theta}_F) - \varphi_R\Omega^2\right]\sin\ \Omega t\right\} . \qquad (3.3.10)$$

The resulting shear moment is,

$$\vec{M}_s = \vec{e} \times \vec{F}_s \qquad (3.3.11a)$$

and, considering only the moment about the Y_R axis,

$$M_s = eF_s . \qquad (3.3.11b)$$

Integrating over a revolution, the average pitch fuselage moment, $(M_S)_{\theta_F}$, and roll fuselage moment, $(M_S)_{\varphi_F}$, in fuselage axes, are

$$(M_s)_{\theta_F} = \int_0^{2\pi} M_s \cos\ \psi\ d\psi = +eN_b\left(\frac{\rho_B R^2}{2}\right)\left\{\frac{-(\ddot{\theta}_R+\ddot{\theta}_F) - 2\Omega(\dot{\varnothing}_R+\dot{\varnothing}_F) + \theta_R\Omega^2}{2}\right\} \qquad (3.3.12)$$

$$(M_s)_{\varphi_F} = \int_0^{2\pi} M_s \sin\ \psi\ d\psi = +eN_b\left(\frac{\rho_B R^2}{2}\right)\left\{\frac{-(\ddot{\varnothing}_R+\ddot{\varnothing}_F) + 2\Omega(\dot{\theta}_R+\dot{\theta}_F) + \varnothing_R\Omega^2}{2}\right\} \qquad (3.3.13)$$

Moments Due to Airload Shear at Flapping Hinge

The aerodynamic shear force, $L(r,\beta,\dot{\beta},t)$ of Fig. 3.3.1 is found by integrating the spanwise lift over the rotor azimuth. For small flapping angles,

$$\left(M_A\right)_{\theta_F} = -\frac{1}{2\pi}\int_0^{2\pi} eL \sin\psi d\psi \tag{3.3.14}$$

$$\left(M_A\right)_{\varphi_F} = -\frac{1}{2\pi}\int_0^{2\pi} eL \cos\psi d\psi \tag{3.3.15}$$

where

$$L = \frac{1}{2}\rho ac\Omega^2 R^3 \int_{\frac{-}{e}}^{1} \left(u_T^2\theta - u_p u_T\right)dr \ . \tag{3.3.16}$$

Substitution of Eqs. (A.19) and (A.20) into Eqs. (3.3.14)-(3.3.16), (with $\zeta(t) = 0$)

$$\left(M_A\right)_{\theta_F} = -eN_B\left(\frac{1}{2}\rho ac\Omega^2 R^3\right)\left[\frac{-\mu_x\beta_0}{4} + \frac{\mu_y}{2}(\theta_0-\lambda) + \frac{\theta_c}{6} + \left(\frac{\dot\theta_R + \dot\theta_F}{6\Omega}\right) + \frac{\phi_R}{6}\right] \tag{3.3.17}$$

$$\left(M_A\right)_{\theta_F} = -eN_B\left(\frac{1}{2}\rho ac\Omega^2 R^3\right)\left[\frac{\mu_y\beta_0}{4} + \frac{\mu_x}{2}(\theta_0-\lambda) + \frac{\theta_s}{6} + \left(\frac{\dot\phi_F + \dot\phi_R}{6\Omega}\right) - \frac{\theta_R}{6}\right] \tag{3.3.18}$$

Combining Eqs. (3.3.12), (2.2.13), (2.2.17) and (2.2.18), we may write the equations for the total fuselage moment from the rotor shear force at the flapping hinge,

$$\left(M_e\right)_{\theta_F} = +e\left\{-\theta_R'\left(+\frac{a}{6}\right) - \phi_R'(\eta) + \theta_R\left(\frac{\eta}{2}\right) - \phi_R\left(\frac{a}{6}\right) - \theta_F'\left(\frac{\eta}{6}\right) - \phi_F'(\eta)\right.$$

$$\left. +\mu_x\left(\frac{a}{4}\beta_0\right) - \mu_y\left(\frac{a}{2}[\theta_0-\lambda]\right) - \theta_c\left(\frac{a}{6}\right) + \theta_R''\left(\frac{-\eta}{2}\right) + \theta_F''\left(\frac{-\eta}{2}\right)\right\} \tag{3.3.19}$$

$$\left(M_e\right)_{\varphi_F} = +c\left\{\theta_R'(\eta) - \phi_R'\left(\frac{\mathcal{A}}{6}\right) + \theta_R\left(\frac{\mathcal{A}}{6}\right) + \phi_R\left(\frac{\eta}{2}\right) + \theta_F'(\eta) - \phi_F'\left(\frac{\mathcal{A}}{6}\right)\right.$$

$$\left. -\mu_x\left(\frac{\mathcal{A}}{2}\left[\theta_0-\lambda\right]\right) - \mu_y\left(\frac{\mathcal{A}}{4}\beta_0\right) - \theta_s\left(\frac{\mathcal{A}}{6}\right) - \phi_F''\left(\frac{\eta}{2}\right) - \phi_R''\left(\frac{\eta}{2}\right)\right\} \qquad (3.3.20)$$

where

$$\mathcal{A} = \frac{1}{2}\rho a c N_B \Omega^2 R^3$$

$$\eta = \rho_B N_B \Omega^2 R^2/2$$

$$(\,)' = \frac{1}{\Omega}(\dot{})$$

Inplane Rotor Forces

The rotor produces drag as well as lift. The sources of this drag are the profile drag of the blades and the induced losses due to tilt of the local lift vector at each spanwise element. Although the profile drag was neglected in the blade equations of Chapter 2, it will be retained here to account for its effect on speed damping at hover. The induced drag terms which are proportional to rotor rate are very important in high speed climb as discussed in HA2.

The origin of the rotor inplane forces is shown in Fig. 3.3.2. The differential inplane forces are, for small inflow angle, φ ,

$$dF_x \approx d\mathfrak{D}[-\sin\psi] + d\mathfrak{L}[\beta\cos\psi - \varphi\sin\psi] \qquad (3.3.21)$$

$$dF_y \approx d\mathfrak{D}[-\cos\psi] - d\mathfrak{L}[\varphi\cos\psi + \beta\sin\psi] \qquad (3.3.22)$$

where

$$\varphi = \tan^{-1}\frac{u_p}{u_T} \approx u_p/u_T \ . \qquad (3.3.23)$$

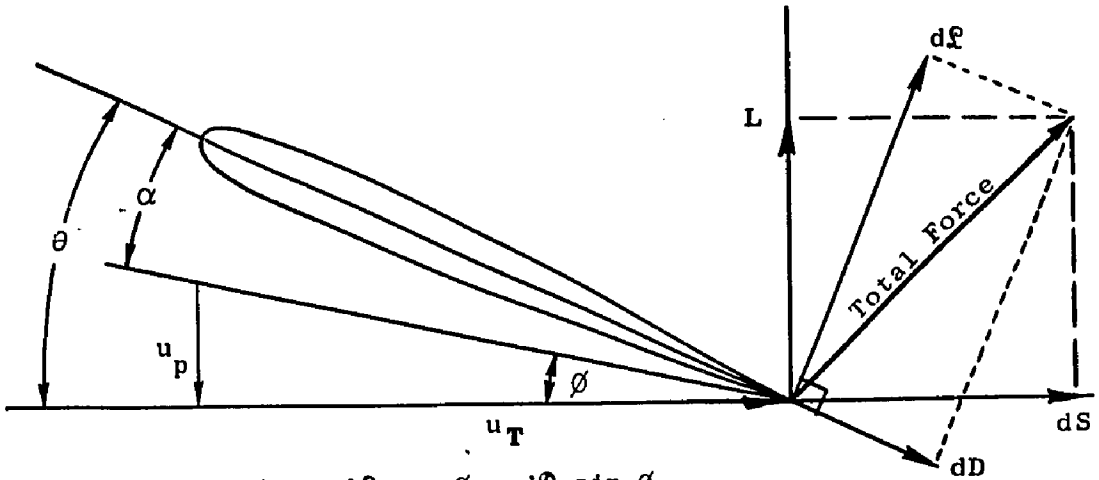

$$dL = d\mathfrak{L} \cos \phi - d\mathfrak{D} \sin \phi$$

$$dS = d\mathfrak{L} \sin \phi - d\mathfrak{D} \cos \phi$$

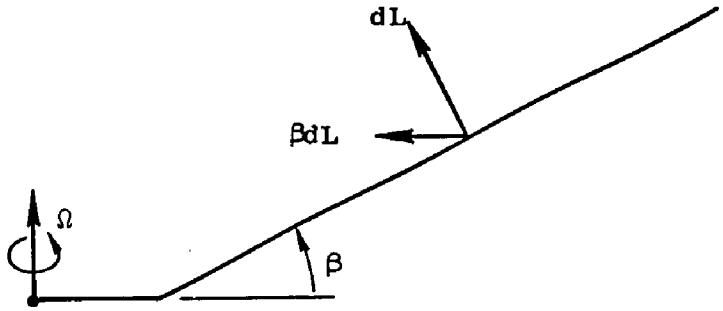

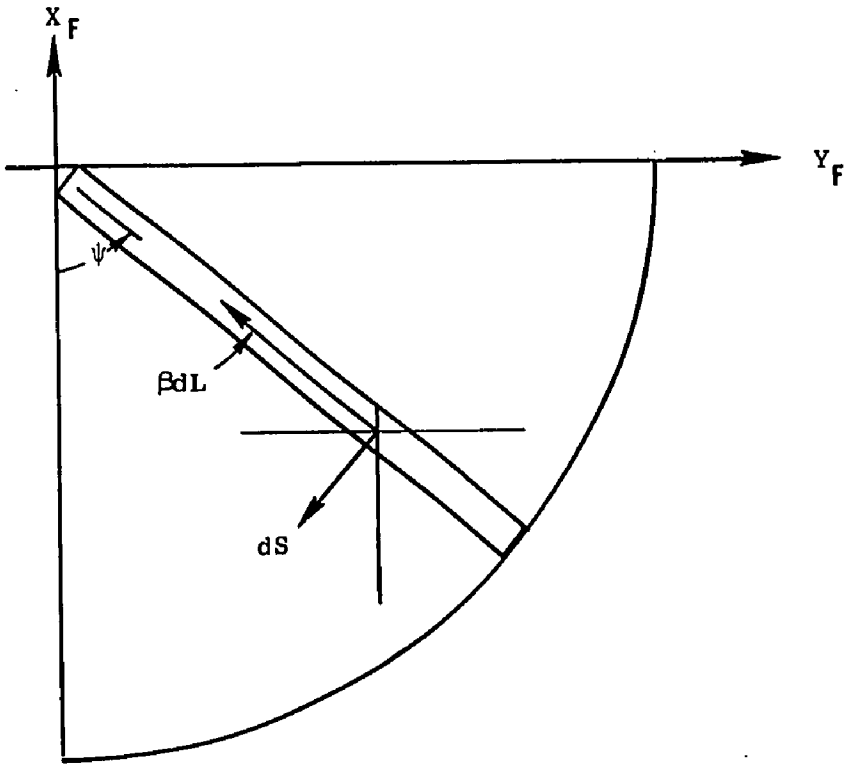

Fig. 3.3.2. SCHEMATIC OF INPLANE ROTOR FORCES

The profile drag is given by the approximation,

$$d\mathfrak{D} = \frac{1}{2}\rho abc\Omega^2 R^2 u_T^2 c_{d_o} \tag{3.3.24}$$

where c_{d_o} is the airfoil drag coefficient.

The integrated inplane forces are then,

$$F_{x_F} = \frac{1}{4\pi}\rho N_B c\Omega^2 R \int_0^{2\pi}\int_0^1 \left[a\left(\theta u_T^2 - u_p u_T\right)\left(\beta\cos\psi - u_p/u_T \sin\psi\right) - u_T^2 c_{d_o}\sin\psi\right] dx\, d\psi \tag{3.3.25}$$

$$F_{y_F} = \frac{1}{4\pi}\rho N_B c\Omega^2 R \int_0^{2\pi}\int_0^1 \left[-a\left(\theta u_T^2 - u_p u_T\right)\left(\beta\sin\psi + u_p/u_T\cos\psi\right) - u_T^2 c_{d_o}\cos\psi\right] dx\, d\psi\ . \tag{3.3.26}$$

Substitution of Eq. (3.2.1) into Eqs. (3.3.25) and (3.3.26), and integrating,

$$F_{x_F} = -\mu_x\left[\sigma a\left(\frac{c_{d_o}}{2a} + \frac{\theta_0\lambda}{2} + \frac{\beta_0^2}{4}\right)\right] + \mu_y\left[\frac{3}{2}\sigma a\beta_0\left(\frac{\theta_0}{2} - \lambda\right)\right] - \theta_R\left[T - \sigma a\frac{\lambda}{4}\right]$$

$$+ \phi_R\left[\sigma a\frac{\beta_0}{6}\right] + \theta'_R\left[\frac{\sigma a\beta_0}{6}\right] + \phi'_R\left[\sigma a\left(\frac{\theta_0}{6} - \frac{\lambda}{2}\right)\right] + \theta'_F\left[\frac{\sigma a\beta_0}{6}\right]$$

$$+ \phi'_F\left[\sigma a\left(\frac{\theta_0}{6} - \frac{\lambda}{2}\right)\right] + \theta_c\left[\frac{\sigma a\beta_0}{6}\right] - \theta_s\left[\sigma a\frac{\lambda}{4}\right] \tag{3.3.27}$$

$$F_{y_F} = -\mu_x\left[\frac{3}{4}\,a\beta_0\left(\frac{\theta_0}{2} - \lambda\right)\right] - \mu_y\left[a\left(\frac{c_{d_o}}{2a} + \frac{\theta_0\lambda}{2} + \frac{\beta_0^2}{4}\right)\right] + \theta_R\left[a\,\frac{\beta_0}{6}\right]$$

$$+ \phi_R\left[T - a\,\frac{\lambda}{4}\right] + \theta'_R\left[a\left(\frac{\theta_0}{6} - \frac{\lambda}{2}\right)\right] - \phi'_R\left[a\,\frac{\beta_0}{6}\right] + \theta'_F\left[a\left(\frac{\theta_0}{6} - \frac{\lambda}{2}\right)\right]$$

$$- \phi'_F\left[a\,\frac{\beta_0}{6}\right] - \theta_c\left[a\,\frac{\lambda}{4}\right] - \theta_s\left[a\,\frac{\beta_0}{6}\right]. \qquad (3.3.28)$$

The corresponding fuselage pitch and roll moments are then

$$\left(M_H\right)_{\theta_F} = -hF_{x_F} \qquad (3.3.29)$$

$$\left(M_H\right)_{\varphi_F} = hF_{y_F} \qquad (3.3.30)$$

Total Rotor Forces on Fuselage

The total moment on the fuselage from the rotor is

$$\left(M_{\theta_F}\right) = \left(M_{K_\beta}\right)_{\theta_F} + \left(M_e\right)_{\theta_F} + \left(M_H\right)_{\theta_F} \qquad (3.3.31)$$

$$\left(M_{\varphi_F}\right) = \left(M_{K_\beta}\right)_{\varphi_F} + \left(M_e\right)_{\varphi_F} + \left(M_H\right)_{\varphi_F} \qquad (3.3.32)$$

where the terms on the right hand side of Eq. (3.3.31) are Eqs. (3.3.6), (3.3.12) and (3.3.27), respectively, and the right hand side of Eq. (3.3.32) is found in Eqs. (3.3.7), (3.3.13), and (3.3.28), respectively.

The total longitudinal and lateral rotor forces are F_{x_F} and F_{y_F}, respectively.

The rotor aerodynamic forces have been derived in terms of μ_x and μ_y, nondimensionalized velocities in the rotor plane. In the vehicle axes, let u_F equal the longitudinal velocity and v_F the lateral velo-

city of the vehicle mass center. Then,

$$\mu_x = \bar{u} - h\theta_F' \tag{3.3.33}$$

$$\mu_y = \bar{v} + h\varphi_F' \tag{3.3.34}$$

where

$$\bar{u} = u_F/\Omega R \tag{3.3.35}$$

$$\bar{v} = v_F/\Omega R \ . \tag{3.3.36}$$

The equations (3.3.33)-(3.3.36) are substituted into the moment equations of Eqs. (3.3.31) and (3.3.32).

3.4 A Tenth Order Roll-Pitch-Horizontal Translation Model

Based on the derivations of the previous sections, the hovering vehicle may be modeled as two coupled rigid bodies. The rotor is modeled as an axially symmetric, spinning, "rigid" wing that can be tilted, but not displaced, with respect to the fuselage. The rotor thus has two degrees of freedom: pitch (θ_R) and roll (φ_R) relative to the fuselage. The fuselage itself is modeled as a rigid body with pitch inertia, I_{θ_F}, roll inertia, I_{φ_F}, and mass, m_v. The fuselage degrees of freedom are pitch (θ_F), roll (φ_F), and the velocity along the vehicle axes, $\bar{u}$ and $\bar{v}$. As discussed in the introduction, the vertical and directional motions of the fuselage are assumed decoupled from this roll-pitch-horizontal translation model of the vehicle. For notational convenience, this model will be termed the TRBM, or two rigid body model.

It is assumed that the displacement of the rotor mass center due to rotor tilt is negligible so that the vehicle center of mass is essentially fixed in the fuselage. In addition, this vehicle mass center is assumed to be located directly under the rotor hub. Then the equations for the TRBM are found by substituting Eqs. (3.3.31) and (3.3.32) into

$$I_{\theta_F}\theta_F'' = M_{\theta_F} \tag{3.4.1}$$

$$I_{\varphi_F}\varphi_F'' = M_{\varphi_F} \tag{3.4.2}$$

$$m_v\bar{u}' = F_{x_F} - m_v g\theta_F/\Omega^2 R \tag{3.4.3}$$

$$m_v\bar{v}' = F_{y_F} + m_v g\varphi_F/\Omega^2 R \tag{3.4.4}$$

where

$I_{\theta_F}, I_{\varphi_F}$ = pitch and roll inertias of vehicle

m_v = mass of vehicle

g = acceleration of gravity.

The result is Eqs. (3.4.5)-(3.4.10) below:

Fuselage Pitch and Roll

$$I_\theta'\theta_F'' = \bar{u}\left[\bar{h}B\left(\frac{c_{d_o}}{2a} + \frac{\theta_0\lambda}{2} + \frac{\beta_0^2}{4}\right) + \bar{e}B\left(\frac{\beta_0}{4}\right)\right] + \bar{v}\left[-\frac{3}{2}\bar{h}B\beta_0\left(\frac{\theta_0}{2} - \lambda\right) - \frac{\bar{e}B}{2}(\theta_0 - \lambda)\right]$$

$$+ \theta_R\left[\frac{hT}{\Omega^2} - \bar{h}B\frac{\lambda}{4} + \bar{e}\frac{P}{2} + \frac{N_s}{2}I_\beta\omega_F^2\right] + \varphi_R\left[-\left(\bar{h}\beta_0 + \bar{e}\right)\frac{B}{6}\right] + \theta_R'\left[-\left(\bar{h}\beta_0 + \bar{e}\right)\left(\frac{B}{6}\right)\right]$$

$$+ \varphi_R'\left[-\bar{h}B\left(\frac{\theta_0}{6} - \frac{\lambda}{2}\right) - \bar{e}P\right] + \theta_F'\left[-\left(\bar{h}\beta_0 + \bar{e}\right)\left(\frac{B}{6}\right) - \bar{h}^2B\left(\frac{c_{d_o}}{2a} + \frac{\theta_0\lambda}{2} + \frac{\beta_0^2}{4}\right) - \bar{h}\bar{e}B\left(\frac{\beta_0}{4}\right)\right]$$

(eq. cont.)

$$+ \phi_F' \left[-\bar{h}B\left(\frac{\theta_0}{6} - \frac{\lambda}{2}\right) - \bar{e}P - \frac{3}{2}\bar{h}^2 B\beta_0\left(\frac{\theta_0}{2} - \lambda\right) - \frac{\bar{h}\bar{e}B}{2}(\theta_0 - \lambda) \right] + \theta_R''\left(-\bar{e}\,\frac{P}{2}\right)$$

$$+ \theta_c\left[-\left(\bar{h}\beta_0 + \bar{e}\right)\left(\frac{B}{6}\right)\right] + \theta_s\left[\bar{h}B\,\frac{\lambda}{4}\right] \qquad (3.4.5)$$

$$I_{\phi_F}'\phi_F''' = \bar{u}\left[-\frac{3}{2}\,\bar{h}B\beta_0\left(\frac{\theta_0}{2} - \lambda\right) - \frac{\bar{e}B}{2}(\theta_0 - \lambda)\right] - \bar{v}\left[\bar{h}B\left(\frac{c_{d_o}}{2a} + \frac{\theta_0\lambda}{2} + \frac{\beta_0^2}{4}\right) + \frac{\bar{e}B}{4}\beta_0\right]$$

$$+ \theta_R\left[\left(\bar{h}\beta_0 + \bar{e}\right)\left(\frac{B}{6}\right)\right] + \phi_R\left[\frac{hT}{\Omega^2} - \bar{h}B\,\frac{\lambda}{4} + \frac{\bar{e}P}{2} + \frac{N_\beta}{2}I_\beta\omega_F^2\right] + \theta_R'\left[\bar{h}B\left(\frac{\theta_0}{6} - \frac{\lambda}{2}\right) + \bar{e}P\right]$$

$$- \phi_R'\left[\left(\bar{h}\beta_0 + \bar{e}\right)\left(\frac{B}{6}\right)\right] + \theta_F'\left[\bar{h}B\left(\frac{\theta_0}{6} - \frac{\lambda}{2}\right) + \bar{e}P + \frac{3}{2}\bar{h}^2 B\beta_0\left(\frac{\theta_0}{2} - \lambda\right) + \frac{\bar{e}\bar{h}B}{2}(\theta_0 - \lambda)\right]$$

$$+ \phi_F'\left[-\left(\bar{h}\beta_0 + \bar{e}\right)\left(\frac{B}{6}\right) - \bar{h}^2 B\left(\frac{c_{d_o}}{2a} + \frac{\theta_0\lambda}{2} + \frac{\beta_0^2}{4}\right) - \bar{e}\bar{h}\beta_0\left(\frac{B}{4}\right)\right]$$

$$- \phi_R''\left(\frac{\bar{e}P}{2}\right) - \theta_s\left[\left(\bar{h}\beta_0 + \bar{e}\right)\left(\frac{B}{6}\right)\right] - \theta_c\left[\bar{h}B\,\frac{\lambda}{4}\right] \qquad (3.4.6)$$

where

$$B = \frac{1}{2}\,\rho acNR^4$$

$$P = \frac{1}{2}\,\rho_B NR^3$$

$$I_\theta' = I_\theta\left(1 + \frac{\bar{e}P}{2}\right)$$

$$I_\phi' = I_\phi\left(1 + \frac{\bar{e}P}{2}\right)$$

$$\omega_R^2 = \left(\frac{K_\beta}{I_\beta/\Omega^2} - 1\right)$$

Fuselage Translation

$$m_v \bar{u}' = -\bar{u}\left[D\left(\frac{c_{d_o}}{2a} + \frac{\theta_0\lambda}{2} + \frac{\beta_0^2}{4}\right)\right] + \bar{v}\left[\frac{3}{2} D\beta_0\left(\frac{\theta_0}{2} - \lambda\right)\right] - \theta_R\left[\frac{T}{\Omega^2 R} - D\,\frac{\lambda}{4}\right]$$

$$+ \phi_R\left[D\,\frac{\beta_0}{6}\right] + \theta_R'\left[\frac{D\beta_0}{6}\right] + \phi_R'\left[D\left(\frac{\theta_0}{6} - \frac{\lambda}{2}\right)\right] + \theta_F'\left[\frac{D\beta_0}{6} + \bar{h}D'\left(\frac{c_{d_o}}{2a} + \frac{\theta_0\lambda}{2} + \frac{\beta_0^2}{4}\right)\right]$$

$$+ \phi_F'\left[D\left(\frac{\theta_0}{6} - \frac{\lambda}{2}\right) + \bar{h}D'\beta_0\left(\frac{\theta_0}{2} - \lambda\right)\right] + \theta_c\left[\frac{D\beta_0}{6}\right] - \theta_s\left[D\,\frac{\lambda}{4}\right] - \frac{m_v g}{\Omega^2 R}\,\theta_F \qquad (3.4.7)$$

$$m_v \bar{v}' = -\bar{u}\left[\frac{3}{2} D\beta_0\left(\frac{\theta_0}{2} - \lambda\right)\right] - \bar{v}\left[D\left(\frac{c_{d_o}}{2a} + \frac{\theta_0\lambda}{2} + \frac{\beta_0^2}{4}\right)\right] + \theta_R\left[D\,\frac{\beta_0}{6}\right] + \phi_R\left[\frac{T}{\Omega^2 R} - D\,\frac{\lambda}{4}\right]$$

$$+ \theta_R'\left[D\left(\frac{\theta_0}{6} - \frac{\lambda}{2}\right)\right] - \phi_R'\left[D\,\frac{\beta_0}{6}\right] + \theta_F'\left[D\left(\frac{\theta_0}{6} - \frac{\lambda}{2}\right) + \bar{h}\,\frac{3}{2} D'\beta_0\left(\frac{\theta_0}{2} - \lambda\right)\right]$$

$$+ \phi_F'\left[-D\,\frac{\beta_0}{6} - \bar{h}D'\left(\frac{c_{d_o}}{2a} + \frac{\theta_0\lambda}{2} + \frac{\beta_0^2}{4}\right)\right] - \theta_c\left[D\,\frac{\lambda}{4}\right] - \theta_s\left[D\,\frac{\beta_0}{6}\right] + \frac{m_v g}{\Omega^2 R}\,\phi_F \qquad (3.4.8)$$

where

$$D = \frac{1}{2}\,\rho a c N_B R^2$$

$$D' = \frac{1}{2}\,\rho a c N_B R^3 \ .$$

Rotor Pitch and Roll

$$\theta_R'' + \gamma'\theta_R' + \omega_R^2\theta_R + 2\phi_R' + \gamma'\phi_R + \theta_F''\left(1 + \frac{3}{2}\bar{h}\beta_0\right) + \gamma'\theta_F'\left(1 + \frac{4}{3}\bar{h}\beta_0\right)$$

$$+ \phi_F'\left[2\left(1 + \frac{3}{2}\frac{\bar{e}}{1-\bar{e}}\right) + \gamma'\bar{h}\left(\frac{8}{3}\theta_0 - 2\lambda\right)\right] - \frac{4}{3}\gamma'\beta_0\bar{u} + \gamma'\left(\frac{8}{3}\theta_0 - 2\lambda\right)\bar{v} = -\gamma'\theta_c$$

(3.4.9)

and,

$$\phi_R'' + \gamma'\phi_R' + \omega_R^2\phi_R - 2\theta_R' - \gamma'\theta_R + \phi_F''\left(1 + \frac{3}{2}\bar{h}\beta_0\right) + \gamma'\left(1 + \frac{4}{3}\beta_0\bar{h}\right)\phi_F'$$

$$+ \left(-2\left[1 + \frac{3}{2}\frac{\bar{e}}{1-\bar{e}}\right] - \bar{h}\gamma'\left[\frac{8}{3}\theta_0 - 2\lambda\right]\right)\theta_F' + \gamma'\left(\frac{8}{3}\theta_0 - 2\lambda\right)\bar{u} + \frac{4}{3}\gamma'\beta_0\bar{v} = -\gamma'\theta_s$$

(3.4.10)

Transformation to Canonical Form

It is desired to transform the six differential equations of the TRBM to the ten first order differential equations of the state

$$x' = Fx + G\theta_{con}$$

where

$$x^T = (\theta_R, \varphi_R, q_R, p_R, \theta_F, \varphi_F, q_F, p_F, \bar{u}, \bar{v})$$

$$\theta_{con}^T = (\theta_c, \theta_s)$$

and

$$q_R = \theta_R' \ , \quad p_R = \varphi_R' \ , \quad q_F = \theta_F' \ , \quad p_F = \varphi_F' \ , \quad \bar{u} = \frac{u}{\Omega R} \ , \quad \bar{v} = \frac{v}{\Omega R} \ ,$$

and

$$( )' = \frac{1}{\Omega} \frac{d}{dt} ( ) \ .$$

To effect this transformation, it is necessary to solve Eqs. (3.4.5), (3.4.6), (3.4.9), and (3.4.10) simultaneously for θ_F'',φ_F'',θ_R'' and φ_R''. Defining the right hand sides of these equations by

$$\mathcal{R} = \left(\mathcal{R}_{\ddot{\theta}_R} \mathcal{R}_{\ddot{\varphi}_R} \mathcal{R}_{\ddot{\theta}_F} \mathcal{R}_{\ddot{\varphi}_F} \right)^T \ ,$$

it is found that

$$(\theta_R'', \varphi_R'', \theta_F'', \varphi_F'')^T = \mathcal{B}\mathcal{R} \tag{3.4.11}$$

where

$$\mathcal{B} = \begin{bmatrix} \frac{1}{1 - A_1 B_1} & 0 & \frac{-B_1}{1 - A_1 B_1} & 0 \\ 0 & \frac{1}{1 - A_2 B_1} & 0 & \frac{-B_1}{1 - A_2 B_1} \\ \frac{A_1}{1 - A_1 B_1} & 0 & \frac{1}{1 - A_1 B_1} & 0 \\ 0 & \frac{-A_2}{1 - A_2 B_1} & 0 & \frac{1}{1 - A_2 B_1} \end{bmatrix} \tag{3.4.12}$$

and $A_1 = \bar{e}P/2I'_\theta$, $A_2 = \bar{e}P/2I'_\phi$, $B_1 = 1 + (3/2)\bar{h}\beta_0$.

In the hover analysis, the equation (3.4.7) is programmed to form the canonical state equations.

TRBM Eigensystem for a Vehicle with a Fully Articulated Rotor

In Table 3.4.1 the elements of the 10X10 matrix F and the 10X2 matrix G are given for a Sikorsky S-61 helicopter. For controls fixed ($\theta_c = \theta_s = 0$) , the characteristic frequencies (eigenvalues) computed using this F matrix are shown in Table 3.4.1 and Fig. 3.4.1. The eigenvalues computed for this vehicle in a hover study by Sikorsky engineers (C01) are also shown in Table 3.4.2 and it is apparent that there is reasonable agreement.

The controls-fixed response of this vehicle is characterized by two pairs of unstable low frequency oscillatory roots, a pair of stable low frequency oscillatory roots, and two pairs of higher frequency, highly damped oscillatory roots. These latter roots are associated with the coupled responses of the rotor modes. The high frequency mode is associated with nutation of the rotor plane while the lower frequency is associated with the precession of the rotor plane.

The unstable roots are well known to VTOL pilots, while their low frequency does allow their manual control, it is tedious and tiring. The low frequency stable fuselage oscillation is a pitch-roll mode. In most analyses, the longitudinal and lateral degrees of freedom are decoupled, which yields two real roots instead of this coupled pitch-roll oscillatory root.

The eigenvectors corresponding to the eigenvalues of Table 3.4.2 are shown in Figs. 3.4.2 and 3.4.3. The eigenvector components are identified by the state to which they correspond. By definition, if the initial conditions of the system are proportional to the eigenvector corresponding to any eigenvalue, s_i , then only the mode involving $e^{s_i t}$ is excited [ZA1]. For example, if the initial condition is $\varphi_F = 1.0$, $\theta_F \cong$

Table 3.4.1. ELEMENTS OF 10×10 F MATRIX AND 10×2 G MATRIX FOR S-61 SIKORSKY HELICOPTER (TRBM)

```
  MU = C.CO     VELOCITY =     C.000 KNCTS
   RCTOR CT=   0.0055958          2CT/AS=   0.0250150          INFLCW RATIO=   0.0528953
    TRIM COLLECTIVE=    8.8457758 DEGS.          CCNING=   5.9117521 CEGS.
**********************************************************************************************
OPEN LOCP DYNAMICS MATRIX....     CMBS=     0.07895   C1=      0.00545   C2=      0.00000
   0.00000   0.00000   1.00000   0.00000   C.00000   0.00000   0.00000   0.00000   0.00000   0.00000
   0.00000   0.00000   0.00000   1.00000   0.00000   0.00000   0.00000   0.00000   0.00000   0.00000
  -0.09114  -1.32520  -1.32520  -2.00018  -0.00000  -0.00000  -1.36378  -2.24605   0.18065  -0.40564
   1.31886  -0.12477   2.00066  -1.31886  -C.00000  -0.00000   2.25010  -1.35626  -0.40474  -0.17519
  -0.00000  -0.00000  -0.00000  -0.00000  -0.00000  -0.00000   1.00000   0.00000   0.00000   0.00000
   0.00000   0.00000   0.00000   0.00000   0.00000   0.00000   0.00000   1.00000   0.00000   0.00000
   0.01096  -0.00207  -C.00207   0.00016   0.00000   0.00000  -0.00245   0.00132   0.00178  -0.00029
   0.00777   0.04121  -0.00059  -0.00777  -0.00000  -0.00000  -0.00496  -0.00920  -0.00109  -0.00669
  -0.00108   0.00158   C.00158  -0.00007  -C.00229  -0.00000   0.00672   0.00222  -0.00078   0.00034
   0.00158   0.00108  -C.00007  -0.00158  -C.00000   0.00229   0.00222  -0.00672  -0.00034  -0.00078
THE CONTROL DISTRIBUTION MATRIX IS....
     -0.00000000        -0.00000000
     -0.00000000        -0.00000000
     -1.32520204        -0.10323382
      0.01215588        -1.31886200
     -0.00000000        -0.00000000
     -0.00000000        -0.00000000
     -0.00206652         0.00290812
     -0.01093157        -0.00776800
      0.00157533        -0.00121140
      0.00121140         0.00157533
```

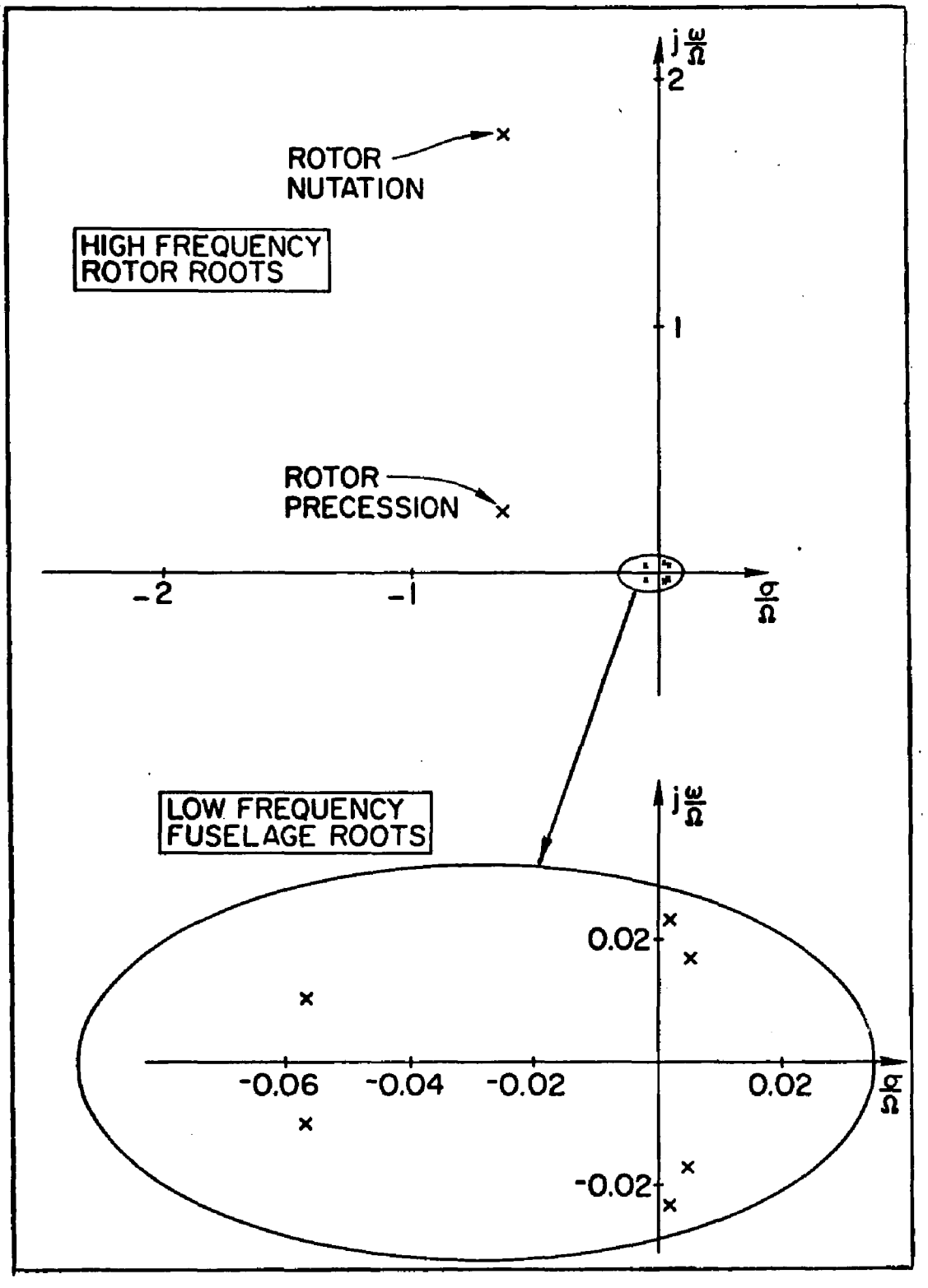

Fig. 3.4.1. CONTROLS FIXED EIGENVALUES FOR 10 × 10 F MATRIX OF TABLE 3.4.1 (TRBM).

Table 3.4.2. COMPARISON OF ROOTS OF 10TH ORDER HOVER MODEL--TRBM AND REF. CO1

	TRBM	(Ref. CO. 1)
1	(.660) ± j(1.79)	-(.64) ± j(1.81)
2	-(.619) ± j(0.245)	-(.60) ± j(0.21)
3	-(.0571) ± j(.0118)	-(.057) ± j(.012)
4	+(.0051) ± j(.0170)	+(.0047) ± j(.018)
5	+(.0017) ± j(.0234)	+(.002) ± j(.024)

0.6 , and $\theta_R \cong 0.2$, then only the fuselage pitch-roll mode corresponding to $s = -.0571 \pm j(.0118)$ will be excited (cf. Fig. 3.4.2, top figure). For reference, the modes are numbered. Modes 1 and 2 are the rotor precessional and nutational modes, respectively. Modes 3, 4, and 5 are fuselage modes. The large magnitude separation of the respective components requires separate scaling in order to portray the relative sizes. M denotes the relative magnitude of the eigenvector length to that of the largest eigenvector, whose length is normalized to unity. Eigenvector components with magnitude less than 0.001 of the largest component are not shown. For the purpose of this discussion, component eigenvectors with relative magnitude greater than or equal to 0.1 are denoted as principal modes.

Table 3.4.2 summarizes the "mode shapes" (eigenvectors) for each eigenvalue (in descending order left to right). The highest frequency mode, the rotor nutation, contains almost no fuselage motions, whereas the rotor precession mode contains some slight fuselage motion. The pitch-roll fuselage motions of the third mode contain significant rotor motions.

The fourth and fifth modes are principally fuselage modes, with only slight rotor motions.

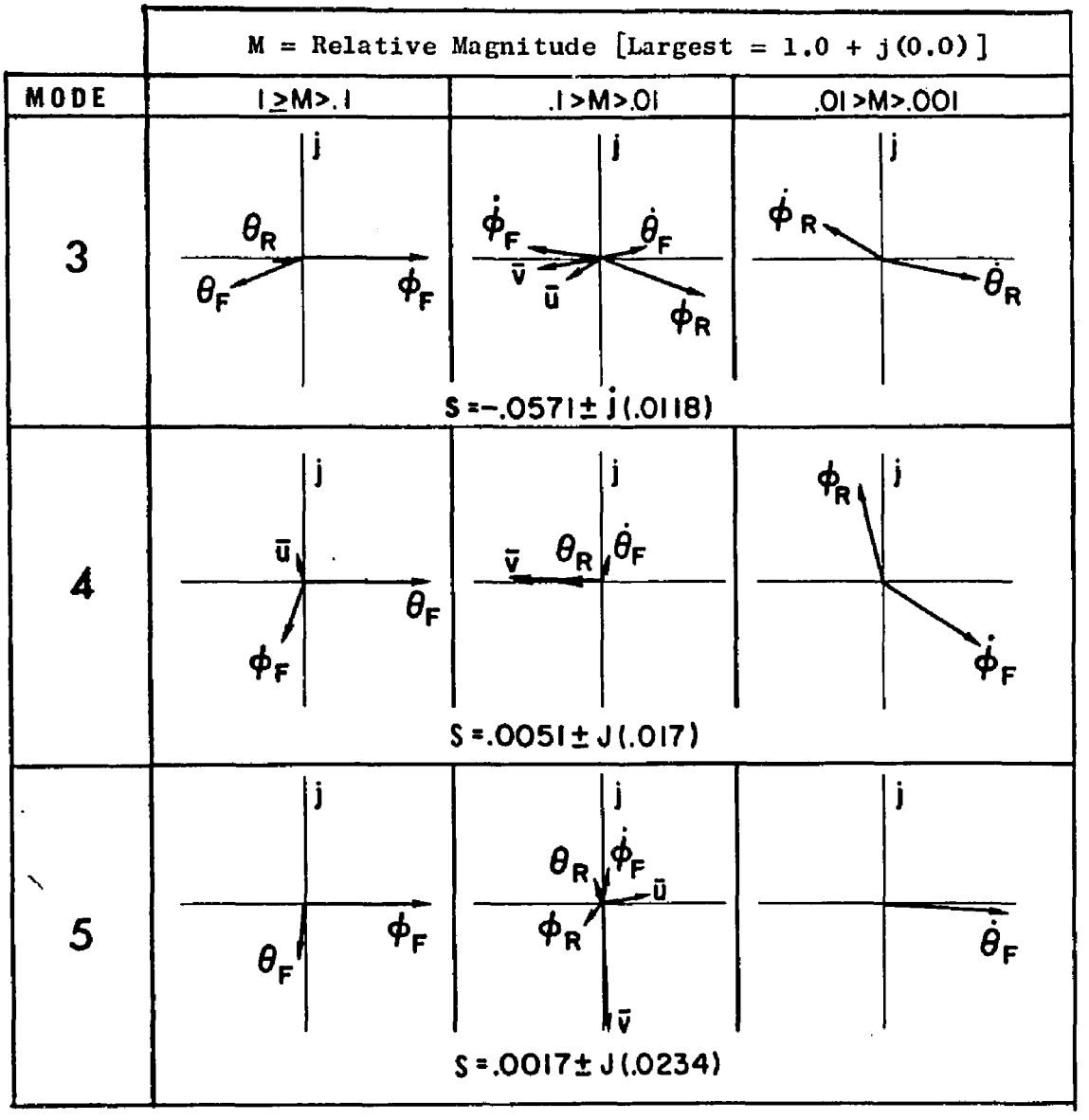

Fig. 3.4.2. OPEN LOOP LOW FREQUENCY EIGENVECTORS FOR TENTH ORDER MODEL (TRBM). (Note: Time measured in units of $1/\Omega$ and velocities in terms of rotor tip speed). The modes are identified by the numbers in the left hand column:
Mode 3: Fuselage Pitch-Roll
Mode 4: Fuselage Pitch-Roll-Longitudinal Velocity
Mode 5: Fuselage Roll-Pitch-Lateral Velocity

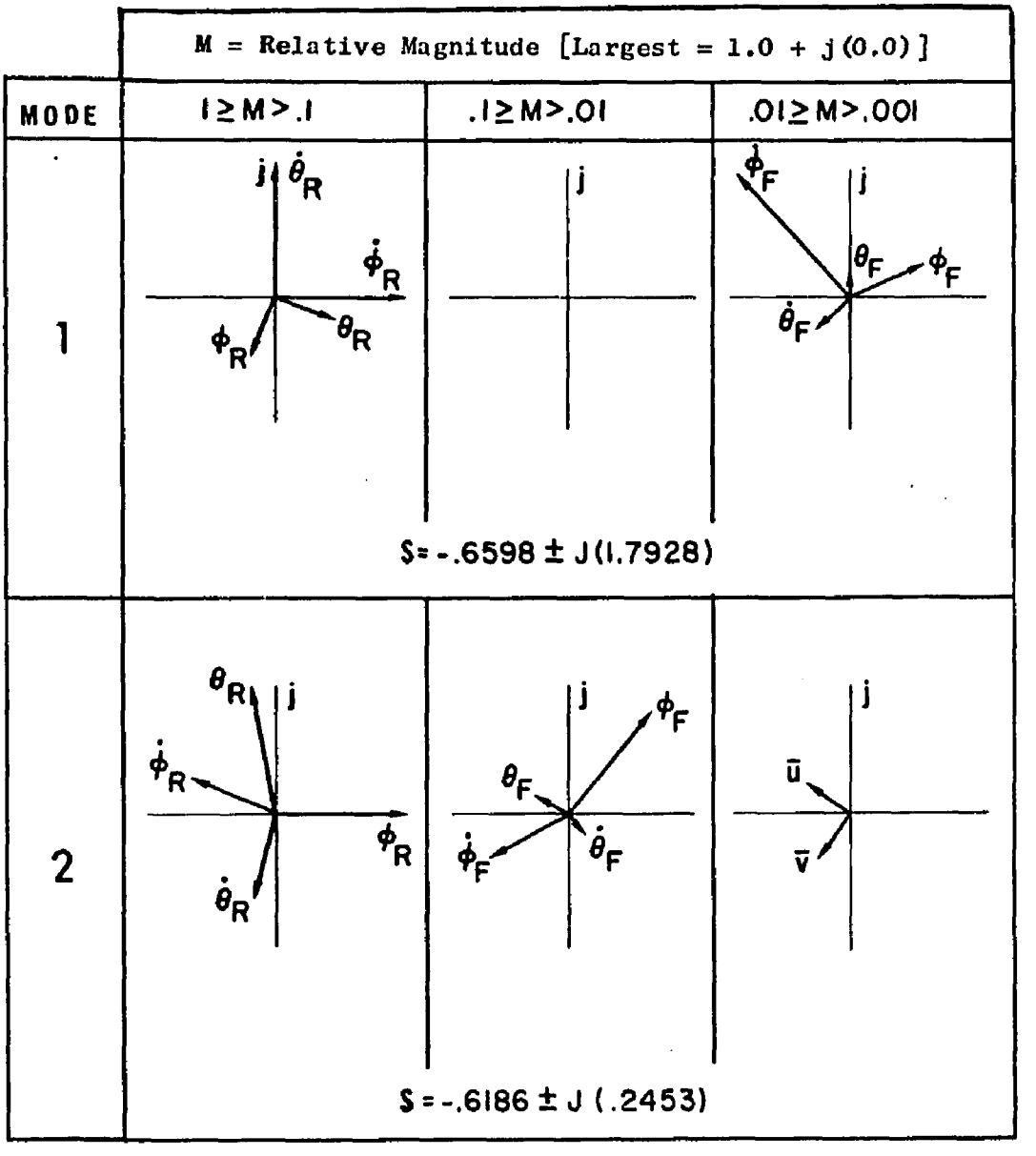

Fig. 3.4.3. OPEN LOOP HIGH FREQUENCY EIGENVECTORS FOR TENTH ORDER MODEL (TRBM). The rotor modes are:
Mode 1: Rotor Nutational
Mode 2: Rotor Precessional
The fuselage state makes no contribution to the principal rotor modes 1 and 2.

Table 3.4.3. RELATIVE MODE SHAPES OF 10TH ORDER OPEN LOOP EIGENVECTORS

		M = Relative Magnitude [Largest = 1.0 ± j(0.0)]			
Mode	s	$.1 < M \leq 1$	$.01 < M \leq .1$	$.001 < M \leq .01$	$.0001 < M \leq .001$
1	-.660 ± j(1.79	$p_R, q_R, \phi_R, \theta_R$	-----	$p_F, \phi_F, q_F, \theta_F$	$\bar{u}$, $\bar{v}$
2	-.617 ± j(.24)	$\phi_R, \theta_R, p_R, q_R$	$\phi_F, p_F, \theta_F, q_F$	$\bar{u}$, $\bar{v}$	---
3	-.057 ± j(.0119)	$\phi_F, \theta_F, \theta_R$	$\phi_R, p_F, \bar{v}, \bar{u}, q_F$	q_R, p_R	---
4	.005 ± j(.017)	$\theta_F, \phi_F, \bar{u}$	$\bar{v}, \theta_R, q_F$	p_F, ϕ_R	q_R, p_R
5	.00017 ± j(.0234)	ϕ_F, θ_F	$\bar{v}, \bar{u}, p_F, \theta_R, \phi_R$	q_F	q_R, p_R

3.5 Rotor Rate (Eighth Order) and Rotor Position (Sixth Order) Roll-Pitch Horizontal Translation Models

Most helicopter controller designs which have been reported represent the rotor dynamics of Eqs. (3.4.9)-(3.4.10) by lower order approximations. Such approximations have been justified by the large separation of rotor frequencies from the fuselage frequencies. The two most common lower order assumptions are:

(i) The "quasi-static" model or "rotor position" model, generally attributed to Hohenemser (HO1). In effect it is assumed that the rotor tip-path-plane can be tilted instantaneously, i.e., θ_R, φ_R are controlled instantaneously by θ_s, θ_c. The forces and moments on the fuselage due to θ_R' and φ_R' are neglected.

(ii) The "precession" or "rotor rate" model, suggested by Miller. It is obtained by neglecting θ_R'' and φ_R'', but retaining the rotor precessional terms θ_R' and φ_R' in both the rotor and fuselage equations. In effect, this produces a "first order lag" between (θ_c, θ_s) and (θ_R, φ_R).

The relationship between the complete rotor equations and the precessional and quasi-static representations is shown in Table 3.5.1.

For this investigation, these lower order assumptions are used in a slightly more general manner. The rotor rate model (RRM) is defined by neglecting $\ddot{\theta}_R$ and $\ddot{\varphi}_R$ but retaining the nutation and precessional rate terms of the rotor response in both θ_R and φ_R. From Eqs. (3.4.9)-(3.4.10), the RRM rotor equations are

$$\theta_R' = \frac{1}{\gamma'^2+4}\left[\left(2-\dot{\omega}_R^2\right)\gamma'\theta_R + \left(2\omega_R^2-\gamma'^2\right)\varphi_R + \left(-4 + 6\,\frac{\bar{e}}{1-\bar{e}} - \gamma'^2 + \bar{h}\gamma'\left[2\alpha^* - \frac{4}{3}\,\gamma'\beta_0\right]\right)\theta_F' \right.$$

(eq. cont.)

$$+\left(\bar{h}\gamma'\left[\frac{8}{3}\beta_0-\gamma'\alpha^*\right]-3\frac{\bar{e}}{1-\bar{e}}\right)\phi_F'+\left(\frac{4}{3}\gamma'\beta_0-2\alpha^*\right)\gamma'\bar{u}$$

$$+\left(\frac{8}{3}\beta_0\gamma'-\gamma'^2\alpha^*\right)\bar{v}-\gamma'^2\theta_c+2\gamma'\theta_s\Bigg] \qquad (3.5.1)$$

$$\phi_R'=\frac{1}{\gamma'^2+4}\left[\left(-\gamma'^2-2\omega_R^2\right)\theta_R-(2+\omega_R^2)\gamma'\phi_R+\left(3\frac{\bar{e}}{1-\bar{e}}+\bar{h}\gamma'\left[\frac{8}{3}\beta_0-\gamma'\alpha^*\right]\right)\theta_F'\right.$$

$$-\left\{4\left(1+\frac{3}{2}\frac{\bar{e}}{1-\bar{e}}\right)+\gamma'^2+\bar{h}\left(2\alpha^*+\frac{4}{3}\gamma'\beta_0\right)\right\}\phi_F'$$

$$\left.+\left(\frac{8}{3}\beta_0+\alpha^*\gamma'\right)\gamma'\bar{u}-\left(2\alpha^*+\frac{4}{3}\gamma'\beta_0\right)\gamma'\bar{v}-2\gamma'\theta_c-\gamma'^2\theta_s\right] \qquad (3.5.2)$$

where

$$\alpha^*=\frac{8}{3}\theta_0-2\lambda$$

$$\gamma'=\gamma/8\ .$$

These two equations are then substituted into the equations (3.4.5) through (3.4.8) to eliminate rotor rate terms in the fuselage equations. The resulting eighth order system is the RRM.

Equations (3.5.1) and (3.5.2) may be reduced to Miller's precession model by neglecting the nutation damping of θ_R and φ_R, to yield

$$\theta_R' = \frac{1}{2}\left[-\gamma'\theta_R - \left\{2\left(1 + \frac{3}{2}\frac{\bar{e}}{1-\bar{e}}\right) - \bar{h}\gamma'\alpha^*\right\}\theta_F' + \gamma'\left(1 + \frac{4}{3}\beta_0\bar{h}\right)\phi_F'\right.$$

$$\left. -\gamma'\alpha^*\bar{u} + \frac{4}{3}\gamma'\beta_0\bar{v} + \gamma'\theta_s\right] \qquad (3.5.3)$$

$$\phi_R' = \frac{1}{2}\left[-\gamma'\phi_R - \gamma'\left(1 + \frac{4}{3}\bar{h}\beta_0\right)\theta_F' - \left\{2\left(1 + \frac{3}{2}\frac{\bar{e}}{1-\bar{e}}\right) + \gamma'\bar{h}\alpha^*\right\}\phi_F'\right.$$

$$\left. + \left(\frac{4}{3}\gamma'\beta_0\right)\bar{u} - \gamma'\alpha^*\bar{v} - \gamma'\theta_c\right] \qquad (3.5.4)$$

The lowest order approximation is the sixth order rotor position model (RPM). This is obtained from Eqs. (3.4.9) and (3.4.10) by neglecting all terms in the rotor and fuselage equations which contain rotor acceleration and rate. Then the rotor equations become:

$$\theta_R' = \frac{1}{\omega_R^4 + \gamma'^2}\left[\left\{\bar{h}\gamma'^2\alpha^* - \gamma'\omega_R^2\left(1 + \frac{4}{3}\bar{h}\beta_0\right) - 2\gamma'\left(1 + \frac{3}{2}\frac{\bar{e}}{1-\bar{e}}\right) + \bar{h}\gamma'^2\alpha^*\right\}\theta_F'\right.$$

$$+ \left\{-2\omega_R^2\left(1 + \frac{3}{2}\frac{\bar{e}}{1-\bar{e}}\right) - \omega_R^2\gamma'\bar{h}\alpha^* + \gamma'^2\left(1 + \frac{4}{3}\beta_0\bar{h}\right)\right\}\phi_F'$$

$$\left. + \left\{\frac{4}{3}\gamma'\omega_R^2\beta_0 - \gamma'^2\alpha^*\right\}\bar{u} + \left\{\frac{4}{3}\gamma'^2\beta_0 - \omega_R^2\gamma'\alpha^*\right\}\bar{v} - \omega_R^2\gamma'\theta_c + \gamma'^2\theta_s\right]$$

(3.5.5)

$$\phi'_R = \frac{1}{\omega_R^4+\gamma'^2}\left[\left\{2\omega_R^2\left(1+\frac{3}{2}\frac{\bar{e}}{1-\bar{e}}\right)-\bar{h}\gamma'\alpha^*\omega_R^2-\gamma'^2\left(1+\frac{4}{3}\bar{h}\beta_0\right)\right\}\theta'_F\right.$$

$$+\left\{-2\gamma'\left(1+\frac{3}{2}\frac{\bar{e}}{1-\bar{e}}\right)-\gamma'^2\bar{h}\alpha^*-\gamma'\omega_R^2\left(1+\frac{4}{3}\bar{h}\beta_0\right)\right\}\phi'_F$$

$$\left.+\left\{\frac{4}{3}\gamma'^2\beta_0+\gamma'\omega_R^2\alpha^*\right\}\bar{u}+\left\{-\gamma'^2\alpha^*-\frac{4}{3}\gamma'\omega_R^2\beta_0\right\}\bar{v}-\gamma'^2\theta_c-\gamma'\omega_R^2\theta_s\right] \tag{3.5.7}$$

These equations are then substituted into the fuselage equations to eliminate the rotor completely from the system representation.

The F and G matrices for the sixth and eighth order models are shown in Tables 3.5.2 and 3.5.3. Note they are not simply partitions of the F and G matrices of the tenth order system.

Characteristic Frequencies and Modes for the Sixth and Eighth Order Models

The characteristic frequencies computed for the three models of the S-61 helicopter are shown in Table 3.5.4. This table demonstrates that, for this aircraft (with no hub restraint), the neglect of rotor dynamics has little effect on the characteristic frequencies of the fuselage modes. The RRM yields lower real and imaginary parts for the rotor precession frequency. Also the highest frequency of the RPM differs significantly from the corresponding frequency of the complete model.

The mode shapes for the RPM and RRM are shown in Figs. 3.5.1 and 3.5.2. The low frequency modes for each eigenvalue are almost the same as for the complete system. The mode shapes are summarized in Table 3.5.5.

The mode shapes of the lowest frequency fuselage modes also show little dependence on the particular model calculated. The most observable

Table 3.5.1. REPRESENTATION OF ROTOR DYNAMICS

Model	$\dot{x} = Ax + Gu$	$x(s) = H(s)\,u(s)$
Complete Rotor	$\begin{pmatrix} \dot{\theta}_R \\ \dot{\phi}_R \\ \dot{q}_R \\ \dot{p}_R \end{pmatrix} = \begin{pmatrix} 0 & 0 & 1 & 0 \\ 0 & 0 & 0 & 1 \\ -\omega_R^2 & -\gamma' & -\gamma' & -2 \\ \gamma' & -\omega_R^2 & 2 & -\gamma' \end{pmatrix} \begin{pmatrix} \theta_R \\ \phi_R \\ q_R \\ p_R \end{pmatrix} + \begin{pmatrix} 0 & 0 \\ 0 & 0 \\ -1 & 0 \\ 0 & -1 \end{pmatrix} \begin{pmatrix} \gamma'\theta_c \\ \gamma'\theta_s \end{pmatrix}$	$\begin{pmatrix} \theta_R \\ \phi_R \end{pmatrix} = \frac{\gamma'}{\left[s^2 + \gamma' s + \omega_R^2\right]^2 + \left[2s + \gamma'\right]^2} \begin{pmatrix} \left[s^2 + 2\gamma' s + \omega_R^2\right] & 2s + \gamma' \\ -2s - \gamma' & -\left[s^2 + 2\gamma' s + \omega_R^2\right] \end{pmatrix} \begin{pmatrix} \theta_c \\ \theta_s \end{pmatrix}$
Rotor Rate	$\begin{pmatrix} \dot{\theta}_R \\ \dot{\phi}_R \end{pmatrix} = \begin{pmatrix} 0 & -\gamma'/2 \\ -\gamma'/2 & 0 \end{pmatrix} \begin{pmatrix} \theta_R \\ \phi_R \end{pmatrix} + \frac{\gamma'}{2} \begin{pmatrix} -1 & 0 \\ 0 & -1 \end{pmatrix} \begin{pmatrix} \theta_c \\ \theta_s \end{pmatrix}$	$\begin{pmatrix} \theta_R \\ \phi_R \end{pmatrix} = \gamma' \begin{pmatrix} 0 & \frac{1}{2s + \gamma'} \\ \frac{-1}{2s + \gamma'} & 0 \end{pmatrix} \begin{pmatrix} \theta_c \\ \theta_s \end{pmatrix}$
Rotor Position	$\begin{pmatrix} \theta_R \\ \phi_R \end{pmatrix} = \begin{pmatrix} \theta_s \\ -\theta_c \end{pmatrix}$	$\begin{pmatrix} \theta_R \\ \phi_R \end{pmatrix} = \begin{pmatrix} \theta_s \\ -\theta_c \end{pmatrix}$

Table 3.5.2. ELEMENTS OF 8×8 F MATRIX AND 8×2 G MATRIX FOR ROTOR RATE MODEL (RRM)
(States are θ_R, ϕ_R, θ_F, ϕ_F, q_F, p_F, $\bar{u}$, $\bar{v}$)

```
  MU = 0.00     VELOCITY =     0.000 KNOTS
   ROTOR CT=    0.0055556          2CT/AS=    0.0250150          INFLOW RATIO=    0.0528953
    TRIM COLLECTIVE=    8.8457758 DEGS.          CONING=    5.9117521 DEGS.
**********************************************************************************************
OPEN LOOP DYNAMICS MATRIX....     OMBS=      0.07895   C1=       0.00545   C2=       0.00000
  -0.47894   -0.27843   -0.00000   -0.00000   -1.12396   -0.06279    0.18298   -0.03014
   0.27843   -0.47894   -0.00000   -0.00000    0.06279   -1.12396   -0.03014   -0.18298
  -0.00000   -0.00000   -0.00000   -0.00000    1.00000    0.00000    0.00000    0.00000
   0.00000    0.00000    0.00000    0.00000    0.00000    1.00000    0.00000    0.00000
   0.01189   -0.00155   -0.00000   -0.00000   -0.00011    0.00193    0.00138   -0.00026
   0.00570    0.04368    0.00000    0.00000   -0.00708   -0.00041   -0.00094   -0.00508
  -0.00185    0.00117   -0.00229   -0.00000    0.00495    0.00219   -0.00049    0.00031
   0.00117    0.00185    0.00000    0.00229    0.00219   -0.00495   -0.00031   -0.00049
THE CONTROL DISTRIBUTION MATRIX IS....
     -0.30582747          0.46075702
     -0.46075702         -0.30582747
     -0.00000000         -0.00000000
     -0.00000000         -0.00000000
     -0.00149421          0.00189147
     -0.00694610         -0.00548726
      0.00112379         -0.00046548
      0.00195731          0.00202687
```

Table 3.5.3. ELEMENTS OF 6×6 F MATRIX AND 6×2 G MATRIX FOR ROTOR POSITION MODEL (RPM)
(States are θ_F, ϕ_F, q_F, p_F, $\bar{u}$, $\bar{v}$)

```
   MU = 0.00     VELOCITY =     0.000 KNOTS

   ROTOR CT=    0.0055958          2CT/AS=    0.0250150          INFLOW RATIO=    0.0528953
    TRIM COLLECTIVE=    8.8457758 DEGS.          CONING=    5.9117521 DEGS.
*****************************************************************************************
OPEN LOOP DYNAMICS MATRIX....     CMRS=     0.07895    C1=      0.00545   C2=      0.00000
     0.00000      0.00000      1.00000      0.00000      0.00000      0.00000
     0.00000      0.00000      0.00000      1.00000      0.00000      0.00000
     0.00000      0.00000     -0.02022      0.01570      0.00492      0.00165
     0.00000      0.00000     -0.05767     -0.07425      0.00604     -0.01807
    -0.00229     -0.00000      0.00723     -0.00163     -0.00093     -0.00028
    -0.00000      0.00229     -0.00163     -0.00723      0.00028     -0.00093
THE CONTROL DISTRIBUTION MATRIX IS....
     -0.00000000        -0.00000000
     -0.00000000        -0.00000000
     -0.00065129         0.01393479
     -0.00070598        -0.00239175
      0.00006956        -0.00238110
     -0.00045174         0.00305175
```

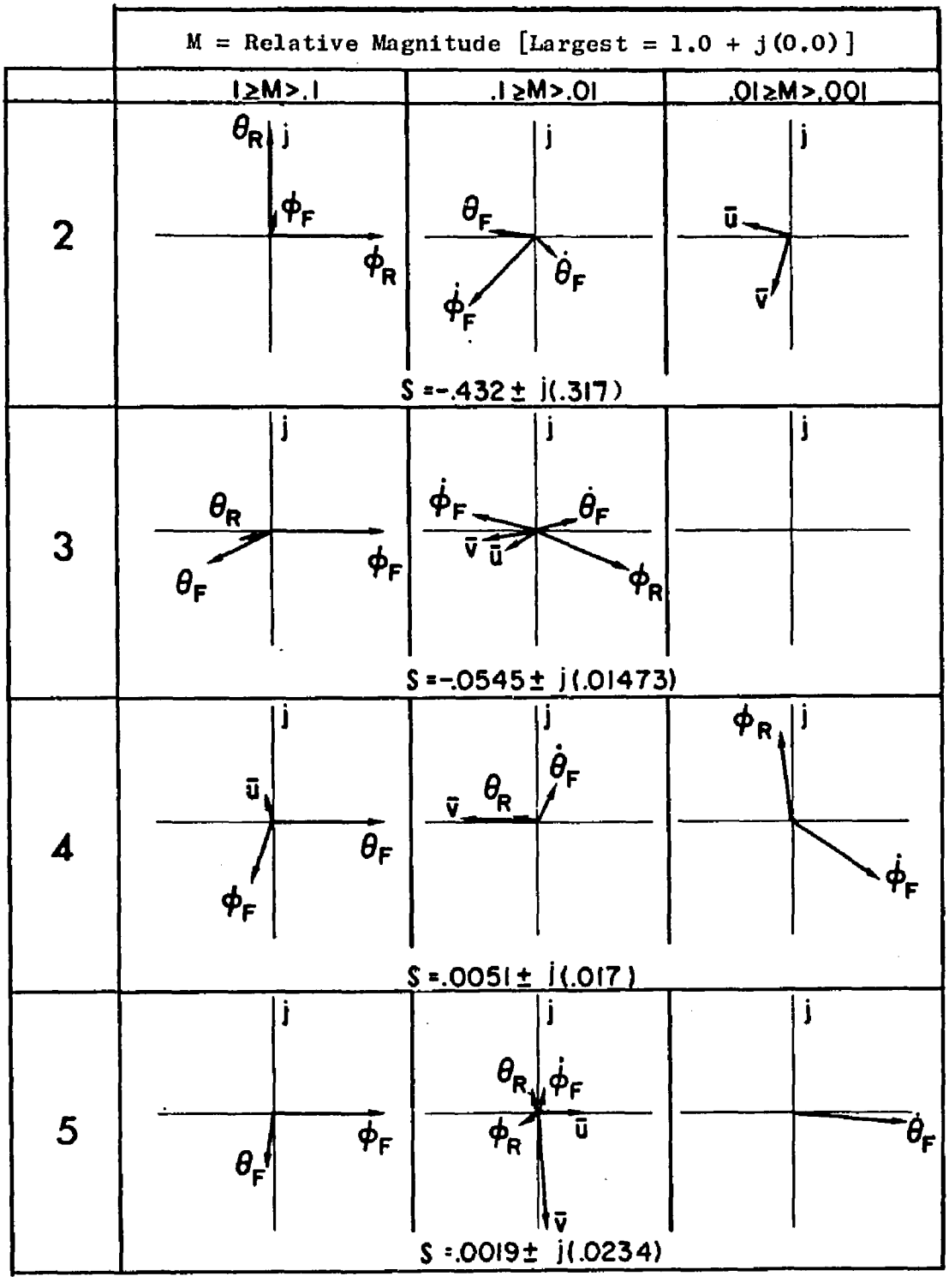

Fig. 3.5.1. OPEN LOOP EIGENVECTORS FOR EIGHTH ORDER MODEL (RRM) (cf. Figs. 3.4.2 and 3.4.3). The principal nutation mode of the rotor (mode 2) has a fuselage roll contribution of about 10 per cent of the rotor roll. The fuselage modes (3, 4, 5) are about the same as for the TRBM.

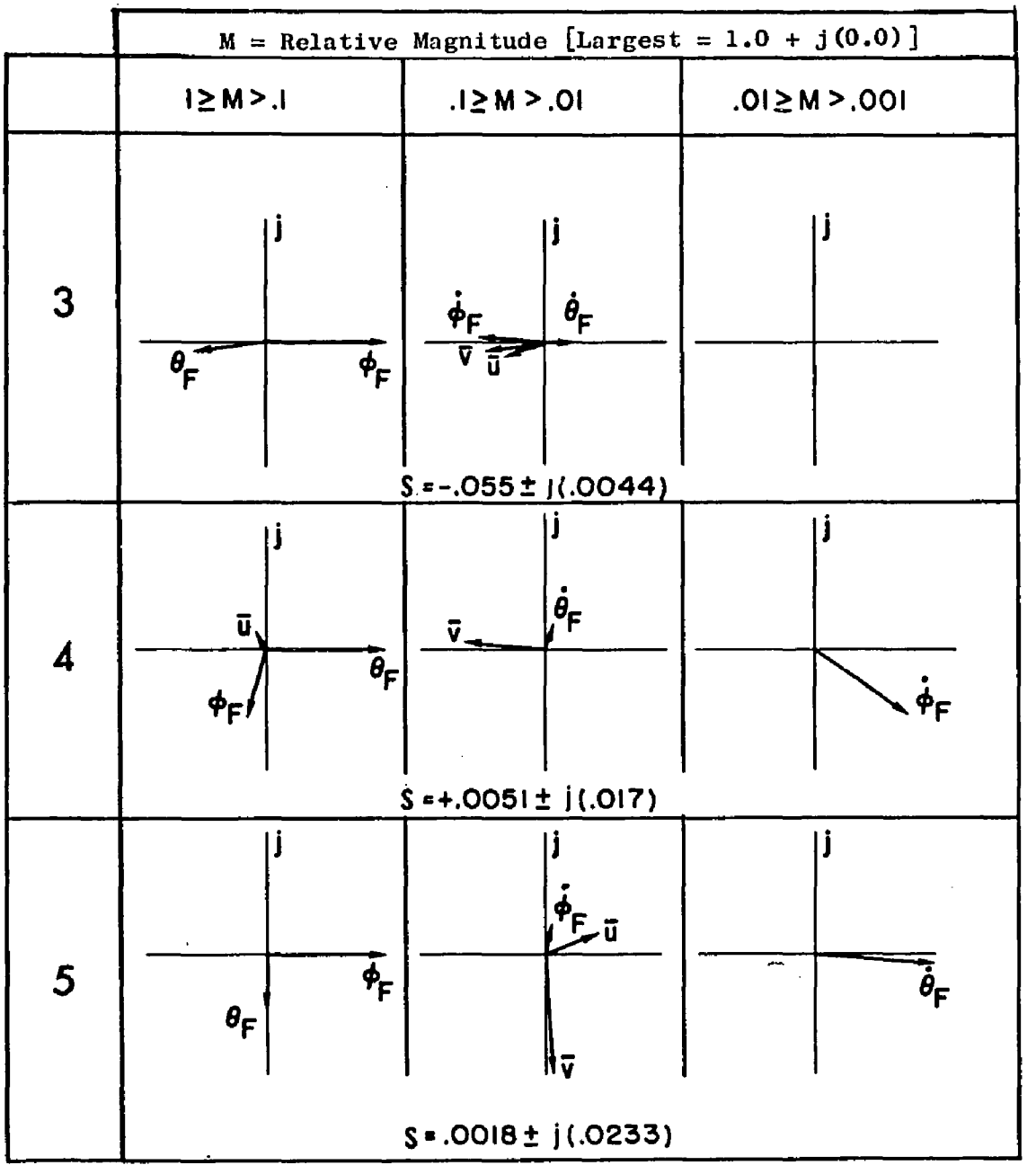

Fig. 3.5.2. OPEN LOOP EIGENVECTORS FOR SIXTH ORDER MODEL (RPM) (cf. Figs. 3.4.2 and 3.4.3). The fuselage modes (3, 4, 5) are almost the same as for RRM and TRBM.

Table 3.5.4. EFFECT OF REDUCED ORDER ROTOR APPROXIMATIONS ON HOVER CHARACTERISTIC FREQUENCIES

	Two Rigid Body Model (TRBM)	Rotor Rate Model (RRM)	Rotor Position Model (RPM)
1	-.660 ± j(1.793)	-----	-----
2	-.619 ± j(0.245)	-.432 ± j(.317)	-----
3	-.057 ± j(0.012)	-.055 ± j(.015)	-.055 ± j(.0044)
4	+.0051 ± j(0.017)	+.0051 ± j(.017)	+.0051 ± j(.017)
5	+.0017 ± j(0.023)	+.0019 ± j(.023)	+.0018 ± j(.023)

Table 3.5.5. OPEN LOOP EIGENVECTORS FOR RRM AND RPM

	Open Loop Eigenvectors for RRM			
	s	$.1 < M \leq 1$	$.01 < M \leq .1$	$.001 < M \leq .01$
2	-.432 ± j(.316)	ϕ_R, θ_R, ϕ_F	p_F, θ_F, q_F	$\bar{u}$, $\bar{v}$
3	-.054 ± j(.015)	$\phi_F, \theta_F, \theta_R$	$\phi_R, p_F, \bar{v}, \bar{u}, q_F$	----
4	+.0051 ± j(.017)	$\theta_F, \phi_F, \bar{u}$	$\bar{v}$, θ_R, q_F	p_F, ϕ_F
5	+.0019 ± j(.023)	ϕ_F, θ_F	$\bar{v}, \bar{u}, p_F, \theta_R, \phi_R$	q_F
	Open Loop Eigenvectors for RPM			
	s	$.1 < M \leq 1$	$.01 < M \leq .1$	$.001 < M \leq .01$
3	-.055 ± j(.0044)	ϕ_F, θ_F	$p_F, \bar{v}, \bar{u}, q_F$	----
4	+.005 ± j(.017)	$\theta_F, \phi_F, \bar{u}$	$\bar{v}$, q_F	p_F
5	+.0018 ± j(.023)	ϕ_F, θ_F	$\bar{v}, \bar{u}, q_F$	q_F

differences occur in the pitch-roll mode with the eigenvalue whose real part is about -.05. This mode, which depends more strongly on the rotor dynamics, does show a variation in imaginary part, although only a slight variation in the fuselage response.

3.6 Eigensystem Analysis of a Hypothetical Hingeless Rotored Vehicle

The fully articulated model of Section 3.5 demonstrated that the rotor dynamics have little effect on the open loop response of the fuselage. In this section, a hypothetical modification of that vehicle will be made. It is assumed that a very stiff blade restraint is added which is equivalent to increasing the blade flapping natural frequency, ω_F, to $\sqrt{3}\Omega$. An offset, $\bar{e}$, of .05 is retained. Such a representation is valid for a hingeless rotor near hover where higher harmonic modes of the blade bending are small.

The open loop root plot for the tenth order TRBM, as a function of $(\omega_F/\Omega)^2$ is shown in Fig. 3.6.1.* The increase in rotor fuselage coupling by increasing the blade stiffness causes the pitch-roll eigenvalues to become real and increases the damping in the fuselage modes. However, the low frequency rotor mode becomes less stable.

The effect on the open loop dynamics for $(\omega_F/\Omega)^2 = .3$ is evaluated for the TRBM, RRM, and RPM models in Table 3.6.1 and Figs. 3.6.2 through 3.6.5.

Table 3.6.1 indicates little change on the low frequency fuselage eigenvalues as the model is reduced, although the real roots of the pitch-roll mode decrease noticeably in the RPM calculation. An examination of the eigenvectors of mode 3 shows that the mode corresponding to the more stable of the two eigenvalues has a higher contribution from roll relative to pitch as we go from the RRM to the RPM.

---

*The characteristic equation of the TRBM cannot be factored into the form

$$1 + \left(\frac{\omega_F}{\Omega}\right)^2 G = 0 \ .$$

Thus Fig. 3.6.1 is <u>not</u> a conventional "root locus" plot.

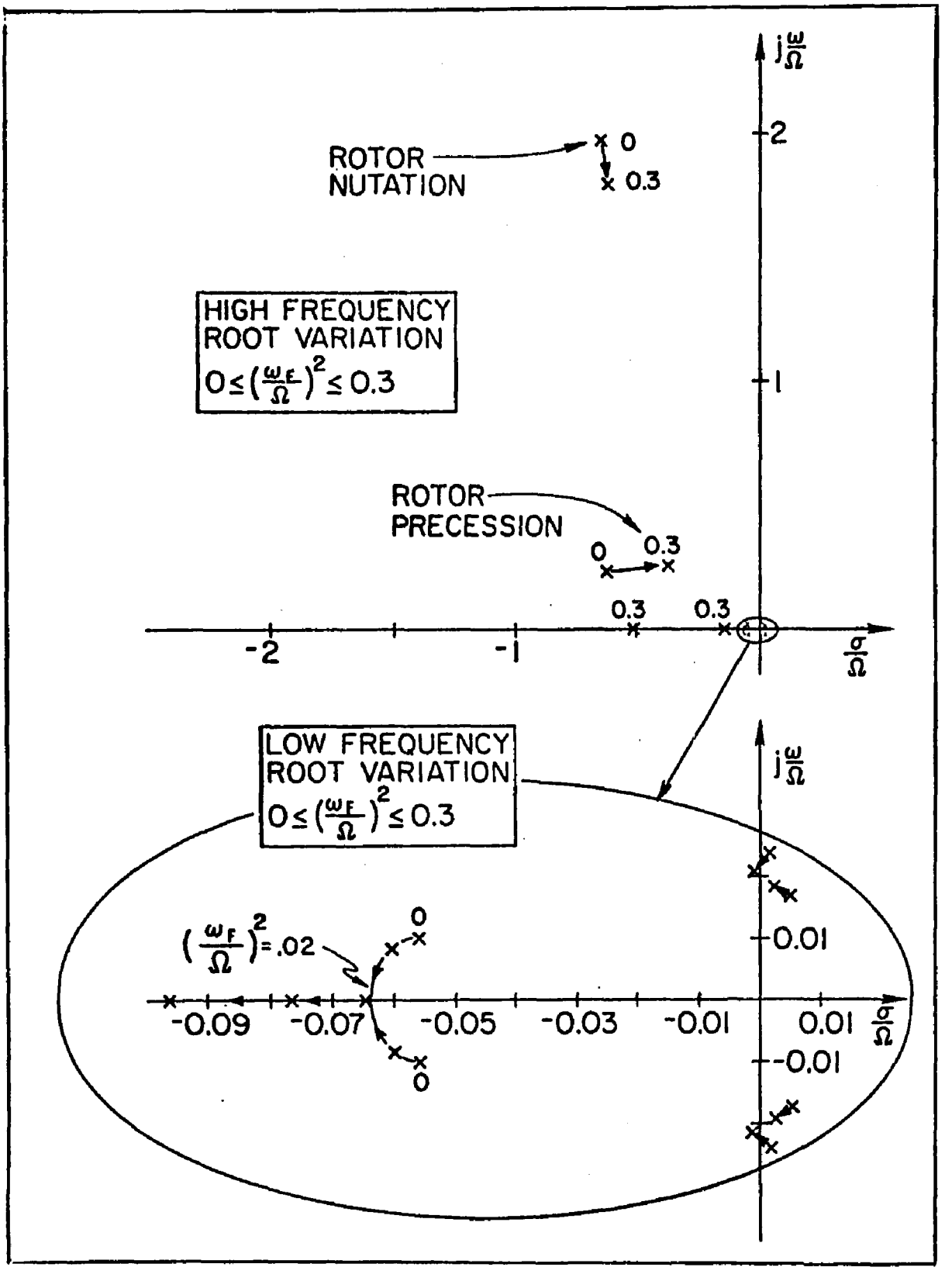

Fig. 3.6.1. CONTROLS-FIXED EIGENVALUES OF TRBM WITH HINGELESS ROTOR.

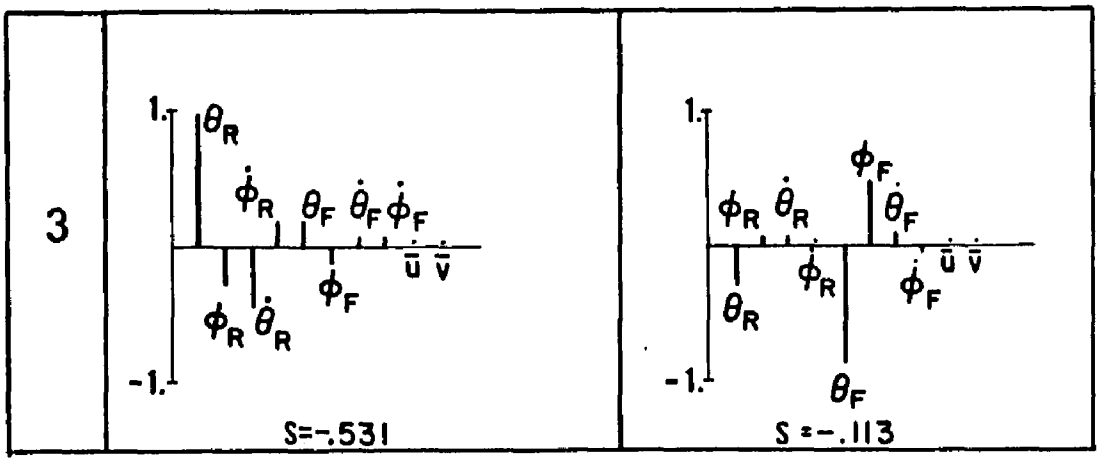

(Bar graph of relative state contributions to the real eigenvectors of fuselage pitch roll mode. Real eigenvector components normalized by square root of sum of squares of components.)

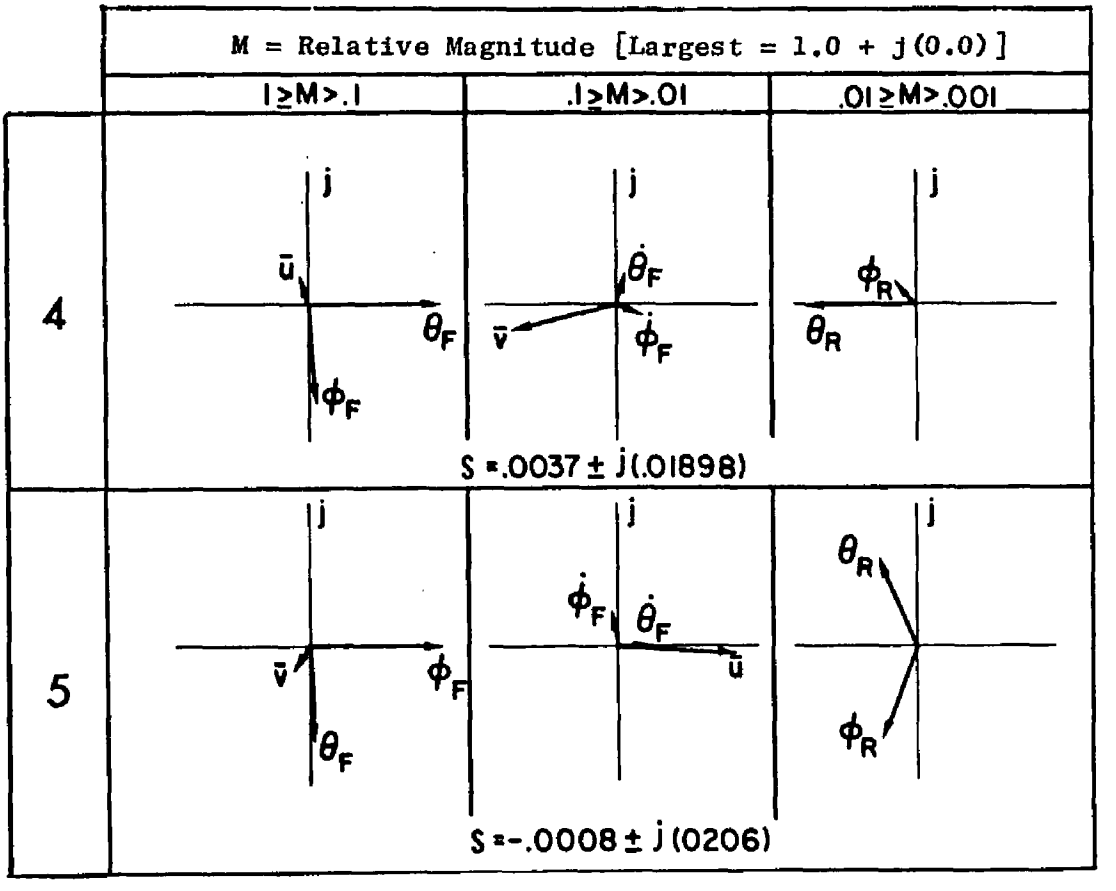

Fig. 3.6.2. OPEN LOOP LOW FREQUENCY EIGENVECTORS FOR TENTH ORDER HYPOTHETICAL HINGELESS-ROTORED MODEL (TRBM). The fuselage pitch-roll mode (3) consists of real eigenvectors.

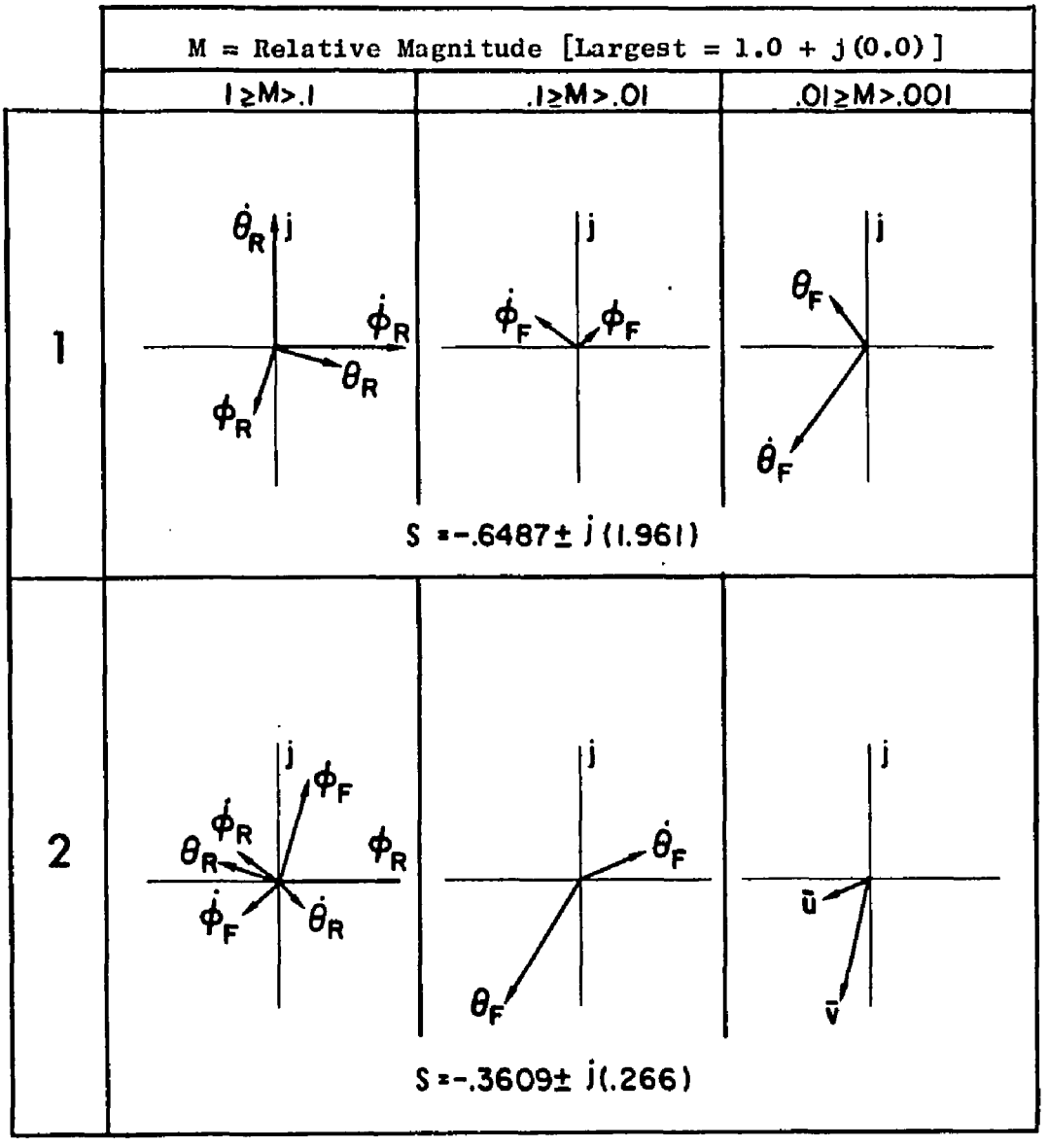

Fig. 3.6.3. OPEN LOOP HIGH FREQUENCY EIGENVECTORS FOR HINGELESS ROTOR TRBM. The rotor nutation mode has large contributions from fuselage roll angle and rate as opposed to the same mode for the articulated rotor model.

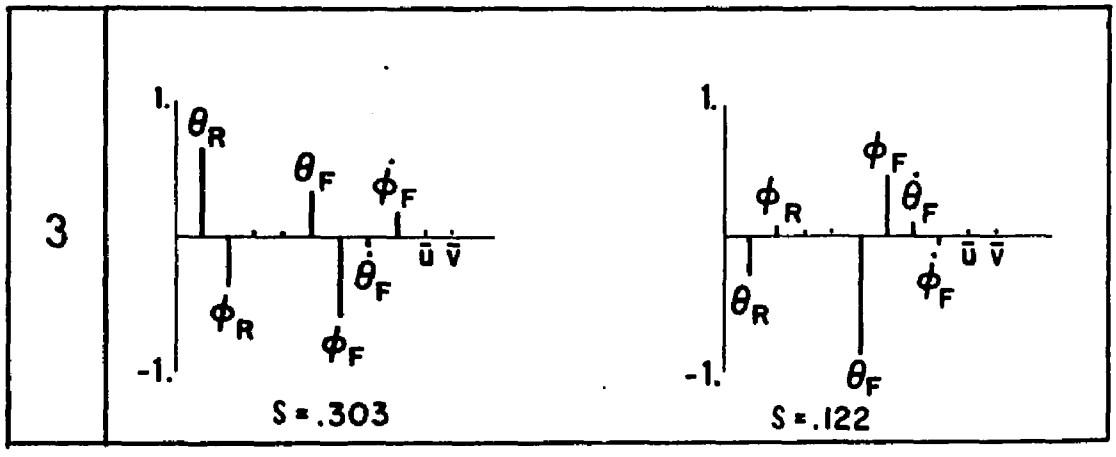

(Bar graph of relative state contributions to the real eigenvectors of fuselage pitch roll mode. Real eigenvector components normalized by square root of sum of squares of components.)

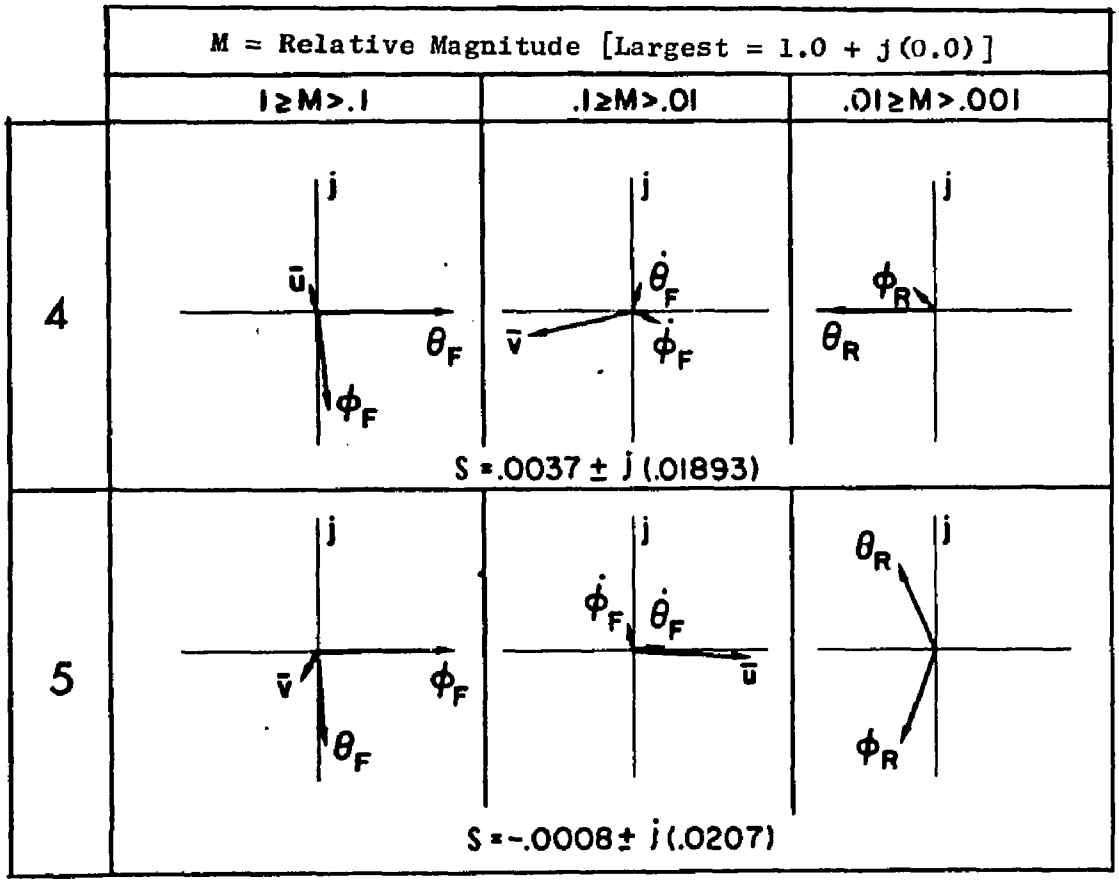

Fig. 3.6.4. OPEN LOOP LOW FREQUENCY EIGENVECTORS FOR EIGHTH ORDER HINGELESS ROTOR MODEL (RRM). The fuselage eigenvectors are nearly the same as for the hingeless rotor TRBM (cf. Fig. 3.6.2).

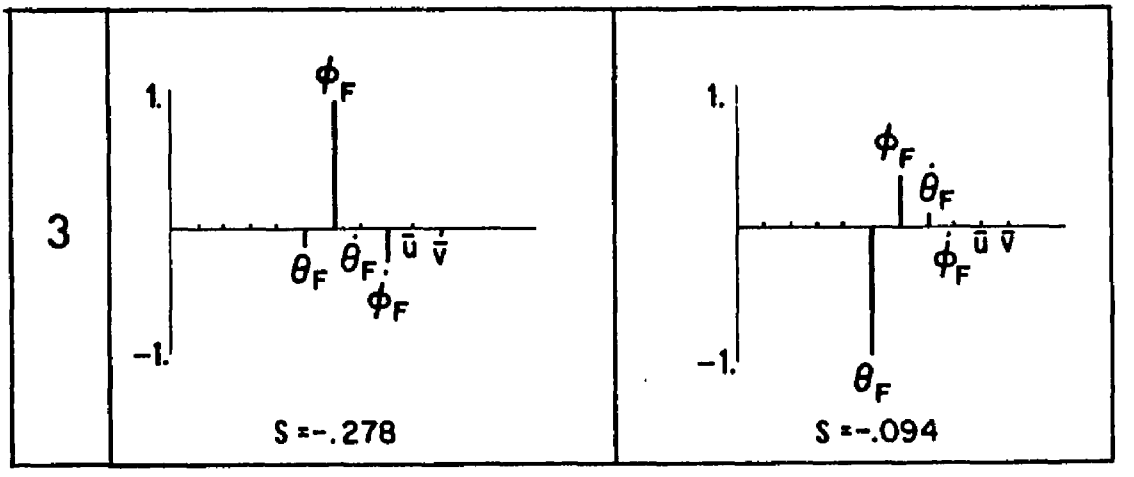

(Bar graph of relative state contributions to the real eigenvectors of fuselage pitch roll mode. Real eigenvector components normalized by square root of sum of squares of components.)

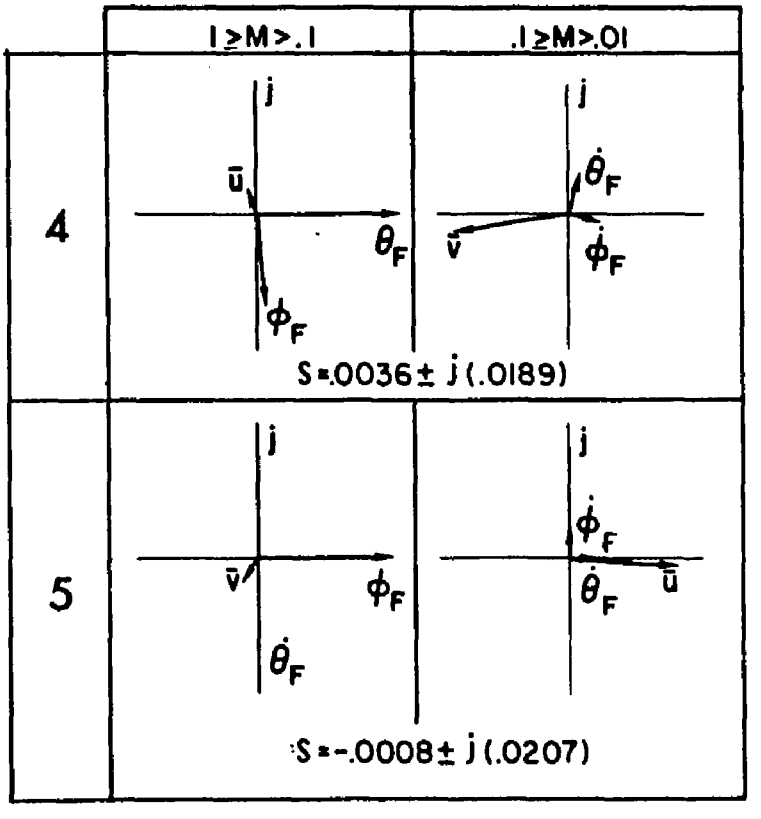

Fig. 3.6.5. OPEN LOOP LOW FREQUENCY EIGENVECTORS FOR SIXTH ORDER HINGELESS ROTOR MODEL (RPM). The fuselage pitch-roll mode (3) has a higher contribution from fuselage roll angle than either the TRBM or RRM.

Table 3.6.1. COMPARISON OF HYPOTHETICAL HINGELESS ROTORED TRBM CHARACTERISTIC FREQUENCIES WITH REDUCED ROTOR MODEL FREQUENCIES.

TRBM	RRM	RPM
$-.649 \pm j(1.961)$	---	---
$-.361 \pm j(0.266)$	$-.340 \pm j(0.341)$	---
$-.531$	$-.303$	$-.278$
$-.113$	$-.122$	$-.094$
$+.0037 \pm j(0.019)$	$+.0037 \pm j(0.019)$	$+.0036 \pm j(0.019)$
$-.0008 \pm j(0.021)$	$-.0008 \pm j(0.021)$	$-.0008 \pm j(0.021)$

3.7 Summary

The two rigid body model of the longitudinal-lateral translation and pitch-roll dynamics of a hovering rotary-wing VTOL are derived in this chapter. The equations for this model are referenced to fuselage axes. This model is used to calculate the controls-fixed natural response of a helicopter with an articulated rotor and with a hingeless rotor. The response consists of two high frequency rotor modes and three lower frequency fuselage modes. Each mode is decomposed into the relative eigenvector contribution from each state of the model.

Rotor-fuselage coupling is most evident in the highest frequency fuselage mode, which consists mostly of fuselage pitch and roll. The model response with a fully articulated rotor or a hingeless rotor shows that a component of rotor pitch with relative eigenvector magnitude of about 15 per cent of the largest fuselage state eigenvector (c.f. Figs. 3.4.2 and 3.6.2). Whereas the low frequency rotor precession mode is almost uncoupled from the fuselage in the articulated rotor model, the stronger mechanical coupling of the hingeless rotor model has a rotor precessional mode consisting of fuselage, as well as rotor, pitch-roll natural response. In both rotor models, the high frequency rotor natural mode is almost uncoupled from the fuselage response. Similarly, the low frequency fuselage modes are nearly uncoupled from the rotor modes.

The effect of reduced order rotor models on rotor-fuselage coupling is most pronounced on frequency on the fuselage pitch-roll mode. For the

articulated rotor model, the fuselage state contribution to the eigenvectors of the fuselage modes is nearly the same for the full rotor model, the rotor rate model, and the rotor position model. However, although the real parts of the fuselage eigenvalues are about the same in the fuselage modes, the imaginary part of the fuselage pitch-roll mode for the sixth order model is an order of ten lower than for the complete model (cf. Figs. 3.4.2, 3.5.1, and 3.5.2). The fuselage pitch-roll mode for the hingeless rotor model consists of only real eigenvalues and eigenvectors. The real eigenvalues of this mode are changed significantly by reduction of the rotor model, although the mode shades are nearly the same (cf. Figs. 3.6.2, 3.6.3, and 3.6.4). For the complete model, the fuselage pitch-roll eigenvalues are -.531 and -.113, while for the sixth order mode, they become -.303 and -.122, respectively.

Chapter IV

COMPUTATIONAL ASPECTS OF MODAL ANALYSIS AND CONTROL SYNTHESIS

4.1 Introduction

The theory of the design of controls for linear multivariable systems is well developed. Various techniques for linearization of nonlinear systems have greatly expanded the applicability of these design methods (BR1). Basically, modern techniques of control synthesis consist of quadratic synthesis methods and of pole assignment methods. The latter methods seek to determine the feedback control gains on system state variables to obtain some preselected eigenvalues ("poles"). The former methods are based on the minimization of a quadratic functional, wherein the specification of weighting coefficients determines the feedback control gains. Both methods are iterative. The pole assignment to a specific closed-loop pole pattern or the choice of a particular set of weighting coefficients may require unrealistic control responses or produce excessive excursions in some state variables, and new poles or weighting coefficients may have to be selected.

Solution Methods of the Matrix Riccati Equation

The iterative nature of design by quadratic synthesis is frequently cited as a disadvantage. Selection of weighting coefficients and solution of the associated matrix Riccati equation may have to be performed several times in order to determine a satisfactory closed loop response. However, there are certain initial guesses at the coefficients which reduce the iterative cycle (BR1). In addition, new and efficient techniques for solution of the matrix Riccati equation have been developed which reduce the labor of obtaining the closed loop response.

The most direct method of solving the matrix Riccati equation is simply by integrating the equation from a specified boundary condition to steady state, which exists uniquely if the system is observable and controllable (KA1).

A related method (KA2) is solution by approximate quadrature. This

technique is characterized by the determination of the transition matrix of the $2n \times 2n$ matrix of the state and the adjoint equations over an interval. Most simply, it is found (BR1) that the solution of the Riccati equation may be written as:

$$S(t) = \Lambda(t)\ X(t)^{-1} , \qquad (4.1.1)$$

where $\Lambda(t)$ and $X(t)$ are $n \times n$ submatrices of the transition matrix of the state and adjoint equations. Computationally, t is a discrete sequence with preselected intervals of Δt . The solution process is then one of iterating on $S(t)$ until some steady value is attained.

An alternate approach (KL1) solves the matrix Riccati equation by reducing it to a general linear matrix equation, which is solved iteratively for the steady state solution.

All of these methods suffer from the same disadvantage. Specifically, if the eigenvalues of the closed-loop system are widely separated, the convergence and accuracy of the algorithms become dependent on smaller iteration intervals, and solutions are attained with longer computation times.

Such problems are avoided for constant coefficient systems by a method based on the modal analysis of the $2n \times 2n$ state and adjoint equations. The theoretical basis of these methods was established by McFarland (MC1) and Potter (PO1), and is known most generally as Potter's Method. The method is also discussed in (OD1) and (VA1). The following sections present a summary of the modal analysis along with new derivations and details of the implementation developed for studies of succeeding chapters.

4.2 Quadratic Synthesis Using Matrix Riccati Equations

The following discussion presents the quadratic synthesis method with emphasis on the computational aspects of the solution by matrix Riccati equations. These computational aspects are determined with reference to a novel formulation of the smoothing problem.

4.2.1 Smoothing with Pre-Flight, In-Flight, and Post-Flight Data

Consider the minimization, by choice of $u(t)$ and $x(t_o)$, of

$$J = \frac{1}{2}\,[x(t_o)-x_o]^T P_o^{-1}\,[x(t_o)-x_o]$$

$$+ \frac{1}{2}\int_{t_o}^{t_f} [z-Hx]^T R^{-1}[z-Hx] + [u-\bar{u}]^T Q^{-1}[u-\bar{u}]dt$$

$$+ \frac{1}{2}\,[x(t_f)-x_f]^T P_f^{-1}[x(t_f)-x_f] \qquad (4.2.1)$$

where

$$\dot{x} = Fx + Gu \qquad (4.2.2)$$

and:

x_o = pre-flight estimate of initial state, $x(t_o)$

P_o = error covariance $E[x(t_o)-x_o][x(t_o)-x_o]^T$

$z(t)$ = in-flight measurements of system output, Hx, where

$E[z(t)-H(t)x(t)][z(\tau)-H(\tau)x(\tau)]^T = R(t)\delta(t-\tau)$

$\bar{u}(t)$ = estimate of external forcing function, where

$E[u(t)-\bar{u}(t)][u(t)-\bar{u}(\tau)]^T = Q(t)\delta(t-\tau)$

x_f = an independent estimate of terminal state, $x(t_f)$

P_f = error covariance, $E[x(t_f)-x_f][x(t_f)-x_f]^T$

Euler-Lagrange Equations

Let

$$\mathcal{H} = \frac{1}{2}\,(z-Hx)^T R^{-1}(z-Hx) + \frac{1}{2}\,(u-\bar{u})^T Q^{-1}(u-\bar{u}) + \lambda^T(Fx+Gu)\,. \qquad (4.2.3)$$

Then, the Euler-Lagrange equations (BR1) become,

$$\dot{\lambda}^T = -\frac{\partial H}{\partial x} = (z-Hx)^T R^{-1} H - \lambda^T F \tag{4.2.4}$$

$$0 = \frac{\partial H}{\partial u} = (u-\bar{u})^T Q^{-1} + \lambda^T G \tag{4.2.5}$$

where

$$\lambda^T(t_f) = -\frac{\partial J}{\partial x(t_f)} = [x(t_f)-x_f]^T P_f^{-1} \tag{4.2.6}$$

$$\lambda^T(t_o) = \frac{\partial J}{\partial x(t_o)} = -[x(t_o)-x_o]^T P_o^{-1} \ . \tag{4.2.7}$$

Substituting Eq. (4.2.5) into Eqs. (4.2.4) and (4.2.2), and rearranging, the Euler-Lagrange equations are:

$$\begin{pmatrix} \dot{x} \\ \dot{\lambda} \end{pmatrix} = \begin{bmatrix} F & -GQG^T \\ -H^T R^{-1} H & -F^T \end{bmatrix} \begin{pmatrix} x \\ \lambda \end{pmatrix} + \begin{pmatrix} G\bar{u} \\ H^T R^{-1} z \end{pmatrix} \tag{4.2.8}$$

$$\tag{4.2.9}$$

$$x(t_f) = x_f + P_f \lambda(t_f) \tag{4.2.10}$$

$$x(t_o) = x_o - P_o \lambda(t_o) \tag{4.2.11}$$

where

$$u(t) = \bar{u}(t) - QG^T \lambda \ . \tag{4.2.12}$$

Equations (4.2.8)-(4.2.11) constitute a two point boundary problem. The solution of this problem may be obtained by the sweep method, as discussed in BR1, where an assumed particular solution is suggested by the <u>form</u> of the boundary conditions. However, for this formulation, there are two possible assumed solutions.

The Forward-Then-Backward Solution Using a Matrix Riccati Equation

The boundary condition (4.2.11) suggests the assumption,

$$x(t) = x_F(t) - P_F(t)\lambda(t) \tag{4.2.13}$$

where $x_F(t)$ and $P_F(t)$ are to be determined. Differentiating Eq. (4.2.13) and substituting Eqs. (4.2.8) and (4.2.9), the assumption (4.2.13) yields the forward Kalman-Bucy filter:

$$\dot{x}_F = Fx_F + P_F H^T R^{-1}(z - Hx_F) + G\bar{u} \qquad x_F(t_o) = x_o \tag{4.2.14}^*$$

$$\dot{P}_F = FP_F + P_F F^T + GQG^T - P_F H^T R^{-1} H P_F \qquad P_F(t_o) = P_o \ . \tag{4.2.15}^*$$

Equation (4.2.15) is a matrix Riccati equation, which, with Eq. (4.2.14), is integrated forward to $t = t_f$. At this terminal time, $x(t_f)$ and $\lambda(t_f)$ may be determined from Eqs. (4.2.10) and Eq. (4.2.13), evaluated at $t = t_f$:

$$\lambda(t_f) = [P_f + P_F(t_f)]^{-1}[x_F(t_f) - x_f] \tag{4.2.16}$$

$$x(t_f) = [P_f^{-1} + P_F^{-1}(t_f)]^{-1}[P_f^{-1}x_f + P_F^{-1}(t_f)x_F(t_f)] \ . \tag{4.2.17}$$

---

*If P_o is very large, it may be more convenient to use

$$\dot{y}_F = -(F^T + S_F GQG^T)y_F + H^T R^{-1} z + S_F G\bar{u} \tag{4.2.14a}$$

$$\dot{S}_F = -S_F F - F^T S_F - S_F GQG^T S_F + H^T R^{-1} H \tag{4.2.15a}$$

where

$$y_F \triangleq S_F x_F$$

$$S_F \triangleq P_F^{-1}$$

Alternately, $x_F(t)$ and $P_F(t)$ could be stored on the forward integration. Then, using Eq. (4.2.17) as the boundary condition, integrate Eq. (4.2.8) backward, computing λ from Eq. (4.2.13) and u from Eq. (4.2.12):

$$\dot{x} = Fx - GQG^T P_F^{-1}(x_F - x) + G\bar{u} \ . \tag{4.2.18}$$

Still another alternative, again using stored $x_F(t)$ and $P_F(t)$, is to integrate Eq. (4.2.9) backward, using Eq. (4.2.16) as the boundary condition, computing x from Eq. (4.2.13) and u from Eq. (4.2.12):

$$\dot{\lambda} = -F^T\lambda - H^T R^{-1} H(x_F - P_F\lambda) + H^T R^{-1} z \tag{4.2.19}$$

or

$$\dot{\lambda} = -(F^T - H^T R^{-1} H P_F)\lambda + H^T R^{-1}(z - Hx_F) \ . \tag{4.2.20}$$

The Backward-Then-Forward Solution Using a Matrix Riccati Equation

Eq. (4.2.10) suggests the assumption

$$x(t) = x_B(t) + P_B(t)\lambda(t) \tag{4.2.21}$$

where $x_B(t)$ and $P_B(t)$ are to be determined. Differentiating Eq. (4.2.21) and substituting Eqs. (4.2.8) and (4.2.9), then (4.2.21), yields the backward Kalman-Bucy Filter:

$$-\dot{x}_B = -Fx_B + P_B H^T R^{-1}(z - Hx_B) \qquad x_B(t_f) = x_f \tag{4.2.22}*$$

$$-\dot{P}_B = -FP_B - P_B F^T + GQG^T - P_B H^T R^{-1} H P_B \qquad P_B(t_f) = P_f \tag{4.2.23}*$$

*If P_f is very large, it may be more convenient to use

$$-\dot{y}_B = (F^T - S_B GQG^T)y_B + H^T R^{-1} z \tag{4.2.22a}$$

(footnote cont.)

After Eqs. (4.2.22) and (4.2.23) are integrated backward to $t = t_o$, $x(t_o$ and $\lambda(t_o)$ may be determined from Eq. (4.2.11) and Eq. (4.2.21) evaluated at $t = t_o$:

$$\lambda(t_o) = [P_o + P_B(t_o)]^{-1}[x_o - x_B(t_o)] \tag{4.2.24}$$

$$x(t_o) = [P_o^{-1} + P_B^{-1}(t_o)]^{-1}[P_o^{-1}x_o + P_B^{-1}(t_o)x(t_o)] \ . \tag{4.2.25}$$

Note that Eq. (4.2.25) is an identity for $P_o^{-1} = 0$.

The Euler-Lagrange equations (4.2.8)-(4.2.9) could then be integrated forward using Eqs. (4.2.4)-(4.2.26) as boundary conditions yielding the optimal estimate of x and the optimal estimate of u from Eq. (4.2.12).

Alternately, $x_B(t)$ and $P_B(t)$ could be stored on backward integration. Then Eq. (4.2.8), using Eq. (4.2.25) as a boundary condition, is integrated forward, computing λ from Eq. (4.2.21), and u from Eq. (4.2.12):

$$\dot{x} = Fx + GQG^T P_B^{-1}(x_B - x) + G\bar{u} \ . \tag{4.2.26}$$

Still another alternative, again using stored x_B and P_B, is to integrate Eq. (4.2.9) forward, using Eq. (4.2.24) as a boundary condition, computing x from Eq. (4.4.21) and u from Eq. (4.2.12):

---

*(footnote continued from previous page)

$$-\dot{S}_B = S_B F + F^T S_B - S_B GQG^T S_B + H^T R^{-1} H \tag{4.2.23a}$$

where

$$y_B = S_B x_B$$

$$S_B = P_B^{-1} \ .$$

$$\dot{\lambda} = -F^T\lambda - H^T R^{-1} H(x_B + P_B\lambda) + H^T R^{-1} z \qquad (4.2.27)$$

or

$$\dot{\lambda} = -(F^T + H^T R^{-1} H\, P_B)\lambda + H^T R^{-1}(z - Hx_B) \; . \qquad (4.2.28)$$

Combination of Forward and Backward Solutions at an Intermediate Time

At an intermediate time $t = t_1$ (where $t_o < t_1 < t_f$), it is simple to solve Eqs. (4.2.13) and (4.2.21) simultaneously to obtain $x(t_1)$ and $\lambda(t_1)$:

$$x(t_1) = [P_F^{-1} + P_B^{-1}]^{-1}[P_F^{-1}x_F + P_B^{-1}x_B]\Big|_{t=t_1} \qquad (4.2.29)$$

$$\lambda(t_1) = (P_F + P_B)^{-1}(x_F - x_B)\Big|_{t=t_1} \; . \qquad (4.2.30)$$

This is Fraser's solution (FR2). It involves solution of two matrix Riccati equations, (4.2.15) and (4.2.23). Fraser also shows that the error covariance of the smoothed estimate $x(t_1)$ is $P_S(t_1)$, where

$$P_S^{-1} = P_F^{-1} + P_B^{-1} \; . \qquad (4.2.31)$$

4.2.2 Follower with Initial, In-Flight, and Final Goals

Analogous to the smoothing problem in which a measurement function, $z(t)$, is given, there is a follower problem in which it is desired that a system output follow a prescribed function, $y(t)$. The analogous quadratic control synthesis problem is to minimize, by choice of $u(t)$ and $x(t)$, the functional,

$$J = \frac{1}{2}\,[x(t_o) - x_o]^T S_o [x(t_o) - x_o] + \frac{1}{2}\int_{t_o}^{t_f} [(y-\mathcal{C}x)^T A(y-\mathcal{C}x)$$

$$+ (u-\bar{u})^T B(u-\bar{u})dt] + \frac{1}{2}\,[x(t_f)-x_f]^T S_f [x(t_f) - x_f] \qquad (4.2.32)$$

where

$$\dot{x} = Fx + Gu \qquad (4.2.33)$$

and

(x_o, S_o) = desired initial conditions and weighting matrix

(x_f, S_f) = desired final conditions and weighting matrix

$y(t)$ = desired output history, $\mathcal{C}x$, with weighting matrix A

$\bar{u}$ = desired control history, u , with weighting matrix B

Equivalence to Smoother Problem

The follower is mathematically identical to the smoothing problem. The only differences are in nomenclature:

Follower	y	$\mathcal{C}$	A	B	S_o	S_f	S_F	S_B
Smoother	z	H	R^{-1}	Q	P_o^{-1}	P_f^{-1}	P_F^{-1}	P_B^{-1}

The regulator problem is a special case of the follower problem with $y(t) = 0$, $S_o^{-1} = 0$, and $\bar{u}(t) = 0$.

Euler-Lagrange Equations

Let

$$\mathcal{H} = \frac{1}{2}\,(y-\mathcal{C}x)^T A(y-\mathcal{C}x) + \frac{1}{2}\,(u-\bar{u})B(u-\bar{u}) + \lambda^T(Fx+Gu) \ .$$

It follows that:

$$\begin{pmatrix}\dot{x}\\ \dot{\lambda}\end{pmatrix} = \begin{pmatrix} F & -GB^{-1}G^T \\ -\mathcal{C}^T A \mathcal{C} & -F^T \end{pmatrix}\begin{pmatrix}x\\ \lambda\end{pmatrix} + \begin{pmatrix} G\bar{u} \\ \mathcal{C}^T A y\end{pmatrix}$$

$$\lambda(t_o) = -S_o[x(t_o)-x_o]$$

$$\lambda(t_f) = S_f[x(t_f)-x_f]$$

where

$$u(t) = \bar{u}(t) - B^{-1}G^T\lambda \ .$$

The backward-then-forward solution is of primary interest here since it is a feedback solution; it requires storing the backward solution $x_B(t), S_B(t)$, or alternately, $y_B(t), S_B(t)$, where

$$y_B = S_B x_B$$

$$\dot{y}_B = -(F^T - S_B G B^{-1} G^T) y_B - \mathcal{C}^T A y + S_B G \bar{u}$$

$$\dot{S}_B = -S_B F - F^T S_B + S_B G B^{-1} G^T S_B - \mathcal{C}^T A \mathcal{C} \ .$$

4.3 Quadratic Synthesis Using Eigenvector Decomposition

The previous sections have reviewed the Euler-Lagrange equations and the matrix Riccati equation method for their solution. The eigenvector decomposition method is, in some respects, simpler and leads to more accurate solutions than the Riccati equation method. The eigenvector decomposition can only be applied to constant coefficient systems.

Symmetry of Eigenvalues of the Euler-Lagrange Equations

Consider the determination of the eigensystem of Eqs. (4.2.8)-(4.2.9). Assuming solutions of the form

$$x = \bar{x}\, e^{st}$$

$$\lambda = \bar{\lambda}\, e^{st} \ .$$

The homogeneous equations become:*

$$\begin{bmatrix} F-sI & -Y \\ -W & -F^T-sI \end{bmatrix} \begin{pmatrix} \bar{x} \\ \hline \bar{\lambda} \end{pmatrix} = 0 \ . \tag{4.3.1}$$

If the second set of equations is multiplied by -1, interchanged with the first set of equations, and the order of $\bar{x}$ and $\bar{\lambda}$ interchanged, the resulting equations are

$$[\bar{\lambda}^T \quad \bar{x}^T] \begin{bmatrix} F+sI & -Y \\ W & F^T-sI \end{bmatrix} = 0 \ . \tag{4.3.2}$$

If s is replaced by $-s$ in Eq. (4.3.2), it is seen that the coefficient matrix is the same as in Eq. (4.3.1); hence, if s_i is a root of the characteristic equation of the determinant of the coefficient matrix, then $-s_i$ is also a root. This result is well-known (LE1, RY1) and may be alternately stated. The eigenvalues of Eq. (4.3.1) are symmetrical about the imaginary axis, since for every $s_i \triangleq (s_i)_+ = \sigma_i \pm j\omega_i$, $(\sigma_i > 0)$, there is a $(s_i)_- = -\sigma_i \mp j\omega_i = -s_i$.

It also follows that the characteristic equation of Eq. (4.3.1) contains only even powers of s :

$$s^m + a_1 s^{m-1} + a_2 s^{m-2} + \ldots a_{m-1} s + a_m = 0$$

where $m = 2n$.

It is therefore convenient to decompose s_i by defining

*For the follower, $Y = GB^{-1}G^T$, $W = \mathcal{C}^T A \mathcal{C}$; while for the smoother, $Y = GQG^T$, $W = H^T R^{-1} H$. For notational convenience, the matrix of coefficients of the Euler-Lagrange equations will be denoted by $\mathcal{F}$.

$$\mathcal{S} = \left[\begin{array}{c|c} \mathcal{S}_+ & 0 \\ \hline 0 & \mathcal{S}_- \end{array}\right] \tag{4.3.3}$$

where

$$\mathcal{S}_+ = \text{diag}[(s_1)_+, (s_2)_+ \ldots (s_n)_+] = -\mathcal{S}_- \ . \tag{4.3.4}$$

Eigenvector Decomposition of the Euler-Lagrange Equations

The eigenvalue decomposition $\mathcal{S}$ suggests an eigenvector decomposition

$$T \triangleq \begin{pmatrix} X_+ & X_- \\ \Lambda_+ & \Lambda_- \end{pmatrix} \triangleq [T_+ \quad T_-] \tag{4.3.5}$$

where the $2n \times n$ matrices

$$T_+ \triangleq \begin{pmatrix} X_+ \\ \Lambda_+ \end{pmatrix} \qquad T_- \triangleq \begin{pmatrix} X_- \\ \Lambda_- \end{pmatrix}$$

are the orderings of the n eigenvectors associated with $\mathcal{S}_+$ and $-\mathcal{S}_+$, respectively.

The homogeneous solutions of the Euler-Lagrange equations may then be written

$$\begin{bmatrix} x(t) \\ \lambda(t) \end{bmatrix} = \sum_{i=1}^{n} \xi_{o_i} \begin{pmatrix} x_+^{(i)} \\ \lambda_+^{(i)} \end{pmatrix} e^{s_i(t-t_o)} + \sum_{i=1}^{n} \eta_{o_i} \begin{pmatrix} x_-^{(i)} \\ \lambda_-^{(i)} \end{pmatrix} e^{s_i(t_f-t)} \tag{4.3.6}$$

where the ξ_{o_i} and η_{o_i} are constants and the eigenvectors corresponding to the s_i are denoted by $[x_+^{(i)}, \lambda_+^{(i)}]^T$ and those corresponding to the $-s_i$ by $[x_-^{(i)}, \lambda_-^{(i)}]^T$.

Alternately,

$$\begin{bmatrix} x(t) \\ \lambda(t) \end{bmatrix} = \begin{bmatrix} x_+^{(1)} & x_+^{(2)} \cdots x_+^{(n)} \\ \lambda_+^{(1)} & \lambda_+^{(2)} \cdots \lambda_+^{(n)} \end{bmatrix} \begin{bmatrix} \xi_{o_1} e^{s_1(t-t_o)} \\ \xi_{o_2} e^{s_2(t-t_o)} \\ \vdots \\ \xi_{o_n} e^{s_n(t-t_o)} \end{bmatrix} + \begin{bmatrix} x_-^{(1)} & x_-^{(2)} \cdots x_-^{(n)} \\ \lambda_-^{(1)} & \lambda_-^{(2)} \cdots \lambda_-^{(n)} \end{bmatrix} \begin{bmatrix} \eta_{o_1} e^{s_1(t_f-t)} \\ \eta_{o_2} e^{s_2(t_f-t)} \\ \vdots \\ \eta_{o_n} e^{s_n(t_f-t)} \end{bmatrix}$$

which is equivalent to the matrix equations,

$$x(t) = X_+ e^{\delta_+(t-t_o)} \xi_o + X_- e^{\delta_+(t_f-t)} \eta_o \qquad (4.3.7)$$

$$\lambda(t) = \Lambda_+ e^{\delta_+(t-t_o)} \xi_o + \Lambda_- e^{\delta_+(t_f-t)} \eta_o \qquad (4.3.8)$$

where

$$X_+ = [x_+^{(1)}, x_+^{(2)} \ldots x_+^{(n)}]$$

$$\Lambda_+ = [\lambda_+^{(1)}, \lambda_+^{(2)} \ldots \lambda_+^{(n)}]$$

and similarly for X_- and Λ_- .

As $(t-t_o) \to \infty$, the modes multiplied by η_o attenuate so that Eqs. (4.3.7) and (4.3.8) become

$$x(t) = X_+ e^{\delta_+(t-t_o)} \xi_o$$

$$\lambda(t) = \Lambda_+ e^{\delta_+(t-t_o)} \xi_o .$$

Upon elimination of $e^{\delta_+(t-t_o)} \xi_o$,

$$\lambda(t) = \Lambda_+ X_+^{-1} x(t) . \qquad (4.3.9)$$

Similarly, for $(t_f - t) \to \infty$,

$$x(t) = X_- e^{\delta_+ (t_f - t)} \eta_o$$

$$\lambda(t) = \Lambda_- e^{\delta_+ (t_f - t)} \eta_o$$

which, upon elimination of $e^{\delta_+(t_f - t)} \eta_o$, become

$$\lambda(t) = \Lambda_- X_-^{-1} x(t) \ . \tag{4.3.10}$$

Relationship to Steady-State Solutions of Matrix Riccati Equations

The quantities $(\Lambda_+ X_+^{-1})$ and $(\Lambda_- X_-^{-1})$ are evidently steady state solutions of the matrix Riccati equations developed in Section 4.2, expressed in terms of the eigenvectors of the Euler-Lagrange equations.

The matrix

$$S_- \triangleq \Lambda_- X_-^{-1} \tag{4.3.11}$$

is the steady state solution obtained by integrating the Riccati equation (4.2.23a) backward in time, i.e.,

$$S_- \triangleq (S_B)_{SS} \ .$$

Similarly,

$$S_+ \triangleq -\Lambda_+ X_+^{-1} \tag{4.3.12}$$

is the steady state solution obtained by integrating the Riccati equation (4.2.15a) forward in time, i.e.,

$$S_+ \triangleq (S_F)_{SS} \ . \tag{4.3.13}$$

The Riccati equations for S_F and S_B, namely, Eqs. (4.2.15a) and (4.2.23a), differ only in the sign of the matrix S :

$$\dot{S}_F = -S_F F - F^T S_F - S_F Y S_F + W \qquad (4.2.15a)$$

$$-\dot{S}_B = S_B F + F^T S_B - S_B Y S_B + W \; . \qquad (4.2.23a)$$

In fact, S_+ and $-S_-$ are steady state solutions of Eq. (4.2.15a), whereas S_- and $-S_+$ are steady state solutions of Eq. (4.2.23a). To show this, Eq. (4.2.15a) may be written as

$$\dot{S}_F = -\frac{1}{2}(S_F - S_+)Y(S_F + S_-) - \frac{1}{2}(S_F + S_-)Y(S_F - S_+) \qquad (4.3.14)$$

and Eq. (4.2.23a) may be written as

$$-\dot{S}_B = -\frac{1}{2}(S_B + S_+)Y(S_B - S_-) - \frac{1}{2}(S_B - S_-)Y(S_B + S_+) \; . \qquad (4.3.15)$$

Obviously, integrating Eq. (4.3.14) forward will result in

$$S_F \Rightarrow \begin{cases} S_+ & \text{if } S(t_o) > -S_- \\ -\infty & \text{if } S(t_o) < -S_- \end{cases} \qquad (4.3.16)$$

Since, in most cases, $S(t_o) \geq 0$ and $S_- > 0$, S_F will converge to S_+ .

Similarly, integrating Eq. (4.3.15) backward will result in

$$S_B \Rightarrow \begin{cases} S_- & \text{if } S(t_f) > -S_+ \\ -\infty & \text{if } S(t_f) < -S_+ \end{cases} \qquad (4.3.17)$$

Again, in most cases $S(t_f) \geq 0$ and $S_+ > 0$, so S_B will converge to S .

If, by mistake, one integrated Eq. (4.3.14) backward instead of forward, $S_F \to S_-$ if $S(t_f) < S_+$ and $S_F \to \infty$ if $S(t_f) > S_+$. Since

$-S_- < 0$, and ∞ is rather large, one would probably suspect a mistake!

Similarly, if Eq. (4.3.15) were integrated forward instead of backward, $S_B \to -S_+$ if $S(t_o) < S_-$ and $S_B \to \infty$ if $S(t_o) > S_+$.

Eigenvalues and Eigenvectors of the Backward Smoother

When the Euler-Lagrange equations (4.2.8)-(4.2.9) for the smoother are integrated forward in time, the modes $x_+^{(i)}$ and $\lambda_+^{(i)}$ eventually dominate, so that Eq. (4.3.9) prevails. Substituting Eq. (4.3.9) into Eq. (4.3.1) gives

$$\delta_+ X_+ = (F + GQG^T S_+) X_+ \quad . \tag{4.3.18}$$

Comparing this with Eq. (4.2.18), it is obvious that

$$(P_F^{-1})_{SS} \triangleq S_+ = -\Lambda_+ X_+^{-1} \quad . \tag{4.3.19}$$

It follows, too, that the eigenvalues and eigenvectors of the backward smoother, Eq. (4.2.18), are δ_+ and $X_+^{(i)}$, so it is stable for backward integration in the steady state.

Eigenvalues and Eigenvectors of the Forward Smoother

Integrating Eq. (4.3.1) backward in time, the modes $x_-^{(i)}, \lambda_-^{(i)}$ eventually dominate and Eq. (4.3.10) prevails. Substituting Eq. (4.3.11) into Eq. (4.3.1) gives

$$-\delta_+ X_- = (F - GQG^T S_-) X_- \quad . \tag{4.3.20}$$

Comparing this with Eq. (4.2.26), it is obvious that

$$(P_B^{-1})_{SS} \triangleq S_- = \Lambda_- X_-^{-1} \tag{4.3.21}$$

and the eigenvalues and eigenvectors of the forward smoother Eq. (4.2.26) are $-s_i$ and $x_-^{(i)}$, so it is stable for forward integration in the steady state.

Eigenvalues and Eigenvectors of the Forward Filter

From Eq. (4.2.13),

$$x_F = x - P_F\lambda \ . \tag{4.3.22}$$

Hence, in the steady state, when P_F = constant, $x_F(t)$ is a linear combination of $x(t)$ and $\lambda(t)$. Again, integrating Eq. (4.3.1) backward in time, the modes $x_-^{(i)}, \lambda_-^{(i)}$ eventually dominate so that the homogeneous solutions satisfy

$$-s_i\begin{bmatrix} x_-^{(i)} \\ \lambda_-^{(i)} \end{bmatrix} = \begin{bmatrix} F & -GQG^T \\ -H^TR^{-1}H & -F^T \end{bmatrix}\begin{bmatrix} x_-^{(i)} \\ \lambda_-^{(i)} \end{bmatrix} \ . \tag{4.3.23}$$

Consider the linear combination

$$x_-^{(i)} + P_F\lambda_-^{(i)} \triangleq x_F^{(i)} \ .$$

From Eq. (4.3.23), this becomes, by direct substitution,

$$-s_i x_F^{(i)} = (F - P_FH^TR^{-1}H)(x_F^{(i)} - P_F\lambda_-^{(i)}) - (GQG^T + P_FF^T)\lambda_-^{(i)}$$

or

$$\begin{aligned} -s_i x_F^{(i)} = {} & (F - P_FH^TR^{-1}H)x_F^{(i)} - (FP_F + P_FF^T + GQG^T \\ & - P_FH^TR^{-1}HP_F)\lambda_-^{(i)} \ . \end{aligned} \tag{4.3.24}$$

But the coefficient of $\lambda_-^{(i)}$ is $\dot{P}_F$ and since in the present consideration, P_F = constant , $\dot{P}_F = 0$. Thus Eq. (4.3.24) is identical to the eigenvalue equation of the Kalman filter Eq. (4.2.14). It follows that the eigenvalues and eigenvector matrix of the forward Kalman filter are:

$$(-\lambda_+) \quad \text{and} \quad (X_- + P_F\Lambda_-) \; . \tag{4.3.25}$$

Thus the forward Kalman filter is stable. It is shown in Appendix B that

$$X_- + P_F\Lambda_- \equiv X_- - X_+(\Lambda_+)^{-1}\Lambda_- = \Lambda_+^{-T} \; . \tag{4.3.26}$$

Eigenvalues and Eigenvectors of the Backward Filter

From Eq. (4.2.21), and an argument precisely parallel to that just presented above, the eigenvalues and eigenvector matrix of the backward Kalman filter, Eq. (4.2.22) are

$$(\lambda_+) \quad \text{and} \quad (X_+ - P_B\Lambda_+), \tag{4.3.27}$$

showing that this filter is stable for backward integration. It is also shown in Appendix B that

$$X_+ - P_B\Lambda_+ \equiv X_+ - X_-(\Lambda_-)^{-1}\Lambda_+ \equiv \Lambda_-^{-T} \; . \tag{4.3.28}$$

Eigenvalues and Eigenvectors of the Follower-Regulator

Integrating Eq. (4.3.1) backward in time, the modes $X_-^{(i)}, \lambda_-^{(i)}$ eventually dominate and Eq. (4.3.10) prevails. Substituting Eq. (3.3.8) into Eq. (4.3.1) gives

$$-\lambda_+ X_- = (F - GB^{-1}G^TS_-)X_- \; . \tag{4.3.29}$$

Comparing this with Eq. (4.2.26), replacing Q by B^{-1} and P_B^{-1} by S_B, it is obvious that

$$(S_B)_{SS} \equiv S_- \equiv \Lambda_- X_-^{-1} \tag{4.3.30}$$

and the eigensystem of the follower regulator is

$$-s_i \ , \quad x_-^{(i)} \ , \tag{4.3.31}$$

showing that it is stable for forward integration in the steady state.

The Smoothed Covariance Matrix

It is shown in Appendix B that the eigenvector matrix, T, is symplectic, and that this implies

$$\Lambda_-(X_-)^{-1} - \Lambda_+(X_+)^{-1} = (X_- X_+^T)^{-1} \ . \tag{B.9}$$

Using Eqs. (4.3.19) and (4.3.21), this gives

$$(P_B^{-1})_{SS} + (P_F^{-1})_{SS} = (X_- X^T)^{-1} = (P_S^{-1})_{SS} \tag{4.3.32}$$

where $(P_S)_{SS}$ is the smoothed covariance in the steady-state (cf. Eq. (4.2.31)).

An Example

The equations of a damped harmonic oscillator with a rate measurement may be written:

$$\dot{x}_1 = x_2$$

$$\dot{x}_2 = -\omega^2 x_1 - 2\zeta\omega x_2 + \omega^2 u$$

$$z = x_2 + v$$

where

$$E\{u\} = 0 \qquad E\{uu^T\} = q\delta(t-\tau)$$

$$E\{v\} = 0 \qquad E\{vv^T\} = r\delta(t-\tau)$$

and q and r are the respective power spectral densities of u and v.

It is desired to determine estimates of x_1 and x_2 from the measurement of the velocity.

The homogeneous canonical equations are:

$$\begin{pmatrix} \dot{x}_1 \\ \dot{x}_2 \\ \dot{\lambda}_1 \\ \dot{\lambda}_2 \end{pmatrix} = \begin{bmatrix} 0 & 1 & 0 & 0 \\ -\omega^2 & -2\zeta\omega & 0 & -q\omega^4 \\ 0 & 0 & 0 & \omega^2 \\ 0 & -1/r & -1 & 2\zeta\omega \end{bmatrix} \begin{pmatrix} x_1 \\ x_2 \\ \lambda_1 \\ \lambda_2 \end{pmatrix}$$

from which the characteristic equation is

$$(s^2 + 2\omega\zeta' s + \omega^2)(s^2 - 2\omega\zeta' s + \omega^2) = 0$$

where

$$\zeta' = \sqrt{\zeta^2 + \frac{q\omega^2}{4r}} \, .$$

Then

$$\Lambda = \omega \, \mathrm{diag}\left[(\zeta' + j\sqrt{1-\zeta'^2}), (\zeta' - j\sqrt{1-\zeta'^2}), (-\zeta' - j\sqrt{1-\zeta'^2}), (-\zeta' + j\sqrt{1-\zeta'^2})\right] .$$

Normalizing the eigenvectors on a unit length of λ_2, the i^{th} column of T is

$$T_i = \begin{bmatrix} -\frac{r}{s_i^2}\,(s_i^2 - 2\zeta\omega s_i + \omega^2) \\ -\frac{r}{s_i}\,(s_i^2 - 2\zeta\omega s_i + \omega^2) \\ \omega^2/s_i \\ 1 \end{bmatrix}$$

from which

$$\Lambda_+^{-1} = \frac{s_1 s_2}{\omega^2 (s_2 - s_1)} \begin{bmatrix} 1 & -1 \\ -\frac{\omega^2}{s_2} & -\frac{\omega^2}{s_1} \end{bmatrix}.$$

The steady-state error covariance of the forward filter is then

$$P_F = -X_+ \Lambda_+^{-1} = r \begin{bmatrix} -\frac{2\zeta}{\omega} + \frac{(s_1+s_2)}{s_1 s_2} & 0 \\ 0 & -2\zeta\omega + (\zeta_1+\zeta_2) \end{bmatrix}$$

where

$$s_1 = \omega[\zeta' + j\sqrt{1-\zeta'^2}] \quad \text{and} \quad s_2 = \omega[\zeta' - j\sqrt{1-\zeta'^2}]$$

or

$$P_F = \frac{r}{\omega}\begin{bmatrix} -2\zeta+2\sqrt{\zeta^2+q\omega^2/4r} & 0 \\ 0 & (-2\zeta+2\sqrt{\zeta'^2+q\omega^2/4r})/\omega^2 \end{bmatrix} .$$

The eigenvalues of the forward Kalman filter are

$$s_1 = -\zeta'\omega - j\omega\sqrt{1-\zeta'^2}$$

$$s_2 = -\zeta'\omega + j\omega\sqrt{1-\zeta'^2}$$

and the corresponding eigenvectors of the filter response are

$$X_1 = \begin{pmatrix} -\frac{1}{\omega}[-\zeta'-j\sqrt{1-\zeta'^2} \\ 1 \end{pmatrix} \quad X_2 = \begin{pmatrix} \frac{1}{\omega}[-\zeta'+j\sqrt{1-\zeta'^2} \\ 1 \end{pmatrix}$$

which is the same as the columns of $(\Lambda_+^{-1})^T$, as discussed in Eq. (4.3.23).

The steady-state error covariance of the backward filter is then

$$P_B = X_-\Lambda_-^{-1} = \frac{r}{\omega}\begin{bmatrix} 2\zeta'+2\sqrt{\zeta^2+q\omega^2/4r} & 0 \\ 0 & \omega^2[2\zeta+2\sqrt{\zeta^2+q\omega^2/4r}] \end{bmatrix}$$

and finally, the steady-state error covariance of the smoothed estimate, P_S , is

$$P_S = [P_F^{-1} + P_B^{-1}]^{-1}$$

or

$$P_S(t) = \begin{bmatrix} \dfrac{\omega q}{4\sqrt{\zeta^2 + \dfrac{\omega^2 q}{4r}}} & 0 \\ 0 & \dfrac{\omega^3 q}{4\sqrt{\zeta^2 + \dfrac{\omega^2 q}{4r}}} \end{bmatrix} .$$

For high order systems it is more economical to use Eq. (4.3.32) for the determination of the steady state $P_S(t)$, since only one inversion is required (in the normalization of T by Eq. (B.9), whereas three inversions are required by the use of Eq. (4.2.31)). For a numerical illustration, let $2\zeta = q = r = \omega = 1$. The normalized T is then

$$T = [T_1 \quad T_1^* \quad T_2 \quad T_2^*]$$

where

$$T_1^T = \left\{\left[(j-1)\left(1-\frac{\sqrt{2}}{2}\right)\right], \left[1-\sqrt{2}\right], \left[\frac{1-j}{\sqrt{2}}\right], 1\right\}$$

$$T_2^T = \left\{\left[-j\,\frac{\sqrt{2}}{4}\left(1+\frac{\sqrt{2}}{2}\right)\right], \left[\frac{\sqrt{2}}{8}\,(1+\sqrt{2})\,(j-1)\right], \left[-j/4\right], \left[-\frac{\sqrt{2}}{8}\,(1-j)\right]\right\}$$

and T_1^* and T_2^* are the conjugate complexes of T_1 and T_2, from which, by direct matrix multiplication,

$$X_- X_+^T = \begin{bmatrix} \dfrac{1}{2\sqrt{2}} & 0 \\ 0 & \dfrac{1}{2\sqrt{2}} \end{bmatrix}$$

which is numerically equal to $P_S(t)$ above with the given parameters. Note that the symplectic normalization (Appendix B) of the n eigenvec-

tors does not affect P_F or P_B since both are defined as the product of one matrix with the inverse of another with the same normalization. Hence,

$$P_F = -X_+ \Lambda_+^{-1} = \begin{bmatrix} -1+\sqrt{2} & 0 \\ 0 & -1+\sqrt{2} \end{bmatrix}$$

$$P_B = X_- \Lambda_-^{-1} = \begin{bmatrix} 1+\sqrt{2} & 0 \\ 0 & 1+\sqrt{2} \end{bmatrix}$$

for both the normalized and nonnormalized eigenvectors. Because of the optimality of the smoothed estimate, $P_S(t)$ is never larger than P_F, the forward filter estimate covariance. Since the damping ratio, ζ, is positive, $P_B > P_F$.

For this example only x_2 is modeled as driven and measured by different random noise signals, and this results in a simple diagonal form for the steady covariance solutions. In general, of course, the covariance is only symmetric.

4.4 Determining Mean Square Stochastic Response

One valuable measure of performance of a controller is the average behavior of the controlled system in the presence of random disturbances. For statistically stationary processes, determination of this average response requires solution of a linear matrix equation of the form

$$FP + PF^T = -Q \qquad (4.4.1)$$

where F is constant and P and Q are positive definite symmetric matrices.

An exact method is proposed for solution of (4.5.1) which is especially suited to the results of the preceding sections of this chapter. Let F_c be the closed loop system matrix, Λ_- its eigenvalue matrix, and X_- its eigenvector matrix. Then

$$F_c = X_- \delta_- X_-^{-1} ;$$

substituting into (4.2.1),

$$X_- \delta_- X_-^{-1} P + P T^{-T} \delta_-^T X_-^T = -Q . \qquad (4.4.2)$$

Premultiplying by T^{-1} and postmultiplying by T^{-T},

$$\delta_- (X_-^{-1} P X_-^{-T}) + (X_-^{-1} P X_-^{-T}) \delta_-^T = -X_-^{-1} Q X_-^{-T} .$$

Let

$$P' = X_-^{-1} P X_-^{-T}$$

$$Q' = X_-^{-1} Q X_-^{-T} .$$

Then

$$\delta_- P' + P' \delta_-^T = -Q' .$$

If $\delta_- = \mathrm{diag}(s_i)$, the elements of P' are

$$P'_{ij} = - \frac{Q'_{ij}}{s_i + s_j} \qquad (4.4.3)$$

and

$$P = X_- P' X_-^T .$$

This method of solution requires only $n \times n$ matrix multiplications and n matrix inversions. However, the requirement that δ_- be diagonal means that, in general, complex arithmetic will be required. Then computer storage and time requirements both increase. If δ_- is not diagonal,

then an alternate method must be used (Sec. 4.5).

4.5 Computational Considerations

It has been shown that the eigenvalue decomposition of the Euler-Lagrange equations has many advantages over determining the steady state solution of the matrix Riccati equation for quadratic synthesis. However, for high order systems the method depends on an extremely accurate procedure for evaluation of the eigenvalues and eigenvectors of an unsymmetric matrix. Procedures of the required accuracy have not been available until recently.

For these studies, an excellent computer program, based on the QR algorithm of Francis, was used. This program calculates the eigensystem of an unsymmetrical real matrix. With modifications by J. H. Wilkenson and his students, it is believed to be the most efficient routine available at the time of this writing.

The outputs of this program are the complex eigenvalues and eigenvectors. From a computational point of view, it is undesirable to use complex arithmetic for the matrix operations discussed in the previous sections. Fortunately, this problem may be circumvented by transforming the eigenvector to real form, a well-known technique in the analysis of linear systems.

There are many ways to transform a matrix to real form. The eigenvectors T of the system $\dot{z} = \mathfrak{F}z$ are given by the solution of*

$$\mathfrak{F}T = T\Lambda \ . \tag{4.5.1}$$

Defining $z = Tz'$ gives the normalized system

$$\dot{z}' = T^{-1}\mathfrak{F}Tz' \tag{4.5.2}$$

where $T^{-1}\mathfrak{F}T$ is a complex diagonal matrix (for no repeated roots of Λ). There is no loss of generality in assuming Λ to be wholly complex, so

*$z = \begin{bmatrix} x \\ \lambda \end{bmatrix}$, cf. Appendix B.

$$\mathcal{A} = \text{diag}[(\sigma_1+j\omega_1),(\sigma_1-j\omega_1)\ldots(\sigma_{2n}+j\omega_{2n}),(\sigma_{2n}-j\omega_{2n}] \qquad (4.5.3)$$

where σ_i and ω_i are the real and imaginary parts of s_i. It is readily verified that the block diagonal matrix

$$\mathcal{K} = \text{diag}\left\{\frac{1}{2}\begin{pmatrix}1 & -j\\ 1 & j\end{pmatrix}\ ;\ \ldots\ \frac{1}{2}\begin{pmatrix}1 & -j\\ 1 & j\end{pmatrix}\right\} \qquad (4.5.4)$$

transforms $\mathcal{A}$ to a block diagonal real matrix

$$\begin{aligned}\mathcal{B} &= \mathcal{K}^{-1}\mathcal{A}\mathcal{K}\\ &= \text{diag}\left\{\begin{pmatrix}\sigma_1 & \omega_1\\ -\omega_1 & \sigma_1\end{pmatrix}\ ;\ \ldots\ \begin{pmatrix}\sigma_{2n} & \omega_{2n}\\ -\omega_{2n} & \sigma_{2n}\end{pmatrix}\right\}.\end{aligned} \qquad (4.5.5)$$

Substituting $\mathcal{K}$ into Eq. (4.5.1) gives

$$\mathcal{F}(T\mathcal{K}) = (T\mathcal{K})\mathcal{B} \qquad (4.5.6)$$

and since $\mathcal{F}$ and $\mathcal{B}$ are real, $(T\mathcal{K})$ is also real. Let

$$T = [(p_1+jq_1)\,|\,(p_1-jq_1)\,|\ldots|\,(p_{2n}+jq_{2n})\,|\,p_{2n}-jq_{2n}] \qquad (4.5.7)$$

where $(p_i \pm jq_i)$ are the complex eigenvectors of $s_i = \sigma_i \pm j\omega_i$ and p_i is the $2n\times1$ column matrix of the real parts of the eigenvectors, and q_i the corresponding imaginary parts. Then the real eigenvector matrix $T\mathcal{K}$ is

$$T\mathcal{K} = [p_1,q_1\ldots p_{2n},q_{2n}] \qquad (4.5.8)$$

Substituting the $2n\times2n$ matrix

$$T = \begin{bmatrix} X_+ & X_- \\ \Lambda_+ & \Lambda_- \end{bmatrix}$$

into Eq. (4.5.8), the first n columns of $T\mathcal{K}$ are

$$(T\mathcal{K}) = \begin{bmatrix} X_+\mathcal{K} \\ \Lambda_+\mathcal{K} \end{bmatrix}$$

and from Eq. (4.3.1)

$$P_F^{-1} = -(\Lambda_+\mathcal{K})(X_+\mathcal{K})^{-1} = -\Lambda_+ X_+^{-1} \ .$$

A similar argument for the second n columns gives Eq. (4.3.30). Hence, because the steady solutions of the Riccati equations are defined in terms of the same columns of T, the result does not depend on the column normalization of T. Note, however, that the cross column product, $X_- X_+^{-T}$, does depend on this normalization (cf. example). The use of the real transformation reduces storage and time requirements over that required for complex multiplications.

A most important feature of the QR method is its insensitivity to widely separated eigenvalues, a fundamental characteristic of the rotary-wing VTOL problem of this research. Solution of the Riccati equation to steady state by any quadrature method known must use time steps no larger than some fraction of the shortest period of the closed loop system. For many high order systems, this would produce extremely large computer time expenditures.

For these studies, only real arithmetic was used. This precluded the use of the highly efficient method of Section 4.4 (because of the block diagonal form of $\mathcal{J}$) for the solution of the general linear matrix equation (4.5.1).

There are two real arithmetical methods for solving (4.5.1). Generally, it will be necessary to implement both on a digital computer. One

method is iterative and approximate, while the other is exact.

The iterative procedure approaches the equation

$$\dot{P} = F_c P + P F_c + Q \ . \tag{4.5.9}$$

A method, called Stein's method, is proposed in (SK1) for solving Eq. (4.5.1) as the steady state solution of Eq. (4.5.9). Use of this method is recommended in (SK1) for solution of Eq. (4.5.1). A quadrature of (4.5.9), the method doubles the integration interval each step. For high order systems, however, with large separation of the elements of F, this writer has found sufficiently large errors (on the order of 30 per cent) without significant computation time decrease, that the exact methods are deemed preferable.*

Exact methods are discussed in (BE1). It is shown that the solution for P is unique for all Q if the eigenvalues of F are stable. Bellman suggests using the Kronecker product to solve for P. This requires writing the n^2 elements of P and Q into a n^2 column (by rows). Then the elements of P are determined by solution of

$$\mathcal{A}(p_{11}\ p_{12} \cdots p_{21} \cdots p_{nn})^T = (q_{11}\ q_{12} \cdots q_{21} \cdots q_{nn})$$

where $\mathcal{A}$ is defined by the Kronecker product, $\otimes$,

$$\mathcal{A} = F \otimes I_n + I_n \otimes F$$

$$= \begin{bmatrix} F_c+f_{11}^c I_n & f_{12}^c I_n & \cdots & f_{1n}^c I_n \\ f_{21}^c I_n & F_c+f_{22}^c I_n & \cdots & \\ \vdots & \vdots & \cdots & \vdots \\ f_{n1}^c I_n & f_{2n}^c I_n & \cdots & F_c+f_{nn}^c I_n \end{bmatrix}$$

*This author has subsequently learned that Stein's method has been developed further by Honeywell, Inc.

for a tenth order system solution of P using this method requires inversion of a 100×100 matrix.

However, the order of the solution may be reduced because there are only $n(n+1)/2$ distinct elements of the P matrix, since it is symmetrical. The cost of this reduction of order is a more complicated $\mathcal{A}$ coefficient matrix.

A modification of Chen's algorithm*(CH1) will provide the required $\mathcal{A}$ matrix. The $\mathcal{A}$ matrix is of dimension $n(n+1)/2$ by $n(n+1)/2$. Number the columns of $\mathcal{A}$ by the pair (k,l), and the rows of $\mathcal{A}$ by the pair (i,j). i,j,l, and k run to n inclusively, the sequencing corresponding to the distinct elements of P which the $\mathcal{A}$ coefficients multiply. Hence, if P is 2×2, the $\mathcal{A}$ is 3×3 and $(k,l) = \{(1,1), (1,2),(2,2)\}$. The required algorithm is then based on the truth table:

$$\mathcal{A}(\cdot,\cdot) = \begin{cases} 2f_c(j,l) & \text{if } k = i, l \neq j \\ 2f_c(i,k) & \text{if } k \neq i, l = j \end{cases}$$

$$\begin{cases} 2f_c(i,l) & \text{if } k = j, l \neq i \\ 2f_c(j,k) & \text{if } k \neq j, l \neq i \\ 0 & \text{if } k \neq j, l \neq i \end{cases}$$

$$\begin{cases} 2f_c(i,k) & \text{if } k = j, l = i \\ 2f_c(i,k)+2f_c(j,l) & \text{if } k \neq j, l \neq i \,. \end{cases}$$

The 2×2 P matrix then gives the $\mathcal{A}$ matrix,

(i,j) \ (k,l)	(1,1)	(1,2)	(2,2)
1,1	$2f_{11}^c$	$2f_{12}^c$	0
1,2	$2f_{21}^c$	$2f_{11}^c+2f_{22}^c$	$2f_{12}^c$
2,2	0	$2f_{21}^c$	$2f_{22}^c$

then

$$\mathcal{A}P = -Q \,. \tag{4.5.10}$$

* A later equivalent implementation of form of $\mathcal{A}$, due to Bingulac (B11), is used in OPTSYS (Sec. 4.6).

Although $P = -\mathcal{A}^{-1}Q$, it has been found that it is much faster computationally to solve the $n(n+1)/2$ linear algebraic equations of (4.5.10).

4.6 The OPTSYS Computer Program

The theory of this chapter has been used to develop a double precision IBM 360 computer program. Although written originally to synthesize controllers for rotary-wing VTOL aircraft, the program is adaptable to synthesize controllers for other multivariable systems and to smoothing and filter synthesis with little modification.

The program considers the constant coefficient linear system with stationary statistics:

$$\mathbf{x} = \mathbf{F}\mathbf{x} + \mathbf{G}\mathbf{u} + \Gamma\mathbf{w} \tag{4.6.1}$$

$$\mathbf{z} = \mathbf{H}\mathbf{x} + \mathbf{v} \tag{4.6.2}$$

where

$\mathbf{x}$ = state vector $(n\times 1)$

$\mathbf{u}$ = control vector $(m\times 1)$

$\mathbf{w}$ = white noise vector $(q\times 1)$; the statistics of $\mathbf{w}$ are: $E(\mathbf{w}) = 0$, $E(\mathbf{w}\mathbf{w}^T) = Q\delta(t-\tau)$ where Q is the power spectral density matrix of $\mathbf{w}$

$\mathbf{z}$ = measurement vector $(p\times 1)$

$\mathbf{v}$ = white noise vector $(p\times 1)$; the stationary statistics of $\mathbf{v}$ are: $E(\mathbf{v}) = 0$, $E(\mathbf{v}\mathbf{v}^T) = R(t-\tau)$ where R is the power spectral matrix of $\mathbf{v}$.

The quadratic performance (or cost) index is the expected value of

$$J = \tfrac{1}{2}\mathbf{x}^T A\mathbf{x} + \tfrac{1}{2}\mathbf{u}^T B\mathbf{u}$$

in the statistical steady state. A is the state weighting coefficient matrix and B is the control weighting coefficient matrix.

The program implicitly assumes the certainty equivalence, or separation, principle. This states that the optimal feedback in the ensemble average sense for the system (4.6.1), (4.6.2) is the optimal deterministic controller preceded by the optimal filter of the state estimates. Therefore, a three part computation schedule was constructed, any part of which may be bypassed, Table 4.6.1. The program scheduling is determined by binary options at computation initiation.

The stationary statistical response of the state and control are determined from the linear matrix equation,

$$(F-GC)\hat{X} + \hat{X}(F-GC)^T + M = 0$$

where

$$M = \begin{cases} \Gamma^T Q \Gamma & \text{for perfect measurements of the state} \\ & \text{and } X \text{ the covariance of the state} \\ KRK^T & \text{for filtered estimates of the state and} \\ X = \hat{X} + P & \text{the covariance of state estimate;} (K = PH^T R^{-1}) \end{cases}$$

and where

X = covariance of state, $E[x(t)x(t)^T]$

$\hat{X}$ = covariance of estimate, $E[\hat{x}(t)\hat{x}(t)^T]$

P = estimate error covariance, $E[(x(t)-\hat{x}(t))(x(t)-\hat{x}(t))^T]$

The control covariance is

$$E\{uu^T\} = C\hat{X}C^T .$$

The actual covariance matrices are not generally required, so only the variances, the square roots of the diagonal elements of the covariance matrix, are printed out.

A summary of the program input requirements and output option is

given in Table 4.6.1.

Table 4.6.1. OPTSYS INPUT REQUIREMENTS AND OUTPUT OPTIONS

	INPUT	OUTPUT
DETERMINISTIC CONTROLLER	F,G A,B	• F,G,A,B • eigenvalues and eigenvectors of F • eigenvalues and eigenvectors of $F-GB^{-1}G\ S_\infty$ • steady state solution of Riccati equation, S_∞ • control gains, $B^{-1}G\ S_\infty$ • (F-GC)
KALMAN FILTER	F,H Q,R	• F,H,Q,R • eigenvalues and eigenvectors of $F-PH^TR^{-1}H$ • steady state covariance of filter error and estimate errors • Kalman filter gains, PH^TR^{-1} • $F-PH^TR^{-1}H$
STATIONARY STATISTICS OF CLOSED LOOP DYNAMICS	(F-GC) Γ,Q K,R	• controlled steady state RMS response in presence of random disturbances with or without perfect measurements • control RMS responses

For the results of Chapter 6, perfect state knowledge is assumed, so that the filter is not required, and

$$P = 0$$

$$\hat{X} = X \ .$$

A typical output for this calculations is shown in Fig. 4.6.1, which is a solution for hingeless rotor characteristics at hover (Chapters 4 and 6). Since no filter is assumed to be required, only the deterministic controller data are printed.

OUTPUT	MATRIX
OPEN LOOP DYNAMICS MATRIX.... OMBS= 0.37895 C1= 0.00545 C2= 0.02881 0.00000 0.00000 1.00000 0.00000 0.00000 0.00000 0.00000 0.00000 0.00000 0.00000 0.00000 0.00000 0.00000 1.00000 0.00000 0.00000 0.00000 0.00000 0.00000 0.00000 -0.42573 -1.32613 -1.32613 -2.00017 -0.00000 -0.00000 -1.35626 -2.24609 0.14116 -0.40584 1.32234 -0.55477 2.00065 -1.32234 -0.00000 -0.00000 2.25023 -1.35145 -0.40550 -0.13637 -0.00000 -0.00000 -0.00000 -0.00000 -0.00000 -0.00000 1.00000 0.00000 0.00000 0.00000 0.00000 0.00000 0.00000 0.00000 0.00000 0.00000 0.00000 1.00000 0.00000 0.00000 0.04234 -0.00124 -0.00124 0.00016 0.00000 0.00000 -0.00158 0.00136 0.00157 -0.00011 0.00467 0.15515 -0.00059 -0.00467 -0.00000 -0.00000 -0.00511 -0.00594 -0.00042 -0.00590 -0.00108 0.00123 0.00123 -0.00007 -0.00229 -0.00000 0.00576 0.00172 -0.00068 0.00027 0.00123 0.00108 -0.00007 -0.00123 -0.00000 0.00229 0.00172 -0.00576 -0.00027 -0.00068	F
THE CONTROL DISTRIBUTION MATRIX IS.... -0.00000000 -0.00000000 -0.00000000 -0.00000000 -1.32612596 -0.00321273 0.01207475 -1.32233580 0.00000000 -0.00000000 -0.00000000 -0.00000000 -0.00124369 0.00290796 -0.01092928 -0.00467429 0.00123261 -0.00121140 0.00121140 0.00123261	G
THE STATE COST MATRIX IS.... 0.00000 1.00000 0.00000 0.00000 0.00000 0.00000 0.00000 0.00000 0.00000 0.00000 0.00000 0.00000 1.00000 0.00000 1.00000 0.00000 0.00000 0.00000 0.00000 0.00000 0.00000 0.00000 0.00000 0.00000 0.00000 1.00000	A
THE CONTROL COST MATRIX IS.... 1.00000 0.00000 0.00000 1.00000	B

Fig. 4.6.1. TYPICAL OUTPUT OF OPTSYS (DETERMINISTIC CONTROLLER ONLY)*

(Figure 4.6.1 continued)

*The state vector is

$$(\theta_R,\ \phi_R,\ \dot{\theta}_R,\ \dot{\phi}_R,\ \theta_F,\ \phi_F,\ \dot{\theta}_F,\ \dot{\phi}_F,\ \bar{u},\ \bar{v})$$

The control vector is

$$(\theta_c, \theta_s)$$

Angles are in radians, time in units of $1/\Omega$, length in units of R where Ω = spin angular velocity of rotor = 21.3 rad sec^{-1}, R = rotor radius = 31.0 ft.

OUTPUT	MATRIX
OPEN LOOP EIGENVALUES AND EIGENVECTORS..... COMPLEX EIGENVALUE(1)..... COMPLEX EIGENVECTOR(1)..... (-0.448695261+J(1.96095836) (0.448368371+J(-0.160447418) (-0.152055491+J(-0.459653851 (-0.015455491+J(0.970379501 (1.000000001+J(0.000000001 (-0.002721731+J(0.003931011 (0.015409091+J(0.010302901 (-0.005942981+J(-0.007887221 (-0.030199151+J(0.023533141 (0.000479981+J(0.000267941 (-0.000296911+J(0.000424721 COMPLEX EIGENVALUE(2)..... COMPLEX EIGENVECTOR(2)..... (-0.360861141+J(0.265836051 (-0.477642831+J(0.134251161 (1.000000001+J(0.000000001 (0.136673941+J(-0.175420711 (-0.360861141+J(0.265836051 (-0.059443031+J(-0.097079621 (0.232712191+J(0.761669221 (0.047257941+J(0.019230161 (-0.286455921+J(-0.212993531 (-0.003885211+J(-0.001717651 (-0.001949961+J(-0.009363301 COMPLEX EIGENVALUE(3)..... COMPLEX EIGENVECTOR(3)..... (0.003675431+J(0.018976531 (-0.007951581+J(-0.000171601 (-0.001575101+J(0.001737731 (-0.000025971+J(-0.000151521 (-0.000038771+J(-0.000023501 (1.000000001+J(0.000000001 (0.021188181+J(-0.690816571 (0.003675431+J(0.018976531 (0.013187181+J(-0.002136971 (-0.020845101+J(0.114430181 (-0.078759821+J(-0.016674541 COMPLEX EIGENVALUE(4)..... COMPLEX EIGENVECTOR(4)..... (-0.000793261+J(0.020637681 (-0.002864231+J(0.005926281 (-0.002194501+J(-0.003726531 (-0.000120031+J(-0.000063811 (0.000078651+J(-0.000042331 (0.001056191+J(-0.679102261 (1.000000001+J(0.000000001 (0.014014261+J(0.000560501 (-0.000793261+J(0.020637681 (0.075271351+J(-0.004059261 (-0.006086661+J(-0.111119811 REAL EIGENVALUE (1)..... REAL EIGENVECTOR(1)..... (-0.530943711+J(-0.000000001 (0.825651111 (-0.254410231 (-0.438374261 (0.127893801 (-0.131510921 (-0.067904411 (0.069824901 (0.004372161 (0.000407261 REAL EIGENVALUE (2)..... REAL EIGENVECTOR(2)..... (-0.113050441+J(-0.000000001 (-0.253281811 (0.041538541 (0.028633621 (-0.004695951 (-0.866131111 (0.413033821 (0.097916501 (-0.046693661 (-0.025147441 (-0.010028611	EIGENVALUES AND EIGENVECTORS OF F

(Figure 4.6.1 continued)

OUTPUT	MATRIX

```
EIGENSYSTEM OF THE OPTIMAL CLOSED LOOP SYSTEM....

COMPLEX EIGENVALUE( 1).....          COMPLEX EIGENVECTOR( 1).....

( -0.648590668)+J( 1.961154588)      (  0.448347688)+J(  0.140411208)
                                     ( -0.152008738)+J(  0.459631478)
                                     ( -0.015426008)+J( -0.970348698)
                                     (  1.000000008)+J(  0.000000008)
                                     ( -0.002721708)+J( -0.003929478)
                                     (  0.015403018)+J( -0.010303668)
                                     ( -0.005941038)+J(  0.007886308)
                                     ( -0.030197338)+J( -0.023524838)
                                     (  0.000479768)+J( -0.000267818)
                                     ( -0.000297018)+J( -0.000426748)

COMPLEX EIGENVALUE( 2).....          COMPLEX EIGENVECTOR( 2).....

( -0.325950468)+J(  0.384456428)     ( -0.360881528)+J( -0.213586858)
                                     (  1.000000008)+J(  0.000000008)
                                     (  0.035508148)+J(  0.208354268)
                                     ( -0.325950468)+J( -0.384456428)
                                     ( -0.024230608)+J(  0.072005948)
                                     ( -0.111811458)+J( -0.629040628)
                                     (  0.035581128)+J( -0.014154768)
                                     ( -0.205393718)+J(  0.248022718)
                                     ( -0.003127758)+J(  0.001275728)
                                     (  0.001705178)+J(  0.005852518)

COMPLEX EIGENVALUE( 3).....          COMPLEX EIGENVECTOR( 3).....

( -0.162369458)+J(  0.159858888)     (  1.000000008)+J(  0.000000008)
                                     ( -0.073650568)+J(  0.020751798)
                                     ( -0.162369458)+J( -0.159858888)
                                     (  0.015275968)+J(  0.008404248)
                                     (  0.011971538)+J( -0.854820988)
                                     (  0.049797938)+J(  0.170576408)
                                     ( -0.138594548)+J(  0.136883058)
                                     (  0.019182498)+J( -0.035657048)
                                     (  0.000997088)+J( -0.016438008)
                                     ( -0.007584998)+J(  0.002012478)

COMPLEX EIGENVALUE( 4).....          COMPLEX EIGENVECTOR( 4).....

( -0.002573278)+J(  0.000237068)     (  0.004531618)+J( -0.006871658)
                                     (  0.011456538)+J(  0.000665588)
                                     ( -0.000013298)+J(  0.000016618)
                                     ( -0.000029328)+J( -0.000004448)
                                     ( -0.382093368)+J(  0.593543368)
                                     ( -0.668132878)+J(  0.038092588)
                                     (  0.001072478)+J( -0.001441518)
                                     (  0.001728318)+J(  0.000060368)
                                     ( -0.296138408)+J(  0.591442568)
                                     (  1.000000008)+J(  0.000000008)

REAL EIGENVALUE   ( 1).....          REAL EIGENVECTOR( 1).....

( -0.938495018)+J( -0.000000008)     ( -0.786396418)
                                     (  0.335777808)
                                     (  0.423470548)
                                     ( -0.180814678)
                                     ( -0.118860538)
                                     (  0.172911988)
                                     (  0.064005808)
                                     ( -0.093112248)
                                     ( -0.004244088)
                                     ( -0.001302788)

REAL EIGENVALUE   ( 2).....          REAL EIGENVECTOR( 2).....

( -0.453408858)+J( -0.000000008)     (  0.457498508)
                                     ( -0.621497608)
                                     ( -0.207433878)
                                     (  0.281792518)
                                     (  0.100911318)
                                     ( -0.472946578)
                                     ( -0.045754088)
                                     (  0.214438168)
                                     (  0.001805908)
                                     (  0.006843128)
```

EIGENVALUES AND EIGENVECTORS OF $(F-GC)$, λ_i AND X_i

(Figure 4.6.1 continued)

OUTPUT	MATRIX
THE RICATTI GAIN MATRIX 0.77491522 0.16401462 0.22740786 -0.20699558 1.75540116 0.16401462 1.09512030 0.37966893 0.21022139 -0.39100841 0.22740786 0.37966893 0.17216085 0.01789161 0.28797795 -0.20699558 0.21022139 0.01789161 0.11733103 -0.61832713 1.75540116 -0.39100841 0.28797795 -0.61832713 8.37658553 0.45842869 1.76823667 0.61112113 0.29934667 0.02034260 10.93620524 -2.50655044 1.70226027 -4.02856618 31.90621770 1.62205023 5.11660295 1.91590824 0.74430501 0.32315269 -0.49014984 0.34883581 0.11647794 -0.00231123 -0.72982764 0.09554750 1.72074826 0.42371102 0.33151794 -0.23895825 0.45842869 10.93620524 1.62205023 -0.49014984 0.09954750 1.76823667 -2.50655044 5.11660295 0.34883581 1.72074826 0.61112113 1.70226027 1.91590824 0.11647794 0.42371102 0.29934667 -4.02856618 0.74430501 -0.00231123 0.33151794 0.02034260 31.90621770 0.32315269 -0.72982764 -0.23895825 4.91309124 -0.35227333 10.09065013 -1.12651120 5.13377455 -0.35227333 181.95371498 2.04166146 3.67939000 -12.56333825 10.09065013 2.04166146 26.77255669 -2.28900175 5.40044184 -1.12651120 3.67939000 -2.28900175 447.36034003 -28.72935241 5.13377455 -12.56333825 5.40044184 -28.72935241 288.92088647	$(S_B)_{SS}$
THE CONTROL GAINS ARE: 0.33588356 0.55123936 0.25049066 0.02503545 0.44362441 0.51182394 2.56534760 2.82317156 -0.38256510 0.28670340 -0.29792362 0.30871007 0.02783607 0.16999108 -0.91826308 0.43829867 -5.82127599 1.10015268 0.55326173 0.11058801	$C = -B^{-1}G^T(S_B)_{SS}$
THE CLOSED LOOP DYNAMICS MATRIX IS.. 0.00000 0.00000 1.00000 0.00000 0.00000 0.00000 0.00000 0.00000 0.00000 0.00000 0.00000 0.00000 0.00000 1.00000 0.00000 0.00000 0.00000 0.00000 0.00000 0.00000 -0.87020 -2.05813 -1.65840 -2.03392 -0.58535 -1.21060 -4.73953 -5.99350 0.64671 -0.78640 1.72035 -0.95634 1.96687 -1.54682 1.21961 -0.56857 9.97889 -2.77213 -1.14172 -0.27914 -0.00000 -0.00000 -0.00000 -0.00000 -0.00000 -0.00000 1.00000 0.00000 0.00000 0.00000 0.00000 0.00000 0.00000 0.00000 0.00000 0.00000 0.00000 1.00000 0.00000 0.00000 0.04106 -0.00103 -0.00147 0.00062 -0.00322 0.00014 -0.02170 0.00105 0.00366 -0.00015 0.00240 0.15168 -0.00346 -0.00574 -0.00056 -0.01201 -0.00593 -0.04193 0.00118 -0.00955 -0.00031 0.00154 0.00151 -0.00024 -0.00063 0.00059 0.01597 0.00387 -0.00182 0.00049 0.00127 0.00213 0.00021 -0.00099 -0.00059 0.00394 -0.00235 -0.00098 -0.00005 -0.00020	$F-GC = F - GB^{-1}G^T(S_B)_{SS}$
THE CONTROL COVARIANCE 0.00000789 0.00002124 0.00002124 0.00081781	$E\{uu^T\}$
STATE RMS RESPONSE 2.35876086 1.85605115 2.19473362 2.84379112 1.43164074 0.86339684 0.19356609 0.25417080 0.18664480 0.15035600	CONTROL RMS RESPONSE 0.16091000 1.63842972
	$E\{xx^T\}$

4.7 Time-Varying Solutions of the Constant Coefficient Homogeneous Euler-Lagrange Equations

Generally, only the steady state solution of the matrix Riccati equation is desired to implement constant coefficient controllers or estimators. However, for optimal open loop control or estimation, the transient of the time-varying solution of the Riccati equation may be desired.

Unfortunately, the complete time-varying solution is inherently a ratio of two time varying matrices. Consequently, the complete solution requires the inversion of an $n \times n$ matrix for each value of time when a continuous unsteady solution is desired.

The ξ_o and η_o of Eqs. (4.3.7)-(4.3.8) may be determined easily since the eigenvector matrix, T, is symplectic (see Appendix B);

$$\xi_o = e^{-\delta_+(t-t_o)}[\Lambda_-^T x(t) - X_-^T \lambda(t)] \tag{4.7.1}$$

$$\eta_o = e^{-\delta_+(t_f-t)}[-\Lambda_+^T x(t) + X_+^T \lambda(t)] \tag{4.7.2}$$

and the ξ_o and η_o are determined by the boundary conditions of $x(t)$ and $\lambda(t)$. The homogeneous boundary condition of the regulator problem, for example, yields

$$\xi_o = e^{-\delta_+(t_f-t_o)}[\Lambda_- - S_f X_-]^T[-\Lambda_+ + S_f X_+]^{-T}\eta_o \ . \tag{4.7.3}$$

Defining the symmetric matrix, E,

$$E = [\Lambda_- - S_f X_-]^T[-\Lambda_+ + S_f X_+]^{-T} \ . \tag{4.7.4}$$

Substitution of (4.7.3) into Eqs. (4.3.7) and (4.3.8) yields

$$x(t) = [+X_+ e^{-\delta_+(t_f-t)}_E \; e^{-\delta_+(t_f-t)} + X_-]e^{\delta_+(t_f-t)}\eta_o \qquad (4.7.5)$$

$$\lambda(t) = [+\Lambda_+ e^{-\delta_+(t_f-t)}_E \; e^{-\delta_+(t_f-t)} + \Lambda_-]e^{\delta_+(t_f-t)}\eta_o \; . \qquad (4.7.6)$$

Now, $x(t_o)$ is given for the regulator problem, and this determines $x(t)$ and $\lambda(t)$;

$$x(t) = X_-[I+X_-^{-1}X_+ e^{-\delta_+(t_f-t)}_E \; e^{-\delta_+(t_f-t)}]e^{-\delta_+(t-t_o)}]$$
$$\cdot \; [I+X_-^{-1}X_+ e^{-\delta_+(t_f-t_o)}_E \; e^{-\delta_+(t_f-t_o)}]^{-1}X_-^{-1}x(t_o) \qquad (4.7.7)$$

$$\lambda(t) = \Lambda_-[I+\Lambda_-^{-1}\Lambda_+ e^{-\delta_+(t_f-t)}_E \; e^{-\delta_+(t_f-t)}]e^{-\delta_+(t-t_o)}]$$
$$\cdot \; [I+X_-^{-1}X_+ e^{-\delta_+(t_f-t_o)}_E \; e^{-\delta_+(t_f-t_o)}]^{-1}X_-^{-1}x(t_o) \; . \qquad (4.7.8)$$

Equations (4.7.7) and Eq. (4.7.8) are the optimal open loop solutions of $x(t)$ and $\lambda(t)$ from $x(t_o)$. Equation (4.7.8) gives the open loop control since $u(t) = -B^{-1}G^T\lambda(t)$. Several cases of Eqs. (4.7.7) and (4.7.8) are of interest.

Case A: $S_f \to \infty$ (infinite weighting on terminal state)

Since E may be rewritten as

$$E = X_+^{-1}[I-S_f^{-1}\Lambda_+X_+^{-1}]^{-1}[S_f^{-1}\Lambda_-X_-^{-1}-I]X_- \; ,$$

it is obvious that $E \to X_+^{-1}X_-$ as $S_f \to \infty$. Then, from Eq. (4.7.7) and (4.7.8),

$$\lim_{S_f \to \infty} x(t_f) = 0 \qquad \lim_{S_f \to \infty} \lambda(t_f) = \infty$$

and the optimal trajectory goes to zero at t_f .

Case B: $t_f \to \infty$ (infinite time of regulation)

Equations (4.7.7) and (4.7.8) immediately become

$$x(t) = (X_- e^{-\delta_+(t-t_o)} X_-^{-1}) x(t_o) \tag{4.7.9}$$

$$\lambda(t) = (\Lambda_- e^{-\delta_+(t-t_o)} X_-^{-1}) x(t_o) \ . \tag{4.7.10}$$

Again, it is seen that the eigenvectors and eigenvalues of the optimal state response are X_- and δ_-, respectively.

Case C: $t \to t_o$ (continuous control law)

Equations (4.7.7) and (4.7.8) give the sampled data response if $x(t_o)$ is regarded as a new sample of the state. The continuous response is therefore obtained by letting $t \to t_o$, or

$$x(t) = x(t) \quad \text{(identity)} \tag{4.7.11}$$

$$\lambda(t) = \Big\{ \Lambda_- [I + \Lambda_-^{-1} \Lambda_+ e^{-\delta_+(t_f-t)} E \, e^{-\delta_+(t_f-t)}]$$

$$\cdot \, [I + X_-^{-1} X_+ e^{-\delta_+(t_f-t)} E \, e^{-\delta_+(t_f-t)}]^{-1} X_-^{-1} \Big\} x(t) \ . \tag{4.7.12}$$

The term in the outer brackets is obviously $S(t)$, since $\lambda(t) = S(t)x(t)$. It is obvious that, as $t_f \to \infty$,

$$\lim_{t_f \to \infty} S(t) = \Lambda_- X_-^{-1}$$

which is precisely Eq. (4.3.11) for $(S_B)_{SS}$, where

$$S_B(t) = \Lambda_- [I + \Lambda_-^{-1} \Lambda_+ e^{-\delta_+(t_f-t)} E \, e^{-\delta_+(t_f-t)}]$$

$$\cdot \, [I + X_-^{-1} X_+ e^{-\delta_+(t_f-t)} E \, e^{-\delta_+(t_f-t)}]^{-1} X_-^{-1} \ . \tag{4.7.13}$$

As mentioned previously, the time-varying solution requires the inversion of an $n \times n$ matrix for each time. Note that the boundness of $S_B(t)$ depends on the invertibility of X_- and the second term in brackets of Eq. (4.7.13). Since $E = -X_-^{-1}X_+$ for $S_f = \infty$, the bracketed term is identically zero at t_f for infinite weighting. At other times, the value of the second brackets depends not only on the eigenvectors of the system, but also on the boundary conditions. This is related to the conjugate point condition of optimization problems (BR1). Alternately, if X_-^{-1} does not exist, a function only of the system dynamics, the system is uncontrollable.

By a similar derivation, the solution of the covariance for the smoother problem is

$$P_F(t) = -X_+[I-X_+^{-1}X_- e^{-\delta_+(t-t_o)} D\, e^{-\delta_+(t-t_o)}] \cdot [I-\Lambda_+^{-1}\Lambda_- e^{-\delta_+(t-t_o)} D\, e^{-\delta_+(t-t_o)}]^{-1}\Lambda_+^{-1} \qquad (4.7.14)$$

where

$$D \triangleq (X_- + P_o\Lambda_-)^{-1}(X_+ + P_o\Lambda_+) \qquad (4.7.15)$$

and P_o is assumed given.

4.8 Summary

The solution of a matrix Riccati equation is fundamental to the technique of quadratic synthesis for control systems. Various solution techniques for this equation are available. One very powerful method is based on the eigensystem of the constant coefficient Euler-Lagrange equations.

The derivation of the Euler-Lagrange equations for the smoothing problem with pre-flight, in-flight and post-flight data is given. Assuming a particular solution from the form of the initial boundary condition

of these equations, a forward Riccati equation and the forward Kalman-Bucy filter equation are obtained. Using stored solutions of these equations, the solution of the backward Euler-Lagrange equations may be found, and hence the smoothed estimate of the state. Similarly, assuming a particular solution from the form of the terminal boundary condition of the Euler-Lagrange equations, the backward Riccati equation and Kalman-Bucy filter equation may be determined. Solution of these equations can then be used to find the smoothed state estimate from the forward Euler-Lagrange equations.

The information form of the Riccati equation for the smoother is obtained by replacing the covariance by its inverse. By making a simple correspondence of matrices between the smoothing problem and the follower problem, it is found that the backward information Riccati equation is the same as the Riccati equation of the follower problem.

The solution of the matrix Riccati equation may be expressed in terms of the eigenvectors of the coefficient matrix of the Euler-Lagrange equations. This fact is used to determine the steady-state solutions for the smoother Riccati equation and the follower Riccati equation. It is also found that the steady state solution of the Fraser smoother may be expressed in terms of the eigenvectors of the Euler-Lagrange equations.

A very important characteristic of the stable eigenvalues of the matrix of the Euler-Lagrange equations is that they are the closed loop eigenvalues of the optimal regulator or estimator. Furthermore, the eigenvectors of the optimal controller or estimator may be obtained from the coefficient matrix eigenvectors without further computation.

A new computer program is given for implementing this theory. The program uses the highly efficient QR algorithm of Francis to determine the required eigensystem. In addition, the steady state RMS response of the closed loop system may be obtained.

The time-varying solution of the matrix Riccati equation may also be expressed in terms of the eigensystem of the homogeneous Euler-Lagrange equations. However, this solution requires a significant amount of computer time and storage.

Chapter V

CONTROLLER SYNTHESIS FOR A ROTARY WING VTOL AIRCRAFT NEAR HOVER

5.1 Introduction

In this chapter, a feedback controller is designed based on the tenth order rotor fuselage TRBM (two rigid body model) presented in Chapter 3. The performance of this controller is compared to controllers designed for the eighth order RRM (rotor rate model) and the sixth order RPM (rotor position model) on the basis of a quadratic cost which penalizes on deviations of fuselage state. These controllers are compared on the basis of the closed loop eigenvalues (frequency and relative stability) and eigenvectors (principal modal response), required control gain magnitude, and RMS response of the state and control to a random external excitation.

The design of regulators by quadratic synthesis specifies a control law which is a linear combination of all of the system states (or estimates of the states). Hence, three controllers are of interest. The TRBM controller and RRM controller are designed on the tenth order and eighth order rotor fuselage dynamics, respectively, while the RPM controller is designed on the sixth order fuselage model. Since two controls are available, the TRBM control law is determined by the twenty gains of Eqs. (5.1.1) and (5.1.2):

$$\theta_c = K_{\theta_R}\theta_R + K_{\phi_R}\phi_R + K_{q_R}q_R + K_{p_R}p_R + K_{\theta_F}\theta_F + K_{\phi_F}\phi_F + K_{q_F}q_F + K_{p_F}p_F + K_{\bar{u}}\bar{u} + K_{\bar{v}}\bar{v} \qquad (5.1.1)$$

$$\theta_s = L_{\theta_R}\theta_R + L_{\phi_R}\phi_R + L_{q_R}q_R + L_{p_R}p_R + L_{\theta_F}\theta_F + L_{\phi_F}\phi_F + L_{q_F}q_F + L_{p_F}p_F + L_{\bar{u}}\bar{u} + L_{\bar{v}}\bar{v} \qquad (5.1.2)$$

For the RRM controller, and RPM controller,

$$K_{q_R} = K_{p_R} = L_{q_R} = L_{p_R} = 0$$

and for the RPM controller, the additional gains

$$K_{\theta_R} = K_{\phi_R} = L_{\theta_R} = L_{\phi_R} = 0 \ .$$

Of particular interest is the use of the RPM controller, requiring only the fuselage states, on the TRBM dynamics whose controller requires both fuselage and rotor states. Since the RPM controller would be easier to implement because of its independence of the rotor state, it is important to be able to evaluate its degradation in performance relative to the TRBM controller. Figures 5.1.1 and 5.1.2 diagram the evaluation of the three controllers on their respective models and on the TRBM.

5.2 Design of Three Different Controllers Using the Two Rigid Body, Rotor Rate and Rotor Position Models

The control designs for this study are performed with the methods of Chapter 4. The A and B weighting matrices are taken to be diagonal and the basic control laws are designed with unity weighting factors on the fuselage states, $\theta_F, \phi_F, \bar{u}$, and $\bar{v}$ and on the control, θ_s and θ_c. This selection of common weighting factors is based on the desire to evaluate all the control systems on the same performance index, and therefore no weighting is placed on the rotor states, i.e.,

$$J = \lim_{t_f \to \infty} \int_0^{t_f} [\theta_F^2 A_{\theta_F} + \phi_F^2 A_{\phi_F} + \bar{u}^2 A_{\bar{u}} + \bar{v}^2 A_{\bar{v}} + \theta_c^2 B_{\theta_c} + \theta_s^2 B_{\theta_s}]dt \ . \quad (5.2.1)$$

For each controller, the resulting closed loop eigenvalues and eigenvectors are found, as well as the control gains and closed loop dynamics matrix. These control gains, all dimensionless, are shown in Table 5.2.1.

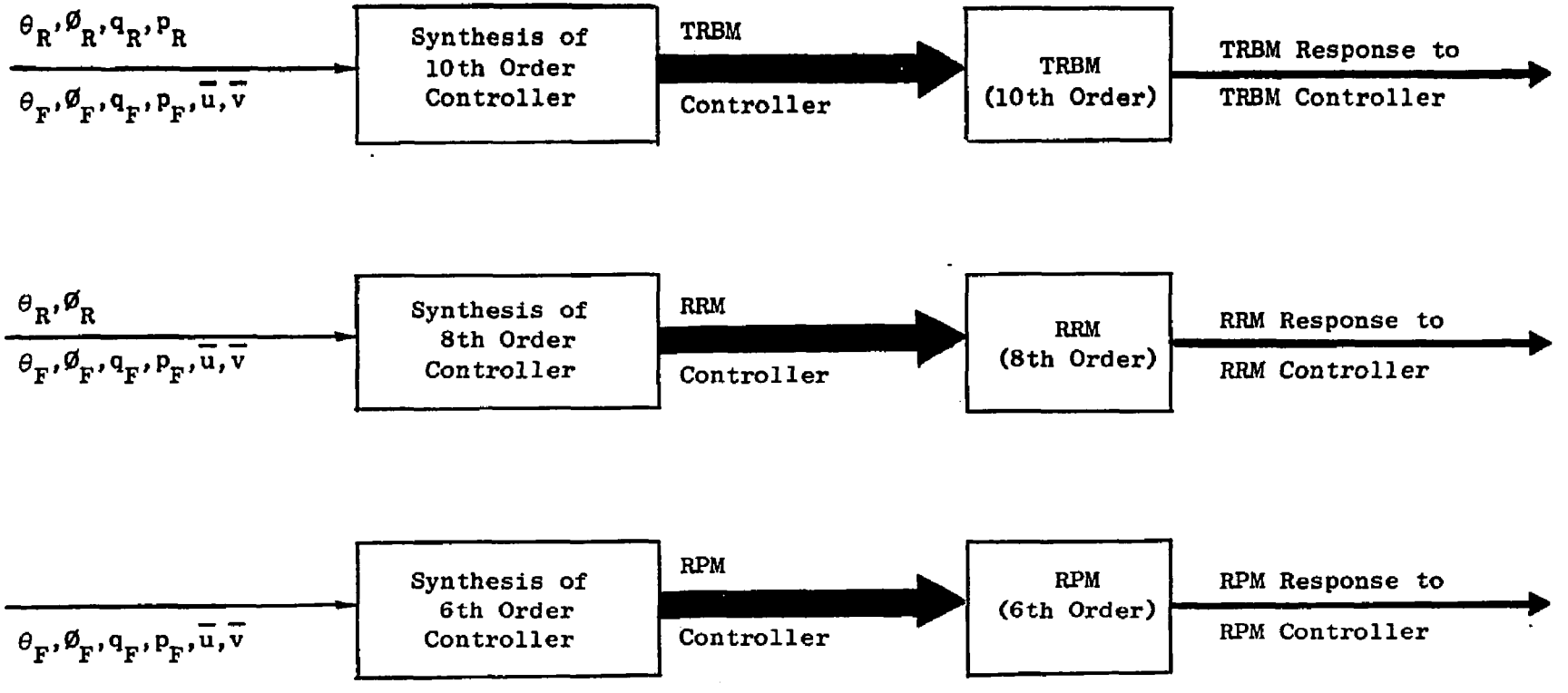

Fig. 5.1.1. SCHEMATIC OF TRBM, RRM, AND RPM CONTROLLER DESIGNS WITH EVALUATION ON THE RESPECTIVE MODELS.

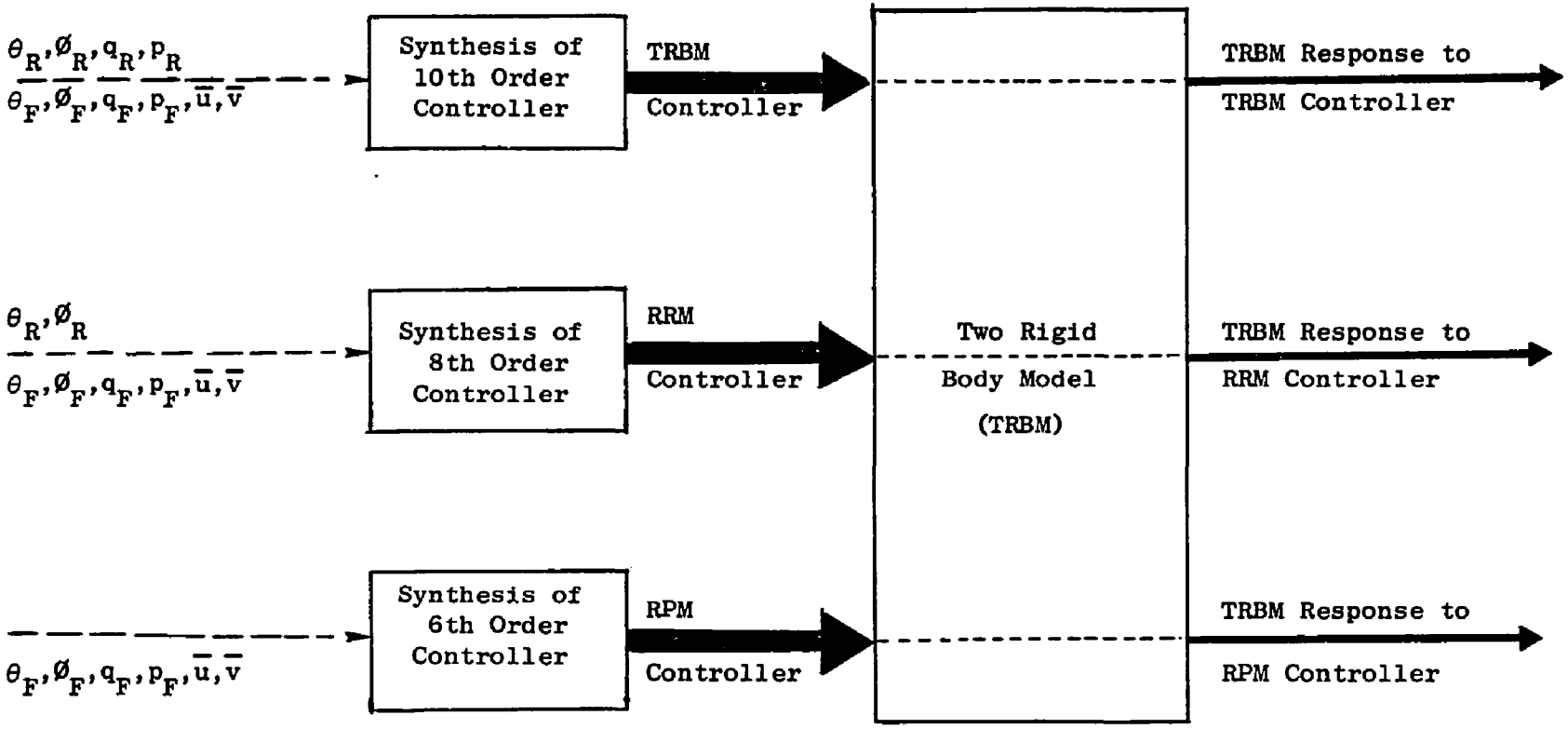

Fig. 5.1.2. SCHEMATIC OF TRBM, RRM, AND RPM CONTROLLERS ON TRBM.

Table 5.2.1. CONTROL GAINS FOR TRBM, RRM, RPM ($A_{\theta_F} = A_{\phi_F} = A_{\bar{u}} = A_{\bar{v}} = B_{\theta_c} = B_{\theta_s} = 1.0$)
(Cf. Figs. 5.1.1 and 5.1.2)

θ_c	K_{θ_R}	K_{ϕ_R}	K_{q_R}	K_{p_R}	K_{θ_F}	K_{ϕ_F}	K_{q_F}	K_{p_F}	$K_{\bar{u}}$	$K_{\bar{v}}$
TRBM(10)	.26	.31	.15	-.02	.28	.98	2.37	5.77	-.23	.25
RRM(8)	.24	.31	0	0	.27	.98	2.12	5.90	-.22	.25
RPM(6)	0	0	0	0	.18	1.00	.37	4.98	-.15	.32
θ_s	L_{θ_R}	L_{ϕ_R}	L_{q_R}	L_{p_R}	L_{θ_F}	L_{ϕ_F}	L_{q_F}	L_{p_F}	$L_{\bar{u}}$	$L_{\bar{v}}$
TRBM(10)	-.16	.17	.02	.09	- .99	.27	-11.4	.77	.63	-.06
RRM(8)	-.16	.16	0	0	-1.00	.26	-11.5	.68	.64	-.07
RPM(6)	0	0	0	0	-1.02	.17	-10.6	.25	.68	-.13

Several conclusions may be drawn from the gains of Table 5.2.1. First, even though no weighting is placed on the rotor state in the TRBM controller synthesis, the gain required of the rotor pitch angle is about the same as the fuselage pitch angle--slightly less than a third of a degree of lateral cyclic per degree of pitch. Also, the TRBM rotor roll angle feedback gain to the lateral cyclic is about a third of the fuselage roll angle feedback gain. The longitudinal cyclic has a rotor pitch gain which is about a fifth of the fuselage pitch gain and a rotor roll angle gain which is about two-thirds of the fuselage roll angle gain. Second, the RRM controller has almost the same gains as the TRBM controller for these weightings, with the exception, of course, of the rotor rate gains. The RPM controller indicates the need for less cross-coupling between pitch attitude and lateral cyclic (and roll attitude and longitudinal cyclic). This is due to the fuselage coupling which is neglected by neglecting the rotor. Third, the feedback gains on the "decoupled" state variables are comparable in magnitude to the usual state variables. Hence, the longitudinal-lateral decoupling, which is almost always assumed in the dynamic analysis and control design of hovering vehicles, is definitely <u>not</u> a good assumption for this vehicle.

5.3 Closed Loop Vehicle Response Using the Three Controllers with Their Respective Models

Using the three sets of feedback gains of Table 5.2.1, each with the model used in designing the gain, the closed-loop eigenvalues were computed and are shown in Table 5.3.1.

Table 5.3.1. CLOSED LOOP EIGENVALUES OF TRBM, RRM, AND RPM (cf. Fig. 5.1.1).

Mode	TRBM (Order 10)	RRM (Order 8)	RPM (Order 6)
1	-.66 ± j(1.79)	---	---
2	-.617 ± j(.242)	-.426 ± j(.314)	---
3	-.17 ± j(.160)	-.168 ± j(.154)	-.162 ± j(.157)
4	-.087 ± j(.090)	-.087 ± j(.090)	-.085 ± j(.081)
5	-.0027 ± j(.0003)	-.0027 ± j(.0003)	-.0026 ± j(.0004)

There is little difference between the low frequency closed loop eigenvalues. However, there are large changes in the feedback gains on the fuselage rate ($K_{q_F}, K_{p_F}, L_{q_F}$ and L_{p_F}) in going from the TRBM to the RPM. Without feedback on rotor rate (and position), it is necessary to have higher gains on the fuselage rates.

The mode shapes corresponding to the low frequency closed loop eigenvalues are shown in Fig. 5.3.1. The fuselage coordinates have about the same magnitude and phase for each mode, except that the RPM does not contain the strong effect of the lateral rotor positions on the mode 3. The lowest frequency eigenvector is independent of the model.

The mode shapes corresponding to the high frequency closed-loop eigenvalues of TRBM and RRM are shown in Fig. 5.3.2. The position coordinates (θ_R and ϕ_R) are about the same, in the second mode.

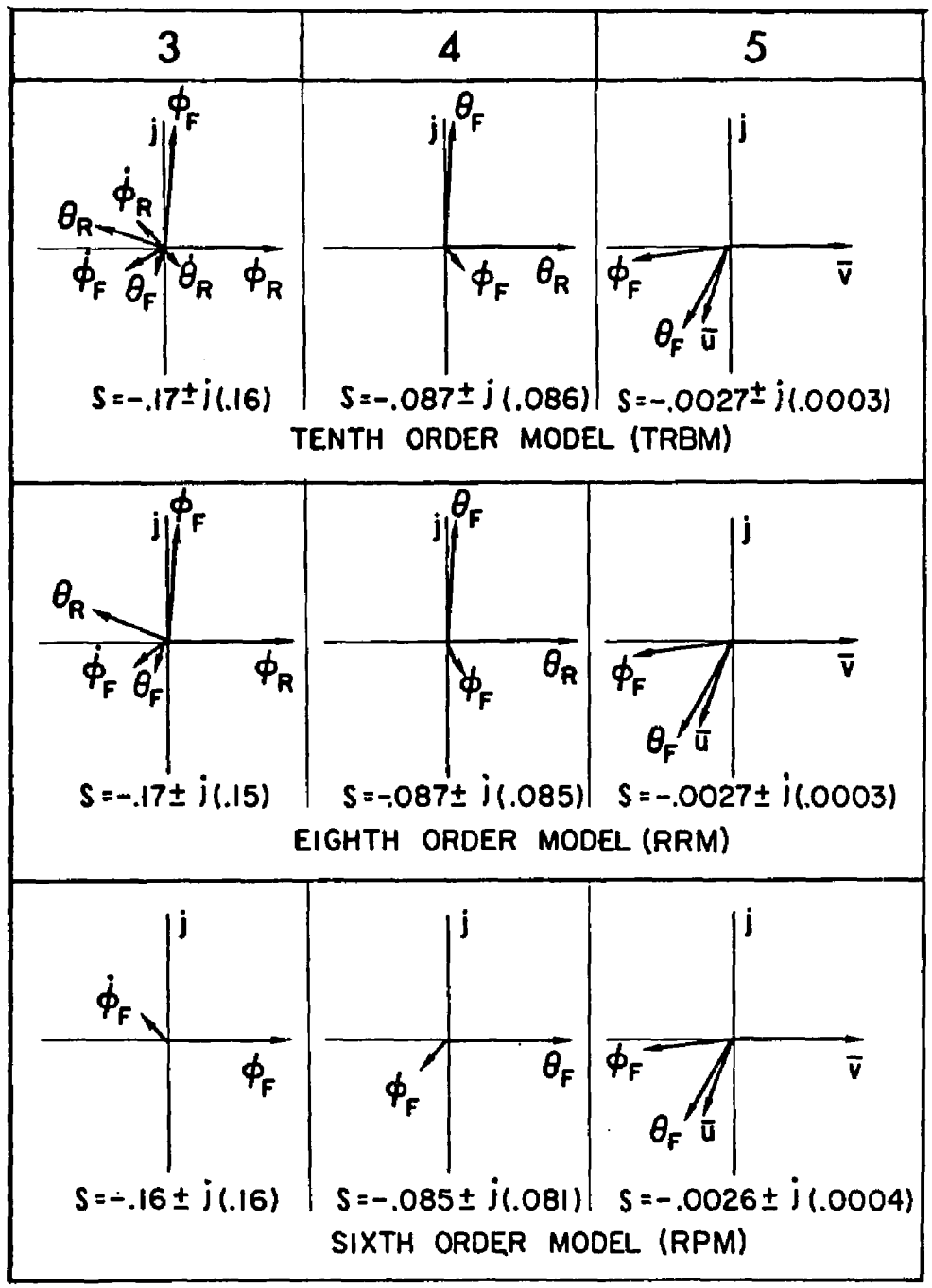

Fig. 5.3.1. MODE SHAPES CORRESPONDING TO THE THREE LOW FREQUENCY CLOSED LOOP EIGENVALUES. These modes have almost identical eigenvector components of the fuselage states. Only mode 5 has no contribution from the rotor state in the principal mode (cf. Fig. 5.1.1).

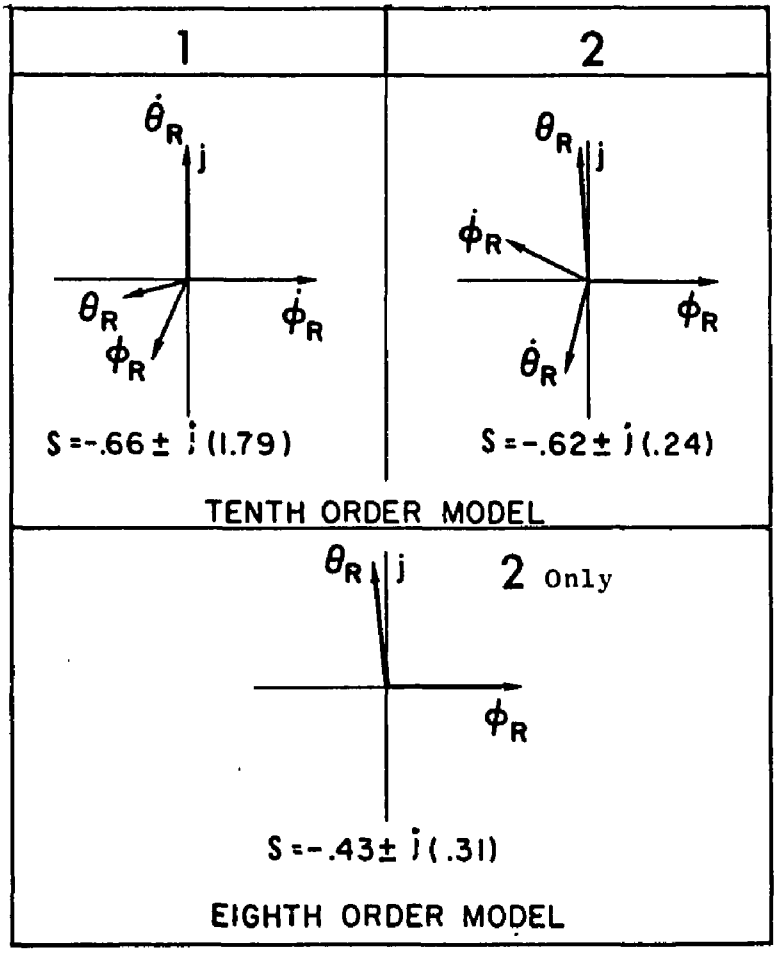

Fig. 5.3.2. MODE SHAPES CORRESPONDING TO TWO HIGH FREQUENCY CLOSED LOOP EIGENVALUES (TRBM AND RRM). The rotor position is represented the same in the precession mode, 2, of both rotor models (the eighth order model has no nutation mode, of course) (cf. Fig. 5.1.1).

5.4 Closed-Loop Vehicle Response Using the Three Controllers with the Complete Model

Next, the closed-loop eigenvalues and eigenvectors are computed using the RRM and RPM feedback gains in Table 5.2.1 with the complete tenth order model. The closed-loop eigenvalues are shown in Table 5.4.1 and, for comparison, the eigenvalues using the TRBM feedback gains are repeated from Table 5.3.1.

Table 5.4.1. CLOSED LOOP EIGENVALUES OF TRBM WITH RRM CONTROLLER AND RPM CONTROLLER (cf. Fig. 5.1.2)

Mode	TRBM	TRBM (RRM Controller)	TRBM (RPM Controller)
1	-.66 ± j(1.79)	-.508 ± j(1.89)	-.708 ± j(1.71)
2	-.617 ± j(0.242)	-.608 ± j(.165)	-.364 ± j(.450)
3	-.17 ± j(.160)	-.18 ± j(.161)	-.22 ± j(.083)
4	-.087 ± j(.090)	-.088 ± j(.084)	-.10 ± j(.10)
5	-.0027 ± j(.0003)	-.0024 ± j(.0007)	-.0024 ± j(.0006)

The three lower frequencies are about the same for all the controllers, except for mode 3 where the frequency using the RPM gains differs significantly. The two high frequency eigenvalues vary considerably depending on which set of control gains is used.

The eigenvectors for modes 3, 4, and 5 are shown in Fig. 5.4.1 and the eigenvectors for modes 1 and 2 are shown in Fig. 5.4.2. Mode 5 contains primarily fuselage motions and modes 1 and 2 contain primarily rotor motions, whereas modes 2 and 3 contain fuselage and rotor motions of about the same magnitude.

It would appear that using the two lower order models to design feedback gains for the complete model gives reasonable closed-loop behavior. However, it is shown in the next section that the mean square response of the vehicle in the presence of a random rotor torque differs depending on whether there is adequate rotor information fed back to anti-

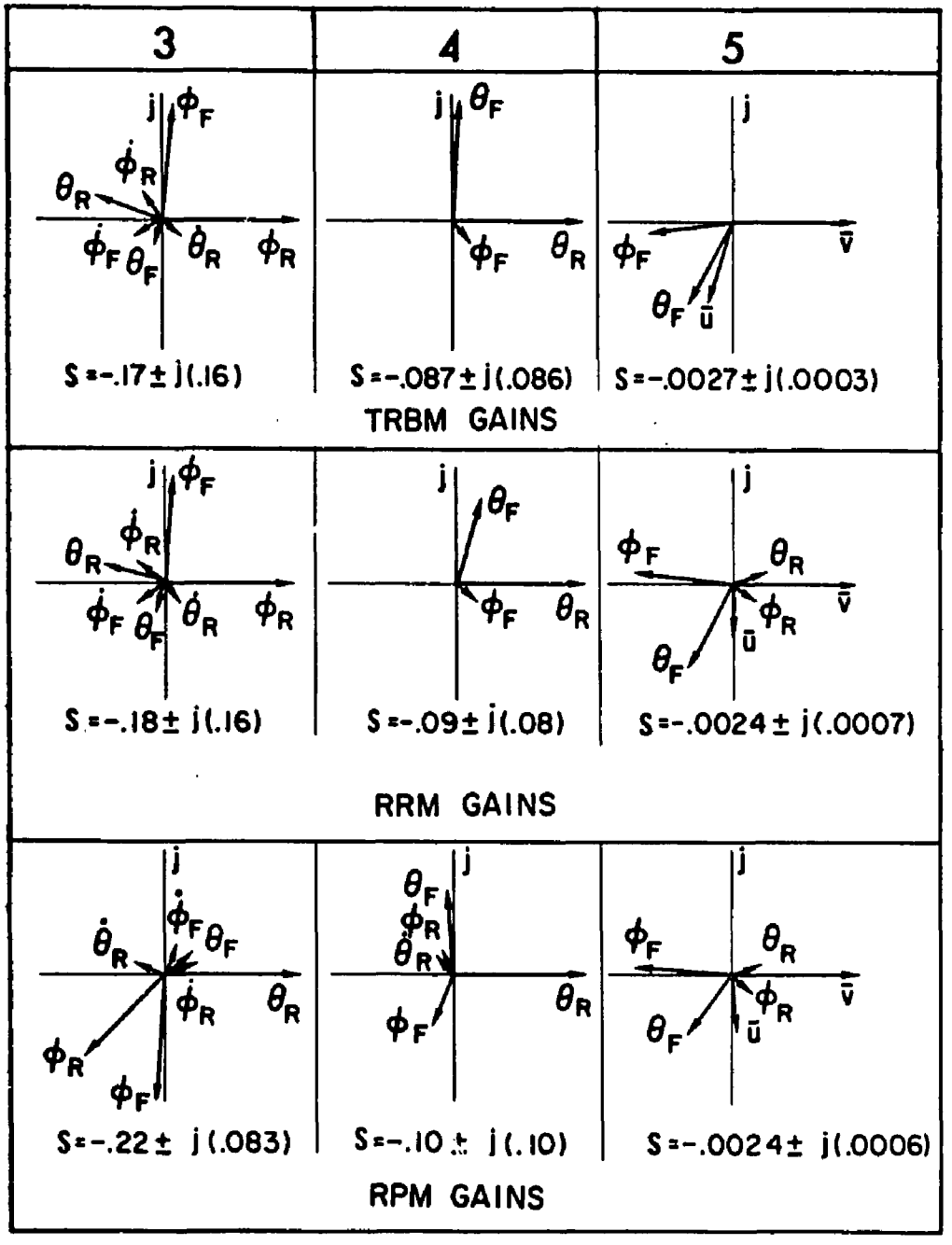

Fig. 5.4.1. COMPARISON OF LOW FREQUENCY MODE SHAPES USING FULL ORDER FEEDBACK (TRBM GAINS) WITH MODE SHAPES USING REDUCED ORDER FEEDBACK (RRM AND RPM) GAINS . The TRBM response with TRBM and RRM gains is almost the same for modes 1, 2, and 3. The RPM gains on the TRBM changes the phase relations on mode 3 where the rotor has slightly more pitch response (cf. Fig. 5.1.2).

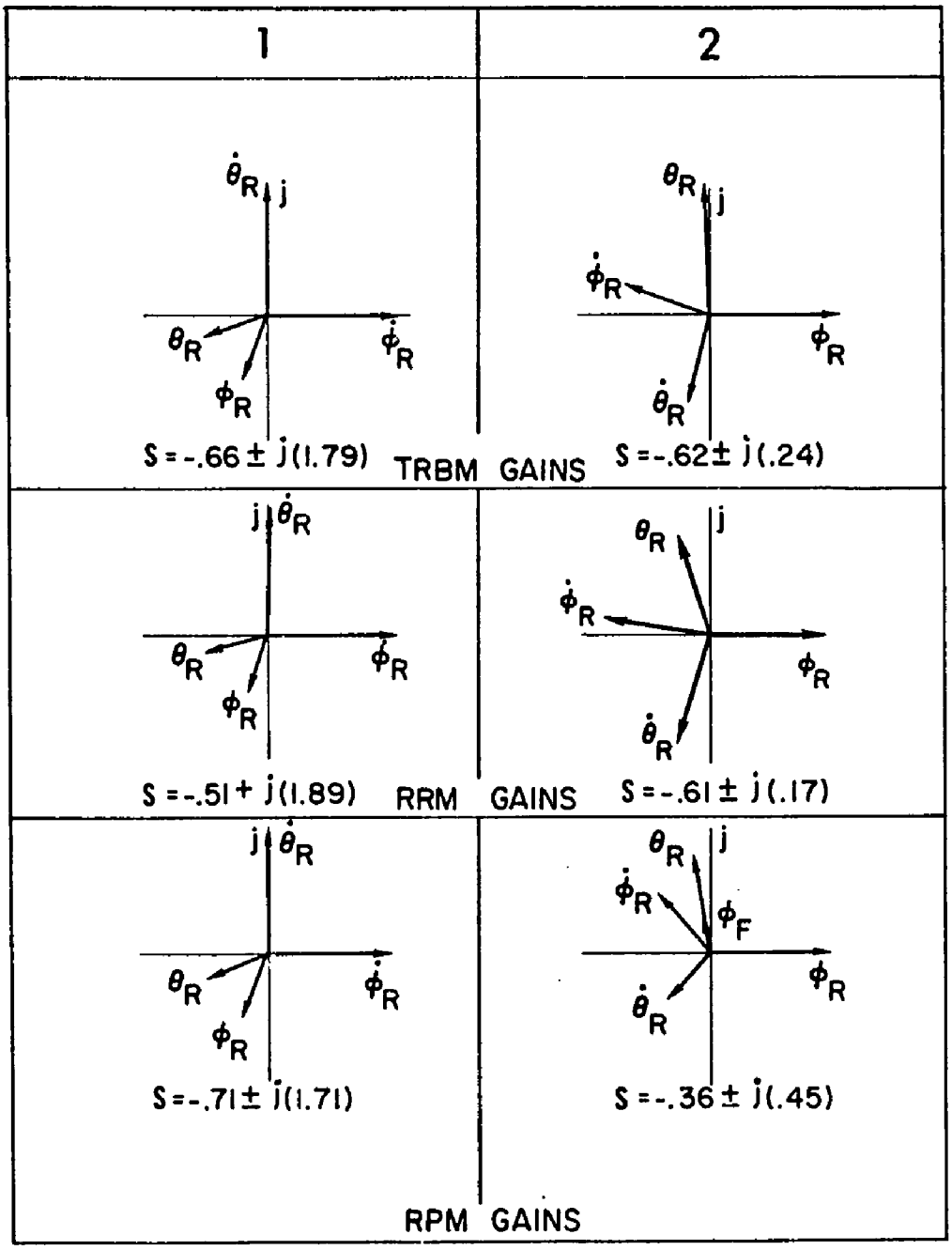

Fig. 5.4.2. COMPARISON OF HIGH FREQUENCY MODE SHAPES USING FULL ORDER FEEDBACK (TRBM GAINS) WITH MODE SHAPES USING REDUCED ORDER FEEDBACK (RRM AND RPM GAINS). The nutation mode, 1, reflects little change with the various controllers. The precession mode, 2, has a fuselage roll component with the RPM controller which is absent from the other two controllers (cf. Fig. 5.1.2).

cipate the effect of rotor disturbances. What is worse, it is shown below that if the designer tries to tighten up the control by weighting the fuselage pitch and roll angles more heavily in the quadratic performance index, he can drive the controlled vehicle unstable by using feedback gains designed on the basis of the lower order models.

This latter possibility is explored by increasing the weighting factors on θ_F and ϕ_F by factors of $\sqrt{10}$ and 10, while maintaining all other weighting factors at unity. The resulting feedback gains are then used as partial state feedback on the complete model and the subsequent performance evaluated.

Table 5.4.2 shows the feedback gains and Table 5.4.3 shows the eigenvalues of the sixth order closed loop system as a function of the weighting factors A_{θ_F} and A_{ϕ_F}. As A_{θ_F} and A_{ϕ_F} are increased, the magnitude of the gains increases and the closed-loop frequency increases, but response appears reasonable. However, when these control gains are used with the tenth order model, the closed-loop eigenvalues are quite different (see Table 5.4.4). As A_{θ_F} and A_{ϕ_F} are increased, the frequency of the first mode <u>decreases</u> and the damping of the second and fifth modes decreases, and, in fact, these modes become <u>unstable</u> for $A_{\theta_F} = A_{\phi_F} = 100$!

In summary, for an articulated rotary-wing VTOL, the rotor position model is satisfactory for calculation of loose control of fuselage motions, if relative stability is the criterion of performance. However, for tight control of fuselage motions it is necessary to use the two rigid body model to assure stable closed-loop response of the rotor fuselage motion.

Table 5.4.2. EFFECTS OF WEIGHTING FACTORS ON FEEDBACK GAINS OF THE RPM CONTROLLER (cf. Fig. 5.1.1).

$A_{\theta_F}=A_{\phi_F}$	K_{θ_R}	K_{ϕ_F}	K_{q_F}	K_{p_F}	$K_{\bar{u}}$	$K_{\bar{v}}$
1	.18	1.00	.36	4.98	-.15	.32
10	.37	3.15	.86	9.77	-.097	-.028
100	.88	9.97	1.70	18.40	.0085	-.238
	L_{θ_F}	L_{ϕ_F}	L_{q_F}	L_{p_F}	$L_{\bar{u}}$	$L_{\bar{v}}$
1	-1.02	.17	-10.59	.25	.68	-.13
10	-3.16	.37	-19.78	.48	.69	-.205
100	-9.97	.87	-36.37	.89	.54	-.174

Table 5.4.3. CLOSED LOOP EIGENVALUES OF THE SIXTH ORDER RRM AS THE FUSELAGE ATTITUDE WEIGHTING FACTORS OF THE QUADRATIC COST ARE INCREASED (cf. Fig. 5.1.1).

Open Loop (RPM)	Closed Loop		
	$A_{\theta_F} = A_{\phi_F} = 1$	$A_{\theta_F} = A_{\phi_F} = 10$	$A_{\theta_F} = A_{\phi_F} = 100$
$-.055 \pm j(.0044)$	$-.168 \pm j(.154)$	$-.285 \pm j(.282)$	$-.505 \pm j(.50)$
$.0051 \pm j(.017)$	$-.087 \pm j(.090)$	$-.149 \pm j(.147)$	$-.264 \pm j(.263)$
$.0018 \pm j(.023)$	$-.0027 \pm j(.0003)$	$-.0011 \pm j(.00017)$	$-.0012$
			$-.00032$

Table 5.4.4. EFFECT OF WEIGHTING FACTORS IN QUADRATIC COST ON CLOSED LOOP EIGENVALUES USING RPM CONTROLLER ON TENTH ORDER MODEL.

$A_{\theta_F} = A_{\phi_F} = 1$	$A_{\theta_F} = A_{\phi_F} = 10$	$A_{\theta_F} = A_{\phi_F} = 100$
-.71 ± j(1.71)	-.782 ± j(1.64)	-.97 ± j(1.50)
-.36 ± j(.45)	-.201 ± j(.702)	+.05 ± j(.99)
-.22 ± j(.08)	-.149 ± j(.231)	-.15 ± j(.41)
-.10 ± j(.10)	-.305 ± j(.069)	-.49
-.0024 ± j(.0006)	-.0014	-.40
	-.00023	+.0004
		-.0012

Unstable

Table 5.4.5. TRBM AND RRM FEEDBACK GAINS FOR $A_{\theta_F} = A_{\phi_F} = 100$.

θ_c	K_{θ_R}	K_{ϕ_R}	K_{q_R}	K_{p_R}	K_{θ_F}	K_{ϕ_F}	K_{q_F}	K_{p_F}	$K_{\bar{u}}$	$K_{\bar{v}}$
RRM	.66	-.97	0	0	3.5	9.4	17.1	26.1	-.17	-.29
TRBM	.87	-.99	.42	-.02	4.4	9.1	21.8	25.7	-.22	-.30
θ_s	L_{θ_R}	L_{ϕ_R}	$L_{\theta'_R}$	$L_{\phi'_R}$	L_{θ_F}	L_{ϕ_F}	$L_{\theta'_F}$	$L_{\phi'_F}$	$L_{\bar{u}}$	$L_{\bar{v}}$
RPM	-.50	.58	0	0	-9.4	3.5	-43.9	7.4	.41	-.16
TRBM	-.44	.69	.08	.28	-9.1	4.2	-42.4	8.8	.39	-.15

Table 5.4.6. CLOSED LOOP EIGENVALUES WITH $A_{\theta_F} = A_{\phi_F} = 100$

RPM with RPM Controller (Cf. Fig. 5.1.1)	RRM with RRM Controller (Cf. Fig. 5.1.1)	TRBM with TRBM Controller (Cf. Figs. 5.1.1, 5.1.2)
----	----	-.66 ± j(1.79)
----	-.37 ± j(.58)	-.48 ± j(.58)
-.51 ± j(.50)	-.58 ± j(.12)	-.23 ± j(.29)
-.26 ± j(.26)	-.23 ± j(.28)	-.71
----	----	-.66
-.0003	-.0003	-.0003
-.0012	-.0014	-.0014

TRBM with RPM Controller (Cf. Fig. 5.1.2)	TRBM with RRM Controller (Cf. Fig. 5.1.2)
-.97 ± j(1.5)	-.247 ± j(2.10)
+.05 ± j(.99)	-.413 ± j(.53)
-.15 ± j(.41)	-.24 ± j(.28)
-.49	-.71
-.40 unstable	-.66
+.0004	+.0004
-.0012	-.0012

5.5 Mean Square Response of the Controlled Vehicle in the Presence of a Random Rotor Torque

In the previous section, the closed-loop vehicle response was evaluated largely on the basis of stability. In this section we evaluate the closed-loop response on the basis of the vehicle's mean square response to a random forcing function. We again consider the response using each one of the three sets of feedback gains designed using the tenth, eighth, and sixth order models of the roll-pitch-horizontal translation motions of the S-61 vehicle near hover (see Table 5.2.1).

The random disturbance was taken to be a roll axis torque on the rotor; it was taken to be a zero-mean white noise process. In terms of an equivalent cyclic pitch disturbance, it may be interpreted as having a root mean square magnitude of 4 degrees with a correlation time of .15 of a rotor revolution; this yields a power spectral density of

$$[2(4)^2(.15)(2\pi)]/[(57.3)^2] \cong .01 \text{ rad}^2 \quad \text{(time unit)}.$$

The calculation of mean square response was done using another part of the OPTSYS computer program (Chapter 4). If $X = E(xx^T)$ is the 10X10 covariance matrix of the mean square TRBM state response, then it is necessary to solve the linear matrix equation:

$$(F-GC)X + X(F-GC)^T + \Gamma Q \Gamma^T = 0 \qquad (5.6.1)$$

where F is the 10X10 open loop TRBM dynamics matrix, G is the 10X2 TRBM control distribution matrix, C is the 2X10 matrix of feedback gains, Q is the power spectral density of the white noise forcing function, and Γ is a 10X1 forcing function distribution vector (all zeroes here except the fourth element which is unity). If $U = E(uu^T)$ is the 2X2 covariance matrix of the mean square cyclic control response, then

$$U = CXC^T . \qquad (5.6.2)$$

The root mean square values of the state and control variables (the square roots of the diagonal elements of X and U) are given in Table 5.5.1 for the random lateral rotor torque described above.

The significant differences in response for the three different controllers are primarily in the ϕ_F and θ_c response (the fuselage roll angle and lateral cyclic pitch control). Using gains from the sixth order controller, the RMS value of ϕ_F is about three times higher than the RMS value of ϕ_F using either the eighth or tenth order controllers! The value of θ_c is three times the TRBM value for both the RRM and RPM. Also, the RMS roll rates for the RPM are about twice those of the TRBM and RRM. The differences are smaller for the other state and control responses. Clearly, there is significant degradation in response using the sixth order controller in this case.

Table 5.5.1. ROOT MEAN SQUARE VEHICLE RESPONSE TO A RANDOM LATERAL ROTOR TORQUE USING THREE DIFFERENT CONTROLLER DESIGNS. The RPM controller response in fuselage roll and roll rate is degraded 2 or 3 to 1 relative to the TRBM controller. Lateral cyclic pitch is increased by about 3 to 1 for both RPM and RRM controllers (cf. Fig. 5.1.2).

Model	Position Response				Rate Response						Control	
	θ_R (Degs)	ϕ_R (Degs)	θ_F (Degs)	β_F (Degs)	q_R (Deg/Sec)	p_R (Deg/Sec)	q_F (Deg/Sec)	p_F (Deg/Sec)	u (Ft/Sec)	v (Ft/Sec)	θ_c (Deg)	θ_s (Deg)
TRBM	2.59	1.89	.64	.12	61.1	71.1	.15	.14	7.01	6.80	.22	1.09
RRM	2.73	1.98	.64	.10	76.6	86.4	.15	.12	7.14	6.13	.58	1.14
RPM	3.03	2.26	.71	.29	72	83.5	.18	.24	8.25	5.14	.68	1.12

5.6 Controller Design and Evaluation for a Hingeless Rotored VTOL Aircraft

In this section, the controller design and evaluation for the hingeless rotored VTOL vehicle of Chapter 3 is shown. As with the articulated rotor of the previous sections of this chapter, the TRBM, RRM, and RPM controllers are designed with diagonal A and B cost matrices and unit weightings of $\theta_F, \phi_F, \bar{u}, \bar{v}, \theta_s$ and θ_c.

The control gains (dimensionless) are shown in Table 5.6.1.

Table 5.6.1. CONTROL GAINS FOR HINGELESS ROTOR TRBM, RRM, RPM. Each controller is designed with $A_{\theta_F} = A_{\phi_F} = A_{\bar{u}} = A_{\bar{v}} = A_{\theta_s} = A_{\theta_c} = 1$.

θ_c	K_{θ_R}	K_{ϕ_R}	K_{q_F}	K_{p_R}	K_{θ_F}	K_{ϕ_F}	K_{q_F}	K_{p_F}	$K_{\bar{u}}$	$K_{\bar{v}}$
TRBM	.34	.55	.25	.03	.44	.91	2.57	2.82	-.38	.29
RRM	.28	.54	0	0	.41	.93	2.24	2.88	-.35	.30
RPM	0	0	0	0	.36	.95	1.31	2.11	-.31	.32
θ_s	L_{θ_R}	L_{ϕ_R}	L_{q_R}	L_{p_R}	L_{θ_F}	L_{ϕ_F}	L_{q_F}	L_{p_F}	$L_{\bar{u}}$	$L_{\bar{v}}$
TRBM	-.30	.31	.03	.17	-.91	.44	-5.82	1.10	.55	.11
RRM	-.31	.29	0	0	-.94	.40	-5.93	.93	.57	.09
RPM	0	0	0	0	-.95	.36	-5.04	.56	.60	.06

The control gains for TRBM show that the rotor pitch gain is a higher fraction of the fuselage pitch gain in both direct and cross feedback channels, as compared with the gains for the articulated rotor. In addition, the cross-coupling gains are higher in the fuselage state. This increase in cross-coupling gain is a direct result of the increase in hub restraint.

The closed-loop eigenvalues for the gains of Table 5.6.1 are shown in Table 5.6.2. The eigenvectors, with magnitudes between 1 and .1, for modes 3, 4, and 5, are shown in Fig. 5.6.1.

The lowest frequency eigenvalues, corresponding to modes 4 and 5, are relatively unaffected by the order of the rotor representation. Mode 2 also demonstrates less change between the TRBM and RRM than for the articulated rotor mode 2 (Fig. 5.3.1).

Next, the eigensystem of the TRBM with the TRBM, RRM, and RPM con-

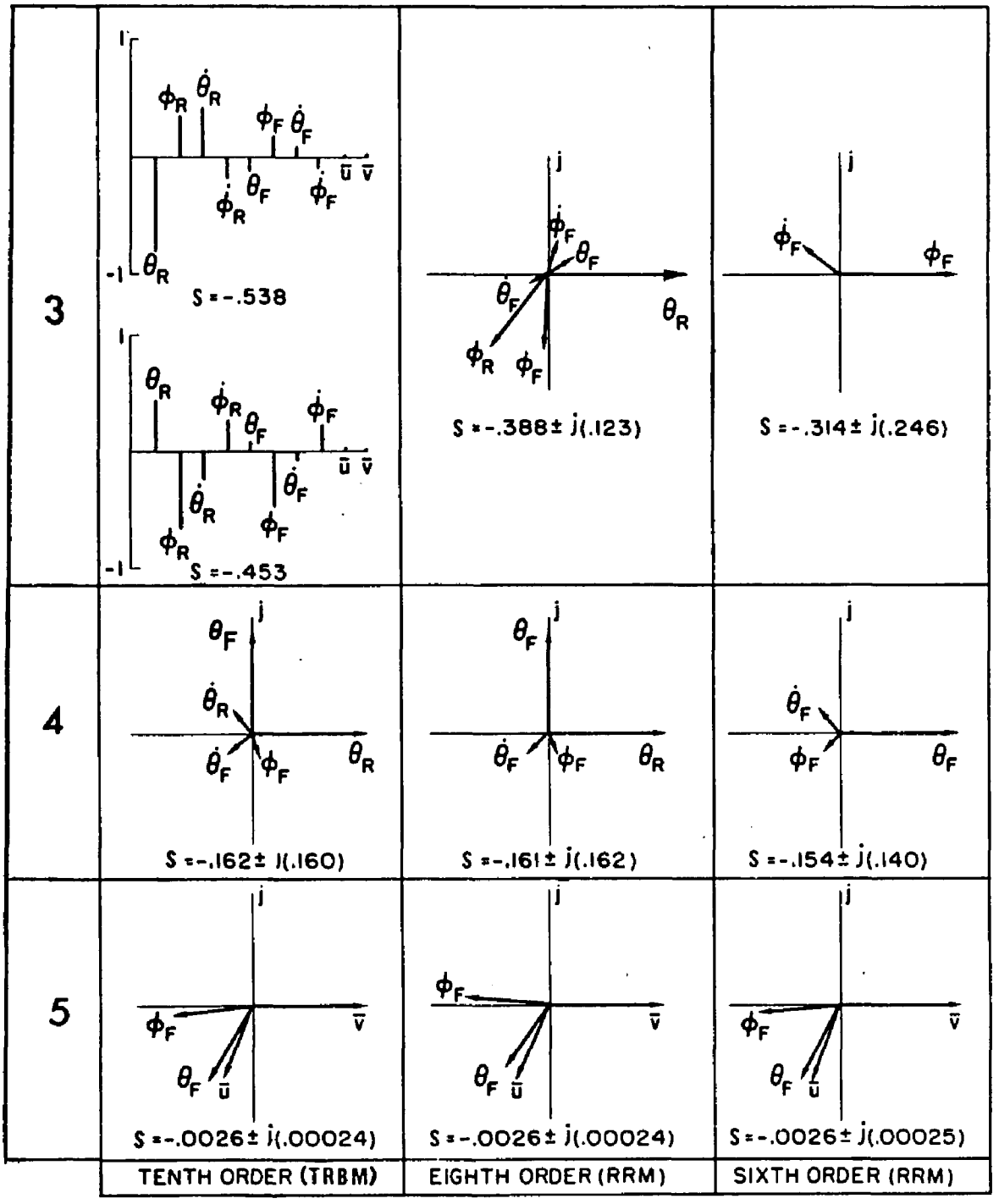

Fig. 5.6.1. MODE SHAPES CORRESPONDING TO THE LOW FREQUENCY CLOSED-LOOP EIGENVALUES (HINGELESS ROTOR). The response of fuselage modes 4 and 5 is almost the same for each order model. The large mode 3 contribution of θ_R to the TRBM and RRM closed loop eigenvector is absent in the RPM closed loop response (cf. Fig. 5.1.1).

Table 5.6.2. CLOSED LOOP EIGENVALUES OF TRBM, RRM, AND RPM (HINGELESS ROTOR MODEL) (cf. Fig. 5.1.1).

MODE	TRBM	RRM	RPM
1	-.65 ± j(1.96)	---	---
2	-.33 ± j(.38)	-.30 ± j(.42)	---
3	-.54 -.45	-.39 ± j(.12)	-.31 ± j(.25)
4	-.16 ± j(.16)	-.16 ± j(.16)	-.16 ± j(.14)
5	-.0026 ± j(.00024)	-.0026 ± j(.00024)	-.0026 ± j(.00025)

trollers is evaluated. The eigenvalues of modes 1 through 5 are shown in Table 5.6.3 and the corresponding mode shades in Fig. 5.6.2 and 5.6.3.

Table 5.6.3. CLOSED LOOP EIGENVALUES OF TRBM WITH TRBM, RRM, AND RPM CONTROLLERS (HINGELESS ROTOR) (cf. Fig. 5.1.2).

MODE	TRBM	RRM	RPM
1	-.65 ± j(1.96)	-.38 ± j(2.08)	-.68 ± j(1.85)
2	-.33 ± j(.38)	-.31 ± j(.39)	-.22 ± j(.60)
3	-.54 -.45	-.56 -.43	-.32 -.28
4	-.16 ± j(.16)	-.16 ± j(.16)	-.17 ± j(.26)
5	-.0026 ± j(.00024)	-.0025 ± j(.00039)	-.0025 ± j(.00031)

The TRBM and RRM controllers give almost identical closed-loop TRBM eigensystems. The RPM controller, on the other hand, produces lower rotor damping in mode 3. Hence, for this vehicle, the RPM controller is not the more conservative design.

Finally, the controllers are evaluated on the basis of the random disturbance discussed in Section 5.5. The root-mean square response of

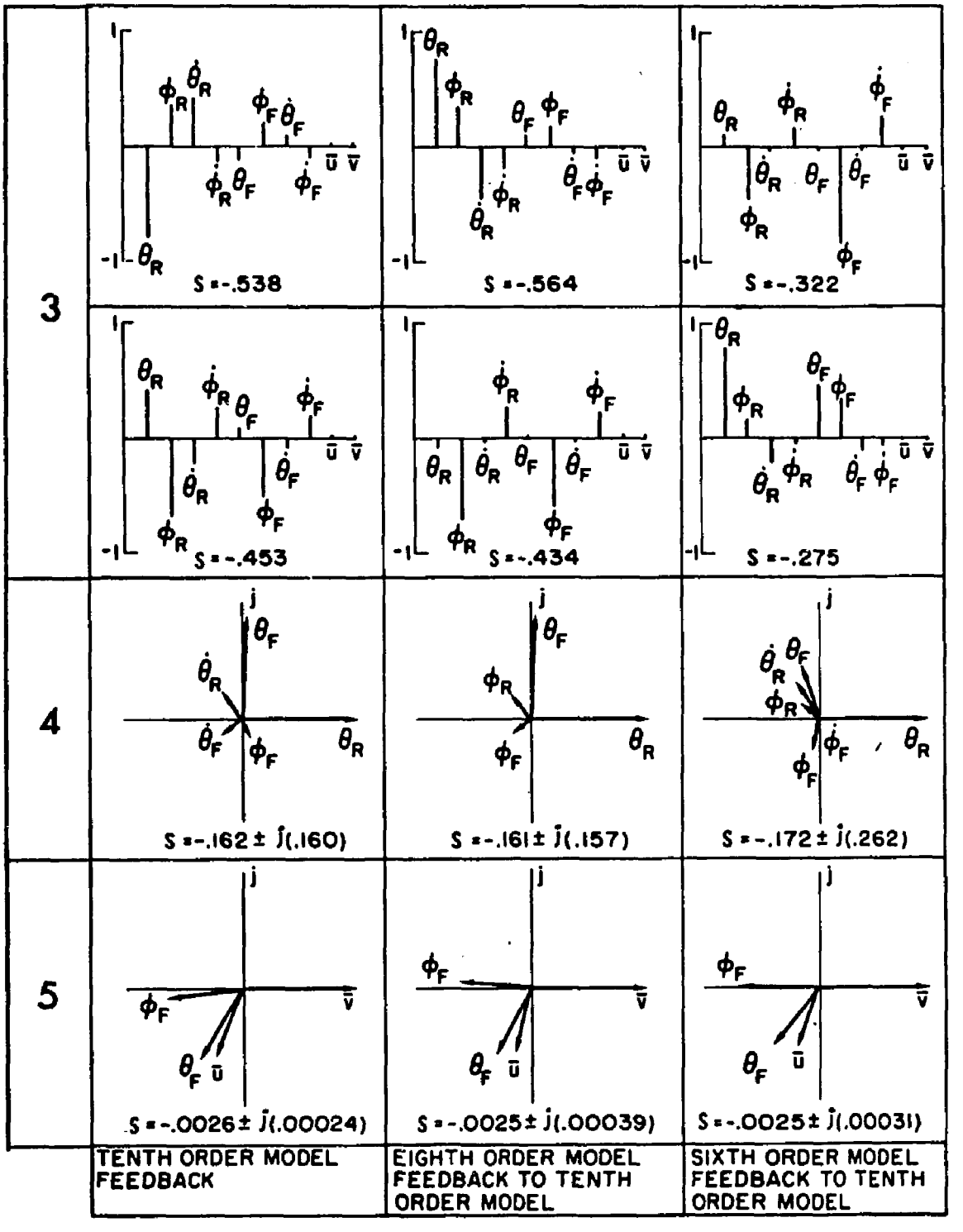

Fig. 5.6.2. COMPARISON OF LOW FREQUENCY MODE SHAPES USING FULL ORDER FEEDBACK (TRBM GAINS) WITH MODE SHAPES USING REDUCED ORDER FEEDBACK (RRM AND RPM GAINS)--(HINGELESS ROTOR MODEL). The TRBM and RRM controllers give similar closed loop eigenvectors for modes 3, 4, and 5. The RPM controller on the TRBM gives less damping and more rotor pitch response to mode 3. For this case, mode 4 is also affected by the RPM controller (cf. Fig. 5.1.2).

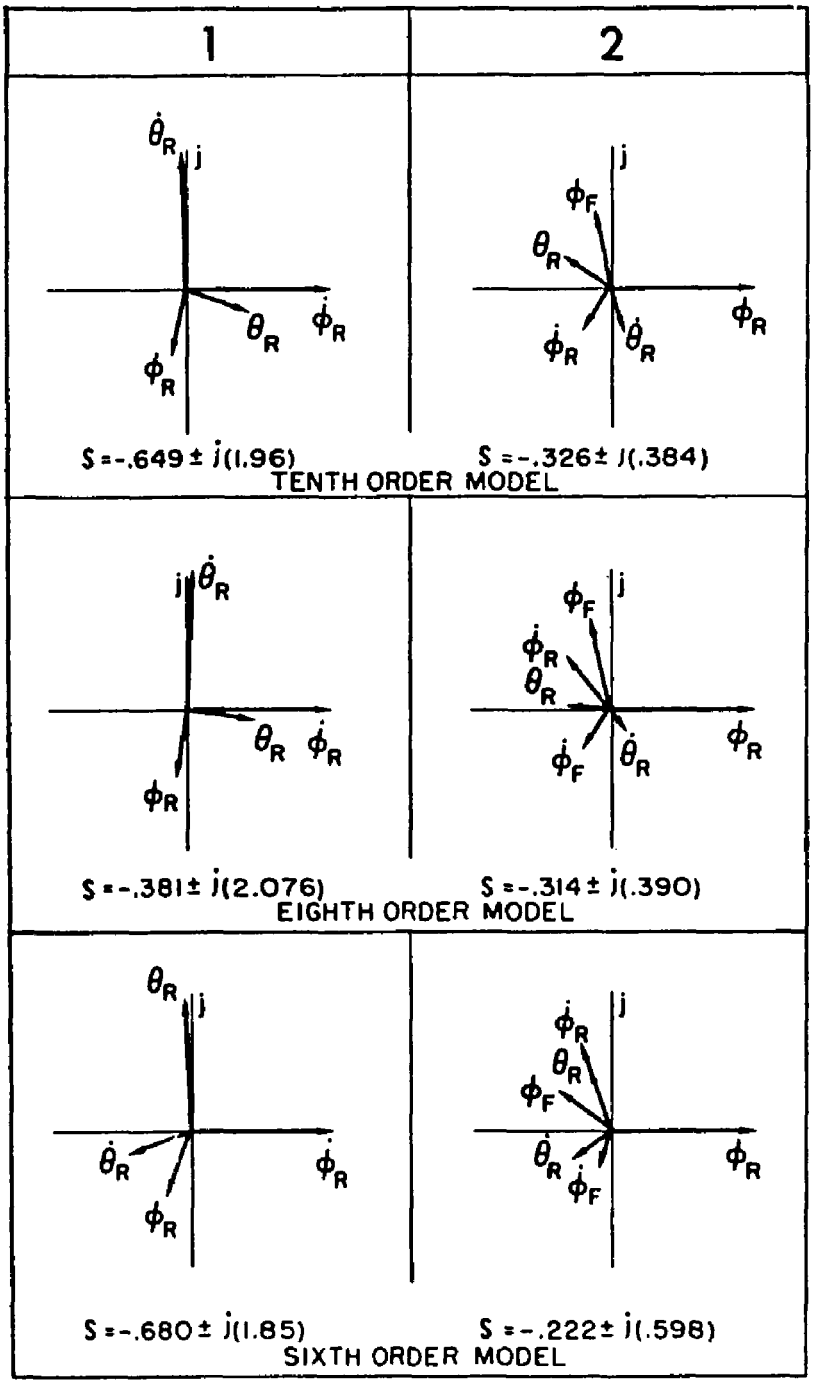

Fig. 5.6.3. ROTOR MODES WITH GAINS FROM TRBM, RRM, AND RPM. The RPM controller gives less damping in the precessional rotor mode than either the TRBM or RRM controllers (cf. Fig. 5.1.2).

the state and control variables is given in Table 5.6.4. The most significant difference of the controllers is found in the lateral cyclic RMS response where the RPM controller produces noticeably more control response. In addition, the rotor and fuselage angular responses are larger than with the TRBM controller. A comparison with the RMS responses of the articulated rotor (Table 5.5.1) shows that the controlled fuselage response levels are higher for the hingeless rotor than for the articulated rotor.

Table 5.6.4. ROOT MEAN SQUARE VEHICLE RESPONSE TO A RANDOM LATERAL ROTOR TORQUE USING THREE DIFFERENT HINGELESS ROTOR CONTROLLER DESIGNS (cf. Fig. 5.1.2).

	Position				Rate						Control	
Model	θ_R (Degs)	ϕ_R (Degs)	θ_R (Degs)	ϕ_F (Degs)	q_R (Deg/Sec)	p_R (Deg/Sec)	q_F (Deg/Sec)	p_F (Deg/Sec)	u (Ft/Sec)	v (Ft/Sec)	θ_c (Deg)	θ_s (Deg)
TRBM	2.32	1.79	.94	.57	66.3	79.3	3.84	5.13	6.33	13.0	.15	1.61
RRM	2.64	2.07	.96	.51	86.5	96.6	3.90	4.52	6.68	12.20	1.03	1.77
RPM	2.05	2.25	1.13	.57	72.5	85.6	5.34	7.45	7.25	10.75	.94	1.77

5.7 Summary

This chapter contains some very important results of the application of quadratic synthesis to the design of controllers for rotary-wing VTOL aircraft control systems.

Three mathematical models of increasing complexity were constructed for a typical articulated-rotor and a hypothetical hingeless rotor helicopter near hover: (a) conventional "rotor position model" (RRM) that treats the fuselage and the rotor as a single rigid body, (b) "two rigid body model" (TRBM) that treats the fuselage and rotor as coupled rigid bodies, and (c) a "rotor rate model" (RRM) that includes the rotor precession dynamics but neglects the rotor nutation dynamics.

The OPTSYS program was used to design state variable feedback controllers for the roll-pitch-horizontal translation motions of the vehicle, which are represented by sixth, eighth, and tenth order models for the

RPM, the RRM, and the TRBM, respectively.

These control systems were first evaluated on the basis of the closed-loop modal response of the TRBM. It was found that neglecting the rotor dynamics completely in the vehicle control design (RPM) leads to deteriorated response, and, in some cases of the articulated rotor, unstable closed-loop response of the vehicle. The control designed using the rotor rate model was better, but it also produced deteriorated response and instability in the full articulated rotor model when controls for very tight regulation were synthesized.

The control systems were also evaluated on the basis of the mean square response of the closed-loop system when the rotor was subjected to a random roll torque. The root mean square values of lateral cyclic pitch and fuselage roll attitude were considerably higher for the RPM controller than for either the RRM controller or the TRBM controller.

Chapter VI

EFFECT OF FORWARD SPEED AND ROTOR PLANE FEEDBACK ON BLADE STABILITY

6.1 Introduction

The methods of quadratic synthesis are useful in designing controllers for constant coefficient models of rotary-wing VTOL aircraft. However, a constant coefficient representation is obtained by averaging the rotor blade motions over one revolution, which implicitly assumes that the blade motions are stable. In fact, forward moving rotor blades are susceptible to flutter type instabilities due to blade elasticity and to parametric excitation arising from the periodicity of the airloads on the rotor.

The parametric excitation instability is the subject of this chapter. It is an important low frequency phenomenon which may be treated by non-flexible blade approximations. Such a treatment serves as a basis upon which flexible blade representations may be evaluated. In the following sections the effect of rotor plane pitch and roll feedback on the stability of periodically excited blade motions is investigated. Only a single blade is considered for this purpose. The analysis and its solution may be extended to include an arbitrary number of blades.

6.2 Computer Analysis of Periodic Excitation of Rotor Motions

The blade equations of Chapter 2 are linear differential equations with periodically varying coefficients. Second order periodic systems may be solved by reduction of the equation to a classical Hill equation, for which solutions have been tabulated (MA1, HI1). For higher order systems, Floquet theory is the basic modern computational approach. The implementation of this theory to the determination of the stability of a system of linear differential equations with periodically varying coefficients is discussed in Appendix C. Given a computer program to evaluate the transition matrix over one rotor revolution, and another program to determine its eigenvalues and eigenvectors, the analysis of system

stability reduces to writing the differential equations. Any order system may be modeled, as long as it is linear. For the purpose of this study, only the flapping and inplane motions of a single blade are considered. This approach therefore assumes that:

- Blade is infinitely stiff in torsion;
- Fuselage effects on the blade motion may be neglected.

The governing equations are then Eqs. (2.4.3) and (2.4.4).

At high speeds, it is necessary to include the effects of reverse flow on the retreating blade. This flow region is discussed in Chapter 2. The reverse flow region for a given μ is approximated by a circle at $y = -R\mu/2$ at $\psi \approx 3\pi/2$ (see Fig. 2.3.2). This representation is continuous.

A typical output of the program is shown in Table 6.1.1. Three sets of numbers are printed. The TRIM STATE is the result of subroutine TRIM which, given the blade C_T and advance ratio μ, calculates the collective pitch, coning angle, inflow ratio, and induced velocity triangular distribution factor. The CHARACTERISTIC MULTIPLIERS are the eigenvalues of the full revolution transition matrix. If any of these have magnitude greater than unity, instability is indicated. Finally, the eigenvalues of the equivalent linear system (of constant coefficients) is printed along with the normalized eigenvectors of the transition matrix. The real parts of these roots are proportional to the damping of the mode, while the imaginary part is mode frequency to within an integer power of $2\pi j/T_R$. A partial program listing is given in Appendix D.

6.3 Simple Flapping with Reverse Flow

Initial computations with the program were made with only the flapping equations. The reason for this is twofold. First, the simplest equation applicable to the overall study could be used to check out the program. Second, there is a previous study of this simple case.

The cited report (LO1) applies the method of mean coefficients to determine rotor blade stability in normal and reversed flow. The results

Table 6.1.1. FLOQUET STABILITY PROGRAM OUTPUT

```
 TRIM STATE
 ----------
   MU = 0.60
   ALP=    0.00000000
   CT =    0.00869528
   THO=    3.22732014
   LAM=    0.00724607
   BO =    4.58754259
   VK =    1.31428652


CHARACTERISTIC MULTIPLIERS
 -0.68693131        -0.00000000
 -0.07746225        -0.00000000
 -0.98727901        -0.00000000
 -0.16308341        -0.00000000


COMPLEX EIGENVALUE( 1).....          REAL EIGENVECTOR( 1).....

( -0.05976602)+J(  0.50000002)       ( -0.97425049)
                                     (  0.01077062)
                                     ( -0.19980164)
                                     (  0.10391955)

COMPLEX EIGENVALUE( 2).....          REAL EIGENVECTOR( 2).....

( -0.40608871)+J(  0.50000002)       ( -0.99578466)
                                     (  0.00729344)
                                     (  0.08527959)
                                     ( -0.03297135)

COMPLEX EIGENVALUE( 3).....          REAL EIGENVECTOR( 3).....

( -0.00203760)+J(  0.50000002)       ( -0.75119725)
                                     (  0.49135510)
                                     (  0.40751711)
                                     (  0.18793597)

COMPLEX EIGENVALUE( 4).....          REAL EIGENVECTOR( 4).....

( -0.28864594)+J(  0.50000002)       (  0.99827864)
                                     ( -0.00694660)
                                     (  0.05362470)
                                     (  0.02271306)
```

of this application are correlated with results of Shutler and Jones (SH1). These researchers had previously determined a series solution to this problem.

The equation studied in LO1 is

$$\frac{d^2\beta}{dt^2} + C^{\beta}_{\dot{\beta}} \frac{d\beta}{dt} + C^{\beta}_{\beta}\beta = 0 \qquad (6.3.1)$$

where, from Chapter 2,

$$C^{\beta}_{\dot{\beta}} = \gamma'\Omega(1 + \frac{4}{3}\mu \sin\psi)$$

$$C^{\beta}_{\beta} = \Omega^2(1 + \frac{4}{3}\gamma'\mu \cos\psi + \gamma'\mu \sin 2\psi)$$

$$\gamma' = \gamma/8 \ .$$

Equation (2.4.3) reduces to Eq. (6.3.1) if ζ-β coupling is neglected and only linear terms are retained.

The governing parameters are γ' and μ. Figure 6.3.1 shows stable and unstable points on a plot of γ' vs. μ. Solid lines represent boundaries of flapping frequency change (from LO1) and the dashed line the stability boundary, also from LO1. Regions $\diamond$ and $\square$ represent frequency $\frac{1}{2}$, or 1, respectively. In Regions A and B, the frequency varies continuously. No reverse flow is considered in this figure.

Using successive Lock numbers, $\gamma = 9.15$, $\gamma = 11.2$, and $\gamma = 15.2$, the parameter μ was swept from 0 to 1.4 in steps of 0.2. With the exception of one point at $\gamma = 9.15$ and $\mu = 1.4$, all points correlate with the boundaries of LO1, both in frequency and damping. The discrepancy of the one point is ascribed to the approximate nature of the analysis of LO1.

Figure 6.3.2 is a plot of the same parameters with the exception that a more realistic high-μ environment, reverse flow, is simulated. Here again, the correlation with LO1 is excellent, even to the discontinuity at

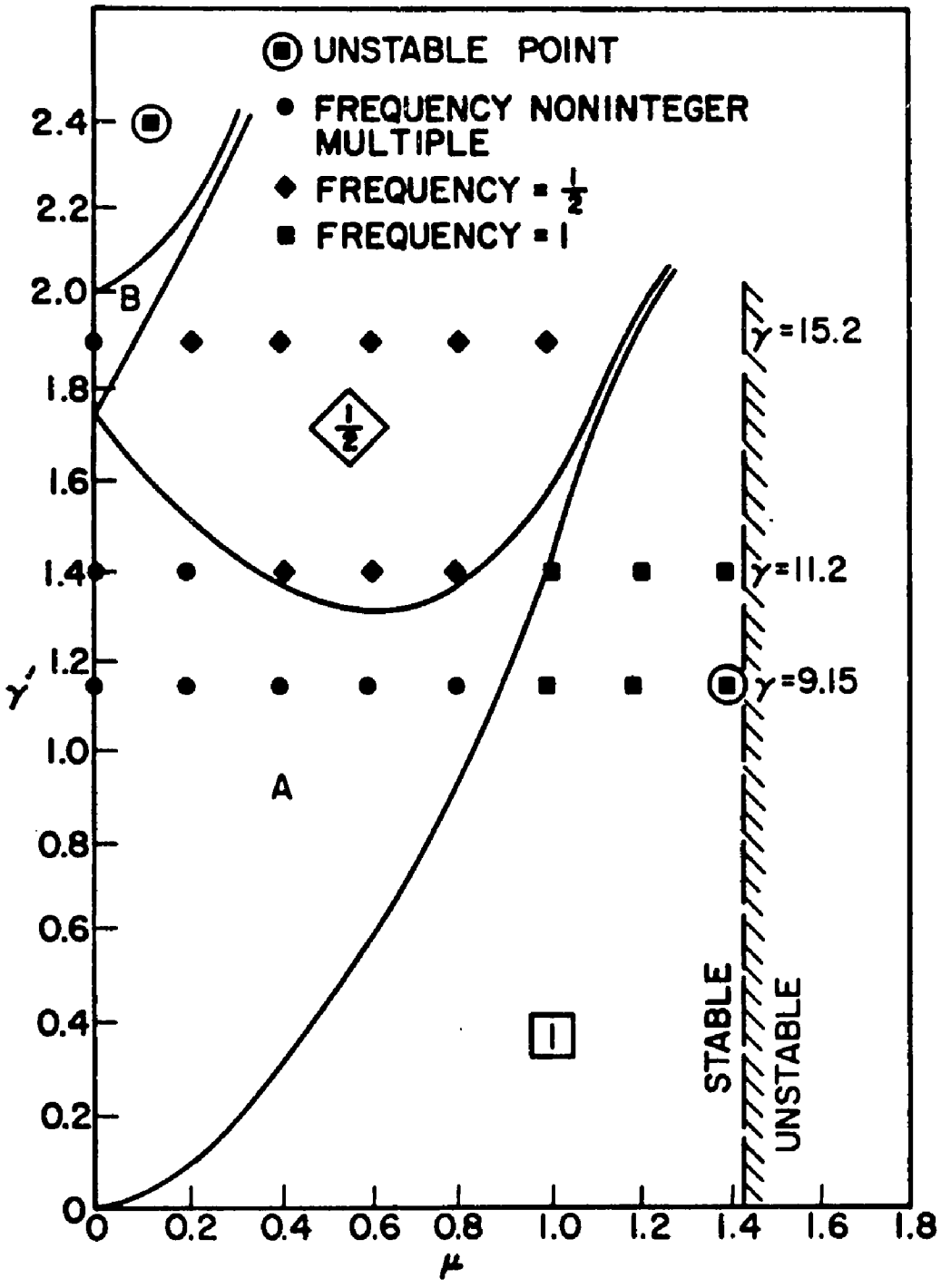

Fig. 6.3.1. CORRELATION OF STABILITY REGIMES WITH LOWIS (LO 1). (No reverse flow and no flap-lag coupling.)

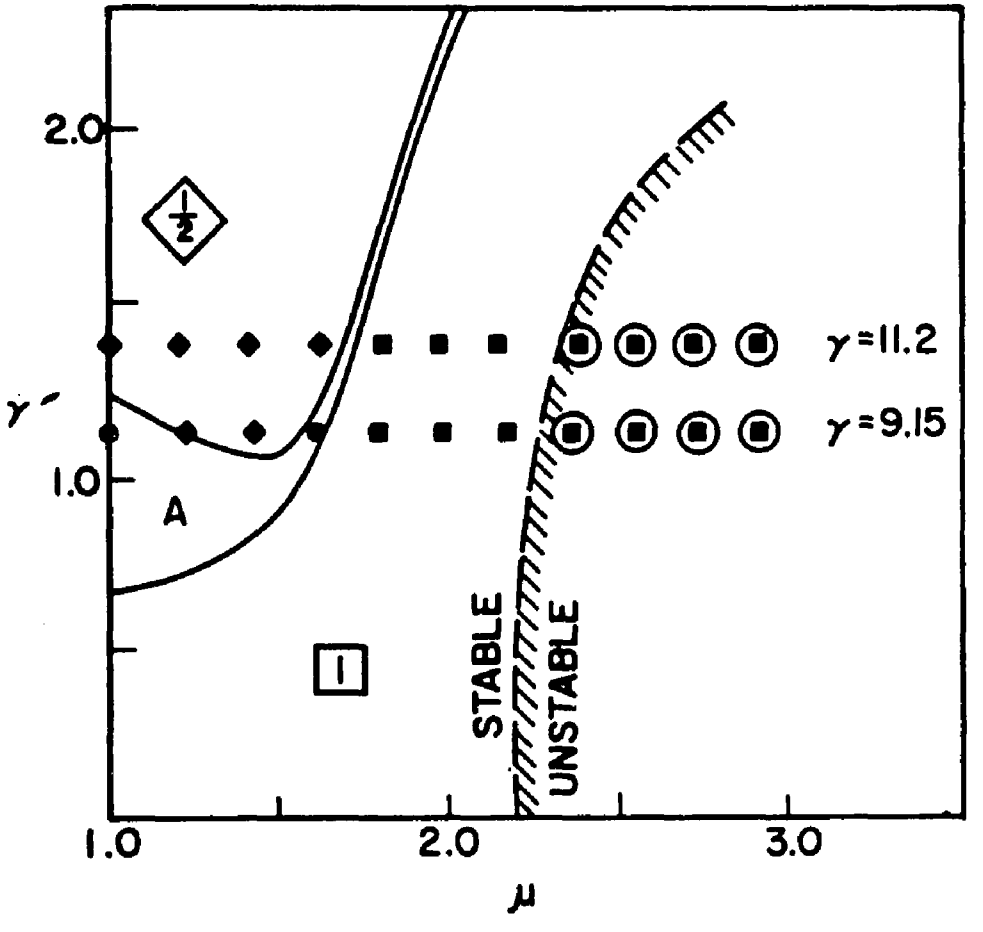

Fig. 6.3.2. CORRELATION WITH REVERSE FLOW STABILITY REGIMES WITH LOWIS (LO 1). (No flap-lag coupling.)

$\mu = 0.6$, $\gamma = 9.15$.

The reverse flow simulation used in this figure is not exactly the same as discussed in Chapter 2. Following the technique employed in LO1, it is assumed that at $\mu = 1.0$, a reverse flow region is encountered. Hence, from $\mu = 1.0$ to $\mu = 2.8$, the lift is reversed in the region of the rotor disc greater than $\psi = \pi$ and $|\psi| \leq |\sin(1/\mu)|$. Reverse flow considerations considerably extend the calculated stability boundaries.

To extend the results of LO1, the program was modified as discussed in Chapter 2. The results of a Lock number sweep are shown in Fig. 6.3.3. A reduction in the size of the continuously variable frequency band occurs at $\mu = 4$ with this reversed flow model, with a corresponding enlargement of the once-per-rev region. However, the final boundary is identical with the simpler representation as well as the results for Lock numbers on the order of 8.0 and below. The boundaries shown in the vicinity of $.8 < \mu < 1.4$ and $10 < \gamma < 14$ are calculated for a 6° integration step size. This increment is too large for this region and a more accurate detail could be produced with a small step size in this region. However, from a practical viewpoint, the accuracy as shown was deemed sufficient.

An alternate representation of the results of Fig. 6.3.3 is found by plotting $Re(s_\beta)$, which is proportional to the damping of the modal response, vs. μ . Figure 6.3.4 shows such a plot for $\gamma = 11.2$, which as seen from Fig. 6.3.3 crosses all the frequency ranges of interest. Figure 6.3.4 is based on a simple flapping model with no reverse flow, while Fig. 6.3.5 is based on a model with continuous reverse flow. Two branches are shown for each case. The significance of these two branches is discussed in Appendix C. It is sufficient to note here that the lower branch determines the system stability limit. Also shown in the frequency content of the branches. The two points shown (as opposed to lines) indicate existence of the continuous frequency transition from $\frac{1}{2}$ per rev to 1 per rev.

It is concluded that consideration of the reversed flow is neces-

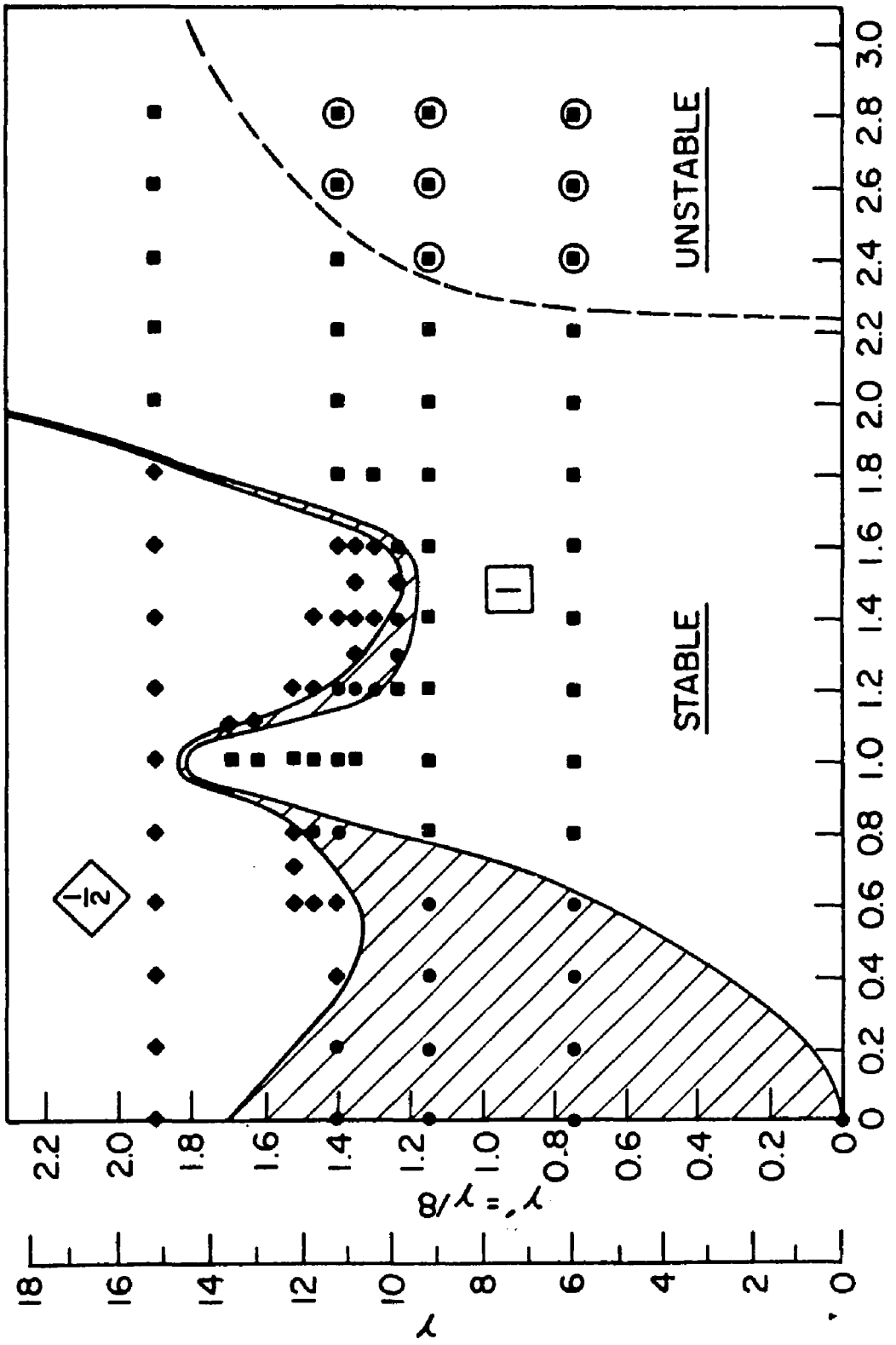

Fig. 6.3.3. STABILITY REGIMES WITH CONTINUOUS REPRESENTATION OF REVERSE FLOW. (No flap-lag coupling. Cf. Fig. 6.3.1 for symbol legend.)

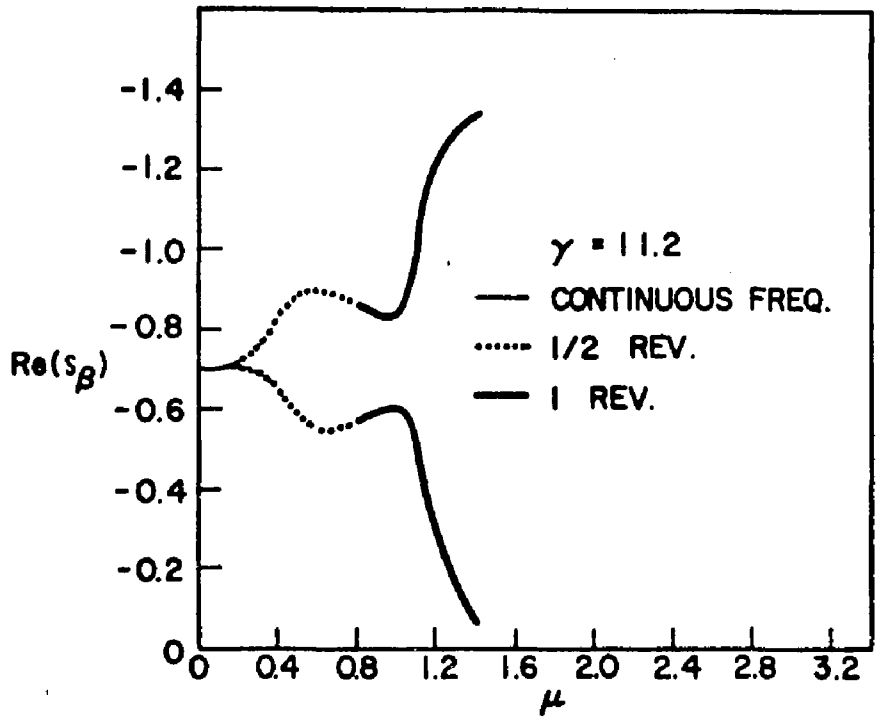

Fig. 6.3.4. VARIATION OF $Re(s_\beta)$ WITH μ , $\gamma' = 11.2$. (No reverse flow and no flap-lag coupling. Cf. Fig. 6.3.1.)

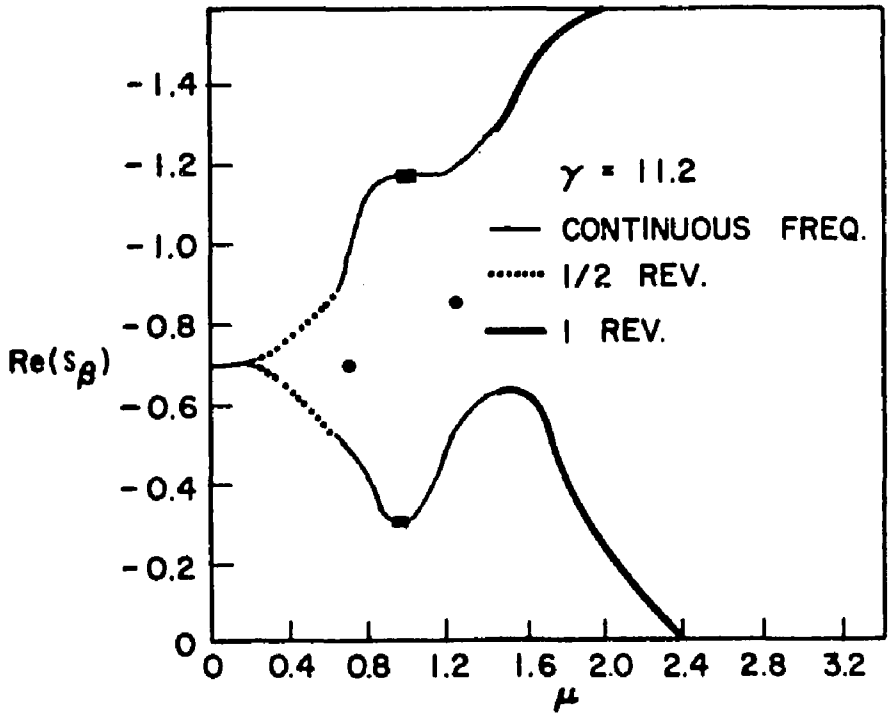

Fig. 6.3.5. VARIATION OF $Re(s_\beta)$ WITH μ , $\gamma = 11.2$. (No flap-lag coupling. Cf. Fig. 6.3.3.)

sary to demonstrate the fact that, for a simple blade with uncoupled flap-lag motions, no instability occurs below $\mu = 1$.

6.4 Flap-Lag Instability at Low μ and γ

The results presented in Fig. 6.3.3 demonstrate three distinct stable modes of behavior for the simplest blade flapping case. Most modern blades have Lock numbers on the order of 6. The results of the simple flapping study indicate that such blades should not be susceptible to the one-half-per-rev natural frequency, nor should they be unstable at low advance ratios.

However, such blades do exhibit a frequency entrainment at advance ratios as low as 0.5 (FR2); this is thought to be caused by unstable pitching moment due to reverse flow. The existence of such an instability depends on the particular blade system under consideration, as indicated by the parameters of Eq. (2.4.3) and (2.4.4). The presence of rotor blade position and rate feedback to blade pitch angle, or rotor plane feedback to θ_o,θ_s and θ_c , will also affect the blade stability.

Equivalence of Blade Flapping State Feedback with Rotor State Feedback

Since a single blade is used in this study, only blade feedback to blade pitch angle is modeled. However, a given rotor plane feedback law, such as Eqs. (5.1.1) and (5.1.2), can be made equivalent to blade flapping feedback.

Substitution of the first harmonic approximation for flapping angle, Eq. (3.2.1), into the blade feedback law, and neglecting the β_o term,

$$\theta = \bar{K}_\beta \beta + \bar{\bar{K}}_{\dot\beta} \dot\beta \qquad (6.4.1)$$

gives

$$\theta = [-\bar{K}_\beta \theta_R - \bar{\bar{K}}_{\dot\beta} (\dot\theta_R + \Omega\varphi_R)]\cos\psi + [-\bar{K}_\beta \varphi_R - \bar{\bar{K}}_{\dot\beta} (\dot\varphi_R - \Omega\theta_R)]\sin\psi \qquad (6.4.2)$$

where θ is the instantaneous blade pitch angle of the blade at azimuth angle Ψ.

Equating the sine and cosine coefficients of Eq. (6.4.2) with those of Eq. (3.2.2),

$$\theta_c = -\bar{K}_\beta \theta_R - \bar{\bar{K}}_\beta (\dot{\theta}_R + \Omega \varphi_R) \tag{6.4.3}$$

$$\theta_s = -\bar{K}_\beta \varphi_R - \bar{\bar{K}}_\beta (\dot{\varphi}_R - \theta_R \Omega) \ . \tag{6.4.4}$$

Solving for $\bar{K}_\beta$ and $\bar{\bar{K}}_\beta$ yields

$$\begin{bmatrix} \bar{K}_\beta \\ \bar{\bar{K}}_\beta \end{bmatrix} = \frac{1}{\theta_R \dot{\varphi}_R - \varphi_R \dot{\theta}_R - \Omega(\theta_R^2 + \varphi_R^2)} \begin{bmatrix} -\dot{\varphi}_R + \theta_R \Omega & \dot{\theta}_R + \varphi_R \Omega \\ \varphi_R & -\theta_R \end{bmatrix} \begin{bmatrix} \theta_c \\ \theta_s \end{bmatrix} \tag{6.4.5}$$

(6.4.6)

where θ_c and θ_s are given by Eqs. (5.1.1) and (5.1.2) as linear combinations of the rotor plane states and fuselage states.

The equations (6.4.5) and (6.4.6) give the equivalence of blade flapping feedback gains to the rotor plane and fuselage feedback gains, since θ_c and θ_s are specified by Eqs. (5.1.1) and (5.1.2). In general, the equivalent blade flapping gains are time-varying since rotor plane state and fuselage state are time-varying.*

At a steady rotor plane angle, $\dot{\theta}_R$ and $\dot{\varphi}_R$ are zero. If φ_R is also zero, then Eqs. (6.4.5) and (6.4.6) give a feedback gain equivalence for this study,

$$\bar{K}_\beta = -K_{c\theta_R}$$

$$\bar{\bar{K}}_\beta = K_{s\varphi_R}/\Omega \ .$$

*The rotor state can be obtained by resolving each blade flapping angle into the non-rotating shaft frame and averaging.

Flap-Lag Instability for a Hypothetical Rotor

In order to examine the possibility of instability, a hypothetical rotor was chosen, the parameters of which are shown in Table 6.4.1. This rotor is characterized by centrally hinged blades with a flapping frequency higher than one-per-rev and negligibly small inplane stiffness.

Table 6.4.1. HYPOTHETICAL ROTOR SYSTEM PARAMETERS

T	γ	σ	$\bar{e}_\beta$	$\bar{e}_\zeta$	ω_β/Ω	ω_ζ/Ω	ζ_o
18,000 lbs.	6	.12	0	.15	1.15	0	0

A constant feedback gain from blade flapping to blade pitch was of the form:

$$\Delta\theta = -\bar{K}_\beta\beta \qquad (\bar{K}_\beta = -.4, 0, +.4) \qquad (6.4.7)$$

From Eq. (6.4.5), this gain is equivalent to a longitudinal rotor plane gain on θ_R and a steady state rotor φ_R of zero. In addition, the feedback law of Eq. (6.4.7) may be implemented by introduction of the so-called delta-3 hinge (SE1, HA1), or electrical measurement of β. The value of $\bar{K}_\beta = -.4$ is to include the effect of the delta-3, which may give an increase in blade pitch angle with flapping angle.

Figure 6.4.1 illustrates the case with no flap-lag coupling and the continuous representation of reversed flow. The blade is stable to $\mu = 2.4$.*

Figure 6.4.2 depicts the Re(s) dependence of advance ratio for $\bar{\bar{K}}_\beta = 0$ with flap-lag coupling. The flapping mode begins $\frac{1}{2}$ per rev transient motion at $\mu = .2$, although no instability is predicted until $\mu > 1$. The inplane mode, on the other hand, demonstrates a significant loss in damping at $\mu = .2$ when the flapping mode begins the execution of $\frac{1}{2}$ per rev transient motions. Instability at $\mu = 1$ is indicated.

*Only the low damping branch is plotted, since it is of primary interest.

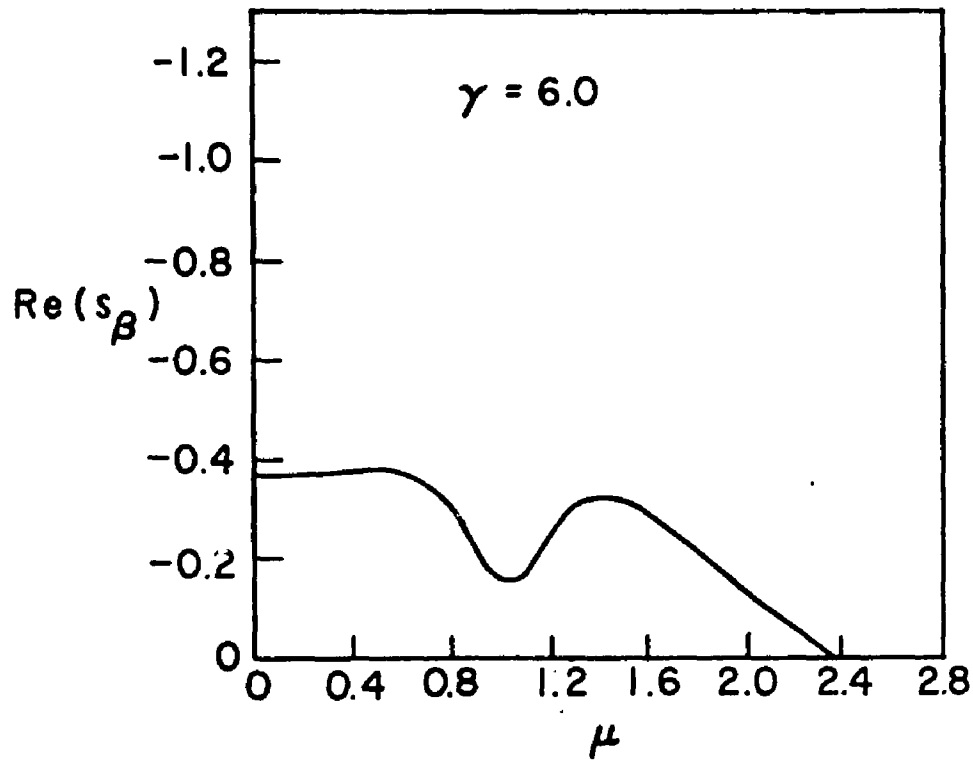

Fig. 6.4.1. EFFECT OF VELOCITY ON $Re(s_\beta)$: $\bar{K}_\beta = \beta_0 = 0$. (No flap-lag coupling, but with reverse flow.) Flapping is unstable at $\mu \cong 2.4$.

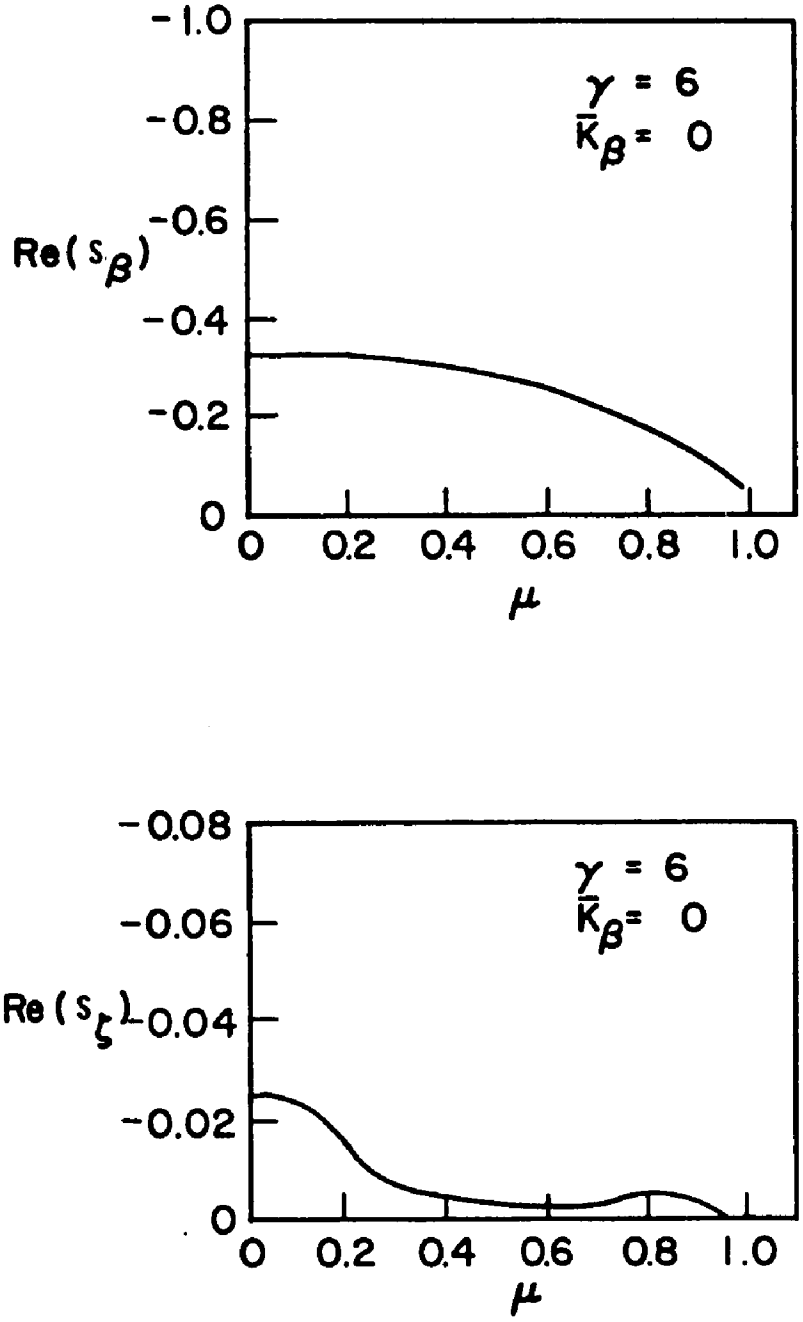

Fig. 6.4.2. EFFECT OF VELOCITY ON $Re(s_\beta)$ AND $Re(s_\zeta)$: $\bar{K}_\beta = 0$. Instability is predicted at about $\mu = 0.95$ when flap-lag coupling is considered, as opposed to the no flap-lag coupling stability limit of $\mu \cong 2.4$ (cf. Fig. 6.4.1).

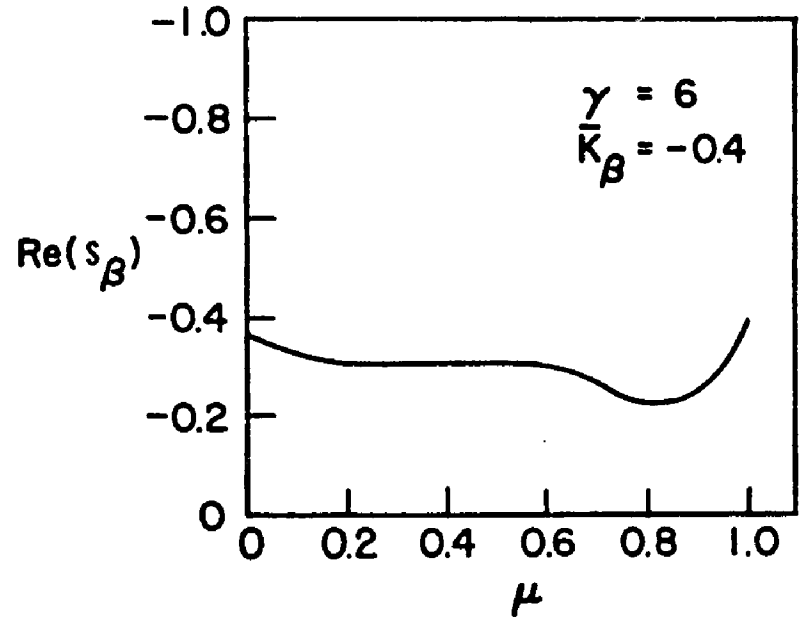

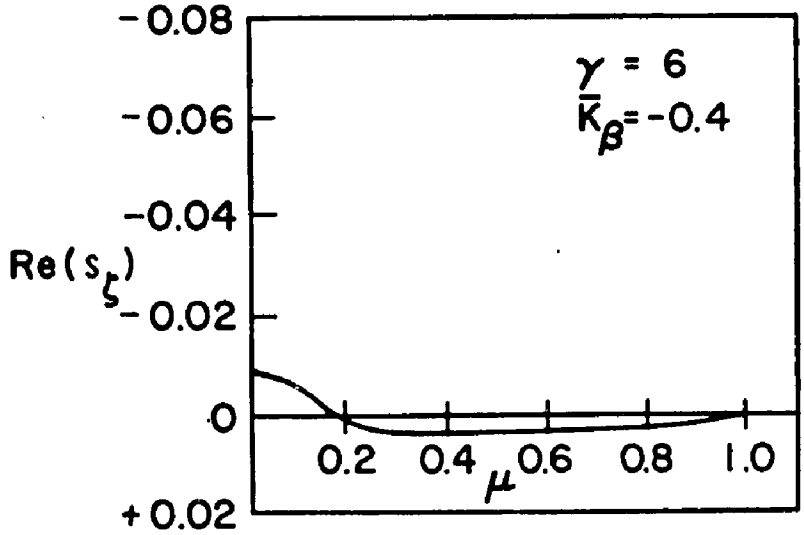

Fig. 6.4.3. EFFECT OF VELOCITY ON $Re(s_\beta)$ AND $Re(s_\zeta)$: $\bar{K}_\beta = -.4$. Instability is predicted at $\mu \cong 0.2$.

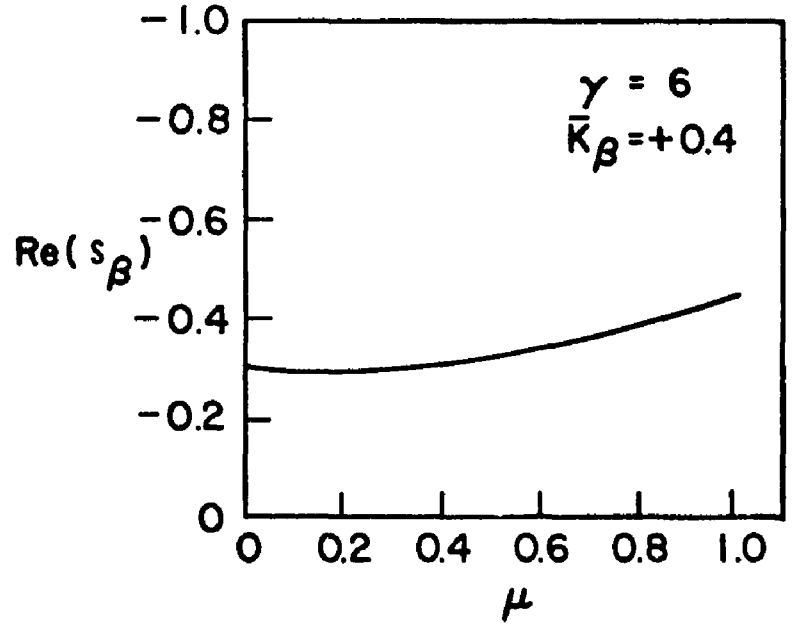

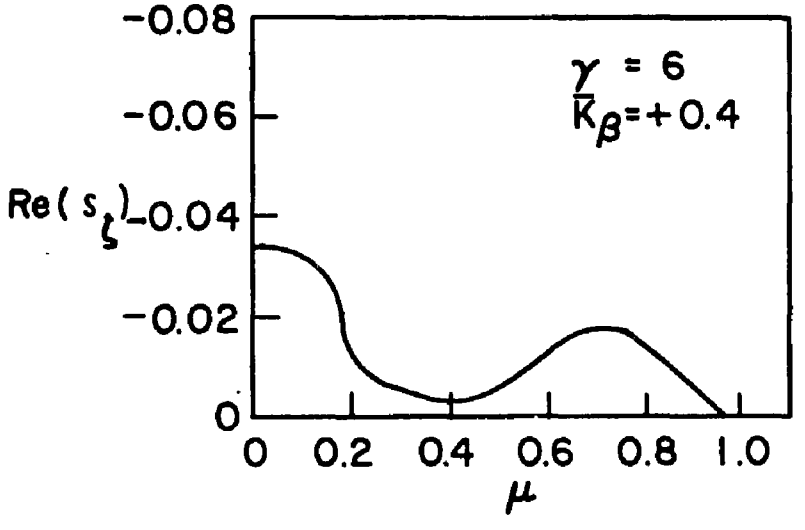

Fig. 6.4.4. EFFECT OF VELOCITY ON $Re(s_\beta)$ AND $Re(s_\zeta)$: $\bar{K}_\beta = +.4$. Instability is predicted at $\mu \cong 0.95$.

Use of the blade feedback gain, $\bar{K}_\beta = -.4$, gives the results of Fig. 6.4.3. There is an improvement of flapping motion damping, with a frequency break at $\mu \sim 0.6$. However, the eigenvalue associated with the lag motion indicates instability from $\mu = 0.2$ to $\mu = 1.0$.

Figure 6.4.4 shows the case with flap-lag coupling and $\bar{K}_\beta = 0.4$. Here, the eigenvalue associated with flapping never enters a parametric frequency range, and the damping is consistently at a relatively high level. The damping of the inplane eigenvalue is also improved, but there is again instability at $\mu = 1.0$.

For this specific configuration, the flap-lag instability can occur at advance ratios considerably below the boundary of Fig. 6.3.3.

From this example, it is clear that the synthesis of rotary wing VTOL aircraft controls, even for low frequency phenomena, should include an evaluation of rotor blade, as well as rotor plane, response.

6.5 Summary

In this chapter, the stability of flap-lag blade motions with blade or rotor plane feedback is examined.

A computer implementation of multivariable Floquet theory is described. This program evaluates the flap-lag stability of a blade by using the QR algorithm to determine the eigenvalues of the transition matrix over one revolution.

The equivalence of blade feedback and rotor plane feedback to blade pitch is shown. For slowly varying rotor plane angles, the blade gain is expressed in terms of the rotor plane position and the rotor position gains.

A hypothetical rotor is used to demonstrate the speed dependence of flap-lag instability. It is concluded that such calculations are necessary in the complete evaluation of a rotor control system.

Chapter VII

CONCLUSIONS AND RECOMMENDATIONS

7.1 Conclusions

This work covers several different topics. Table 7.1 lists the chapter detailed summaries for reference.

Table 7.1. TOPIC SUMMARIES BY CHAPTER.

CHAPTER	TOPIC	SUMMARY PAGE
I	Introduction	———
II	Blade Equations	64
III	Vehicle Hover Analysis	72
IV	Quadratic Synthesis by Eigenvector Decomposition	118
V	Hover Controller Design	142
VI	Blade Stability	160

This investigation has demonstrated that improved hover controllers for rotary-wing VTOL aircraft may be designed by using feedback of rotor state variables. Indeed, neglect of these states may lead to instabilities in the controlled system which would not be indicated in a lower order model of the aircraft. It was also shown that RMS gust response may be underestimated if the rotor state is neglected in the control design.

A control system designed on the basis of rotor and fuselage models must also be evaluated for its effect on the blade stability, using the periodic blade equations of motion. One particular feedback of rotor state, feedback of flapping angle to blade pitch, was shown to produce blade instability at high advance ratios.

A new and very efficient program was developed for quadratic synthesis of controllers. Coupled with an efficient eigenvector-eigenvalue

routine (the QR algorithm of Francis), it is faster and more accurate than iterative methods for solving the steady-state Riccati equation. In addition, the eigenvector decomposition method gives the closed loop eigenvalues and eigenvectors without the further calculation required by other methods.

The eigenvector decomposition method can also be used to design Kalman filters and smoothers. The Euler-Lagrange equation eigensystem gives the steady state solutions of both the forward and backward Riccati equations, and hence is a new approach to the solution of the Fraser smoother.

It is concluded that the eigenvector decomposition method is a superior technique in the synthesis and evaluation of the solutions of quadratic synthesis problems.

7.2 Recommendations

Further investigations of mathematical models of VTOL vehicles is desirable and should be integrated with a flight test program. Such a program should also be concerned with means of measuring rotor state, i.e., pitch and roll angles of the tip-path plane and their time rates of change.

Since the rotor is subject to intense vibration, it is suggested that an estimation scheme for determining rotor pitch and roll rates from rotor position and/or fuselage state would solve many practical problems of forming control signals for a controller. The OPTSYS computer program is capable of designing such estimators and is already developed. However, further investigation of the modeling of noise sources, both from the vehicle and the measurement system, is needed.

The eigenvector decomposition method of quadratic synthesis may be extended to include periodic systems. This may be accomplished by the discrete analog of the continuous quadratic loss problem. The Floquet representation yields a discrete equivalent system (with a period of one rotor revolution). Having determined this discrete equivalent, the discrete formulae may be used to design controllers for each harmonic of

blade response. The difficulty is reducing the computational requirements of the design procedure to a tractable level.

Finally, the eigenvalue decomposition method should be extended to include the problem of colored noise in the estimation problem and the optimization of step and higher order responses in the control case. Such an investigation would serve a useful purpose by unifying many of the concepts of quadratic synthesis and the so-called frequency domain techniques.

Appendix A

DERIVATION OF BLADE FLAP-PITCH-LAG EQUATIONS OF MOTION

Kinematics

The blade direction cosine matrices of the rotations of Table 2.2.1 are:

$$T_{R/S} = \begin{pmatrix} \cos\psi & \sin\psi & 0 \\ -\sin\psi & \cos\psi & 0 \\ 0 & 0 & 1 \end{pmatrix} \tag{A-1}$$

$$T_{\beta/R} = \begin{pmatrix} \cos\beta & 0 & \sin\beta \\ 0 & 1 & 0 \\ -\sin\beta & 0 & \cos\beta \end{pmatrix} \tag{A-2}$$

$$T_{\zeta/\beta} = \begin{pmatrix} \cos\zeta & \sin\zeta & 0 \\ -\sin\zeta & \cos\zeta & 0 \\ 0 & 0 & 1 \end{pmatrix} \tag{A-3}$$

$$T_{\theta/\zeta} = \begin{pmatrix} 1 & 0 & 0 \\ 0 & \cos\theta & \sin\theta \\ 0 & -\sin\theta & \cos\theta \end{pmatrix} \tag{A-4}$$

where β is positive when the blade is above the plane determined by X_s, Y_s.

The small angle transformation from the inertial frame to fuselage axis is, from Fig. 2.2.1

$$T_{F/I} \approx \begin{pmatrix} 1 & 0 & -\theta_F \\ 0 & 1 & \phi_F \\ \theta_F & -\phi_F & 1 \end{pmatrix} \tag{A-6}$$

and the shaft frame transformation from the fuselage axes is

$$T_{S/F} = \begin{pmatrix} -1 & 0 & 0 \\ 0 & 1 & 0 \\ 0 & 0 & -1 \end{pmatrix} \tag{A-7}$$

For $\Omega = (\omega_x, \omega_y, \omega_z)^T$,

$$(\overline{\Omega x}) \triangleq \begin{bmatrix} 0 & -\omega_z & \omega_y \\ \omega_z & 0 & -\omega_x \\ -\omega_y & \omega_x & 0 \end{bmatrix} \tag{A-8}$$

From Fig. 2.2.2,

$$\underset{F}{\Omega}^{F-I} = (\dot{\phi}_F, \dot{\theta}_F, \dot{\psi}_F)^T \tag{A-9}$$

then from Eq. (A-7)

$$\underset{S}{\Omega}^{F-I} = (\dot{\phi}_{SF}, \dot{\theta}_{SF}, \dot{\psi}_{SF})^T = (-\dot{\phi}_F, \dot{\theta}_F, -\dot{\psi}_F)^T \tag{A-10}$$

and from Eq. (A-1)

$$\Omega_R^{F-I} = \begin{pmatrix} \dot{\phi}_R^F \\ \dot{\theta}_R^F \\ \dot{\psi}_R^F \end{pmatrix} = \begin{pmatrix} -\dot{\phi}_F \cos\psi + \theta_F \sin\psi \\ \dot{\phi}_F \sin\psi + \dot{\theta}_F \cos\psi \\ -\dot{\psi}_F \end{pmatrix} \tag{A-11}$$

and

$$\Omega_R^{R-I} = \Omega_R^{F-I} + (0 \quad 0 \quad \Omega)^T \tag{A-12}$$

for small β, ζ, and θ, Eqs. (A-1) and (A-7) give

$$\Omega_B^{B-I} = \begin{pmatrix} \Omega_x^{B-I} \\ \Omega_{By}^{B-I} \\ \Omega_{Bz}^{B-I} \end{pmatrix} = \begin{pmatrix} -\dot{\phi}_F \cos\psi + \dot{\theta}_F \sin\psi + \Omega\beta - \dot{\beta}\zeta + \dot{\theta} \\ \dot{\phi}_F \sin\psi + \dot{\theta}_F \cos\psi + \Omega\theta - \Omega\zeta\dot{\beta} - \dot{\beta} + \dot{\zeta}\theta \\ -\dot{\psi}_F + \Omega + \dot{\beta}\theta + \dot{\zeta} \end{pmatrix} \tag{A-13}$$

Velocities

The velocity of the origin of the S frame, $\vec{V}^{S-I}$, is

$$\vec{V}_S^{S-I} = T_{S/F}\, T_{V/I}\, V_I^{F-I} + (\vec{\Omega}_S^{F-I} \times) h \tag{A-14}$$

substituting Eqs. (A-6) and (A-7) into (A-14), and since $V_I^{F-I} = (u_I, v_I, w_I)^T$,

$$V_F^{S-I} = \begin{pmatrix} h\dot{\theta}_F - u_F \\ h\dot{\phi}_F + v_F \\ w_F \end{pmatrix} \tag{A-15}$$

where

$$u_F = u_I - w_I\theta_F$$

$$v_F = v_I + w_I\phi_F$$

$$w_F = -w_I - u_I\theta_F + v_I\phi_F .$$

The inertial velocity of a point on the blade centerline is

$$\vec{V}^{\xi-I} = \vec{V}^{S-I} + \vec{\Omega}^{R-I} \times \vec{e} + \vec{\Omega}^{B-I} \times \vec{\xi} . \qquad \text{(A-16)}$$

coordinatizing Eq. (A-16) in the B frame,

$$V_B^{B-I} = V_B^{S-I} + (\Omega_B^{R-I} \times) e_B + (\Omega_B^{B-I} \times) \xi_B \qquad \text{(A-17)}$$

where

$$\Omega_B^{R-I} = T_{\theta/\zeta} T_{\zeta/\beta} T_{\beta/R} \Omega_R^{R-I} \qquad \text{(A-18)}$$

The velocities (inplane and normal only) are then Eqs. (A-19) and (A-20) below. A change of variable,

$$r = \xi + e$$

has been made in these equations. Then

$$V_B^{\xi-I} \triangleq \begin{pmatrix} u_R \\ u_T \\ u_P \end{pmatrix}$$

where

$$u_T = r\Omega + (r-e)(\dot{\zeta} + \dot{\beta}\theta) + [h\dot{\phi}_F + v_F + \zeta u_F] \cos\psi$$
$$+ [-h\dot{\theta}_F + u_F - \zeta v_F] \sin\psi - \theta[w_F] \tag{A-19}$$

$$u_P = (r-e)\ [\dot{\beta} - \dot{\zeta}\theta + \Omega\zeta\beta] - [r\dot{\phi}_F + u_F\theta + v_F\beta] \sin\psi$$
$$- [r\dot{\theta}_F - u_F\beta + v_F\theta] \cos\psi - (w_F) \tag{A-20}$$

and u_R will be neglected.

Equations of Motion

The sum of the external moments about the flapping hinge equals the time rate of change of angular momentum about the hinge plus the moments due to the acceleration of the hinge. Taking point 0 as the hinge,

$$\vec{\dot{H}}^I = \left\{ \vec{\dot{H}}^B + \vec{\Omega}^{B-I} \times \bar{H} \right\} + \left\{ M\bar{R}_{CM} \times \vec{a}^{O-I} \right\} \tag{A-21}$$

where $\vec{H}$ and $\vec{\Omega}^{B-I}$ are defined relative to a blade fixed coordinate system with origin at 0. Hence,

$$\vec{H} = \bar{\bar{I}} \cdot \vec{\Omega}^{B-I} \tag{A-22}$$

$$\bar{\bar{I}} = \begin{bmatrix} I_{xx} & +I_{xy} & 0 \\ +I_{xy} & I_{yy} & 0 \\ 0 & 0 & I_{zz} \end{bmatrix} \tag{A-23}$$

where

$$I_{xy} = -\iiint_{\text{volume}} xy\ dx\ dy\ dz$$

$$I_{xx} = \iiint_{volume} (y^2 + z^2)\, dx\, dy\, dz$$

$$I_{yy} = \iiint_{volume} (x^2 + z^2)\, dx\, dy\, dz$$

$$I_{zz} = \iiint_{volume} (x^2 + y^2)\, dx\, dy\, dz$$

and I_{xz} and I_{yz} are assumed zero due the smallness of the blade thickness relative to the chord and span. For this study, the blade feathering axis is coincident with the blade x principal axis and I_{xy} will be small as shown below.

The first bracketed term of (A-22) is

$$\overset{B}{\vec{H}} + \vec{\Omega}^{B-I} \times \overset{B}{\vec{H}} = \begin{bmatrix} I_{xx}\dot{\Omega}_x + (I_{zz}-I_{yy})\Omega_y\Omega_z + I_{xy}(\dot{\Omega}_y - \Omega_x\Omega_z) \\ I_{yy}\dot{\Omega}_y + (I_{xx}-I_{zz})\Omega_x\Omega_z + I_{xy}(\dot{\Omega}_x + \Omega_y\Omega_z) \\ I_{zz}\dot{\Omega}_z + (I_{yy}-I_{xx})\Omega_x\Omega_y + I_{xy}(\Omega_x^2 - \Omega_y^2) \end{bmatrix} \tag{A-24}$$

where the superscript "B-I" and underscript "B" are understood in the Ω components of the right hand side.

The second bracketed term of (A-22) is found by writing

$$\overset{R}{B}_{CM} = \begin{pmatrix} \eta_{CM} \\ \xi_{CM} \\ 0 \end{pmatrix} \tag{A-25}$$

$$\overset{O-I}{a}_B = T_{\theta/R} \frac{\left\{ \overset{I}{\Omega}^{R-I} \times \vec{e} + \Omega^{R-I} \times (\Omega^{R-I} \times \vec{e}) \right\}}{R} \tag{A-26}$$

Substituting (A-13) into Eq. (A-24), and Eqs. (A-25) and (A-26) into Eq. (A-21) and coordinatizing into the inplane lag frame,

$$M_x = I_{xx}\left[\ddot{\theta} + (\Omega^2+2\Omega\dot{\zeta})\theta - \zeta(\ddot{\beta}+\Omega^2\beta) + (-\ddot{\phi}_F+2\dot{\theta}_F\Omega)\cos\psi + (\ddot{\theta}_F+2\Omega\dot{\phi}_F)\sin\psi\right]$$

$$+ I_{xy}\left[-\ddot{\beta} - (\Omega^2+2\Omega\dot{\zeta})\beta + \ddot{\zeta}\theta + (\ddot{\theta}_F+2\Omega\dot{\phi}_F)\cos\psi + (-\ddot{\phi}_F+2\Omega\dot{\theta}_F)\sin\psi\right]$$

$$- M\, e\eta_{CM}\left[\Omega^2\beta - \Omega^2\zeta\theta + (\ddot{\theta}_F+2\dot{\phi}_F\Omega)\cos\psi + (\ddot{\phi}_F-2\Omega\dot{\theta}_F)\sin\psi\right] \qquad \text{(A-27)}$$

$$M_y = I_{yy}\left[\ddot{\beta} + (\Omega^2+2\Omega\dot{\zeta})\beta - (\ddot{\theta}_F+2\Omega\dot{\phi}_F)\cos\psi + (\ddot{\phi}_F-2\Omega\dot{\theta}_F)\sin\psi\right]$$

$$-I_{xy}\left[\ddot{\theta} + (\Omega^2+2\Omega\dot{\zeta})\theta - (\ddot{\beta}+\Omega^2\beta)\zeta + (\ddot{\phi}_F-2\Omega\dot{\theta}_F)\cos\psi + (\ddot{\theta}_F+2\Omega\phi_F)\sin\psi\right]$$

$$+ Me\,\xi_{CM}\left[\Omega^2\beta - (\ddot{\theta}_F+2\Omega\dot{\phi}_F)\cos\psi - (\ddot{\phi}_F-2\dot{\theta}_F\Omega)\sin\psi\right] \qquad \text{(A-28)}$$

$$M_z = I_{zz}[\ddot{\zeta} - 2\Omega\beta\dot{\beta}] + M\xi_{CM}\left[e\Omega^2\zeta + (\dot{u}_F - h\ddot{\theta}_F)\sin\psi + (\dot{v}_F + h\ddot{\phi}_F)\cos\psi\right]$$

$$-M\eta_{CM}\left[e\Omega^2 + (\dot{u}_F - h\ddot{\theta}_F)\cos\psi - (\dot{v}_F + h\ddot{\phi}_F)\sin\psi\right] \qquad \text{(A-29)}$$

Equations (A-27) - (A-28) may be expressed in terms of blade geometric properties, instead of the inertias I_{yy}, I_{zz}, and I_{xy}. This evaluation is based on the assumption of a flat blade with constant spanwise and chordwise mass distribution.

In each of the equations [(A-27) - (A-29)], divide by the inertia of the axis about which the equation is written, giving equations for M/I for each axis. This division will yield, on the right hand sides, the terms I_{xy}, I_{xx}, I_{xy}/I_{yy}, $Me\eta_{CM}/I_{xx}$, $Me\xi_{CM}/I_{yy}$, and $M\eta_{CM}/I_{zz}$. Those terms not involving I_{xx} may be expressed in terms of the geometric properties of the blades. No assumptions are made regarding I_{xx} in terms of chord properties. Hence,

$$I_{yy} = \rho_B \int_0^{R-e} \xi^2 \, d\xi = \frac{M_B}{3} (R-e)^2$$

for the blade CM a distance $-\eta_{CM}$ behind the feathering axis

$$I_{xy} = -\rho_B \int_0^{R-e} \xi \eta_{CM} \, d\xi = -\frac{M(R-e)}{2} \eta_{CM}$$

and

$$\frac{I_{xy}}{I_{yy}} = -\frac{3}{2} \frac{\eta_{CM}}{1 - \bar{e}}$$

$$\frac{Me\xi_{CM}}{I_{yy}} = \frac{3}{2} \frac{\bar{e}}{1 - \bar{e}}$$

In the inplane equation, it is assumed that $I_{zz} \sim I_{yy}$. Furthermore, since the principal inplane stiffness term is $M\xi_{CM} e\Omega^2 \zeta$, it may be assumed that the offset for the inplane degree of freedom is not the same as the offset for the β degree of freedom. Then,

e_β = effective offset of flapping hinge (first flapping mode)

e_ζ = effective offset of inplane hinge (first inplane mode)

are assumed independent.

Another property of the blade characteristics is the effective stiffness of the first inplane or flapping mode. Denoting the effective flapping stiffness as K_β, the flapping restoring moment is $K_\beta \beta$. The corresponding inplane restoring moment is $K_\zeta \zeta$. These terms are added to Eqs. (A-28) and (A-29), respectively.

The resulting equations are Eqs. (2.2.3) - (2.2.5) of the text.

Appendix B

THE HAMILTONIAN AND SYMPLECTIC PROPERTIES OF THE CANONICAL SYSTEM

The Hamiltonian Property of the Canonical Equations (KA1)

The Hamiltonian of the homogeneous Euler-Lagrange equations may be written, for example, in the regulator problem, as

$$\mathcal{H}[x,\ \lambda,\ t] = \frac{1}{2}\ [x^T\ \lambda^T] \begin{bmatrix} A & F^T \\ F & -GB^{-1}G^T \end{bmatrix} \begin{bmatrix} x \\ \lambda \end{bmatrix} \qquad \text{(B-1)}$$

$$= \frac{1}{2}\ z^T M z$$

where $z = \begin{pmatrix} x \\ \lambda \end{pmatrix}$ and the matrix M is symmetric. If we define

$$\tilde{J} = \begin{pmatrix} 0 & I_n \\ -I_n & 0 \end{pmatrix}$$

then it follows that

$$M = -\tilde{J}\mathcal{F} \qquad \text{where} \quad \mathcal{F} = \begin{bmatrix} F & -GB^{-1}G^T \\ -A & -F^T \end{bmatrix} \qquad \text{(B-2)}$$

Since M is symmetric,

$$\mathcal{F} = \tilde{J}\mathcal{F}^T\tilde{J} \qquad \text{(B-3)}$$

Equations (B-1) through (B-3) define the Hamiltonian property of the canonical system, (4.3.1). This property is closely related to the symplectic property of the transition matrix of the canonical system.

Symplectic Property of the Transition Matrix (OD1, KA1)

It is known that the transition matrix of the Euler-Lagrange equations, $\Phi(t,t_o)$, is symplectic, that is,

$$\Phi^T(t,t_o)\,\tilde{J}\,\Phi(t,t_o) = \tilde{J} \tag{B-4}$$

It follows from (B-4) that

$$\Phi^{-1}(t,t_o) = \tilde{J}^T\Phi^T(t,t_o)\tilde{J} \tag{B-5}$$

The eigenvector decomposition of the transition matrix is

$$\Phi(t,t_o) = Te^{\Lambda(t-t_o)}T^{-1} = e^{\mathcal{J}(t-t_o)} \tag{B-6}$$

where T and Λ are

$$T = \begin{pmatrix} X_+ & X_- \\ \Lambda_+ & \Lambda_- \end{pmatrix} \qquad \Lambda = \begin{pmatrix} \Lambda_+ & 0 \\ 0 & \Lambda_- \end{pmatrix}$$

and

$$\Phi(t_o,t_o) = TT^{-1} = I \tag{B-7}$$

Equations (B-4) and (B-7) require T to be symplectic, for substitutions of (B-6) into (B-4) gives

$$(T^T\tilde{J}T) = e^{\Lambda(t-t_o)}T^T\tilde{J}Te^{\Lambda(t-t_o)}$$

Since $e^{\Lambda(t-t_o)}(\pm\tilde{J})\,e^{\Lambda(t-t_o)} = \pm J$ (identity), Eq. (B-7) requires $\tilde{J} = T^T\tilde{J}T$ and hence T is symplectic, and, by definition

$$T^{-1} = \tilde{J}^TT^T\tilde{J}$$

This specifies a normalization of the T matrix, specifically,

$$X_+^T\Lambda_- - \Lambda_+^TX_- = I \tag{B-8}$$

for which, since $X_+^T \Lambda_+ = \Lambda_+^T X$ from (B.5a)

$$(\Lambda_- X_-^{-1}) - (\Lambda_+ X_+^{-1}) = (X_- X_+^T)^{-1} \qquad \text{(B-9)}$$

Both sides of (B-9) are symmetric.

Appendix C

FLOQUET THEORY

Consider the linear system

$$\dot{x} = F(t)x \tag{C-1}$$

where $F(t)$ is a continuous periodic $n \times n$ matrix, with a lowest common period of T_R. Hence

$$F(t) = F(t + T_R) \quad , -\infty < t < \infty \tag{C-2}$$

Then, if $\Phi(t,t_o)$ is a fundamental matrix of (C-1)

$$\dot{\Phi}(t + T_R,t_o) = F(t + T_R)\ \Phi(t + T_R,t_o)$$

$$= F(t)\ \Phi(t + T_R,t_o) \tag{C-3}$$

Hence $\Phi(t + T_R,t_o)$ is also a fundamental matrix of (C-1). By definition, a fundamental matrix is a solution matrix of the system (C-1) whose columns are linearly independent over the domain of solution definition. Hence $\det|\Phi(t,t_o)| \neq 0$ over that domain and further there exists a nonsingular constant matrix C such that

$$\Phi(t + T_R) = \Phi(t)\ C \quad (-\infty < t < \infty .) \tag{C-4}$$

Equation (C-4) states that, given one set of linearly independent solutions of a linear differential equation, any other set of linearly independent solutions is a linear combination of the given set. Alternately, the columns of a fundamental matrix span the space of solutions of a linear differential equation.

The main result of this appendix is Floquet's theorem. Because of its importance to our studies, two equivalent forms will be given.

Floquet's Theorem (Classical) (SA1)

Given the system $\dot{x} = F(t)x$ with $F(t)$ a continuous periodic matrix of lowest common period T_R, then there exists a nonzero constant $\hat{s}$ and at least one nontrivial solution $x(t)$ such that $x(t + T_R) = \hat{s}x(t)$.

Proof.

From (C-4) $C = \Phi^{-1}(t)\,\Phi(t + T_R)$. Choose $\Phi(t)$ such that $\Phi(0) = I$. Then $C = \Phi(T_R)$ and since $\det|\Phi(t)| \neq 0$,

$$\det|C| \neq 0 .$$

Let $\hat{s}_i$ be a root of the characteristic polynomial of $|C - \hat{s}I|$. Since $\det|C| \neq 0$, $\hat{s} \neq 0$ and there exists a nonzero vector η such that $C\eta = \hat{s}\eta$. Let one solution of (C-1) be $x(t) = \Phi(t)\eta$. Then

$$x(t + T_R) = \Phi(t + T_R)\eta = \Phi(t)\, C\eta$$

$$= \Phi(t)\hat{s}\eta = \hat{s}\,\Phi(t)\eta$$

$$= \hat{s}x(t) .$$

Hence for any $x(t)$ having this property, $\hat{s}$ must be a characteristic root of C. If $\hat{s}_1, \hat{s}_2, \ldots, \hat{s}_m$, $1 \leq m \leq n$ are the distinct eigenvalues of C, then there must exist at least m solutions having this property. This completes the proof.

It is noted that if $x(t)$ is any other fundamental matrix of (C-1), then there exists another constant matrix, D, such that

$$x(t) = \Phi(t)\, D .$$

where

$$x(t + T_R) = \Phi(t + T_R)D = \Phi(t)CD = x(t)D^{-1}CD$$

and $D^{-1}CD$ is a similarity transformation on C, having the same eigenvalues as C.

Floquet's Theorem(Lyapunov) (ZA 1)

Let $x(t)$, $F(t)$, and $\Phi(t)$ be defined as above. Then the fundamental matrix, $\Phi(t,t_o)$, can always be written as

$$\Phi(t,t_o) = K(t,t_o)\exp\left[(t-t_o)B\right] \tag{C-5}$$

where $K(t,t_o)$ is periodic of period T_R and B is a constant $n \times n$ matrix.

Proof.

Define the matrix B

$$e^{T_R B} = C$$

where B is a real or complex constant matrix. Then

$$\Phi(t + T_R,t_o) = \Phi(t,t_o)C = \Phi(t,t_o)e^{T_R B}.$$

Now define $K(t,t_o)$ such that

$$K(t,t_o) \triangleq \Phi(t,t_o)\, e^{-(t-t_o)B}.$$

The nonsingularity of $K(t,t_o)$ is insured by the results of the above discussion. Furthermore, $K(t,t_o)$ is periodic,for

$$K(t + T_R,t_o) = \Phi(t + T_R,t_o)\, e^{-(t-t_o+T_R)B} = \Phi(t,t_o)\, Ce^{-(t-t_o+T_R)B}$$

$$= \Phi(t,t_o)\, e^{T_R B} e^{-T_R B} e^{-(t-t_o)B}$$

$$= \Phi(t,t_o)\, e^{-(t-t_o)B}$$

The theorem is proved by the above calculation.

Note: Lyapunov introduced the theory of reducible systems which gives the significance of this latter statement of Floquet's theorem. Specifically, the system C-1 is reducible if for $t \geq t_o$, there is a matrix $N(t)$ possessing the following properties:

(a) It is bounded, differentiable, and has a bounded inverse

(b) It is such that the application of the time-varying transformation

$$y = N(t)\, x \tag{C-6}$$

transforms the given system into

$$\dot{y} = By$$

$$B = N(t)A(t)\, N^{-1}(t) + \dot{N}(t)N^{-1}(t) \tag{C-7}$$

Definition. Let B be a nonsingular $n \times n$ matrix. Then there exists an $n \times n$ matrix C such that

$$e^{B} = C \tag{C-8}$$

In most texts (BE1, BR 1), this result is stated as a theorem to the effect that every nonsingular matrix has a logarithm. However, for the purposes of this discussion, only the relationship between B and C is required.

Now let the (distinct) eigenvalues of C be $\hat{s}_1, \hat{s}_2, \ldots, \hat{s}_m$, and call these the characteristic multipliers of the system (C-1). Physically, these numbers represent the growth fraction per lowest common period of the mode to which the eigenvalue belongs. Let the numbers $s_1, s_2, \ldots, s_m$ be defined by the complementary relations

$$s_i = \frac{1}{T_R} \ln[\hat{s}_i]$$

$$\hat{s}_i = e^{s_i T_R} \tag{C-10}$$

The s_i are the characteristic exponents of the system. Physically, these numbers represent the eigenvalues of the constant coefficient system related by the reducibility property. These numbers are not unique, for they are determined only to within multiples of $e^{2\pi j/T_R}$, and hence the characteristic exponents are determined only to their real parts. That these real parts represent the damping factor of the period is the main justification for applying Floquet theory to stability determination.

The implementation of this theory to determine the stability of the system discussed in Chapter 6 is presented in Appendix D.

Characteristic Multipliers of a Second Order Periodic System

Consider the differential equation

$$\ddot{\beta} + D(t)\dot{\beta} + S(t)\beta = 0$$

where D and S are continuous functions(of period T_R) in t. This equation may be written in terms of the states $\beta_1 = \beta$ and $\beta_2 = \dot{\beta}_1$ as

$$\begin{pmatrix} \dot{\beta}_1 \\ \dot{\beta}_2 \end{pmatrix} = \begin{pmatrix} 0 & 1 \\ -S(t) & -D(t) \end{pmatrix} \begin{pmatrix} \beta_1 \\ \beta_2 \end{pmatrix}$$

Let $\Phi(t)$ be the fundamental matrix such that $\Phi(0) = I$, and

$$\Phi(t) = \begin{pmatrix} \phi_{11}(t) & \phi_{12}(t) \\ \phi_{21}(t) & \phi_{22}(t) \end{pmatrix} .$$

with $\phi_{21}(t) = \dot{\phi}_{11}(t)$ and $\phi_{22}(t) = \dot{\phi}_{12}(t)$.

The characteristic multipliers are defined as the eigenvalues of $\Phi(T_R)$, and hence

$$\det\left|\Phi(T_R) - \hat{s}I\right| = \hat{s}^2 - \left[\phi_{11}(T_R) + \phi_{22}(T_R)\right]\hat{s} + \det\left|\phi(T_R)\right| = 0$$

where, by the Jacobi-Louiville formula [BE 1]

$$\det|\phi(T_R)| = \exp\left(-\int_0^{T_R} D(t)\,dt\right)$$

and so

$$\hat{s}^2 - \left[\phi_{11}(T_R) + \phi_{22}(T_R)\right]\hat{s} + \exp\left(-\int_0^{T_R} D(t)\,dt\right) = 0$$

Hence, the characteristic multipliers are given by

$$\hat{s} = \frac{\phi_{11}(T_R) + \phi_{22}(T_R)}{2} \pm \sqrt{\frac{\left[\phi_{11}(T_R) + \phi_{22}(T_R)\right]^2}{4} - \det|\phi(T_R)|}$$

$$= \frac{\phi_{11}(T_R) + \phi_{22}(T_R)}{2} \pm \sqrt{\frac{\left[\phi_{11}(T_R) - \phi_{22}(T_R)\right]^2}{4} + \phi_{12}\phi_{21}}$$

Alternately, letting $2m = \phi_{11}(T_R) + \phi_{12}(T_R)$,

$$\hat{s} = m \pm j\sqrt{\det|\phi(T_R)| - m^2}$$

For $|m| < \det|\phi(T_R)|$, this is an imaginary root, while for $|m| \geq \det|\phi(T_R)|$, $\hat{s}$ is real. For $m < \det|\phi(T_R)|$, the locus of s is a circle of radius $\det|\phi(T)|$ in the complex plane.

The condition of frequency and stability is, for the simple second order case, determined by the location of the $\hat{s}$ relative to this circle.

The characteristic multiplier satisfies the equation, for the i^{th} mode,

$$x_i(t + T_R) = \hat{s}_i x_i(t) .$$

If $\hat{s} = +1 + j(0)$, $x(t)$ is of fundamental period $T_R \pmod{2\pi}$; $\hat{s} = -1 + j(0)$, the fundamental period is $2T_R \pmod{2\pi}$. Roots lying on the real

axis to the right of the $\mathrm{Im}(\hat{s})$ axis correspond to frequencies of one per rev, two per rev, etc. and roots on the left side of the $\mathrm{Im}(\hat{s})$ axis correspond to frequencies of 1/2 per rev, 3/2 per rev, etc.

The condition for stability is that $\hat{s}$ be contained within a unit circle centered at the origin in the characteristic multiplier plane (see Fig. C-1).

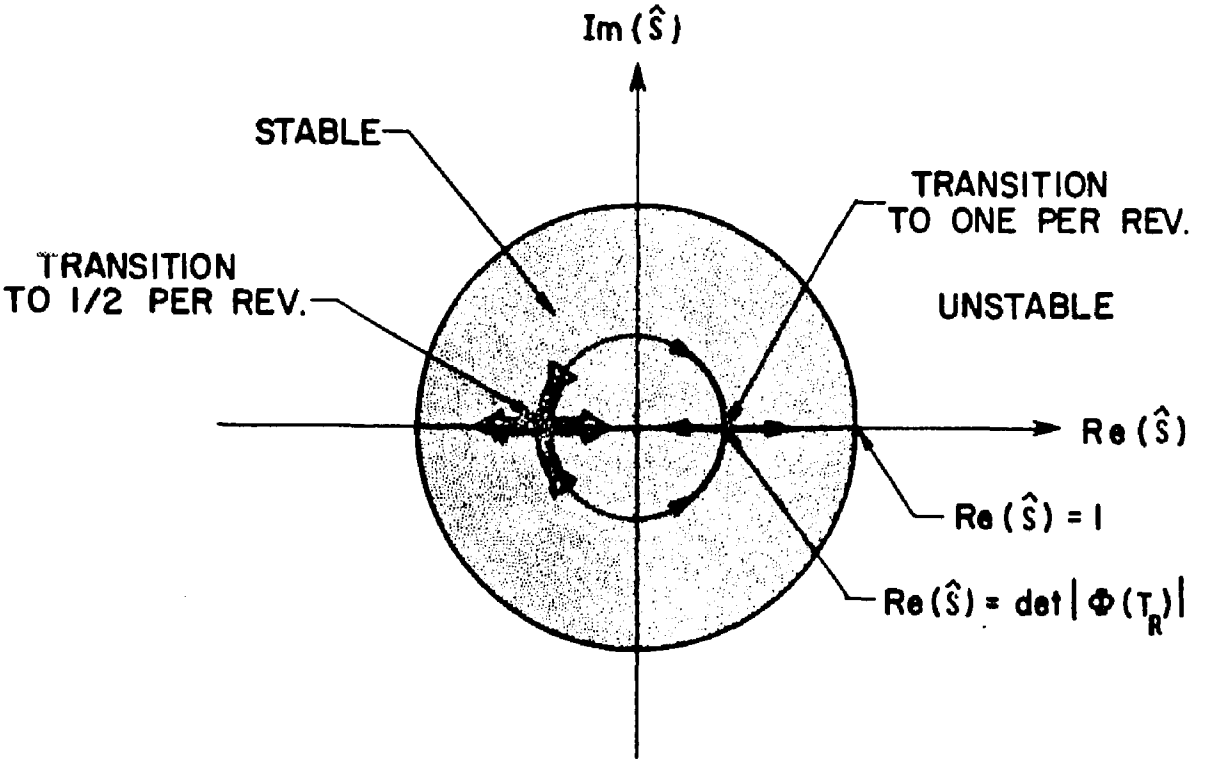

Fig. C-1. LOCI OF CHARACTERISTIC MULTIPLIERS.

The characteristic exponent loci corresponding to the characteristic multiplier loci of Fig. C-1 are discussed in Truxal (TR 1). The characteristic exponent locus for the 1/2 per rev transition is shown in Fig. C-2.

For the same s-plane frequency, there are two damping values, corresponding to the two values of s on the negative real axis of Fig. C-1. The periodic solution occurs when $|\hat{s}| = 1$, or the s-plane locus crosses the $\mathrm{Im}(s)$ axis. This is the branch plotted in the results of Chapter 6.

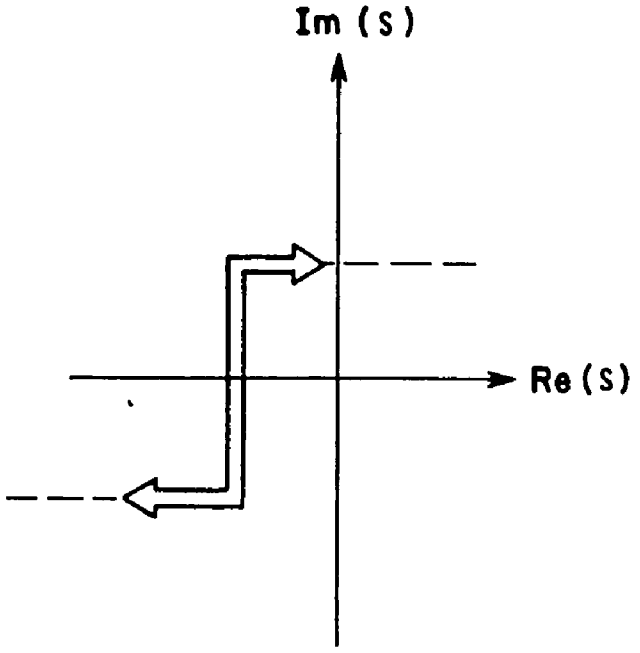

Fig. C-2. CHARACTERISTIC EXPONENT ROOT LOCUS OF 1/2 PER REV TRANSITION.

Appendix D

DESCRIPTION OF BLADE STABILITY PROGRAM

The program written to implement the Floquet solution consists of thirteen subroutines and one main calling routine. All calculations are performed in double precision arithmetic. Numerous options are available for evaluating various combinations of blade parameters, effects of secondary aerodynamic effects, and flight condition. In addition, the structure of the program is such that the order of the system may be increased by simply changing only two or three subroutines. All program options are described by comments and reference to these comments allows tailoring the program to a specific task. A qualitative description of the program flow paths is shown in Fig. D-1. The most important aspect of the use of multivariable Floquet theory discussed in Appendix C is the determination of the characteristic exponents of the system. A secondary, but equally important, aspect is the generation of the transition matrix.

The integration routine is a fourth-order, double-precision implementation of the Runge-Kutta formulae. Other routines with automatic step size control were originally used, but it was found that a step size of 6° in ψ give five-place accuracy of the transition matrix and minimized machine time, so Runge-Kutta was adopted. Greater accuracy can be achieved (at expense of computation time) with smaller step sizes--about one significant figure per halving of step size.

In order to generate the characteristic exponents, subroutine EIG performs the operation of taking the logarithm of these characteristic multipliers, and dividing the result by the lowest common period of the coefficients of the equations. Hence, given the column vectors WR and WI , where the characteristic multipliers are

$$[W]_i = [WR]_i + j[WI]_i ,$$

subroutine EIG generates the column vectors CMR and CMI , where the characteristic exponent is

$$CM_i = \frac{1}{P}\left\{\left[\mathrm{Ln}\left(WR_i^2 + WI_i^2\right)^{\frac{1}{2}}\right] + j \tan^{-1}\frac{WI_i}{WR_i}\right\}.$$

Subroutine CNORM performs the dual function of normalizing the eigenvectors and ordering the eigenvalue-eigenvectors as to the real or complex nature of the eigenvector. The complex eigenvectors are normalized.

The eigenvalue-eigenvector routine consists of nine subroutines, two of which were written in the course of this work, and seven of which were developed in the fall of 1969 by J. H. Wilkenson and his students of the Stanford Computation Center, Mr. Richard Underwood and Mr. Scott Wallace. The latter routines solve for the eigenvalues and non-normalized eigenvectors of a real nonsymmetric matrix of arbitrary order using the QR algorithm in double precision arithmetic. The basic reference for the computation procedures are found in (WI1). This high speed program solves for the eigenvalues and eigenvectors of the transition matrix, giving the characteristic multipliers and the eigenvectors of the Floquet modes, such that the eigenvector component with largest modulus is of the form 1.0 + j(0.0) and all other components normalized on this modulus. The real eigenvectors are normalized such that the sum of their squares is unity.

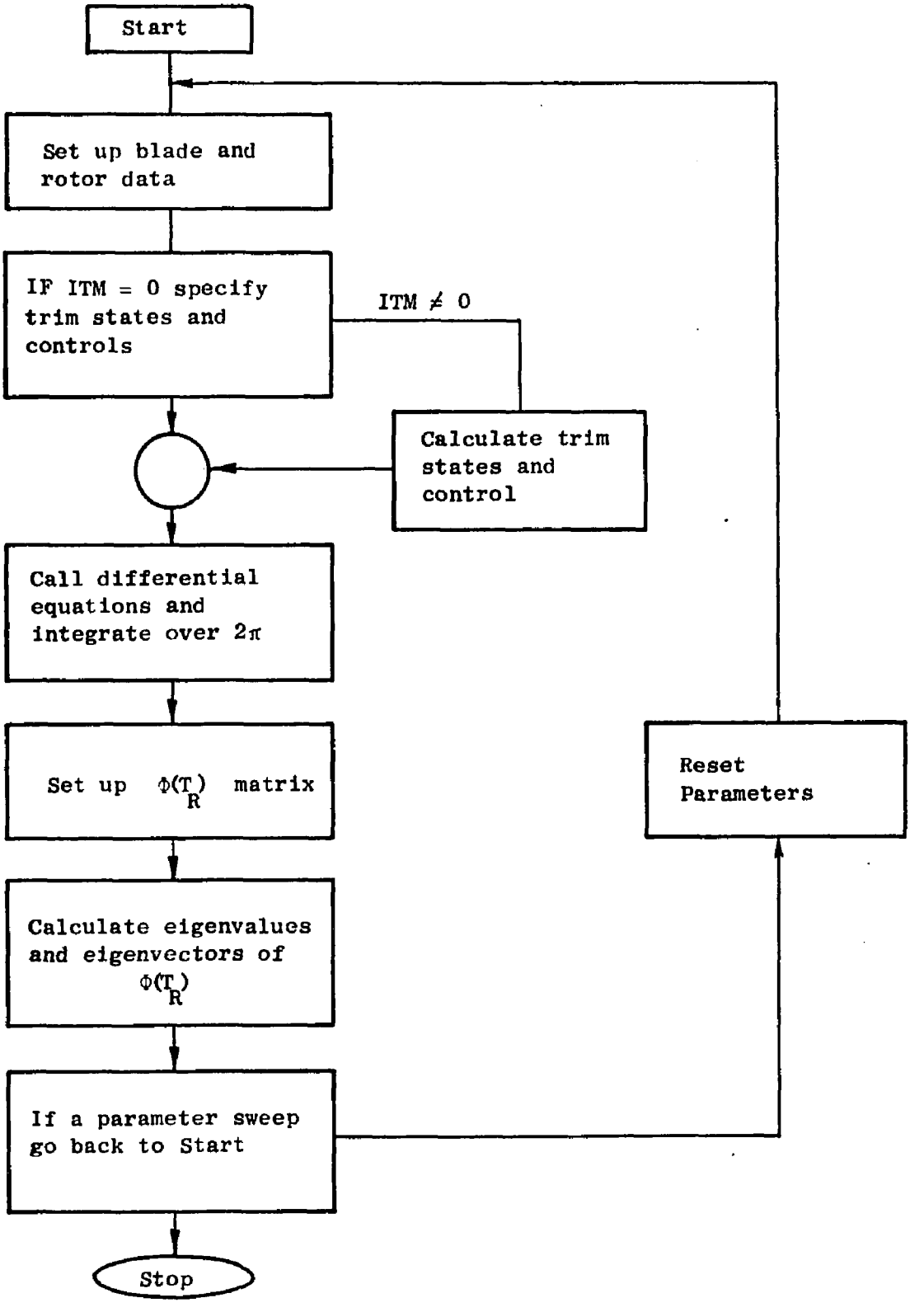

Fig. D-1. BLADE STABILITY PROGRAM SEQUENCING.

```
      IMPLICIT REAL*8 (A-H,O-Z)
      DIMENSION X(5),DX(5)
      REAL*8 A(50,50),BA(50,50),WR(50),WI(50),VEC(50,50)
      REAL*8 LAM,MU,MU2
      COMMON /BLAD/ B,B2,B3,B4,B5,F1,C1,C2,C3,C4,C5,C6,C7,C8,C9,C10,
     1              C11,C12,C13,C14,C15,C16,C17,C18,C19,BA,OMB2,
     2              BO,ZU,OMZ2,THC,CBK,PI,SOL,GAM,ALP,VK
      COMMON /CONT/ ICHECK,IPR,ICS,IVK
      COMMON /COEF/ CB,CDB,CZ,CDZ,CDBZ,CBDZ,CBZ,CIZ,CICZ,CIB,CIDB,
     1              CIBDB,CIZB,CIBDZ,CIDBZ,CBP,SBP,C2BP,S2BP,CDAM,CDAP

    1 FORMAT('1')
    2 FORMAT('1',3X,'MU = ',F4.2,/,4X,'----------')
    3 FORMAT('0INPUT MATRIX....',/)
    4 FORMAT(' ',5X,F12.8,5X,F12.8,5X,F12.8,5X,F12.8)
    5 FORMAT('0DET=',F12.8)
C*************************************************************
C  PROGRAM CONTROL *
C*******************
      NS = 4
      IA  = NS
      MST = NS+1
      PSIMX=6.2831E5D0
C  DP=6.DO FOR FOUR PLACE EIGENVALUE ACCURACY. GO TO DP=1.5D0 FOR MORE
C  ACCURACY IN THESE EIGENVALUES.
      DP  = 6.0D0/57.2957751D0
C  ICHECK=1 FOR CHECK OF EIGEN-SUBROUTINE---OTHERWISE ICHECK=0
      ICHECK=0
C   IPR=-1.....CHARACTERISTIC MULTIPLIERS ONLY
C   IPR= 0.....CHARACTERISTIC MULTIPLIERS AND NORMALIZED EIGENVECTORS
C   IPR=+1.....CHARACTERISTIC EXPONENTS AND NON-NORMALIZED EIGENVECTORS
C             (IF ICHECK=1)
      IPR= 0
C
C  CONTROL OF THE PARAMETRIC DO-LOOP
C   SO=INITIAL VALUE OF THE PARAMETER
C   SF=FINAL VALUE OF THE PARAMETER
C   SDEL=INCREMENT OF THE PARAMETER
C
      SDEL=.2D0
      SO = 0.0D0
      SF = 2.8DC
      ISO=SO/SDEL+.5
      ISF=SF/SDEL+.5
      IO = 1+ISO
      ISM= 1+ISF
C
C ITM=0 IF NO BETA-ZETA COUPLING(BETA-ZETA UNCOUPLING WHEN BO=THC=LAM=0)
      ITM=0
C  ICS=0 IF NO REVERSE FLOW EFFECT
       ICS = 1
C  IVK=0 IF CONSTANT INDUCED VELOCITY IS ASSUMED. IVK=1 IF TRIANGULAR
C  DISTRIBUTION IS ASSUMED.
      IVK = 0
C*************************************************************
C
C  BLADE AND ROTOR PARAMETERS
C
      B   = 1.DO
```

```
32          B2   = B*B
33          B3   = B*B2
34          B4   = B*B3
35          B5   =B*B4
36          CBK  =0.0D0
37          E    = 0.D0
38          EB     = 0.D0
39          EZ     = .15D0
40          GAM = 9.15D0
41          CM   = 25.4D0
42          CMB = 0.00D0
43          CMZ = 0.D0
44          ZO   = 0.D0
      C
      C
      C  CONVERSION OF UNITS
      C
45          BN   = GAM/8.D0
46          ZO   = ZO/57.2957751D0
      C
      C  CALCULATION OF CONSTANTS
      C
47          OMB2   = CMB*CMB+1.5D0*(EB/(1.D0-EB))
48          OMZ2   = CMZ*CMZ+1.5D0*(EZ/(1.D0-EZ))
      C
      C  BEGIN VARIATION OF SVAR
      C
49          DO 1000 IS=IO,ISM
50          SVAR = SDEL*(IS-1)
51          MU     = SVAR
52          MU2    = MU*MU
53          C17    = MU
54          C18    = MU2
55          IF (ITM .EQ. 0) WRITE (6,2) MU
56          EF   = 1.D0/6.283185D0
      C
      C CALCULATION OF TRIM STATES
      C
57          PI     = 3.141592D0
58          THRT   = 0.D0
59          THC    = 0.D0
60          BO     = 0.D0
61          ZO     = 0.D0
62          LAM    = 0.D0
63          VK     = 0.D0
64          CT     = 0.D0
65          IF (ITM .EQ. 0) GO TO 13
66          ALP    = 0.D0
67          RHO    = .002378D0
68          RR     = 25.6D0
69          SOL    = .12D0
70          THRT   = 18000.D0
71          TS     = CM*RR
72          RA     = PI*RR*RR
73          CT     = THRT/(RHO*RA*TS*TS)
74          CALL TRIM(LAM,CT)
      C
      C  CALCULATION OF COEFFICIENTS OF PERIODIC COEFFICIENTS
      C
75        13 C1   = (4.D0/3.D0)*B3
```

```
          C2  = MU*C1
          C3  = LAM*C1
          C4  = MU*LAM*B2
          C5  = LAM*B4
          C6  = MU2*B2
          C7  = MU*B4
          C8  = B4*2.D0
          C9  = .5D0*C7*LAM
          C10 = 2.D0*C2
          C11 = LAM*B3
          C12 = (8.D0/5.D0)*B5
          C13 = C2/2.D0
          C14 = 2.D0*C3
          C15 = C2*LAM
          C16 = C15/2.D0
          C19  = LAM
      C
      C  INTEGRATION OF EQNS
      C
           DO 5000 I=1,NS
           DO 4999 J=1,NS
 4999  X(J) =0.D0
          X(I) =1.D0
          X(5) = 0.D0
  100  CALL RUK(X,DP,MST)
          PSI = X(MST)
      C    PSID=57.2957751D0*X(MST)
      C    PRINT 30,PSID
      C    PRINT 31,(X(J),J=1,MST)
      C 30 FORMAT('0PSI:  (',D20.10,')')
   31  FORMAT(' ',5('(',D20.10,')'))
          IF (PSI-PSIMX) 100,101,101
      C
      C  END OF INTEGRATION AND SET UP THE C MATRIX
      C
    101  DO 4998 J=1,NS
          BA(I,J) = X(J)
 4998  A(J,I) = X(J)
 5000  CONTINUE
      C
      C  THE FOLLOWING STATEMENTS ARE CHECK CALCULATIONS AND
      C  ARE NORMALLY NOT USED
      C
      C     WRITE(6,3)
      C     DO 5001 NI=1,NS
      C5001 WRITE(6,4) (A(NI,NJ),NJ=1,NS)
      C     DET=A(1,1)*A(3,3)-A(3,1)*A(1,3)
      C     WRITE(6,5) DET
      C
      C  CALL THE EIGENVALUE SOLVER
      C
          CALL EIG(NS,IA,EF,A,WR,WI,VEC)
 1000  CONTINUE
          WRITE(6,1)
          RETURN
          END
```

```
      SUBROUTINE BLADE(X,DX,DP)
      IMPLICIT REAL*8 (A-H,O-Z)
      DIMENSION X(5),DX(5)
      DOUBLE PRECISION DP
      COMMON /BLAD/ B,B2,B3,B4,B5,F1,C1,C2,C3,C4,C5,C6,C7,C8,C9,C10,
     1              C11,C12,C13,C14,C15,C16,C17,C18,C19,BN,OMB2,
     2              BO,ZO,CMZ2,THC,CBK,PI,SOL,GAM,ALP,VK
      COMMON /CONT/ ICHECK,IPR,ICS,IVK
      COMMON /COEF/ CB,CDB,CZ,CDZ,CDBZ,CBDZ,CBZ,CIZ,CIDZ,CIB,CIDB,
     1              CIBDB,CIZB,CIBDZ,CIDBZ,CBP,SBP,C2BP,S2BP,CDAM,CDAP
C
C
C  CALCULATION OF PERIODIC COEFFICIENTS
C
C BETA TERMS
C
      CBP = DCOS(X(5))
      SBP = DSIN(X(5))
      C2BP= DCOS(2.DO*X(5))
      S2BP= DSIN(2.DO*X(5))
      CDAP = 1.DO+C2BP
      CDAM = 1.DO-C2BP
      CB   = C2*CBP+C6*S2BP+CBK*(B4+C10*SBP+C6*CDAM)
      CDB  = B4+C2*SBP
      CZ= 2.DO*C4*CBP+VK*(2.DO/3.DO)*C11*CDAP-THO*(C10*CBP+2.DO*C6*S2BP)
      CDZ  = C3+VK*(C5*CBP)-THO*(C8+C10*SBP)
      CDBZ = C2*CBP+CBK*(C8+C10*SBP)
      CBDZ =C2*CBP+CBK*(C8+C10*SBP)
      CBZ  = B4+C2*SBP+C6*CDAP+CBK*(C10*SBP+2.DO*C6*S2BP)
C
C ZETA TERMS
C
      CIZ  = THO*(2.DO*C4+VK*C16*CDAP)
      CIDZ = THO*(C3+VK*C5*CBP)
      CIB  = -4.DO*C4*CBP-CBK*(C3+(2.DO*C4+VK*C15))*SBP+VK*C5*CBP
     1    -VK*(C15*CDAP)+THO*(C2*CBP+C6*S2BP)
      CIDB =-C14-VK*2.DO*C5*CBP+THC*(B4+C2*SBP)
      CIBDB= -C10*CBP-CBK*(B4+C2*SBP)
      CIZB = -C14-CBK*(2.DO*C4*CBP+C16*CDAP)-VK*(2.DO*C4*CBP)
     1    +THO*(B4+C2*SBP+C6*CDAP)
      CIBDZ=-CBK*(C3+VK*C5*CBP)+THC*C2*CBP
      CIDBZ=CIBDZ
C
C CALCULATION OF COEFFICIENTS OF D.E.
C
C BETA D.E.
      IF (C17 .EQ. 0.DO) GO TO 10
      IF (X(5) .GE. PI .AND. ICS .NE. 0) CALL REVS(X,C17,C19)
   10 CFDB  = (CDB)*BN
      CFB   = 1.DO+CMB2+BN*(CB)
      CFDZ  = (2.DO+BN*(CBDZ*BO+CDZ))
      CFZ   = BN*(CZ+CBZ*BO)
C
C ZETA D.E.
      CZDZ  = BN*(CIDZ+CIBDZ*BO)
      CZZ   = OMZ2+BN*(CIZ+CIZB*BO)
      CZDB  = BN*(CIDB)-(2.DO-BN*CIBDB)*BO
      CZB   = BN*(CIB)
C
C BETA AND ZETA D.E.
```

```
      C
148         DX(1) = X(3)*DP
149         DX(2) = X(4)*DP
150         DX(3) = (-CFD8*X(3)-CFB*X(1)-CFDZ*X(4)-CFZ*X(2))*DP
151         DX(4) = (-CZDZ*X(4)-CZZ*X(2)-CZDB*X(3)-CZB*X(1))*DP
152         DX(5) =1.DD*DP
153         RETURN
154         END


155         SUBROUTINE RUK(XF,DP,N)
156         IMPLICIT REAL*8 (A-H,O-Z)
157         DOUBLE PRECISION DP
158         DIMENSION XF(5),UF(5),FF(5),DF(5)
159         CALL  BLADE(XF,DF,DP)
160         DO 101 I=1,N
161     101 UF(I)=XF(I)+0.5D0  *DF(I)
162         CALL BLADE(UF,FF,DP)
163         DO 102 I=1,N
164         DF(I)=DF(I)+2.D0  *FF(I)
165     102 UF(I)=XF(I)+0.5D0  *FF(I)
166         CALL BLADE(UF,FF,DP)
167         DO 103 I=1,N
168         DF(I)=DF(I)+2.D0  *FF(I)
169     103 UF(I)=XF(I)+FF(I)
170         CALL BLADE(UF,FF,DP)
171         DO 104 I=1,N
172     104 XF(I)=XF(I)+(DF(I)+FF(I))/6.0D0
173         RETURN
174         END
```

```
      SUBROUTINE TRIM(LAM,CT)
      IMPLICIT REAL*8 (A-H,O-Z)
      REAL*8 LAM
      COMMON /BLAD/ B,B2,B3,B4,B5,F1,C1,C2,C3,C4,C5,C6,C7,C8,C9,C10,
     1              C11,C12,C13,C14,C15,C16,C17,C18,C19,BN,OMB2,
     2              BO,ZO,OMZ2,THC,CBK,PI,SOL,GAM,ALP,VK
      COMMON /CONT/ ICHECK,IPR,ICS,IVK
    1 FORMAT(' ',1X,'LAMBDA=',F12.8)
    2 FORMAT(1X,'DERIVATIVE IS ZERO')
    3 FORMAT('1',2X,'TRIM STATE',/,3X,'----------',/,
     15X,'MU = ',F4.2,/,5X,'ALP= ',F12.8,/,5X,'CT = ',F12.8,/,
     25X,'THO= ',F12.8,/,5X,'LAM= ',F12.8,/,5X,'BO = ',F12.8,/,
     35X,'VK = ',F12.8,//)
      N=20
      ICT=0
      IF (C17 .NE. 0.DO) GO TO 9
      LAM = DSQRT(CT/2.DO)
      GO TO 55
    9 LAM = CT/(2.DO*C17)
   10 ROOT=DSQRT(C18+LAM*LAM)
      FLAM=LAM-.5DO*CT/ROOT
      DFLAM=1.DO+.5DO*(CT*LAM)/(ROOT**3)
      IF (DFLAM) 40,50,40
   40 ELAMN=LAM-FLAM/DFLAM
      IF (DABS(LAM-ELAMN) .LT. 1.D-6 .OR. ICT .GT .N) GO TO 55
      ICT=ICT+1
      LAM=ELAMN
      GO TO 10
   50 WRITE(6,2)
       GO TO 60
   55 TC    = (2.DO*CT)/(5.73DO*SOL)
      DNTHO=(1.DO/3.DO)+(C18/2.DO)
      THO   = (TC+.5DO*LAM)/DNTHO
      THOD =THO*57.29577951DO
      BO    =(GAM/2.DO)*(.25DO*THC*(1.DO+C18)-(LAM/3.DO))-OMB2
      BOD   = BO*57.29577951DO
      ALPD=ALP*57.29577951DO
      VK = IVK*((4.DO*C17)/(3.DO*LAM))/(1.2DO+C17/LAM)
      WRITE(6,3) C17,ALPD,CT,THOD,LAM,BOD,VK
   60 CONTINUE
      RETURN
      END
```

```
212          SUBROUTINE REVS(X,MU,LAM)
213          IMPLICIT REAL*8 (A-H,O-Z)
214          REAL*8 LAM,MU
215          DIMENSION X(5)
216          COMMON /BLAD/ B,B2,B3,B4,B5,F1,C1,C2,C3,C4,C5,C6,C7,C8,C9,C10,
            1              C11,C12,C13,C14,C15,C16,C17,C18,C19,BN,OMG2,
            2              BC,ZO,CMZ2,THO,CBK,PI,SOL,GAM,ALP,VK
217          COMMON /COEF/ CB,CDB,CZ,CDZ,CBDZ,CBDZ,CBZ,CIZ,CIDZ,CIB,CIDB,
            1              CIBDB,CIZB,CIBDZ,CIDBZ,CBP,SBP,C2BP,S2BP,CDAM,CDAP
218          SBP=DSIN(X(5))
219          SRVPS=DSIN(-1.DO/C17)
220          IF (C17 .LE. 1.DO) GO TO 10
221          IF (DABS(SBP) .LT. DABS(SRVPS)) GO TO 10
222          CB    = -CB
223          CDB   = -CDB
224          CZ    = -CZ
225          CDZ   = -CDZ
226          CBDZ  = -CBDZ
227          CDBZ  = -CDBZ
228          CBZ   = -CBZ
229          CIZ   = -CIZ
230          CIDZ  = -CIDZ
231          CIB   = -CIB
232          CIDB  = -CIDB
233          CIZB  = -CIZB
234          CIBDZ= -CIBDZ
235          CIDBZ= -CIDBZ
236          CIBDB=-CIBDB
237          GO TO 20
238       10 SB    = -MU*SBP
239          SB2   = SB*SB
240          SB3   = SB2*SB
241          SB4   = SB2*SB2
242          SB5   = SB2*SB3
             C
             C  AERODYNAMIC COEFFICIENTS IN THE REVERSED FLOW REGIME
             C
243          SC1   = (4.DO/3.DO)*SB3
244          SC2   = MU*SC1
245          SC3   = LAM*SC1
246          SC4   = MU*LAM*SB2
247          SC5   = LAM*SB4
248          SC6   = (MU*SB)**2
249          SC7   = MU*SB4
250          SC8   = SB4*2.DO
251          SC9   = .5DO*SC7*LAM
252          SC10  = 2.DO*SC2
253          SC11  = LAM*SB3
254          SC12  = (8.DO/5.DO)*SB5
255          SC13  = SC2/2.DO
256          SC14  = 2.DO*SC3
257          SC15  = SC2*LAM
258          SC16  = SC15/2.DO
             C
             C  FLAPPING COEFFICIENTS IN REVERSED FLOW REGIME
             C
259          SCB    = SC2*CBP+SC6*SBP+CBK*(SB4+SC10*SBP+SC6*CDAM)
260          SCDB   = SB4+SC2*SBP
261          SCZ    = 2.DO*SC4*CBP+VK*(2.DO/3.DO)*C11*CDAP
            1 -THO*(SC10*SBP+2.DO*SC6*S2BP)
```

```
262          SCDZ   = SC3+VK*(SC5*CBP)-THO*(SC8+SC10*SBP)
263          SCDBZ  = SC2*CBP+VK*(SC5*CBP)-THO*(SC8+SC10*SBP)
264          SCBDZ  =SC2*CBP+CBK*(SC8+SC10*SBP)
265          SCBZ   = SB4+SC2*SBP+SC6*CDAM+CBK*(SC10*SBP+2.D0*SC6*S2BP)
266          CB     = CB-SCB
267          CDB    = CDB-SCDB
268          CZ     = CZ-SCZ
269          CDZ    = CDZ-SCDZ
270          CDBZ   = CDBZ-SCDBZ
271          CBDZ   =CBDZ-SCBDZ
272          CBZ    = CBZ-SCBZ
         C
         C   ZETA COEFFICIENTS IN THE REVERSED FLOW REGIME
         C
273          SCIZ   = THO*(2.DO*SC4+VK*SC16*CDAP)
274          SCIDZ  = THO*(SC3+VK*SC5*CBP)
275          SCIB   = -4.D0*SC4*CBP-CBK*(SC3+(2.D0*SC4+VK*SC15))*SBP+VK*SC5*CBP
            1     -VK*(SC15*CDAP)+THO*(SC2*CBP+SC6*S2BP)
276          SCIDB =-SC14-VK*2.DO*SC5*CBP+THO*(SB4+SC2*SBP)
277          SIBDB= -SC10*CBP-CBK*(SB4+SC2*SBP)
278          SCIZB = -SC14-CBK*(2.DO*SC4*CBP+SC16*CDAP)-VK*(2.DO*SC4*CBP)
            1     +THO*(SB4+SC2*SBP+SC6*CDAP)
279          SIBDZ=-CBK*(SC3+VK*SC5*CBP)+THO*SC2*CBP
280          SICBZ=SIBDZ
281          CIZ    = CIZ-SCIZ
282          CIDZ   = CIDZ-SCIDZ
283          CIB    = CIB-SCIB
284          CIDB   = CIDB-SCIDB
285          CIBDB= CIBCB-SIBDB
286          CIZB = CIZB-SCIZB
287          CIBDZ= CIBCZ-SIBDZ
288          CIDBZ=CIBDZ
289       20 RETURN
290          END
```

Appendix E

LISTING OF OPTSYS

The following listing is included to complete the discussions of Chapters 3, 4, and 5 with the actual implementation of those chapters. The eigenvalue-eigenvector routine is the same as that used for the Floquet stability analysis.

The subroutines for determining the RPM and RRM are not included, but their implementation is discussed in Chapter 3.

```
      IMPLICIT REAL*8(A-H,O-Z)
C THE FOLLOWING DIMENSIONS ARE ORDER 2N
      DIMENSION A(20,20),RM(20,20),WR(20),WI(20),X(20,20),PRO(20,20),
     1CWR(10),CWI(10),ICNT(20),D(20),INT(20)
C THE FOLLOWING DIMENSIONS ARE OF ORDER N
      DIMENSION BA(10,10),ACL(10,10),SC(10,10),GN(10,10),Q(10,10)
C THE FOLLOWING ARE THE DIMENSIONS FOR THE ESTIMATION SOLUTION AND
C  ARE ARE OF DIMENSION NXNO OR NOXN
      DIMENSION  HO(6,10),FBGE(10,6),RC(6,6),RCI(6,6)
C THE FOLLOWING ARE THE DIMENSIONS OF THE CONTROL SOLUTION AND
C  ARE OF DIMENSION NXNC OR NCXN
      DIMENSION B(2,2),BI(2,2),G(10,2),FBGC(2,10)
C     DIMENSION GM(10,10)
      REAL*4 FMT(20)
C
C***OUTPUT OPTIONS
C---IOL=1 IF THE OPEN LOOP EIGENSYSTEM IS DESIRED-- OTHERWISE IOL=0
C---IE =1 IF THE EIGENVALUES AND EIGENVECTORS OF THE OPEN AND CLOSED
C         LOOP SYSTEM ARE DESIRED
C---IQ=1 IF THE RMS VALUES OF THE CONTROL AND STATE RESPONSES IN
C   THE PRESENCE OF STATE NOISE ARE TO BE FOUND
C---INQ=1 IF THE RMS VALUES OF THE CONTROL AND STATE RESPONSES IN
C         THE PRESENCE OF STATE AND MEASUREMENT NOISE ARE TO BE
C         DETERMINED
      INQ  =  0
      IOL  =  1
      IE   = 1
      IQ   =  0
C***  ORDER OF THE SYSTEM DYNAMICS
C     (NOTE:THE DIMENSIONS OF THE SYSTEM DYNAMICS,CONTROL,
C           MEASUREMENT,AND COST MATRICES MUST BE SPECIFIED
C           IN THE DIMENSION STATEMENTS ABOVE)
      NS = 10
      M = 2*NS
      MH = NS
      N  = M
C***ORDER OF THE CONTROL SYSTEM
C----NC = NUMBER OF SEPARATE CONTROLS
      NC = 2
      NCC = NC
C***ORDER OF THE MEASUREMENT SYSTEM
C     (NOTE:IF ONLY THE CONTROL PROBLEM IS TO BE SOLVED THEN NO=0)
C----NO=NUMBER OF MEASUREMENTS
C----NG=NUMBER OF INDEPENDENT STATE NOISE SOURCES
      NO = 0
      NG = 10
C*****************************************
      NOB = 0
C***INITALIZATION OF MATRICES
      DO  5 I = 1,NS
      DO  5 J = 1,NS
      ACL(I,J) = 0.D0
      SC(I,J) = 0.D0
    5 BA(I,J) = 0.D0
      DO 6 I = 1,NS
      DO 6 J = 1,NC
```

```
     6 G(I,J) = 0.D0
       DO 7 I= 1,NC
       DO 7 J = 1,NC
       B(I,J) = 0.D0
     7 BI(I,J) = 0.D0
       DO  8 I = 1,NG
       DO  8 J = 1,NG
     8 Q(I,J) = 0.D0
       IF (NO.EQ.0) GO TO 11
       DO 9 I = 1,NO
       DO 9 J = 1,NO
       RC(I,J) = 0.D0
     9 RCI(I,J) = 0.D0
       DO 10 I = 1,NO
       DO 10 J = 1,MH
    10 HO(I,J) = 0.D0
C***OPEN LOOP DYNAMICS MATRIX
    11       BN = 5.D0
             BK = 0.D0
             CDRG  = 0.02D0
             CHD = 18.25D0/12.D0
             R   = 31.0D0
             EB=0.05D0
             EN = 93.D0*R*BN
             RS  = R*R
             RHO = .002378D0
             PI  = 3.1416D0
             TPI = 6.2832D0
             ALC = 5.73
             RALC= RHO*ALC
             AREA= PI*RS
             VPI = 46500.D0
             VRI = 12400.D0
             BFI = 1800.D0
             GAM = 10.62D0
             GP  = GAM/8.D0
             WT  = 17500.D0
             THRT= WT
             VM  = WT/32.2D0
             TS  = 660.D0
             CM  =TS/R
             OMS = OM*OM
             H   = 6.62D0
             OMB = 0.05D0
             OMEB = 1.5D0*(EB/(1.D0-EB))
             OMBS = OMB+OMEB
C  SPECIFICATION OF FLIGHT CONDTION
       ALP = 0.D0
       RMU=0.COCO
       RMU2=RMU*RMU
       VFT = RMU*TS
       VKT = VFT/1.689D0
C  CALCULATION OF INFLOW RATIO,LAMBDA, AND COLLECTIVE
       SOL = BN*CHD/(PI*R)
       TCT = THRT/(RHO*AREA*TS*TS)
       CTF = 2.D0*TCT/(ALC*SOL)
       NT=20
       ICT=0
       IF (RMU .NE. 0.D0) GO TO 12
       VLAM = DSQRT(TCT/2.D0)
```

```
      GO TO 20
   12 VLAM = TCT/(2.D0*RMU)
   13 ROOT=DSQRT(RMU2+VLAM*VLAM)
      FLAM=VLAM-.5D0*TCT/ROOT
      DFLAM=1.D0+.5D0*(TCT*VLAM)/(ROOT**3)
      IF (DFLAM) 14,15,14
   14 ELAMN=VLAM-FLAM/DFLAM
      IF (DABS(VLAM-ELAMN) .LT. 1.D-6 .OR. ICT .GT .NT) GO TO 20
      ICT=ICT+1
      VLAM=ELAMN
      GO TO 13
   15 WRITE(6,1095)
 1095 FORMAT(' ','THE DERIVATIVE IS ZERO')
       GO TO 19
   20 DNTHO=(1.D0/3.D0)+(RMU2/2.D0)
      THO  =(CTF+.5D0*VLAM)/DNTHO
      THOD =THO*57.2957751D0
      BO   =((GAM/2.D0)*(.25D0*THO*(1.D0+RMU2)-(VLAM/3.D0)))/(OMBS+1.
      BOD  = BO*57.2957751D0
      ALPD=ALP*57.2957751D0
      THOF =((2.666D0)*THO-2.D0*VLAM)*GP
      WRITE(6,48) RMU,VKT,TCT,CTF,VLAM,THOD,BOD
   19 CONTINUE
   48 FORMAT('1',2X,'MU = ',F4.2,4X,'VELOCITY = ',F8.3,1X,'KNOTS',//,
     14X,'ROTOR CT=',F12.7,9X,'2CT/AS=',F12.7,9X,'INFLOW RATIO=',
     2F12.7,//,5X,'TRIM COLLECTIVE=',F12.7,1X,'DEGS.',9X,'CONING=',
     3F12.7,1X,'DEGS.',/,'*****************************************
     4**********************************************************',
C  ROTOR DEPENDENT COEFFICIENTS
           EL = .5D0*RHO*ALC*BN*CHO*(R**2)
           EM = EL*(R**2)
           HB = H/R
           VPIP=VPI*(1.D0+EB*EN/(2.D0*VPI))
           VRIP=VRI*(1.D0+EB*EN/(2.D0*VRI))
C  TRIM DEPENDENT COEFFICIENTS
           F1 = (CDRG/(2.D0*ALC)+(BO*BO)/4.D0+THO*VLAM/2.D0)
           F2 = 1.5D0*BO*(THO/2.D0-VLAM)
           F3 = THO/6.D0-VLAM/2.D0
           F4 = VLAM/4.D0
           F5 = BO/6.D0
           F6 = HB*BC+EB
           F7 = THO-VLAM
           F8 = BO/4.D0
C  FUSELAGE MOMENT COEFFICIENTS
      CVR = +THRT/(VM*OM*TS)
      GPR = +32.2/(OM*TS)
      C1  = (THRT*H)/(OMS*VPIP)
      C2  = (BN/2.D0)*(BFI/VPIP)*OMB
           CTHE=C1+C2
           CPHI =(VPIP/VRIP)*CTHE
           CM1 = EB*(EN/2.D0)-HB*EM*F4
           CM2 = (EM/6.D0)*F6
           CM3 = HB*EM*F3+EB*EN
           CM4 = HB*EM*F2+EB*(EM/2.D0)*F7
           CM5 = +HB*EM*F1+EB*EM*F8
C  FUSELAGE FORCE COEFFICIENTS
           CF1 = EL*F4/VM
           CF2 = EL*F5/VM
           CF3 = EL*F3/VM
           CF4 = EL*F1/VM
```

```
              CF5 = EL*F2/VM
              OMFS= OMBS+GP*BK
C***SYSTEM DYNAMICS MATRIX
C---ROTOR DYNAMICS
              BA(1,3) = 1.D0
              BA(2,4) = 1.D0
              BA(3,1)= -OMFS
              BA(3,2) = -GP
              BA(3,3) = -GP
              BA(3,4)=-2.D0
              BA(3,6) = 0.D0
              BA(3,7) = -GP*(1.D0+1.333D0*HB*B0)
              BA(3,8) = -(2.D0*(1.D0+OMEB)+HB*THOF)
              BA(3,9) = 1.3333D0*GP*B0
              BA(3,10) =-THOF
              BA(4,1) = GP
              BA(4,2) = -OMFS
              BA(4,3)= 2.D0
              BA(4,4)=-GP
              BA(4,5) =  0.D0
              BA(4,6) = 0.D0
              BA(4,7) = 2.D0*(1.D0+OMEB)+HB*THOF
              BA(4,8) = -GP*(1.D0+1.333D0*HB*B0)
              BA(4,9) = -THOF
              BA(4,10)= -BA(3,9)
              BA(5,7) = 1.D0
              BA(6,8) = 1.D0
C---FUSELAGE DYNAMICS
              BA(7,1) = CTHE+CM1/VPIP
              BA(7,2) = -CM2/VPIP
              BA(7,3) =  BA(7,2)
              BA(7,4) = -CM3/VPIP
              BA(7,7) = -(CM2+HB*CM5)/VPIP
              BA(7,8) = -(CM3+HB*CM4)/VPIP
              BA(7,9) =  CM5/VPIP
              BA(7,10)= -CM4/VPIP
              BA(8,1) =  CM2/VRIP
              BA(8,2) = CPHI+CM1/VRIP
              BA(8,3) = CM3/VRIP
              BA(8,4) =-BA(8,1)
              BA(8,7) = (CM3+HB*CM4)/VRIP
              BA(8,8) = -(CM2+HB*CM5)/VRIP
              BA(8,9) = -CM4/VRIP
              BA(8,10)=-CM5/VRIP
              BA(9,1) = -CVR+CF1
              BA(9,2)= CF2
              BA(9,3) = CF2
              BA(9,4) = CF3
              BA(9,5) = -GPR
              BA(9,7)  = CF2+H*CF4
              BA(9,8)  = CF3+H*CF5
              BA(9,9)  = -CF4
              BA(9,10) = CF5
              BA(10,1) = +CF2
              BA(10,2) =CVR-CF1
              BA(10,3) = +CF3
              BA(10,4) = -CF2
              BA(10,6) = GPR
              BA(10,7) = CF3+H*CF5
              BA(10,8) = -CF2-H*CF4
```

```
            BA(10,9) = -CF5
            BA(10,10)= -CF4
C***CONTROL DISTRIBUTION MATRIX
            G(3,1) = -GP*(1.D0+.5D0*RMU2)
            G(3,2) = 0.D0
            G(4,1) = C.D0
            G(4,2) = -GP*(1.D0+1.5D0*RMU2)
            G(7,1) = -CM2/VPIP
            G(7,2) = HB*EM*F4/VPIP
            G(8,1) = -HB*EM*F4/VRIP
            G(8,2) = -CM2/VRIP
            G(9,1) = EL*F5/VM
            G(9,2) = -EL*F4/VM
            G(10,1)= -G(9,2)
            G(10,2)= +G(9,1)
C SIMULTANEOUS SOLUTION FOR ROTOR AND FUSELAGE ACCELERATIONS
            CB1 = 1.D0+1.5D0*HB*B0+OMEB
            OF1 = (EB*EN/(2.D0*VPIP))
            OF2 = (VPIP/VRIP)*OF1
            DENT = 1.DC-OF1*CB1
            DENP = 1.D0-OF2*CB1
            DO 491 J = 1,NS
            PRO(3,J) = (BA(3,J)-CB1*BA(7,J))/DENT
            PRC(4,J) = (BA(4,J)-CB1*BA(8,J))/DENP
            PRO(7,J) = (-OF1*BA(3,J)+BA(7,J))/DENT
            PRO(8,J) = (-OF2*BA(4,J)+BA(8,J))/DENP
            BA(3,J) = PRO(3,J)
            BA(4,J) = PRO(4,J)
            BA(7,J) = PRO(7,J)
  491       BA(8,J) = PRO(8,J)
            DO 493 I = 1,2
            PRC(3,I) = (G(3,I)-CB1*G(7,I))/DENT
            PRO(4,I) = (G(4,I)-CB1*G(8,I))/DENP
            PRO(7,I) = (-OF1*G(3,I)+G(7,I))/DENT
            PRC(8,I) = (-OF2*G(4,I)+G(8,I))/DENP
            G(3,I) = PRO(3,I)
            G(4,I) = PRO(4,I)
            G(7,I) = PRO(7,I)
  493       G(8,I) = PRO(8,I)
C***STATE COST MATRIX
            SC(1,1) = 0.D0
            SC(2,2) = 0.D0
            SC(5,5) = 1.D0
            SC(6,6) = 1.D0
            SC(9,9) = 1.D0
            SC(10,10) = 1.D0
C***STATE NOISE COVARIANCE
            Q(3,3) = .C0D0
            Q(4,4) = .01D0
C***THE CONTROL COST MATRIX....G(BINVERSE)*GT
C---BINVERSE
       DO 21 I= 1,NC
    21 B(I,I) = 1.D0
       DO 23 I = 1,NC
    23 BI(I,I) = 1/B(I,I)
     3 FORMAT(' ','OPEN LOOP DYNAMICS MATRIX....',4X,'OMBS=',
      1F12.5,3X,'C1=',F12.5,3X,'C2=',F12.5,/)
     4 FORMAT(' ',2X,F8.5,2X,F8.5,2X,F8.5,2X,F8.5,2X,F8.5,2X,F8.5,
      12X,F8.5,2X,F8.5,2X,F8.5,2X,F8.5)
       WRITE(6,3) OMBS,C1,C2
```

```
      DO 5001 NI=1,NS
 5001 WRITE(6,4) (BA(NI,NJ),NJ=1,NS)
           WRITE(6,7004)
 7004 FORMAT('0','THE CONTROL DISTRIBUTION MATRIX IS....',//)
           DO 7005 NI=1,NS
 7005 WRITE(6,7006) (G(NI,NJ),NJ=1,NC)
 7006 FORMAT(2X,F15.8,3X,F15.8)
      WRITE(6,3041)
 3041 FORMAT('0','THE STATE COST MATRIX IS....',//)
      CALL RAPRNT(NS,NS,NS,10,SC,4,'(10(1X,F9.5))')
      WRITE(6,3042)
 3042 FORMAT('0','THE CONTROL COST MATRIX IS....',//)
      CALL RAPRNT(NC,NC,NC,2,BI,3,'(2(1X,F9.5))')
C***EIGENSYSTEM OF THE OPEN LOOP DYNAMICS
      IF (IOL.EQ.0) GO TO 500
      DO 51 I = 1,NS
      DO 51 J = 1,NS
   51 GN(I,J) = BA(I,J)
C*****************************************
      CALL BALANC (10,NS,GN,LOW,IHIGH,D)
      CALL ELMHES (10,NS,LOW,IHIGH,GN,INT)
      CALL HQR2 (10,NS,LOW,IHIGH,GN,CWR,CWI,ACL,ICNT,&46)
      CALL ELMBAK (10,LOW,IHIGH,NS,GN,INT,ACL)
      CALL BALBAK (10,NS,LOW,IHIGH,NS,D,ACL)
C*****************************************
      WRITE(6,2030)
 2030 FORMAT('1','OPEN LOOP EIGENVALUES AND EIGENVECTORS.......')
C     WRITE(6,2040)
      IF(IOL.NE.0) CALL CNORM(CWR,CWI,ACL,NS)
C2040 FORMAT('0OPEN LOOP EIGENVECTORS . . .')
C     CALL RAPRNT(NS,NS,NS,5,X,4,'(5(1X,F15.8))')
C***CALCULATION OF CONTROL GAINS:FORMATION OF CONTROL HAMILTONIAN
C
C    **                          **          ***F AND FT ARE THE OPEN LOOP
C    *                            *             DYNAMICS MATRIX AND TRANSPOSE
C    *     -F          GM*BI*GMT* *          ***BI IS NCXNC CONTROL WEIGHTING
C    *                            *             MATRIX
C    *                            *          ***A IS THE NSXNS STATE WEIGHTING
C    *                            *             MATRIX
C    *       A             FT     *
C    **                          **          ***GM IS THE NSXNC CONTROL
C                                               DISTRIBUTION MATRIX
C*****************************************************************
      IF (NCC.EQ. 0) GO TO 1801
  500 CONTINUE
      DO 24 I = 1,NC
      DO 24 J = 1,MH
      PRO(I,J) = 0.D0
      DO 24 K = 1,NC
   24 PRO(I,J) = PRO(I,J) + BI(I,K)*G(J,K)
      DO 25 I = 1,MH
      DO 25 J = 1,MH
      RM(I,J+MH)=0.D0
      DO 25 K = 1,NC
   25 RM(I,J+MH) = RM(I,J+MH) + G(I,K)*PRO(K,J)
   50 CONTINUE
C***2NX2N HAMILTONIAN MATRIX***************
C---DIAGONAL BLOCKS---M11 AND M22
      DO 26 I = 1,MH
      DO 26 J = 1,MH
```

```
      RM(I,J) = -BA(I,J)
      RM(I+MH,J+MH) = BA(J,I)
C---M21 BLOCK
   26 RM(I+MH,J) =+SC(I,J)
C---M12 BLOCK IS DEFINED IN LINE 25 ABOVE
C  26 RM(I,J+MH) =CC(I,J)
      DO 27 I = 1,M
      DO 27 J = 1,M
   27 A(I,J) = RM(I,J)
C     WRITE(6,1020)
C1020 FORMAT('1','2NX2N HAMILTONIAN MATRIX.....')
C     CALL RAPRNT(20,N,N,10,A,4,'(10(1X,1PD12.5))')
C**************************************
      CALL BALANC (20,N,A,LOW,IHIGH,D)
      CALL ELMHES (20,N,LOW,IHIGH,A,INT)
      CALL HQR2 (20,N,LOW,IHIGH,A,WR,WI,X,ICNT,&46)
      CALL ELMBAK (20,LOW,IHIGH,N,A,INT,X)
      CALL BALBAK (20,N,LOW,IHIGH,N,D,X)
C**************************************
      IF (NOB.EQ.0) WRITE(6,9119)
      IF (NOB.NE.0) WRITE(6,9120)
 9119 FORMAT('1','EIGENSYSTEM OF THE OPTIMAL CLOSED LOOP SYSTEM....')
 9120 FORMAT('1','EIGENSYSTEM OF THE OPTIMAL ESTIMATOR.....')
C     WRITE(6,1030) (WR(I),WI(I),ICNT(I),I=1,N)
C1030 FORMAT('1','EIGENVALUES . . .'/(' ',F15.8,1X,F15.8,1X,I3))
C     WRITE(6,1040)
C1040 FORMAT('CEIGENVECTORS . . .')
C     CALL RAPRNT(M,N,N,5,X,4,'(5(1X,F15.8))')
      CALL RGAIN(M,NS,NC,NOB,IE,RM,WR,WI,X,GN)
      IF (NOB.NE. 0) GO TO 60
      WRITE(6,1401)
 1401 FORMAT('1','THE RICATTI GAIN MATRIX')
      CALL RAPRNT(MH,MH,MH,5,GN,4,'(5(1X,F15.8))')
C  CALCULATION OF FEEDBACK GAIN
C
C***FEEDBACK GAINS---U = -(BINVERSE)*GT*GN
C---CALCULATE GT
      DO 800 I = 1,NC
      DO 800 J = 1,MH
      PRO(I,J) = 0.D0
      DO 800 K = 1,MH
  800 PRO(I,J) = PRO(I,J) +G(K,I)*GN(K,J)
      DO 801 I = 1,NC
      DO 801 J = 1,NS
      FBGC(I,J) = 0.D0
      DO 801 K = 1,NC
  801 FBGC(I,J) = FBGC(I,J) +BI(I,K)*PRO(K,J)
C***THE OPTIMUM FEEDBACK CONTROL GAINS
      DO 802 I = 1,NC
      DO 802 J = 1,NS
  802 FBGC(I,J) = -FBGC(I,J)
      WRITE(6,977)
  977 FORMAT(' ','THE CONTROL GAINS ARE:')
      DO 968 I = 1,NC
  968 WRITE(6,978) (FBGC(I,J),J = 1,NS)
  978 FORMAT(' ',4X,F15.8,4X,F15.8,4X,F15.8,4X,F15.8,4X,F15.8,/,4X,
     1F15.8,4X,F15.8,4X,F15.8,4X,F15.8,4X,F15.8,//)
C***THE CLOSED LOOP DYNAMICS MATRIX
      DO 150 I = 1,NS
      DO 150 J = 1,NS
```

```
      PRO(I,J) = 0.DO
      DO 150 K = 1,NC
  150 PRO(I,J) = PRO(I,J)+G(I,K)*FBGC(K,J)
      DO 160 I = 1,NS
      DO 160 J = 1,NS
  160 ACL(I,J)=BA(I,J)+PRO(I,J)
      WRITE(6,170)
  170 FORMAT(' ','THE CLOSED LOOP DYNAMICS MATRIX IS..',//)
      DO 180 I = 1,NS
  180 WRITE(6,4) (ACL(I,J),J = 1,NS)
      NOB=NO
      IF(NOB.EQ.0) GO TO 388
C***CALCULATION OF FILTER GAINS:FORMATION OF ESTIMATION HAMILTONIAN
C
C    **                          **          ***F AND FT ARE SAME AS FOR
C    *                            *           CONTROL HAMILTONIAN
C    *     F          -GM*Q*GMT*              ***Q IS NGXNG STATE DISTURBANCE
C    *                            *           RCOVARIANCE
C    *                            *          ***R IS NOXNO MEASUREMENT NOIS
C    *                            *           RCOVARIANCE
C    * -HUT*RIN*HO       -FT      *          ***HO IS NOXNS MEASUREMENT MAT
C    **                          **          ***GM IS NSXNG STATE DISTURBAN
C                                             DISTRIBUTION MATRIX
C*****************************************************************
 1801 CONTINUE
      DO 28 I = 1,NO
      DO 28 J = 1,NO
      RC(I,J) = 0.DO
   28 RCI(I,J) = 0.DO
C**COVARIANCE ON THE NOXNO DIAGONAL
      RC(1,1) = 1.D-06
      RC(2,2) = 1.D-06
      RC(3,3) = 1.D-02
      RC(4,4)  =1.D-02
      RC(5,5) = 1.D-02
      RC(6,6) = 1.D-02
      DO 29 I = 1,NO
   29 RCI(I,I) = 1/RC(I,I)
C*** THE MEASUREMENT MATRIX
      HO(1,1) = 1.DO
      HO(2,2) = 1.DO
      HO(3,5) = 1.DO
      HO(4,6) = 1.DO
      HO(5,7)=1.DO
      HO(6,8) = 1.DO
      WRITE(6,3056)
 3056 FORMAT('1','THE MEASUREMENT SCALING MATRIX IS...')
      DO 3057 I =1,NO
 3057 WRITE(6,4) (HO(I,J),J=1,NS)
      WRITE(6,3058)
 3058 FORMAT('0','THE MEASUREMENT COVARIANCE IS...')
      DO 3059 I = 1,NO
 3059 WRITE(6,3060) (RC(I,J),J=1,NO)
 3060 FORMAT('0',2X,(6F14.7))
C**(HOT*RIN*HO===>SC
      DO 30 I = 1,NO
      DO 30 J = 1,MH
      PRO(I,J) = 0.DO
      DO 30 K = 1,NO
   30 PRO(I,J) = PRO(I,J)+RCI(I,K)*HO(K,J)
```

```
      DO 31 I = 1,MH
      DO 31 J = 1,MH
      SC(I,J) = 0.DO
      DO 31 K = 1,NO
   31 SC(I,J) = SC(I,J) + HO(K,I)*PRO(K,J)
C***GM*Q*GMT===>CC
C     Q(1,1) = 1.DO
C     Q(2,2) = 1.DO
C     Q(3,3) = 1.DO
C     Q(4,4) = 0.DO
C     DO 34 I = 1,MH
C     DO 34 J = 1,NG
C  34 GM(I,J)=0.DO
C     DO 45 I=1,MH
C  45 GM(I,I) = 1.DO
C     DO 35 I = 1,NG
C     DO 35 J = 1,MH
C     PRO(I,J) = 0.DO
C     DO 35 K = 1,NG
C  35 PRO(I,J) = PRO(I,J)+Q(I,K)*GM(J,K)
C     DO 36 I = 1,MH
C     DO 36 J = 1,MH
C     RM(I,J+MH) = 0.DO
C     DO 36 K = 1,NG
C  36 RM(I,J+MH) = RM(I,J+MH)+GM(I,K)*PRO(K,J)
      DO 37 I = 1,MH
      DO 37 J = 1,MH
      BA(I,J)=-BA(I,J)
      SC(I,J) = -SC(I,J)
   37 RM(I,J+MH) = -Q(I,J)
      NC = NC
      GO TO 50
C***GO BACK TO 50 TO SET UP THE FILTER HAMILTONIAN
C    AND CALCULATE THE FILTER GAINS
   60 CONTINUE
      DO 61 I= 1,MH
      DO 61 J= 1,NO
      PRO(I,J) = 0.DO
      DO 61 K = 1,NO
   61 PRO(I,J) = PRO(I,J)+HO(K,I)*RCI(K,J)
      DO 62 I = 1,MH
      DO 62 J = 1,NC
      FBGE(I,J) =0.DO
      DO 62 K = 1,MH
   62 FBGE(I,J) = FBGE(I,J)+GN(I,K)*PRO(K,J)
      WRITE(6,1018)
 1018 FORMAT('1','FILTER STEADY STATE GAINS')
      DO 63 I = 1,MH
   63 WRITE(6,1019) (FBGE(I,J),J =1,NO)
 1019 FORMAT(' ',2X,6F15.8)
      IF(INQ.EQ.0) GO TO 388
      DO 65 I = 1,NO
      DO 65 J = 1,MH
      PRO(I,J) = 0.DO
      DO 65 K = 1,NG
   65 PRO(I,J) = PRO(I,J)+RC(I,K)*FBGE(J,K)
      DO 66 I = 1,MH
      DO 66 J = 1,MH
      Q(I,J) = 0.DO
      DO 66 K = 1,NO
```

```
   66 Q(I,J) = Q(I,J)+FBGE(I,K)*PRO(K,J)
  388 CONTINUE
C***THE RMS STATE AND CONTROL RESPONSES
      IF (IQ.EQ.0) GO TO 389
      CALL SCCV(NS,ACL,Q)
      NC = NCC
      DO 190 I = 1,NS
      DO 190 J = 1,NC
      PRO(I,J) = 0.D0
      DO 190 K = 1,NS
  190 PRO(I,J) = PRO(I,J)+Q(I,K)*FBGC(J,K)
      DO 200 I = 1,NC
      DO 200 J = 1,NC
      SC(I,J) = 0.D0
      DO 200 K = 1,NS
  200 SC(I,J) =SC(I,J)+FBGC(I,K)*PRO(K,J)
      IF(INQ.EQ.0) GO TO 503
      WRITE(6,1501)
 1501 FORMAT('0','THE COVARIANCE OF THE ESTIMATION ERROR')
      CALL RAPRNT(MH,MH,MH,5,GN,4,'(5(1X,F15.8))')
      WRITE(6,220)
  220 FORMAT('1','THE COVARIANCE OF THE ESTIMATE..',//)
      CALL RAPRNT(MH,MH,MH,5,Q,4,'(5(1X,F15.8))')
      DO 67 I = 1,MH
      DO 67 J = 1,MH
   67 Q(I,J) = GN(I,J)+Q(I,J)
  503 CONTINUE
      WRITE(6,210)
  210 FORMAT('0','THE STATE COVARIANCE MATRIX..',//)
      CALL RAPRNT(MH,MH,MH,5,Q,4,'(5(1X,F15.8))')
      WRITE(6,221)
  221 FORMAT('1',//,1X,'THE CONTROL COVARIANCE',//)
      DO 230 I = 1,NC
  230 WRITE(6,231) (SC(I,J),J=1,NC)
  231 FORMAT(' ',4X,F15.8,4X,F15.8)
      DO 240 I = 1,NS
  240 Q(I,I) = DSQRT(Q(I,I))*57.293D0
      DO 250 I =1,NC
  250 SC(I,I) = DSQRT(SC(I,I))*57.293D0
      WRITE(6,262)
  262 FORMAT('0',1X,'STATE RMS RESPONSE',20X,'CONTROL RMS RESPONSE',
     1//)
      DO 270 I = 1,NC
  270 WRITE(6,272) Q(I,I),SC(I,I)
  272 FORMAT(' ',F15.8,25X,F15.8)
      NC1=NC+1
      DO 275 I=NC1,NS
  275 WRITE(6,276) Q(I,I)
  276 FORMAT(1X,F15.8)
      GO TO 389
   46 WRITE(6,1060)
 1060 FORMAT('0FAILURE IN HQR2')
  389 WRITE(6,4001)
 4001 FORMAT('1')
      STOP
      END
      SUBROUTINE RAPRNT(NMAX,M,N,L,A,IDIM,FMT)
      REAL*8 A(NMAX,N)
      DIMENSION FMT(IDIM)
      NU=L
```

```
      DO 20 NL=1,N,L
      IF (NU.GT.N) NU=N
      DO 10 I=1,M
   10 WRITE(6,FMT)(A(I,J),J=NL,NU)
      WRITE(6,100)
  100 FORMAT(' ')
   20 NU=NU+L
      RETURN
      END
      SUBROUTINE CDIV (A,B,C,D,E,F)
      IMPLICIT REAL*8 (A-H,O-Z)
C
C     THIS SUBROUTINE COMPUTES THE COMPLEX DIVISION
C
C             E + F*I = (A + B*I)/(C + D*I)
C
      T=C*C+D*C
      E=(A*C+B*D)/T
      F=(B*C-A*D)/T
C
      RETURN
      END
      SUBROUTINE HQR2 (NM,N,LOW,HI,H,WR,WI,F,ICNT,*)
C
      IMPLICIT REAL*8 (A-H,O-Z)
      DIMENSION H(NM,NM),WR(NM),WI(NM),F(NM,NM),ICNT(NM)
      INTEGER HI, HI1, EN, EL
      REAL*8 IP,IV,MA(50),MB(50)
      DATA EPSM / Z3410000000000000 /
      LOGICAL LAST
C
      DO 101 I=1,N
      DO 9101 J=I,N
      F(I,J)=0.0D0
 9101 F(J,I)=0.0D0
  101 F(I,I)=1.0D0
C
      IF (N.GT.2)MA(3)=H(3,1)
      IF (N.LT.4) GO TO 9102
      DO 102 I=4,N
      MA(I)=H(I,I-2)
  102 MB(I)=H(I,I-3)
C
 9102 LOWM1=LOW-1
      HI1=HI+1
C
C
C
      IF (LOWM1.LT.1) GO TO 9103
      DO 103 I=1,LOWM1
      WR(I)=H(I,I)
      WI(I)=0.0D0
  103 ICNT(I)=0
C
 9103 IF (HI1.GT.N) GO TO 9104
      DO 104 I=HI1,N
      WR(I)=H(I,I)
      WI(I)=0.0D0
  104 ICNT(I)=0
C
```

```
 9104 EN=HI
      T=0.0D0

      ----- DETERMINE EIGENVALUE EN

  105 IF (EN.LT.LOW) GO TO 100

          ITS=0
          NA=EN-1
C
C         ----- SEARCH FOR SPLIT
C
  200     L=EN
  106     IF (L.EQ.LOW) GO TO 109
          IF (DABS(H(L,L-1)).LE.EPSM*(DABS(H(L-1,L-1))
     X    +DABS(H(L,L)))) GO TO 109
          L=L-1
          GO TO 106
C
C         ----- TEST FOR CONVERGENCE
C
  109     X=H(EN,EN)
          IF (L.EQ.EN) GO TO 110
          Y=H(NA,NA)
          W=H(EN,NA)*H(NA,EN)
          IF (L.EQ.NA) GO TO 111
          IF (ITS.EQ.30)RETURN1
C
C         ----- COMPUTE SHIFT
C
          IF (ITS.NE.10.AND.ITS.NE.20) GO TO 113
          T=T+X
          DO 112 I=LOW,EN
  112     H(I,I)=H(I,I)-X
          S=DABS(H(EN,NA))+DABS(H(NA,EN-2))
          Y=.75D0*S
          X=Y
          W=-0.4375D0*S*S
C
C         ----- QR ROTATION
C
  113     ITS=ITS+1
          EL=NA-L
          DO 114 MM=1,EL
             M=NA-MM
             Z=H(M,M)
             R=X-Z
             S=Y-Z
             P=(R*S-W)/H(M+1,M)+H(M,M+1)
             Q=H(M+1,M+1)-Z-R-S
             R=H(M+2,M+1)
             S=DABS(P)+DABS(Q)+DABS(R)
             P=P/S
             Q=Q/S
             R=R/S
             IF (M.EQ.L) GO TO 115
             IF (DABS(H(M,M-1))*(DABS(Q)+DABS(R)).LE.EPSM*DABS(P)
     X       *(DABS(H(M-1,M-1))+DABS(Z)+DABS(H(M+1,M+1))))
     X       GO TO 115
  114        CONTINUE
```

```
C
  115     MP2=M+2
          DO 116 I=MP2,EN
  116     H(I,I-2)=0.0D0
          MP3=M+3
          IF (EN.LT.MP3) GO TO 9117
          DO 117 I=MP3,EN
  117     H(I,I-3)=0.0D0
 9117     CONTINUE
C
          DO 118 K=M,NA
             LAST=K.EQ.NA
             IF (K.EQ.M) GO TO 119
             P=H(K,K-1)
             Q=H(K+1,K-1)
             R=0.0D0
             IF (.NOT.LAST)R=H(K+2,K-1)
             X=DABS(P)+DABS(Q)+DABS(R)
             IF (X.EQ.0.0D0) GO TO 118
             P=P/X
             Q=Q/X
             R=R/X
  119        S=0.0D0
             IF (P.EQ.0.0D0) GO TO 1119
             IF (DLOG10(DABS(P)).GE.-38.0D0) S=P*P
 1119        IF (Q.EQ.0.0D0) GO TO 2119
             IF (DLOG10(DABS(Q)).GE.-38.0D0) S=S+Q*Q
 2119        IF (R.EQ.0.0D0) GO TO 3119
             IF (DLOG10(DABS(R)).GE.-38.0D0) S=S+R*R
 3119        S=DSQRT(S)
             IF (P.LT.0)S=-S
             IF (K.EQ.M) GO TO 120
             H(K,K-1)=-S*X
             GO TO 9121
  120        IF (L.NE.M)H(K,K-1)=-H(K,K-1)
 9121        P=P+S
             X=P/S
             Y=Q/S
             Z=R/S
             Q=Q/P
             R=R/P
             DO 121 J=K,N
                P=H(K,J)+Q*H(K+1,J)
                IF (LAST) GO TO 122
                P=P+R*H(K+2,J)
                H(K+2,J)=H(K+2,J)-P*Z
  122           H(K+1,J)=H(K+1,J)-P*Y
  121           H(K,J)=H(K,J)-P*X
             J=MINO(EN,K+3)
             DO 123 I=1,J
                P=X*H(I,K)+Y*H(I,K+1)
                IF (LAST) GO TO 124
                P=P+Z*H(I,K+2)
                H(I,K+2)=H(I,K+2)-P*R
  124           H(I,K+1)=H(I,K+1)-P*Q
  123           H(I,K)=H(I,K)-P
             DO 125 I=LOW,HI
                P=X*F(I,K)+Y*F(I,K+1)
                IF (LAST) GO TO 126
                P=P+Z*F(I,K+2)
```

```
                F(I,K+2)=F(I,K+2)-P*R
  126           F(I,K+1)=F(I,K+1)-P*Q
  125           F(I,K)=F(I,K)-P
  118       CONTINUE
C
C         ----- END OF QR ROTATION
C
          GO TO 200
C
C         ----- ONE REAL ROOT IS DETERMINED
C
  110     H(EN,EN)=X+T
          WR(EN)=H(EN,EN)
          WI(EN)=0.0D0
          IF (EN.NE.1)H(EN,NA)=0.0D0
          ICNT(EN)=ITS
          EN=NA
          GO TO 105
C
C         ----- TWO ROOTS ARE DETERMINED
C
  111     P=(Y-X)/2.0D0
          Q=P*P+W
          Z=DSQRT(DABS(Q))
          X=X+T
          H(EN,EN)=X
          H(NA,NA)=Y+T
          IF (NA.NE.1)H(NA,NA-1)=0.0D0
          ICNT(EN)=-ITS
          ICNT(NA)=ITS
C
          IF (Q.LE.0.0D0) GO TO 201
C
C         ----- TWO REAL ROOTS
C
          IF (P.LT.0.0D0)Z=-Z
          Z=P+Z
          WR(NA)=X+Z
          S=X-W/Z
          WR(EN)=S
          WI(NA)=0.0D0
          WI(EN)=0.0D0
          X=H(EN,NA)
          R=DSQRT(X*X+Z*Z)
          P=X/R
          Q=Z/R
          DO 203 J=NA,N
             Z=H(NA,J)
             H(NA,J)=Q*Z+P*H(EN,J)
  203        H(EN,J)=Q*H(EN,J)-P*Z
          DO 204 I=1,EN
             Z=H(I,NA)
             H(I,NA)=Q*Z+P*H(I,EN)
  204        H(I,EN)=Q*H(I,EN)-P*Z
          DO 205 I=LOW,HI
             Z=F(I,NA)
             F(I,NA)=Q*Z+P*F(I,EN)
  205        F(I,EN)=Q*F(I,EN)-P*Z
          H(EN,NA)=0.0D0
          GO TO 202
```

```
C
C
C          ----- TWO COMPLEX ROOTS
C
  201      WR(NA)=X+P
           WR(EN)=X+P
           WI(NA)=Z
           WI(EN)=-Z
C
  202      EN=EN-2
           GO TO 105
C          ----- END OF EIGENVALUE ITERATION
  100 RNRM=0.0D0
      K=1
      DO 210 I=1,N
      DO 209 J=K,N
  209 RNRM=RNRM+DABS(H(I,J))
  210 K=I
C
C     ----- DETERMINE THE EIGENVECTORS OF THE TRIANGULAR MATRIX STORED
C     ----- IN H AND OVERWRITE THEM ON H
C
      EN=N
  400 IF (EN.LT.2) GO TO 401
C
           P=WR(EN)
           Q=WI(EN)
           NA=EN-1
C
           IF (Q.NE.0.0D0) GO TO 212
C
C          ----- REAL EIGENVECTOR CORRESPONDING TO REAL EIGENVALUE
C
           I=NA
  206      IF (I.LT.1) GO TO 220
C
              S=H(I,EN)
              IP1=I+1
              IF (NA.LT.IP1) GO TO 9214
              DO 214 J=IP1,NA
  214         S=S+H(I,J)*H(J,EN)
 9214         Y=0.0D0
              IF (I.NE.1)Y=H(I,I-1)
  215         Z=P-H(I,I)
              IF (Z.EQ.0.0D0)Z=EPSM*RNRM
              IF (Y.NE.0.0D0) GO TO 9213
C
              H(I,EN)=S/Z
              GO TO 213
C
 9213         I=I-1
              R=H(I,EN)
              IP2=I+2
              IF (NA.LT.IP2) GO TO 9216
              DO 216 J=IP2,NA
  216         R=R+H(I,J)*H(J,EN)
 9216         W=H(I,I)-P
              X=H(I,I+1)
              IF (CABS(W).LE.CABS(Y)) GO TO 217
C
```

```
               RM=Y/W
               Z=(S-RM*R)/(Z+RM*X)
               H(I+1,EN)=Z
               H(I,EN)=(-R-X*Z)/W
               GO TO 213
C
  217          RM=W/Y
               X=(RM*S-R)/(X+RM*Z)
               H(I+1,EN)=X
               H(I,EN)=(-S+X*Z)/Y
C
C
  213     I=I-1
          GO TO 206
C
  220     H(EN,EN)=1.0D0
          GO TO 211
C
C         ----- COMPLEX EIGENVECTOR CORRESPONDING TO COMPLEX EIGENVALUE
C
  212     I=NA
  299     IF (I.LT.1) GO TO 350
C
               R=H(I,EN)
               S=0.0D0
               IP1=I+1
               IF (IP1.GT.NA) GO TO 9301
               DO 301 J=IP1,NA
               R=R+H(I,J)*H(J,NA)
  301          S=S+H(I,J)*H(J,EN)
 9301          CONTINUE
               Y=0.0D0
               IF (I.NE.1)Y=H(I,I-1)
  302          Z=H(I,I)-P
C
               IF (Y.NE.0.0D0) GO TO 9303
C
               CALL CDIV(-R,-S,Z,Q,H(I,NA),H(I,EN))
               GO TO 303
C
 9303          I=I-1
               RA=H(I,EN)
               SA=0.0D0
               IP2=I+2
               IF (NA.LT.IP2) GO TO 9304
               DO 304 J=IP2,NA
               RA=RA+H(I,J)*H(J,NA)
  304          SA=SA+H(I,J)*H(J,EN)
 9304          CONTINUE
               W=H(I,I)-P
               X=H(I,I+1)
               IF (DABS(W)+DABS(Q).LE.DABS(Y)) GO TO 305
C
               CALL CDIV(Y,0.0D0,W,Q,RM,IM)
               R=R-RM*RA+IM*SA
               S=S-RM*SA-IM*RA
               T1=RM*X-Z
               T2=IM*X-Q
               CALL CDIV(R,S,T1,T2,RV,IV)
               T1=-RA-X*RV
```

```
            T2=-SA-X*IV
            CALL CDIV(T1,T2,W,Q,H(I,NA),H(I,EN))
            GO TO 306
C
  305       RM=W/Y
            IM=Q/Y
            RA=RA-RM*R+IM*S
            SA=SA-RM*S-IM*R
            T1=RM*Z-IM*Q-X
            T2=IM*Z+RM*Q
            CALL CDIV(RA,SA,T1,T2,RV,IV)
            H(I,NA)=(IV*Q-RV*Z-R)/Y
            H(I,EN)=-(S+IV*Z+RV*Q)/Y
C
  306       H(I+1,NA)=RV
            H(I+1,EN)=IV
C
C
  303    I=I-1
         GO TO 299
C
  350    H(EN,NA)=1.0D0
         H(EN,EN)=0.0D0
         EN=NA
C
  211 EN=EN-1
      GO TO 400
C
C      ----- END EIGENVECTORS OF TRIANGULAR MATRIX
C
C
  401 IF (WI(1).EQ.0.0D0)H(1,1)=1.0D0
      IF (LOWM1.LT.1) GO TO 9402
      DO 402 I=1,LOWM1
         IP1=I+1
         DO 402 J=IP1,N
  402    F(I,J)=H(I,J)
C
 9402 IF (HI1.GT.N) GO TO 404
      DO 403 I=HI1,N
         IF (I.EQ.N) GO TO 9403
         IP1=I+1
         DO 403 J=IP1,N
  403    F(I,J)=H(I,J)
C
 9403 IF (LOW.GT.HI) GO TO 404
      DO 416 J=HI1,N
      DO 416 I=LOW,HI
         Z=0.CDO
         DO 405 K=LOW,HI
  405    Z=Z+F(I,K)*H(K,J)
  416    F(I,J)=Z
C
  404 J=HI
 9404 IF (J.LT.LOW) GO TO 413
C
         IF (WI(J).EQ.0.0D0) GO TO 407
C
         IP=J-1
         DO 408 I=LOW,HI
```

```
            Y=0.0D0
            Z=0.0D0
            DO 409 K=LOW,J
            Y=Y+F(I,K)*H(K,IP)
  409       Z=Z+F(I,K)*H(K,J)
            F(I,IP)=Y
  408       F(I,J)=Z
         J=IP
         GO TO 406
C
  407    DO 410 I=LOW,HI
            Z=0.0D0
            DO 411 K=LOW,J
  411       Z=Z+F(I,K)*H(K,J)
  410       F(I,J)=Z
C
  406 J=J-1
      GO TO 9404
C
C     ----- END EIGENVECTOR DETERMINATION
C
  413 IF (N.GT.2)H(3,1)=MA(3)
      IF (N.LT.4)RETURN
      DO 415 I=4,N
      H(I,I-2)=MA(I)
  415 H(I,I-3)=MB(I)
C
      RETURN
      END
      SUBROUTINE BALANC (NM,N,A,LOW,HI,D)
C
      IMPLICIT REAL*8 (A-H,O-Z)
      DIMENSION A(NM,NM),D(NM)
      INTEGER HI
      LOGICAL NOCONV
      DATA B,B2 / 16.0D0, 256.0D0 /
C
      L = 1
      K = N
C
C     SEARCH FOR ROWS ISOLATING AN EIGENVALUE AND PUSH THEM DOWN
C
  100 J = K
  101 IF (J.LT.1) GO TO 110
      R = 0.0D0
      DO 102 I = 1,K
  102 R = R+DABS(A(J,I))
      R = R-DABS(A(J,J))
      IF (R.NE.0.0D0) GO TO 103
      D(K) = J
      IF (J.EQ.K) GO TO 203
      DO 201 I = 1,K
         F = A(I,J)
         A(I,J) = A(I,K)
  201    A(I,K) = F
      DO 202 I = L,N
         F = A(J,I)
         A(J,I) = A(K,I)
  202    A(K,I) = F
  203 K = K-1
```

```
      GO TO 100
  103 J = J-1
      GO TO 101
C
C     SEARCH FOR COLUMNS ISOLATING AN EIGENVALUE AND PUSH THEM LEFT
C
  110 J = L
  109 IF (J.GT.K) GO TO 113
      C = 0.0D0
      DO 112 I = L,K
  112 C = C+DABS(A(I,J))
      C = C-DABS(A(J,J))
      IF (C.NE.0.0D0) GO TO 111
      D(L) = J
      IF (J.EQ.L) GO TO 213
      DO 211 I = 1,K
         F = A(I,J)
         A(I,J) = A(I,L)
  211    A(I,L) = F
      DO 212 I = L,N
         F = A(J,I)
         A(J,I) = A(L,I)
  212    A(L,I) = F
  213 L = L+1
      GO TO 110
  111 J = J+1
      GO TO 109
C
  113 LOW = L
      HI = K
      IF (L.GT.K)RETURN
      DO 300 I = L,K
  300 D(I) = 1.0D0
C
C     NOW BALANCE THE MATRIX IN ROWS L THROUGH K
C
  302 NOCONV = .FALSE.
      DO 301 I = L,K
C
         C = C.0D0
         R = C.0D0
         DO 303 J = L,K
         IF (J.EQ.I) GO TO 303
         C = C+DABS(A(J,I))
         R = R+CABS(A(I,J))
  303    CONTINUE
C
         F = 1.0D0
         S = C+R
C
         G = R/B
  304    IF (C.GE.G) GO TO 305
         F = F*B
         C = C*B2
         GO TO 304
C
  305    G = R*B
  306    IF (C.LT.G) GO TO 307
         F = F/B
         C = C/B2
```

```
         GO TO 306
C
  307    IF ((C+R)/F.GE.0.95D0*S) GO TO 301
C
         G = 1.0D0/F
         D(I) = D(I)*F
         NOCONV = .TRUE.
         DO 311 J = L,N
  311    A(I,J) = A(I,J)*G
         DO 312 J = 1,K
  312    A(J,I) = A(J,I)*F
C
  301    CONTINUE
C
      IF (NOCONV) GO TO 302
      RETURN
C
      END
      SUBROUTINE BALBAK(NM,N,LOW,HI,M,D,Z)
C
      IMPLICIT REAL*8 (A-H,O-Z)
      INTEGER HI
      DIMENSION D(NM),Z(NM,NM)
      IF (LOW.GT.HI) GO TO 107
      DO 101 I=LOW,HI
         S=D(I)
         DO 102 J=1,M
  102    Z(I,J)=Z(I,J)*S
  101    CONTINUE
C
  107 IF (LOW.LE.1) GO TO 108
      LOWM1=LOW-1
      DO 103 II=1,LOWM1
         I=LOW-II
         K=D(I)
         IF (K.EQ.I) GO TO 103
         DO 104 J=1,M
            S=Z(I,J)
            Z(I,J)=Z(K,J)
  104       Z(K,J)=S
  103    CONTINUE
C
  108 IF (HI.GE.N)RETURN
      IH=HI+1
      DO 105 I=IH,N
         K=D(I)
         IF (K.EQ.I) GO TO 105
         DO 106 J=1,M
            S=Z(I,J)
            Z(I,J)=Z(K,J)
  106       Z(K,J)=S
  105    CONTINUE
C
      RETURN
      END
      SUBROUTINE ELMHES(NM,N,K,L,A,INT)
C
      IMPLICIT REAL*8 (A-H,O-Z)
      DIMENSION INT(NM),A(NM,NM)
      LM1=L-1
```

```
      KP1=K+1
      IF (LM1.LT.KP1) RETURN
C
      DO 101 M=KP1,LM1
         I=M
         X=0.0D0
         DO 102 J=M,L
            IF (DABS(A(J,M-1)).LE.DABS(X)) GO TO 102
            X=A(J,M-1)
            I=J
  102    CONTINUE
         INT(M)=I
         IF (I.EQ.M) GO TO 103
C
         MM1=M-1
         DO 104 J=MM1,N
            Y=A(I,J)
            A(I,J)=A(M,J)
  104       A(M,J)=Y
         DO 105 J=1,L
            Y=A(J,I)
            A(J,I)=A(J,M)
  105       A(J,M)=Y
C
  103    IF (X.EQ.0) GO TO 101
         MP1=M+1
         DO 106 I=MP1,L
            Y=A(I,M-1)
            IF (Y.EQ.0) GO TO 106
            Y=Y/X
            A(I,M-1)=Y
            DO 107 J=M,N
  107       A(I,J)=A(I,J)-Y*A(M,J)
            DO 108 J=1,L
  108       A(J,M)=A(J,M)+Y*A(J,I)
  106       CONTINUE
  101    CONTINUE
C
      RETURN
      END
      SUBROUTINE ELMBAK (NM,K,L,R,A,INT,Z)
C
      IMPLICIT REAL*8 (A-H,O-Z)
      DIMENSION A(NM,NM),INT(NM),Z(NM,NM)
      INTEGER R
      LMK=L-K-1
      IF (LMK.LT.1)RETURN
      DO 101 MM=1,LMK
         M=L-MM
         MP1=M+1
         DO 102 I=MP1,L
            X=A(I,M-1)
            IF (X.EQ.0) GO TO 102
            DO 103 J=1,R
  103       Z(I,J)=Z(I,J)+X*Z(M,J)
  102       CONTINUE
         I=INT(M)
         IF (I.EQ.M) GO TO 101
         DO 104 J=1,R
            X=Z(I,J)
```

```
            Z(I,J)=Z(M,J)
  104       Z(M,J)=X
  101   CONTINUE
      RETURN
      END
      SUBROUTINE MINV(NM,A,N,D,L,M)
      IMPLICIT REAL*8 (A-H,O-Z)
      DIMENSION A(NM),L(NM),M(NM)
      DOUBLE PRECISION A,D,BIGA,HOLD
      D=1.0D0
      NK=-N
      DO 80 K=1,N
      NK=NK+N
      L(K)=K
      M(K)=K
      KK=NK+K
      BIGA=A(KK)
      DO 20 J=K,N
      IZ=N*(J-1)
      DO 20 I=K,N
      IJ=IZ+I
   10 IF( DABS(BIGA)- DABS(A(IJ))) 15,20,20
   15 BIGA=A(IJ)
      L(K)=I
      M(K)=J
   20 CONTINUE
C
C        INTERCHANGE ROWS
C
      J=L(K)
      IF(J-K) 35,35,25
   25 KI=K-N
      DO 30 I=1,N
      KI=KI+N
      HOLD=-A(KI)
      JI=KI-K+J
      A(KI)=A(JI)
   30 A(JI) =HOLD
C
C        INTERCHANGE COLUMNS
C
   35 I=M(K)
      IF(I-K) 45,45,38
   38 JP=N*(I-1)
      DO 40 J=1,N
      JK=NK+J
      JI=JP+J
      HOLD=-A(JK)
      A(JK)=A(JI)
   40 A(JI) =HOLD
C
C        DIVIDE COLUMN BY MINUS PIVOT (VALUE OF PIVOT ELEMENT IS
C        CONTAINED IN BIGA)
C
   45 IF(BIGA) 48,46,48
   46 D=0.0D0
      RETURN
   48 DO 55 I=1,N
      IF(I-K) 50,55,50
   50 IK=NK+I
```

```
      A(IK)=A(IK)/(-BIGA)
   55 CONTINUE
C
C        REDUCE MATRIX
C
      DO 65 I=1,N
      IK=NK+I
      HOLD=A(IK)
      IJ=I-N
      DO 65 J=1,N
      IJ=IJ+N
      IF(I-K) 60,65,60
   60 IF(J-K) 62,65,62
   62 KJ=IJ-I+K
      A(IJ)=HOLD*A(KJ)+A(IJ)
   65 CONTINUE
C
C        DIVIDE ROW BY PIVOT
C
      KJ=K-N
      DO 75 J=1,N
      KJ=KJ+N
      IF(J-K) 70,75,70
   70 A(KJ)=A(KJ)/BIGA
   75 CONTINUE
C
C        PRODUCT OF PIVOTS
C
      D=D*BIGA
C
C        REPLACE PIVOT BY RECIPROCAL
C
      A(KK)=(1.0D0)/BIGA
   80 CONTINUE
C
C        FINAL ROW AND COLUMN INTERCHANGE
C
      K=N
  100 K=(K-1)
      IF(K) 150,150,105
  105 I=L(K)
      IF(I-K) 120,120,108
  108 JQ=N*(K-1)
      JR=N*(I-1)
      DO 110 J=1,N
      JK=JQ+J
      HOLD=A(JK)
      JI=JR+J
      A(JK)=-A(JI)
  110 A(JI) =HOLD
  120 J=M(K)
      IF(J-K) 100,100,125
  125 KI=K-N
      DO 130 I=1,N
      KI=KI+N
      HOLD=A(KI)
      JI=KI-K+J
      A(KI)=-A(JI)
  130 A(JI) =HOLD
      GO TO 100
```

```
  150 RETURN
      END
      SUBROUTINE SCOV(NM,AVCN,Q)
      IMPLICIT REAL*8 (A-H,O-Z)
      REAL*8 AVCN(NM,NM),Q(NM,NM)
      REAL*8 V(55,55),COV(55),QE(55),LU(55,55)
      DIMENSION L(55,55)
      INTEGER IPS(55)
      REAL DIGITS
      DIGITS=0.D0
      N = NM
      M = N*(N+1)/2
      M2 = M*M
      K = 0
      DO 20 I= 1,N
      DO 20 J = I,N
      K = K+1
      QE(K) =-Q(I,J)
      L(I,J) = K
   20 L(J,I) = K
      DO 30 I = 1,M
      DO 30 J = 1,M
   30 V(I,J) =0.D0
      DO 40 I = 1,N
      DO 40 J = 1,N
      DO 40 K = 1,N
   40 V(L(I,K),L(J,K)) = AVCN(I,J)+V(L(I,K),L(J,K))
      DO 50 I = 1,N
      DO 50 J = 1,M
   50 V(L(I,I),J)=2.D0*V(L(I,I),J)
C     DO 60 I = 1,M
C  60 WRITE(6,103) (V(I,J),J=1,M)
C 103 FORMAT(' ',4X,F15.8,4X,F15.8,4X,F15.8)
      CALL LINSY2(3,M,V,55,QE,COV,LU,IPS,DIGITS,&141,&142,&143)
      K = 0
      DO 80 I = 1,N
      DO 80 J = I,N
      K = K+1
      Q(I,J) =COV(K)
   80 Q(J,I) = Q(I,J)
C     DO 90 I = 1,N
C  90 WRITE(6,100)(Q(I,J),J=1,N)
C 100 FORMAT(' ',4X,F15.8,4X,F15.8,4X,F15.8)
      GO TO 155
  141 WRITE(6,151)
      GO TO 155
  142 WRITE(6,152)
      GO TO 155
  143 WRITE(6,153)
      GO TO 155
  151 FORMAT('****MATRIX WITH A ROW OF ALL ZERO ELEMENTS FOUND')
  152 FORMAT('****ZERO PIVOT ELEMENT FOUND')
  153 FORMAT('****MAXIMUM NUMBER OF ITERATIONS REACHED IN IMPROVE')
  155 CONTINUE
      RETURN
      END
      SUBROUTINE LINSY2(MODE, N, A, IDIM, B, X, LU, IPS, DIGITS,*,*,*
        INTEGER MODE, N, IDIM, IPS(N)
        REAL*8 A(IDIM,N), LU(IDIM,N), B(N), X(N)
        REAL DIGITS
```

```
      EXTERNAL DECMP2, SOLVE2, IMPRV2
      DIGITS = 0.0
      IF (MODE .EQ. 2 .OR. MODE .EQ. 4) GO TO 10
      CALL DECMP2 (N, A, IDIM, LU, IPS, &100, &101)
10    CALL SOLVE2 (N, LU, IDIM, B, X, IPS)
      IF (MODE .LE. 2) RETURN
      CALL IMPRV2(N, A, IDIM, B, X, LU, IPS, DIGITS, &102)
      RETURN
100   RETURN 1
101   RETURN 2
102   RETURN 3
    END
   SUBROUTINE DECMP2 (N, A, IDIM, LU, IPS, *,*)
      INTEGER N, IDIM, IPS(N)
      REAL*8 A(IDIM,N), LU(IDIM,N), DMAX1, DABS
      INTEGER I, J, K, IP, KP, KP1, NM1, IDXPIV
      REAL*8 SCALES(100), EM, BIG, SIZE, PIVOT, ROWNRM, ZERO
      ZERO = 0.0D0
      DO 5 I=1,N
         IPS(I) = I
         ROWNRM = 0.0D0
         DO 2 J=1,N
            LU(I,J) = A(I,J)
            ROWNRM = DMAX1(ROWNRM,DABS(LU(I,J)))
 2       CONTINUE
         IF (ROWNRM .EQ. ZERO) RETURN 1
         SCALES(I) = 1.0/ROWNRM
 5    CONTINUE
      NM1 = N-1
      DO 17 K=1,NM1
         BIG = 0.0D0
         DO 11 I=K,N
            IP = IPS(I)
            SIZE = DABS(LU(IP,K))*SCALES(IP)
            IF (SIZE .LE. BIG) GO TO 11
            BIG = SIZE
            IDXPIV = I
11       CONTINUE
         IF (BIG .EQ. ZERO) RETURN 2
         IF (IDXPIV .EQ. K) GO TO 15
         J = IPS(K)
         IPS(K) = IPS(IDXPIV)
         IPS(IDXPIV) = J
15       KP = IPS(K)
         PIVOT = LU(KP,K)
         KP1 = K+1
         DO 16 I=KP1,N
            IP = IPS(I)
            EM = LU(IP,K)/PIVOT
            LU(IP,K) = EM
            DO 16 J=KP1,N
               LU(IP,J) = LU(IP,J) - EM*LU(KP,J)
16       CONTINUE
17    CONTINUE
      IF (LU(IPS(N),N) .EQ. ZERO) RETURN 2
      RETURN
    END
    SUBROUTINE SOLVE2 (N, LU, IDIM, B, X, IPS)
      INTEGER N, IDIM, IPS(N)
      REAL*8 LU(IDIM,N), B(N), X(N)
```

```
      INTEGER I, J, IP, IP1, IM1, NP1, IBACK
      REAL*8 SUM
      NP1 = N+1
      X(1) = B(IPS(1))
      DO 2 I=2,N
         IP = IPS(I)
         IM1 = I-1
         SUM = 0.0D0
         DO 1 J =1,IM1
            SUM = SUM + LU(IP,J)*X(J)
1        CONTINUE
         X(I) = B(IP) - SUM
2     CONTINUE
      X(N) = X(N)/LU(IPS(N),N)
      DO 4 IBACK =2,N
         I = NP1 - IBACK
         IP = IPS(I)
         IP1 = I+1
         SUM = 0.0D0
         DO 3 J=IP1,N
            SUM = SUM + LU(IP,J)*X(J)
3        CONTINUE
4     X(I) = (X(I)-SUM)/LU(IP,I)
      RETURN
  END
  SUBROUTINE IMPRV2(N, A, IDIM, B, X, LU, IPS, DIGITS, *)
      INTEGER N, IDIM, IPS(N)
      REAL*8 A(IDIM,N), LU(IDIM,N), B(N), X(N), DABS, DMAX1
      REAL*8 DLOG1C
      REAL DIGITS
      REAL*8 R(100), DX(100), EPS, XNORM, DXNORM, T, SUM, ZERO
      INTEGER I, J, ITMAX, ITER, IEXP
      EXTERNAL SOLVE2,DPPUT,IPTOTL
      IEXP = 0
      ZERO = 0.0D0
      EPS = 3.55E-15
      ITMAX = 29
      XNORM = 0.0D0
      DO 1 I=1,N
         XNORM = DMAX1(XNORM,DABS(X(I)))
1     CONTINUE
      IF (XNORM .NE. ZERO) GO TO 3
      DIGITS = -DLOG10(EPS)
      RETURN
3     DO 9 ITER = 1,ITMAX
         DO 5 I=1,N
            DO 4 J=1,N
               CALL DPPUT(-A(I,J),X(J))
4           CALL DPPUT(1.0D0,B(I))
            CALL IPTOTL(R(I))
5        CALL SOLVE2 (N, LU, IDIM, R, DX, IPS)
         DXNORM = 0.0D0
         DO 6 I=1,N
            T = X(I)
            X(I) = X(I) + DX(I)
            DXNORM = DMAX1 (DXNORM,DABS(X(I)-T))
6        CONTINUE
         IF (ITER .EQ. 1) DIGITS = -DLOG10(DMAX1(DXNORM/XNORM,EPS))
         IF (DXNORM .LE. EPS*XNORM) RETURN
9     CONTINUE
```

```
      RETURN 1
      END
      SUBROUTINE  DPPUT(A , B)
      REAL*8  A, B
      COMMON /CPACCC/ R(45)
      REAL*8 R
      REAL*8    X,Y,AL,AH,BL,BH,C
      REAL W
      INTEGER CHC,  EXPT
      EQUIVALENCE  (CHC,W)
C     WE SPLIT UP THE HIGH AND LOW ORDER PARTS OF A AND B.  THAT
C     IS, THE LEFT 6 HEX DIGITS OF THE FRACTION, AND THE RIGHT 8.
      W=A
      AH=W
      AL=A-AH
      W=B
      BH=W
      BL=B-BH
      Y=AH*BH
      W=Y
      X=W
C     WE NOW FIND THE EXPONENT PART OF A*B.  THIS IS DIVIDED BY
C     THREE TO DETERMINE WHERE IN THE ACCUMULATOR WE WILL PLACE A*B.
      W=ABS(W)
      EXPT=CHC/50331648 + 3
      R(EXPT)=R(EXPT) + X
      R(EXPT-2)=R(EXPT-2) + (Y-X)
      Y=AH*BL
      W=Y
      X=W
      W=ABS(W)
      EXPT=CHC/50331648 + 3
      R(EXPT)=R(EXPT) + X
      R(EXPT-2)=R(EXPT-2) + (Y-X)
      Y=AL*BH
      W=Y
      X=W
      W=ABS(W)
      EXPT=CHC/50331648 + 3
      R(EXPT)=R(EXPT) + X
      R(EXPT-2)=R(EXPT-2) + (Y-X)
      W=AL
      C=W
      Y=C*BL
      W=Y
      X=W
      W=ABS(W)
      EXPT=CHC/50331648 + 3
      R(EXPT)=R(EXPT) + X
      R(EXPT-2)=R(EXPT-2) + (Y-X)
      Y=(AL-C)*BL
      W=Y
      X=W
      W=ABS(W)
      EXPT=CHC/50331648 + 3
      R(EXPT)=R(EXPT) + X
      R(EXPT-2)=R(EXPT-2) + (Y-X)
500   RETURN
      END
      SUBROUTINE IPTOTL(IP)
```

```
      REAL*8 IP
      COMMON /DPACCC/ R(45)
      REAL*8 R
      IP  =  0.0D0
      DO  100  I = 1,43
      IP  =  IP + R(46-I)
100   R(46-I)  =  0.0D0
      RETURN
      END
      BLOCK DATA
      COMMON /DPACCC/ R
      REAL*8 R(45)/45*0.0D0/
      END
      SUBROUTINE CNORM(WR,WI,VEC,NS)
      IMPLICIT REAL*8 (A-H,O-Z)
      DOUBLE PRECISION  WR,WI,VEC
      DIMENSION WR(NS),WI(NS),VEC(NS,NS)
      DIMENSION RVEC(10,10),VECRN(10,10),VECIN(10,10),VECR(10,10),
     1          VECI(10,10),VRV(10),VIV(10),VRRV(10),VRIV(10)
    7 FORMAT(' ')
    8 FORMAT('0REAL EIGENVALUE   (',I2,').......',14X,'REAL EIGENVECT
     1(',I2,').......'//1X,'(',F12.8,')+J(',F12.8,')',13X,'(',F12.8,'
     2)
    9 FORMAT(44X,'(',F12.8,')')
   10 FORMAT('0COMPLEX EIGENVALUE(',I2,').......',14X,'COMPLEX EIGENV
     1TOR(',I2,').......'//1X,'(',F12.8,')+J(',F12.8,')',13X,'(',F12.
     2,')+J(',F12.8,')')
   11 FORMAT(44X,'(',F12.8,')+J(',F12.8,')')
C
      LM=0
      LR=0
      LC=0
      DO 999 K =1,NS
      LK =K+1
      REMOD = 0.D0
      IF (DABS(WI(K)).LT.1.D-10) GO TO 998
      IF (LM.EQ.1.AND.K.EQ.NS) GO TO 1000
      IF (LM.EQ.1) GO TO 992
      LC=LC+1
      EMAX = 0.D0
      DO 997 I = 1,NS
      VECR(I,LC)=VEC(I,K)
      VECI(I,LC)=VEC(I,LK)
      CMOD=VECR(I,LC)**2+VECI(I,LC)**2
      IF (CMOD-EMAX)997,990,990
  990 EMAX = CMOD
      M=I
  997 CONTINUE
      VMR = VECR(M,LC)
      VMI = VECI(M,LC)
      EMXIN=1.D0/EMAX
      DO 980 I=1,NS
      VR = VECR(I,LC)
      VI = VECI(I,LC)
      VECRN(I,LC)=EMXIN*(VR*VMR+VI*VMI)
  980 VECIN(I,LC)=EMXIN*(-VR*VMI+VI*VMR)
      VRV(LC)=WR(K)
      VIV(LC)=WI(K)
  992 LM=0
      IF(DABS(WI(K)+WI(LK)).LT.1.D-10) LM=1
```

```
      GO TO 999
  998 LR=LR+1
      DO 996 I=1,NS
      RVEC(I,LR)=VEC(I,K)
  996 REMOD=RVEC(I,LR)**2+REMOD
      RMOD=DSQRT(REMOD)
      DO 995 I=1,NS
  995 RVEC(I,LR)=RVEC(I,LR)/RMOD
      VRRV(LR)=WR(K)
      VRIV(LR)=WI(K)
      IF(K.EQ.NS) GO TO 1000
  999 CONTINUE
C1000 WRITE(6,7)
 1000 CONTINUE
      IF (LC .EQ. 0) GO TO 961
      DO 960 J=1,LC
      WRITE(6,10) J,J,VRV(J),VIV(J),VECRN(1,J),VECIN(1,J)
  960 WRITE(6,11) (VECRN(K,J),VECIN(K,J),K=2,NS)
  961 IF (LR.EQ.0) GO TO 1005
      WRITE(6,7)
      DO 965 J=1,LR
      WRITE(6,8) J,J,VRRV(J),VRIV(J),RVEC(1,J)
  965 WRITE(6,9) (RVEC(K,J),K=2,NS)
 1005 RETURN
      END
```

```
C**********************************************************************
C  SUBROUTINE RGAIN
C--------------------
C
C     THIS SUBROUTINE SEPARATES THE EIGENVECTORS AND EIGENVALUES OF
C     THE EULER-LAGRANGE EQUATIONS BY THE DECOMPOSITION DISCUSSED
C     IN CHAPTER IV AND CALCULATES THE STEADY-STATE SOLUTION OF THE
C     RICCATI EQUATION FOR THE CONTROL OR ESTIMATION PROBLEM
C**********************************************************************
      SUBROUTINE RGAIN(M,NS,NC,NOB,IF,RM,WR,WI,VF,GN)
      IMPLICIT REAL*8 (A-H,O-Z)
      DIMENSION WR(M),WI(M),VF(M,M),GN(NS,NS),RM(M,M)
      DIMENSION  W11(10,10),TC(20,10),W21(10,10),LT(100),MT(100)
      DIMENSION C(10),CI(10),CT(10,10)
      MH = NS
      K = 1
      KP = 1
      KN = 1
   10 IF(K.GT.M) GO TO 200
      IF(WR(K)) 100,5000,50
   50 IF(WI(K)) 80,75,80
C  LOOP 1A---EIGENVECTOR FOR REAL EIGENVALUE,POSITIVE
   75 CONTINUE
C  75 C(KP,KP) = WR(K)
      C(KP) = -WR(K)
      CI(KP) = WI(K)
      DO 76 J = 1,M
   76 TC(J,KP) = VF(J,K)
      DO 77 J = 1,NS
   77 CT(J,KP) = VF(J,K)
      KP = KP+1
      K=K+1
      GO TO 10
C  LOOP 1B---EIGENVECTOR FOR COMPLEX EIGENVALUE,POSITIVE REAL PART
   80 RR = WR(K)
      RI = WI(K)
      C(KP) = - RR
      C(KP+1) = -RR
      CI(KP) = RI
      CI(KP+1) = -RI
     C(KP,KP) = RR
     C(KP,KP+1) =-RI
     C(KP+1,KP) = RI
     C(KP+1,KP+1) = RR
      DO 81 J = 1,M
      FR = VF(J,K)
      FI = VF(J,K+1)
      TC(J,KP) = FR+FI
   81 TC(J,KP+1) = FR-FI
      DO 82 J = 1,NS
      CT(J,KP) = -VF(J,K)
   82 CT(J,KP+1) =- VF(J,K+1)
      KP = KP+2
      K = K+2
      GO TO 10
  100 IF(WI(K)) 120,110,120
```

```
C  LOOP 2A---EIGENVECTOR FOR REAL EIGENVALUE,NEGATIVE REAL PART
  110 CONTINUE
  110 CB(KN,KN) = WR(K)
      DO 95 J= 1,M
   95 TCB(J,KN) = VF(J,K)
      KN = KN+1
      K=K+1
      GO TO 10
C  LOOP 2B---EIGENVECTOR FOR COMPLEX EIGENVALUE,NEGATIVE REAL PART
  120 CONTINUE
  120 RR = WR(K)
      RI = WI(K)
      CB(KN,KN) = RR
      CB(KN,KN+1) = -RI
      CB(KN+1,KN) = RI
      CB(KN+1,KN+1) = RR
      DO 121 J = 1,M
      FR = VF(J,K)
      FI = VF(J,K+1)
      TCB(J,KN) = FR+FI
  121 TCB(J,KN+1) = FR-FI
      KN = KN+2
      K = K+2
      GO TO 10
  200 CONTINUE
C  FORMATION OF W11
      DO 300 I = 1,MH
      DO 300 J = 1,MH
  300 W11(I,J) = TC(I,J)
      KNS = NS+1
C  FORMATION OF W21
      DO 320 I=1,MH
      DO 320 J=1,MH
  320 W21(I,J)= TC(I+MH,J)
C
  326 IF (NOB.EQ.0) GO TO 322
      DO 321 I = 1,MH
      DO 321 J = 1,MH
      W11(I,J)= TC(I+MH,J)
  321 W21(I,J)=-TC(I,J)
  322 CONTINUE
      MHS=MH*MH
C  INVERT W11
      CALL MINV(MHS,W11,MH,DETC,LT,MT)
C
C  CALCULATE THE RGAIN MATRIX
      DO 325 IL=1,MH
      DO 325 JL=1,MH
      GN(IL,JL) = 0.DO
      DO 325 KL=1,MH
  325 GN(IL,JL)=GN(IL,JL)+W21(IL,KL)*W11(KL,JL)
      IF (NOB.EQ.0) GO TO 401
      DO 402 I = 1,MH
      DO 402 J = 1,MH
  402 CT(I,J) = W11(J,I)
  401 IF (IE.NE.0) CALL CNORM(C,CI,CT,NS)
      GO TO 6000
 5000 WRITE(6,1)
    1 FORMAT('1','ZERO EIGENVALUE')
 6000 RETURN
```

REFERENCES

BE1 Bellman, Richard, Stability Theory of Differential Equations, Dover Publications, 1969.

BE2 Bellman, Richard, Introduction to Matrix Analysis, McGraw-Hill Book Co., New York, 1960.

BI1 Bingulac, S. P., "An Alternate Approach to Expanding PA + A'P = -Q," IEEE Trans. on Automatic Control, Feb., 1970, pp. 135-137.

BR1 Bryson, A. E. and Ho, Y. C., Applied Optimal Control, Ginn-Blaisdell, Waltham, Mass., 1969.

BR2 Bryson, A. E. and Frazier, M., "Smoothing for Linear and Nonlinear Dynamic Systems," Wright Patterson Air Force Base, Ohio, Aeronautical Systems Division, TDR-63-119, pp. 353-304, September 1962.

BU1 Buffum, R. S., and Robertson, W. T., "A Hover Augmentation System for Helicopters," J. of Aircraft, Vol. 4, No. 4, July-Aug., 1967.

CH1 Chen, C. F. and Shieh, L. S., "A Note on Expanding PA + A^TP = Q," IEEE Trans. on Automatic Control, February 1968, pp. 122-123.

CO1 Cooper, D., Private communication, December 30, 1970.

CO2 Cooper, D., Hansen, K. C., Kaplita, T. T., "Single Rotor Helicopter Dynamics Following a Power Failure at High Speeds," USAVLABS TR 66-30, June 1966.

CR1 Crimi, Peter, "A Method for Analyzing the Aeroelastic Stability of a Helicopter Rotor in Forward Flight," NASA Report CR-1332, Washington, D. C., August 1969.

CR2 Crossley, T. R., and Porter, B., "Synthesis of Helicopter Stabilization Systems Using Modal Control Theory," presented at AIAA Flight Mechanics Conference, Santa Barbara, Calif., August 1970.

DA1 D'Angelo, Henry, Linear Time-Varying Systems: Analysis and Synthesis, Allyn and Bacon, Boston 1970.

DE1 DeRusso, P. M., Roy, R. J., Close, C. M., State Variables for Engineers, John Wiley & Sons, N.Y., 1965.

DU1 Duven, D. J., "Convergence of the Difference Equation for the Error Covariance Matrix Arising in Kalman Filter Theory,"TR 94900 Engineering Research Institute, Iowa State University, Ames, Iowa, April 1971.

DU2 DuWalt, F., and Daughaday, H., "Flutter of Lightly Loaded Rotors in Forward Flight," presented at V/STOL Technology and Planning Conference, Sept. 24, 1969.

EL1 Ellis, C. W., "Effects of Articulated Rotor Dynamics on Helicopter Control System Requirements," Aeronautical Engineering Review, July 1953, pp. 30-38.

ER1 Erugin, Nikolay P., Linear Systems of Ordinary Differential Equations with Periodic and Quasi-Periodic Coefficients, Academic Press, New York - London, 1966.

FL1 Floquet, G., "Sur les équations différentielles linéaieres," Ann. de l'Ecole Normal Supérieure, Paris, December 1883.

FR1 Fraser, Donald C., "A New Technique for the Optimal Smoothing of Data," Instrumentation Laboratory, M.I.T., Cambridge, Mass., January 31, 1967.

FR2 Fradenburgh, E. A., and Chuga, G. M., "Flight Program of the NH-3A Research Helicopter," JHS, Vol. 13, No. 1, January 1968,

FR3 Francis, J. G. F., "The QR Transformation, Parts I and II, Computer Journal, Vol. 4, No. 3, pp. 265-271, 332-345.

GE1 Gessow, Alfred; Myers, Garry G., Jr., Aerodynamics of the Helicopter, The Macmillan Company, New York, 1952.

GR1 Gray, D. L., Rempfer, P. S., Stevenson, L., "Application of Quadratic Optimization to Helicopter Flight Control," JACC, 1969.

HA1 Hall, W. E., "Application of Floquet Theory to the Analysis of Rotary Wing VTOL Stability," SUDAAR 400, Stanford University, April 1970.

HA2 Hall, W. E., "Prop-Rotor Stability at High Advance Ratios," Journal of the American Helicopter Society, April 1966.

HI1 Hill, G. W., "Mean Motion of the Lunar Perigee," Acta. Math., Vol. 8, January 1886.

HO1 Hohenemser, K., "Contribution to the Problem of Helicopter Stability," Proc. of Fourth Annual Forum, American Helicopter Society, 1948.

HO2 Hohenemser, K., Heaton, Jr., Paul W., "Aeroelastic Instability of Torsionally Rigid Helicopter Blades," Journal of American Helicopter Society, 1967.

HO3 Hohenemser, K., and Peters, D. A., "Application of the Floquet Transition Matrix to Problems of Lifting Rotor Stability," AHS 26th Annual National Forum, June 1970.

HO4 Horvay, G., and Yuan, S. W., "Stability of Rotor Blade Flapping Motion when Hinges are Tilted," J. Ae. Sci., Oct., 1947.

KA1 Kalman, R. E., "A New Approach to Linear Filtering and Prediction Theory," Transactions of the ASME, Journal of Basic Engineering, March 1960.

KA2 Kalman, R. E., and Englar, T. S., "A User's Manual for the Automatic Synthesis Program," NASA CR-475, June 1966.

KL1 Kleinman, D. L., "On an Iterative Technique for Riccati Equation Computations," IEEE Trans. Automatic Control, Vol. AC-13, pp. 114-115, February 1968.

LE1 Letov, A. M., "Analytic Controller Design III," Automation and Remote Control, Vol. 21, June 1960.

LE2 Lee, I., "Study of Linear Feedback Systems with Periodic Parameters Through An Extension of the Floquet Theory," SEL-62-117, December 1962.

LO1 Lowis, O. J., "The Stability of Rotor Blade Flapping Motion at High Tip Speed Ratios," A.R.C., R&M No. 3544, 1968.

MA1 Mathieu, E., "Mémoire sur le mouvement vibratoire d'une membrance de forme elliptique," J. Math. Pures at Appliquée, 1868.

MC1 MacFarlane, A. G. J., "An Eigenvector Solution to the Optimal Linear Regulator Problem," Journal of Electronics and Control, Vol. 14, No. 6, June 1963, pp. 643-654.

MI1 Miller, R. H., "Helicopter Control and Stability in Hovering Flight," Journal of Aeronautical Sciences, August 1948, pp. 453-472.

MI2 Miller, R. H., "A Method for Improving the Inherent Stability and Control Characteristics of Helicopters," Journal of Aeronautical Sciences, June 1950, pp. 363-374.

MI3 Mil, M. L., et al., Helicopters, Vol. 1, Aerodynamics NASA TTE-494, September 1967.

NA1 Narendra, K. S., and Murphy , R. D., "Design of Helicopter Stabilization Systems Using Optimal Control Theory," Journal of Aircraft, Vol. 6, No. 2, 1969.

OD1 O'Donnell, J. J., "Asymptotic Solution of the Matrix Riccati Equation of Optimal Control," Proc. Fourth Annual Allerton Conference on Circuit and System Theory, Oct. 1966, Monticello, Ill., pp. 577-586.

PA1 Payne, P. R., "Induced Aerodynamics of Helicopters," Aircraft Engineering, 1953.

PI1 Pipes, L. A., "Solution of Variable Circuits by Matrices," J. Frankl. Inst., 224: 585-600, 1938.

PI2 Pipes, L. A., "Operational and Matrix Methods in Linear Variable Networks," Phil. Mag., 25: 285-600, 1938.

PO1 Potter, J. E., "Matrix Quadratic Solutions," SIAM J. Applied Math., Vol. 14, No. 3, May 1966, pp. 496-501.

RY1 Rynaski, Edmund G., "Optimal Helicopter Station Keeping," IEEE Transactions on Auto. Control. Vol. AC-11, No. 3, July 1966.

SA1 Sanchez, David A., Ordinary Differential Equations and Stability Theory: An Introduction, W. H. Freeman & Co., 1968.

SE1 Seckel, E., Stability and Control of Airplanes and Helicopters, Academic Press, New York, 1964.

SH1 Shutler, A. G., Jones, J. P., "The Stability of Rotor Blade Flapping Motion,"A.R.C., R&M No. 3178, 1961.

SH2 Shupe, N. K., "A Study of Dynamic Motions of Hingeless Rotored Helicopters," ECOM-3323, August 1970.

SK1 Skelton, G. B., "Investigation of the Effects of Gusts on V/STOL Craft in Transition and Hover," AFFDL-TR-68-35, October 1968.

SI1 Sissingh, G. J., "Dynamics of Rotors at High Advance Ratios," JHS, Vol. 13, No. 3, July 1969, pp. 56-63.

ST1 Stammers, C. W., Ph.D., "The Bending Torsion Flutter of a Hingeless Rotor Blade," I.S.V.R., TR No. 9, October 1968.

ST2 Stammers, C. W., Ph.D., "The Flapping Torsion Flutter of a Helicopter Blade in Forward Flight," I.S.V.R. TR No. 3, February 1968.

TR1 Truxal, John G., Control System Synthesis, McGraw-Hill Book Company, New York, 1955.

VA1 Vaughan, D. R., "A Negative Exponential Solution for the Linear Optimal Regulator Problem," Proc. of 1968 J.A.C.C., Ann Arbor, Mich., June 1968, pp. 717-725.

VA Vaughan, D. R., "A Non-Recursive Solution of the Discrete Matrix Riccati Equation," IEEE Trans. on Automatic Control, October 1970.

WH1 Whittaker, W., and Watson, G. N., A Course of Modern Analysis, Cambridge, 1947.

WI1 Wilkenson, J. H., Martin, R.S., Peters, G., "The QR Algorithm for Real Hessenberg Matrices," Numer. Math., 14, 219-231 (1970).

WO1 Wolkovitch, J. and Johnston, D. E., "Automatic Control Considerations for Helicopters and VTOL Aircraft With and Without Sling Loads," ST1 TR 138-1, Systems Technology, Inc., November 1965.

WO2 Wood, E. R., Hermes, M. E., "Rotor Induced Velocities in Forward Flight by Momentum Theory," AIAA Paper No. 69-224, Presented AIAA/AHS VTOL Research, Design, and Operations Meeting, February 17-19, 1969.

YO1 Young, M. I., "A Theory of Rotor Blade Motion Stability in Powered Flight," J. Am. Helicopter Soc., Vol. 9, No. 3, July 1965.

ZA1 Zadeh, Lofti A. and Desoer, Charles A., Linear System Theory, McGraw-Hill Book Company, New York, 1963.